Root System Plasticity to Water Stress Tolerance in a Food Legume Mungbean,*Vigna radiata* (L.) Wilczek

Thesis submitted to the University of Hyderabad for the award of

Doctor of Philosophy

By

DEBASHREE SENGUPTA

Department of Plant Sciences
School of Life Sciences
University of Hyderabad
Hyderabad 500046
Andhra Pradesh (India)

February, 2013

Regd No. 08LPPH07

Department of Plant Sciences
School of Life Sciences
University of Hyderabad
Hyderabad 500046

DECLARATION

I, Debashree Sengupta, hereby declare that this thesis entitled **"Root system plasticity to water stress tolerance in a food legume, mungbean (*Vigna radiata* (L.) Wilczek)"** submitted by me under the guidance and supervision of Professor Attipalli R. Reddy is an original and independent research work. I also declare that it has not been submitted previously in part or in full to this University or any other University or Institution for the award of any degree or diploma.

Date:

Name: **Debashree Sengupta**

Signature:

Regd. No.: **08LPPH07**

Department of Plant Sciences
School of Life Sciences
University of Hyderabad
Hyderabad 500046

CERTIFICATE

This is to certify that this thesis entitled "**Root system plasticity to water stress tolerance in a food legume, mungbean (*Vigna radiata* (L.) Wilczek)"** is a record of bonafide work done by Ms. Debashree Sengupta, a research scholar for Ph.D. programme in Plant Sciences, Department of Plant Sciences, School of Life Sciences, University of Hyderabad under my guidance and supervision. The thesis has not been submitted previously in part or in full to this or any other University or Institution for the award of any degree or diploma.

Professor Attipalli R Reddy
(Supervisor)

(Head of the Department) **(Dean of the School)**

This thesis is dedicated to my beloved father

Late. Bhawani Prasad Sengupta

Acknowledgements

It's a great privilege for me to express my profound sense of gratitude to my supervisor Prof. Attipalli R. Reddy for providing me the opportunity to work under his invaluable guidance. I thank him for his constant encouragement, support and excellent guidance which helped me to develop my research ideas and scientific writing skills to a great extent.

My sincere thanks to Prof. R.P. Sharma, Dean, School of Life Sciences, Prof. Aparna Dutta Gupta, Prof. Ramanadham and Prof. A. S. Raghavendra, former Deans, School of Life Sciences for allowing me to use the school facilities for my research work.

I thank Prof. Attipalli R. Reddy, Head, Department of Plant Sciences; and Prof. Appa Rao Podile, Former Head, Department of Plant Sciences for allowing me to use the department facilities for my research work.

I also thank Prof. A.S. Raghavendra and Dr. K.P.M.S.V. Padmasree, my Doctoral committee members for their valuable suggestions and kind help.

I would like to express my thankfulness to Prof P.B Kirti for kindly providing his lab facilities and Dr. K Raja Rajesh Kumar for helping me in the RACE experiment.

I thank Proteomics facility, Dr. Madhurarekha, Ms. Monica and Ms. Kalpana for their help in my proteomics work.

I thank Central Instrumentation Laboratory (CIL) and Ms. Nalini for her help in my confocal microscopic studies.

I would like to thank all the faculty members of Life sciences for their timely and useful help whenever needed.

My sincere thanks to my seniors Dr. Girish and Dr. Chalapathi for their help and support.

I thank my present lab mates Anirban Guha, Chaitanya, Sumit, Madhan, Shalini , Harsha, Vamsi and Rajeev for maintaining a cheerful environment in the lab. I specially thank Mr Anirban Guha for all his valuable suggestions, help and friendly support throughout my research tenure.

I am highly grateful to my friends Abhay, Chaitu, Bimo, Jyothi, Prasu, Rama and Narmada for their affection and support throughout my research tenure and also for making my stay in the University a wonderful memory.

I thank Mr. Pandu , Mr. Vinodh, Mr.Lakshman and Mr Ashok for their help in the green house and lab work.

I also thank all the non-teaching staff members of Department of Plant Sciences and School of life Sciences for their help with the official works during my research period.

I thank DBT, DST,CSIR and DST-Nanotechnology for funding in the lab and DST-FIST, UGC-SAP and DBT-CREBB for funding to the department and school.

I acknowledge the financial assistance from CSIR, New Delhi in the form of junior and senior research fellowship.

I also thank DST, New Delhi and CICS, Chennai for providing travel grant for attending the EMBO meeting 2012 in Nice, France.

My special thanks to my husband Manoj for his encouragement and constant support which helped me to achieve this goal and my parents and in-laws for their patience, support and confidence in me.

Debashree

TABLE OF CONTENTS

LIST OF FIGURES AND TABLES

Figures

Tables

Symbols and abbreviations used

2DGE	2-Dimensional gel electrophoresis
6R	Six days after re-watering
ABA	Abscisic acid
ABS	Absorption
ACN	Acetonitrile
ACT	Actin
ADR	Aldose reductase
AKR	Aldo keto reductase
ALR	Aldehyde reductase
ANOVA	Analysis of Variance
APX	Ascorbate Peroxidase
ASA	Ascorbic acid
BLAST	Basic local alignment search tool
BSA	Bovine serum albumin
CHAPS	3-[(3-Cholamidopropyl)dimethylammonio]-1-propanesulfonate
CHCA	α-Cyano-4-Hydroxy Cinnamic Acid
CHI	Chalcone isomerase
Chl	Chlorophyll
CHR	Chalcone reductase
C_i	Internal CO_2 concentration
CRBD	Completely randomized block design
D3	Three days after onset of drought treatment
D6	Six days after onset of drought treatment
DCDHF-DA	Dichlorodihydrofluorescein diacetate
DDW	Double distilled water
DHAR	Dehydroascorbate reductase
DMSO	Dimethyl sulpohoxide
DNPH	Dinitro phenyl hydrazine
DTT	Dithiothreitol
E	Transpiration rate
EDTA	Ethylene diamine tetra acetic acid
ET_O	Electron transport
F_M	Fluorescence Maximum
F_O	Fluorescene Origin
F_V	Variable fluorescence
GAPDH	Glyceraldehyde 3-phosphate dehydrogenase
GPOX	Guaiacol peroxidase
GR	Glutathione reductase
g_s	Stomatal conductance
GSA	Glutamate semialdehyde
GSA-DH	Glutamic-γ-semialdehyde dehydrogenase
GSH	Glutathione (reduced)
GSP	Gene specific primer

GSSG	Glutathione (oxidized)
GST	Glutathione S-transferase
H_2O_2	Hydrogen peroxide
HNE	4-hydroxy-2-nonenal
HSD	3α-hydroxysteroid dehydrogenase
HSP-90	Heat shock protein-90
IEF	Isoelectric focusing
IPCC	Intergovernmental Panel on Climate Change
IPG	Immobilized pH gradient
IPTG	Isopropyl-β-D-thiogalactopyranoside
IRGA	Infra Red Gas Analyzer
KCl	Potassium Chloride
KI	Potassium Iodide
K_m	Michaelis-Menten constant
KOH	Potassium hydroxide
LB	Luria Bertani
Ldw	Leaf Dry Weight
Lfw	Leaf Fresh Weight
LMC	Leaf Moisture Content
Lp_r	Root Hydraulic Conductivity
LRWC	Leaf Relative Water content
Ltw	Leaf Turgid Weight
MALDI-TOF	Matrix Assisted Laser Desorption and Ionisation-Time of Flight
MDA	Malondialdehyde
$MgCl_2$	Magnesium chloride
MIP	Major Intrinsic Protein
MS	Methionine synthase
MS/MS	Mass Spectrometry/Mass spectrometry
NADPH	Nicotinamide adenine dipnucleotide phosphate
NaOH	Sodium hydroxide
NCBI	National Centre for Biotechnology Information
NPK	Nitrogen, Phosphorus, Potassium
NPQ	Non photochemical quenching
NSF	National Science Foundation
OA	Osmotic adjustment
OEC	Oxygen evolving complex
OPT	*O*-phthalaldehyde
ORF	Open reading frame
P5C	Δ^1-Pyrroline-5-Carboxylate
P5CDH	P5C dehydrgenase
P5CR	P5C reductase
PAM	Pulse amplitude modulation
PAR	Photosynthetically active radiation
PC	Pot water holding capacity
PCR	Polymerase chain reaction

PDH	Proline dehydrogenase
PEA	Plant efficiency analyzer
PEG	Poly ethyleneglycol
PEP	Phosphoenol pyruvate
PET	Photosynthetic electron transport
PGA	2-phosphoglycerate
PIP	Plasma membrane intrinsic protein
PMF	Peptide mass fingerprinting
PMSF	Phenyl methane sulfonyl fluoride
P_n	Net CO_2 assimilation rate
p-NB	para-Nitro benzaldehyde
POX	Proline oxidase
PPFD	Photosynthetic photon flux density
PQ	Plastoquinone
PQH_2	Reduced plastoquinone
PSI	Photosystem I
PSII	Photosystem II
PUFA	Poly unsaturated fatty acids
PVP	Polyvinyl pyrrolidone
RACE	Rapid amplification of cDNA ends
RC	Reaction centre
Rdw	Root dry weight
Rfw	Root fresh weight
RLD	Root length density
RMC	Root moisture content
ROS	Reactive oxygen species
Rtw	Root turgid weight
SD	Synthetic dropout
SDS-PAGE	Sodium dodecyl sulphonate-polyacrylamide gel electroporesis
SIP	Small basic Intrinsic Protein
SOD	Superoxide dismutase
TBA	Thiobarbituric acid
TCA	Trichloro acetic acid
TFA	Trifluoroacetic acid
TIP	Tonoplast intrinsic protein
TR_O	Trapping energy
VrP5CS	*Vigna radiata* Δ^1-pyrroline-5-carboxylate synthetase
VrγECS	*Vigna radiata* γ-glutamyl cysteine synthetase
W_D	Pot dry weight
W_P	Plant fresh weight
W_S	Saturated pot weight
WUE_i	Instantaneous water use efficiency
XET	Xyloglucan endotransglucosylase
X-Gal	5-Bromo 4-chloroindolyl-β-D-galactopyranoside
γ-GK	γ-Glutamyl kinase

CHAPTER 1

General Introduction & Experimental Design

INTRODUCTION

Sustainable agricultural crop production in an ever declining arable land area, owing to the increasing urbanization and industrial demands, is a major challenge in our current agricultural system. There is a constant need to minimize yield loss in food crops and maximize productivity to cope up with the perpetually increasing food demand. In order to achieve this goal, analysis of major underlying factors responsible for decreasing crop yield is highly essential. Major contributors inhibiting optimum crop yield were various abiotic stress factors including drought, salinity, heavy metals and high/low temperatures and among these, drought has become one of the most important, owing to its wide array of deleterious effects which deteriorates crop productivity worldwide (Roy et al. 2011). The term drought signifies a condition when the rainfall levels decline below normal range for a continuous stretch of time, which could be weeks, months or even years leading to various water-related problems. It was estimated that in India, approximately over 68% of land area is vulnerable to drought and majority of the drought prone areas were located in the western and peninsular India, which were primarily arid, semi-arid and sub-humid regions. Moreover, due to the recent challenges of global climate change, there are also predictions for occurrence of long lasting droughts, across the globe in the near future (IPCC 2007, NSF 2010).

As limitation of soil water availability to plants usually leads to a considerable loss in grain yield of major crops, it is essential to implement new strategies for crop improvement in drought prone areas, so that yield performance of crops will not be compromised. However, implementation of such crop improvement strategies were not always successful for all cultivated crops and in order to have an appropriate drought-management strategy, it is essential to have a comprehensive knowledge on various drought-induced responses of important crop plants including their physiological and biochemical mechanisms as well as the corresponding genetic regulatory factors. Thus, importance of fundamental research in providing crucial inputs regarding various drought-induced responses of crop plants for optimizing crop performance under water limiting regimes have always been recognized as extremely crucial to ensure the survival of

agricultural crops and sustainable food production under the present and future adverse climatic conditions (Al-Kaisi and Bronner 2009, Mittler and Blumwald 2010).

Strategies for improving crop performance in drought prone areas

Water deficit conditions usually result due to a seasonal decline in soil water availability (erratic monsoons) or may result from drought spells. The intensity, timing and duration of water deficit periods are highly crucial to determine the impact of drought on plants and also the type of drought-management strategy to be utilized. Broadly, there are three major strategies for improving crop performance in areas which are prone to water-deficit periods (**Fig. 1**). Firstly, the use of water reserves for supplementary crop irrigation, which include constructions of river dams, rainwater catchments, recycling of urban waste water and the use of water saving irrigation technologies. Another strategy includes use of regulated deficit irrigation, which is primarily practiced by farmers of semi-arid areas, wherein they carefully reduce the amount and timing of supplementary irrigation without affecting the crop yield. Final strategy which is of particular interest for us, being plant biologists, is the use of selection, breeding or genetic engineering approaches for enhancing drought-tolerance capacity in crop plants. In this strategy, the major targets are to develop crops which can maximize water uptake and minimize water loss and also acquire more photosynthate per unit of water transpired. However, in order to achieve these goals, a clear understanding of immediate drought-induced stress symptoms in crop plants and the corresponding drought tolerance strategies adopted is extremely important.

Though continuous breeding practices for more than 80 years have led to significant enhancement in crop yields under drought prone environments with considerable inputs from fundamental research in understanding physiological and molecular responses of plants to water deficit, there still exists a considerable gap between the “optimum” crop yield potential and the “actual” yield under drought stress. Owing to the complexity of drought tolerance mechanisms, efforts to minimize this ‘yield gap’ in drought prone

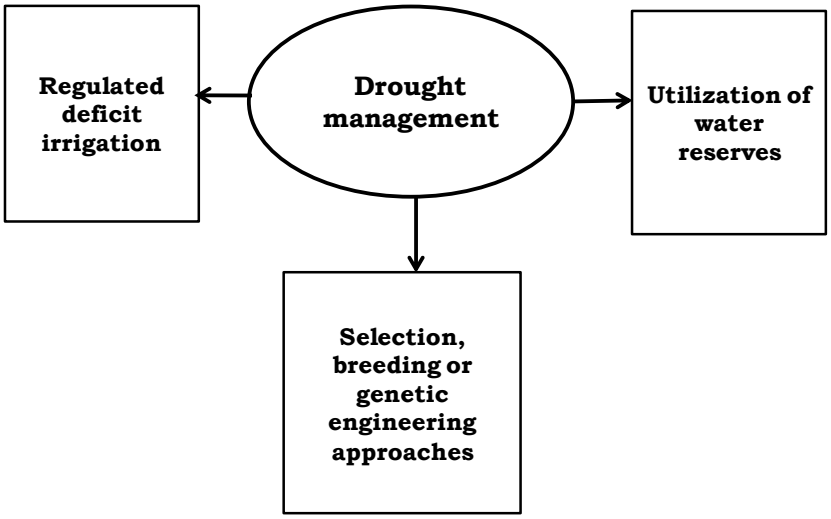

Fig 1. Options for improving crop performance under drought prone environments.

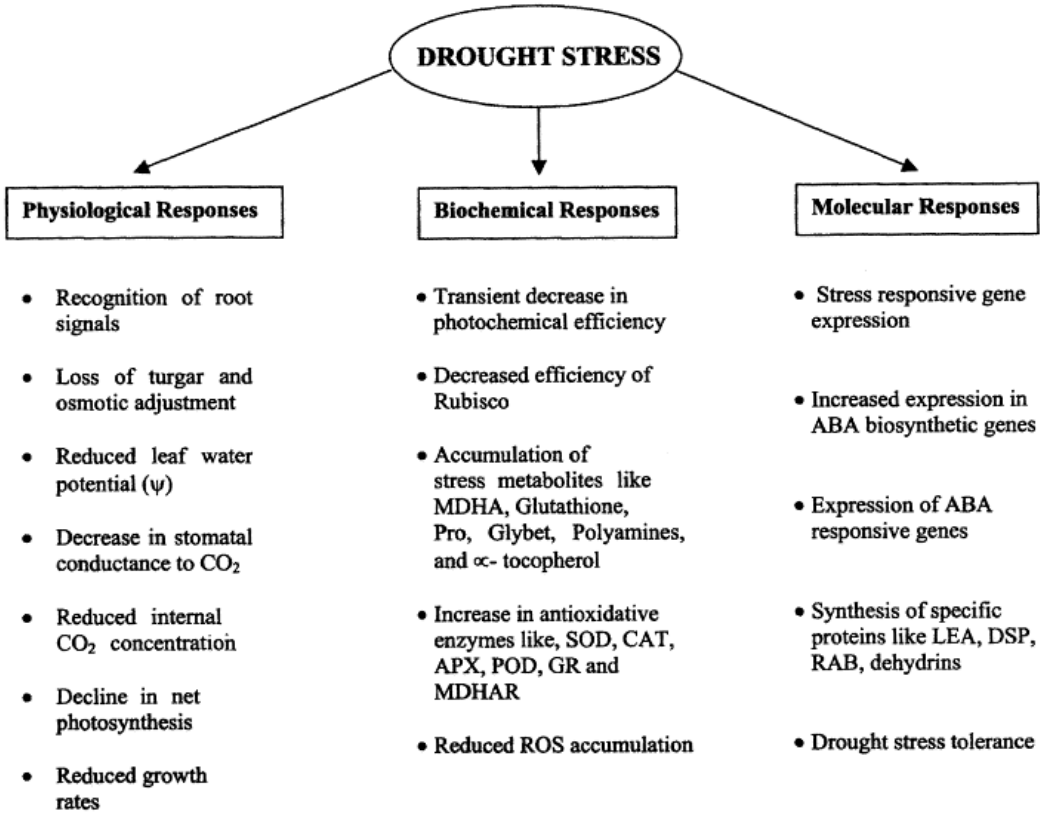

From: Reddy et al. (2004) J Plant Physiol.

Fig 2. General drought-induced physiological, biochemical and molecular responses of higher plants.

environments remained slower than expected. However, since last decade research on crop physiology and genomics have continuously provided crucial inputs towards drought tolerance mechanisms of important crop plants, which could prove highly beneficial and can be utilized by plant breeders for selection, breeding and consecutive crop improvement (Cattivalli et al. 2008). Also, studies on identification of morpho-physiological and metabolic traits, responsible for ensuring better adaptability and higher yield potential under drought stress showed that crop performance under drought could be described as a function of single physiological trait. For example, higher photosynthetic rate or stomatal conductance could be positively correlated to higher yield and better adaptability under water deficit conditions. Also, it was observed that during drought stress, plants maintain soil water absorption and cell turgor pressure through various osmotic adjustments (OA) which were considered to be a key mechanisms in plants under drought and hence OA is considered as an effective selection criterion for drought tolerance (Serraj and Sinclair 2002). Further, identification of such important drought-tolerance traits of crop plants, through fundamental research will contribute significantly towards crop improvement in water limited regimes through breeding or genetic engineering approaches by providing more number of selection criteria.

Drought-induced responses of higher plants

Drought-induced plant responses vary considerably from plant to plant as well as from cellular to whole plant level, depending upon the stress intensity and duration and also the plant genotype and its developmental stage (Farooq et al. 2009). Upon drought perception, plants continuously try to modulate their growth and physiology in order to survive and adapt accordingly and such plasticity in plant response during drought stress is highly essential for conferring drought-tolerance. In general, the first visible drought-induced response in plants is the rapid inhibition of shoot and to a lesser extent root growth, as an increased root to shoot ratio usually help plants to tolerate water deficit conditions.

During drought conditions, the initial physiological symptom is the partial or complete stomatal closure leading to reduced transpiration rate and a concomitant reduction in CO_2 uptake for photosynthesis. Though reduced transpiration rate due to stomatal closure, is considered as an adaptive measure to minimize water loss, reduction in CO_2 uptake leads to diminished leaf carbon fixation. However, as water stress directly inhibits cell division and expansion, total carbon uptake is also reduced due to growth inhibition at the whole plant level (Zhu 2001). Moreover, slower growth is considered to be an adaptive feature for plant survival during drought because it allows plants to divert photosynthates and energy towards production of protective molecules such as antioxidants and osmolytes to defend against drought stress and/or to maintain root growth to maximize water uptake, which were otherwise utilized for shoot growth (Zhu 2002, Chaves et al. 2003). It was shown that under water deficit conditions, the ability to accumulate (and later on remobilize) stem reserves is a beneficial characteristic of various species such as cereals and also some legumes, which help them to maintain their reproductive growth during drought (Blum et al. 1994). However, if drought condition continues further, it leads to interrupted reproductive development, premature leaf senescence, wilting, desiccation and finally death of the plant. A wide range of differential responses of plants to water deficit condition exist, depending upon plant species, growth stage, duration of water limitation and other cross reacting environmental restrains (Yordanov et al. 2000, Reddy et al. 2004, Tester and Bacic 2005, Umezawa et al. 2006, Bartels and Sunkar 2007, Shinozaki and Yamaguchi-shinozaki 2007, Blum 2009, Mittler and Blumwald 2010). A concise summary of various physiological, biochemical and molecular responses of plants under drought stress was given by Reddy et al. 2004 (**Fig. 2**).

There are different strategies adopted by plants to maintain water status and tolerate drought conditions. Under gradually developing water deficit conditions, plants escape dehydration by shortening their life cycle. However, in case of rapid dehydration, photosynthetic machinery is primarily targeted by the induced oxidative stress in the form

of high levels of reactive oxygen species (ROS) (Miller et al. 2008). Under such adverse conditions, the capacity for metabolic protection either constitutive or induced, against the damaging effects of ROS and energy dissipation through chlorophyll (Chl) *a* fluorescence or non-photochemical quenching (NPQ) are the key elements for determining plant survivability under drought conditions (Flexas and Medrano 2002, Foyer and Noctor 2003). Plant's phenotypic plasticity during drought stress which is the capacity of a given plant to alter its physiology and morphology, decides the type of strategy (escape, avoidance or resistance) to be followed for tolerating the drought period (**Fig. 3**). In drought escape, the plant tries to complete its life cycle before the onset of drought. In India, due to erratic monsoons, drought escape strategy could not be targeted by plant breeders for developing tolerant varieties. The other two strategies include 1) drought avoidance; where plants maintain the tissue water potential through enhanced water uptake by efficient root system, stomatal control of transpirational water loss and increased water use efficiency and 2) drought resistance, where plants maintain the turgor through various osmotic adjustments (Bhattacharya and Rajam 2006, Pujni et al. 2007). The latter two strategies were found to be useful for breeding programs in India.

It is now evident that during moderate (sub-lethal) drought conditions, plants use strategies to conserve water by reducing transpiration and exploring enlarged soil volumes to maintain water supply. These strategies include partial stomatal closure, slower shoot growth and enhanced root growth. These responses are coordinated and form parts of a drought avoidance strategy which allow plants to tolerate transient periods of drought and also to survive more severe and persistent drought conditions by premature flowering and reproduction. At cellular level, cell division is reduced and cell expansion is either maintained or decreased, depending upon the level of ABA as well as other factors involved in coordination of the drought responses, mediated maintenance of turgor and cell wall extensibility (Valliyodan and Nguyen 2006). However, it is not necessary that each individual response and the additive effect of several responses lead to drought tolerance.

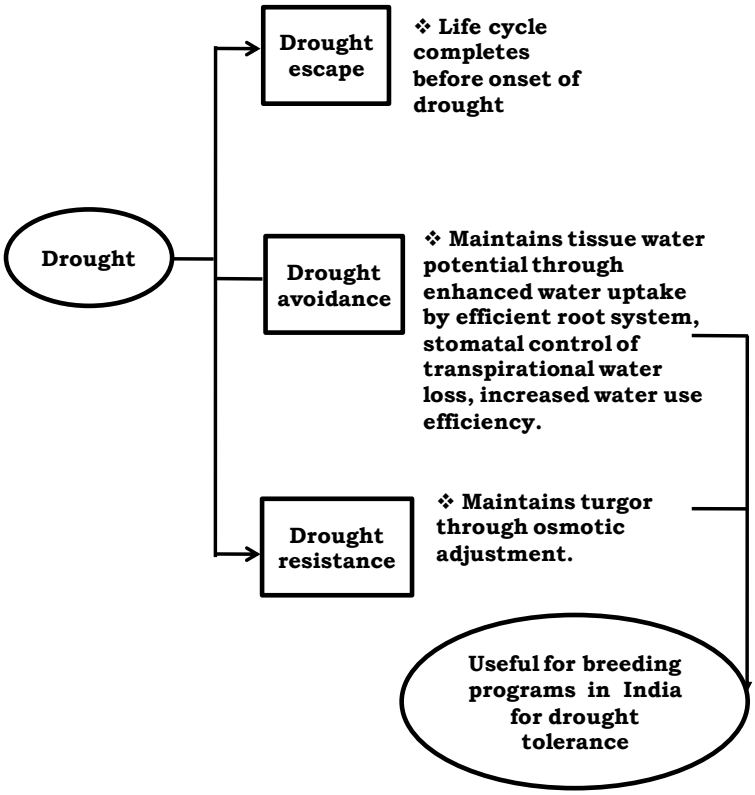

Fig 3. Major strategies adopted by plants for tolerating drought conditions.

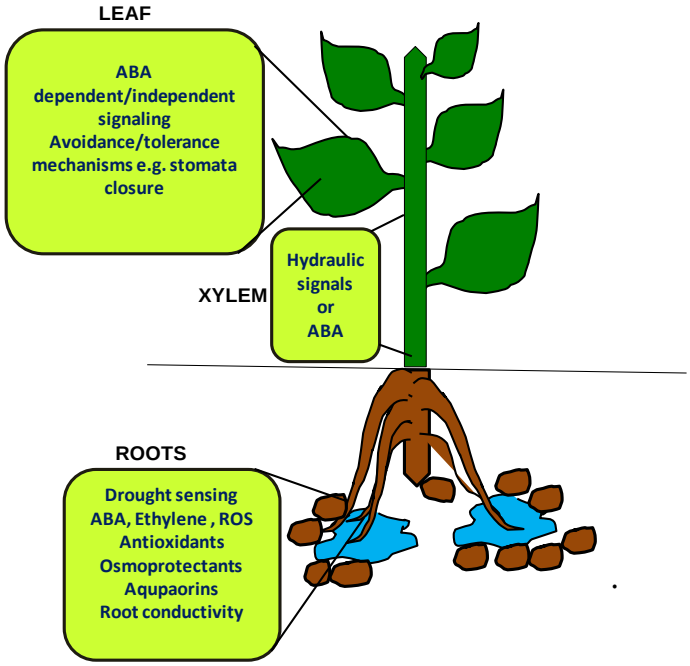

Fig 4. Plant responses during drought stress. Roots senses the declining soil water potential and along with ROS generation gives various responses including ABA and ethylene biosynthesis., antioxidant activities, osmolyte accumulation, root hydraulic conductivity alterations and change in aquaporin expression patterns. Roots tranduces hydraulic or ABA mediated signals through xylem which finally results in plant physiological changes leading to avoidance/ tolerance strategies.

Therefore, to select a promising individual plant response as a target for improving drought tolerance remains highly difficult and requires continuous inputs from fundamental research (Tardieu 2012).

Importance of root system during drought

Drought is usually considered to be a root-borne stress as roots are the primary site of water uptake from soil and thus, importance of maintaining root growth to ensure optimum crop yields during drought stress, is highly important (Gewin 2010). Immediately following drought perception, roots respond through a number of physiological and biochemical adjustments, before transducing the stress signals to the shoot system where further drought avoidance/tolerance mechanisms occur. A diagrammatic representation of such integrated drought-induced plant reponses were illustrated in **Fig. 4**. During drought, soil drying occurs at different rates in different soil layers, as water depletes from the superficial layer quite rapidly when compared to the deeper soil zones. Thus, plants having the ability to develop deeper root system were comparatively more tolerant to drought, than plants having a superficial root growth (Alsina et al. 2011). In dry soils, the ability of a plant to modulate its root distribution towards an efficient water uptake by exploiting the deeper regions of the soil is an important mechanism to tolerate drought. Hence, traits such as deep rooting, root length density (RLD) and root distribution were considered as drought adaptive traits which could be targeted by plant breeders, as selection criteria for drought resistance (Matsui and Singh 2003, Taiz and Zeiger 2006). Deeper root penetration in response to water deficit conditions has been found in cowpea (Matsui and Singh 2003), white clover (Annicchiarico and Piano 2004) and chickpea (Kashiwagi et al. 2006). However, it was observed that root distribution was not significantly affected by drought conditions in soya bean (Benjamin and Nielsen 2006).

Though, it is well established that extensive root systems are vital for plants to cope up with insufficient supplies of water or nutrients. In order to develop drought tolerant crops, it is of prime importance to obtain information regarding various root responses under water deficit conditions, as apart from plant genetic control over root proliferation during drought, the physical, chemical and biological properties of soil also determines the pattern of root growth. Especially during drought stress, physical impedance to root growth is quite significant and needs to be well understood. Owing to the growing importance of root-based information, a significant portion of drought stress research is now diverted towards understanding various root responses during drought conditions. Different informative reviews on root responses have covered various aspects of root morpho-physiological and molecular modulations including root to shoot signaling in response to drought stress (Schachtman and Goodger 2008, Bengough et al. 2011, Gowda et al. 2011). However, the area of "plant root responses" under drought conditions is extensively vast and varies from physiological, anatomical, morphological, biochemical to molecular levels. Hence, the topic is highly difficult to be covered under any single review. To give an idea about the recent developments in root responses under drought stress**,** we tried to consolidate last 5 year reports on various aspects of root response studies, under drought stress conditions in different plant species (**Table 1**).

Despite a considerable amount of work on root growth response, our basic understanding regarding what soil factors limits root growth, for what periods, and under which weather and associated soil water conditions still remains insufficient. It was observed that under water-deficit conditions, roots of drought-tolerant plant varieties continue to grow, whereas the growth of the shoot and leaves are inhibited. This leads to increased root: shoot ratio which as already mentioned, is an important mechanism of plant adaptation to water-deficit conditions and it is important to identify the underlying factors which confers such adaptive responses. Recently, various proteomic-based investigations have been carried out in different crop species to unveil such contributing factors (Yoshimura et al. 2008, Yamaguchi and Sharp 2010). Along with identification of regulatory elements for root growth maintenance, understanding various chemical signals

Table 1. Concise literature review on plant root responses under drought stress conditions of last five years, including plant species, developmental stage at which drought was induced, type of drought treatment followed, resulting plant water status and finally the observed root responses.

Plant	Growth stage	Drought treatment	Water status	Techniques used	Root response observed	Reference
Zea mays	10 day old Seedling	PEG solution for 8 h	-0.7 MPa	Comparative proteomics, RT-PCR	Significant induction of alcohol dehydrogenase 1, fructokinase, aquaporin PIP 2-5, serine /threonine protein kinase receptor, pathogenesis related protein 10 and small heat shock proteins.	Liu et al. 2013
Lotus japonicus	35 day old plants	5 days Water withholding	RWC declined from 88 to 59 %	Biochemical analysis of oxidative stress and antioxidants	Water stress induces a higher nitrosative stress in roots and more oxidative stress in the leaves of *L. japonicas*	Signorelli et al. 2013
Jatropha curcas	1 year old plants	Rainfed	Not mentioned	Root morphology observation and microscopic analysis	*J. curcas* follows a drought avoidance strategy under rainfed condition with a conservative root system	Krishnamurthy et al. 2012
Oryza sativa	Field grown seedlings	Field exp: seasonal drought Greenhous exp: water withholding.	Leaf water potential varied among genotypes	Root morphological, anatomical and aquporin expression analysis,	Drought resistant genotypes showed more stable bleeding rate (*Lp*r) with variation in soil moisture, more responsiveness of root anatomy to drought and higher quaporin expression levels, early in the day.	Henry et al. 2012
Cicer arietinum	4 week old seedlings	Water withholding for 2, 24, 48 and 72 h	Not mentioned	Transcriptomic analysis of oxylipins and biochemical estimation of jasmonates, ABA, aldehydes in roots.	Jasmonates play an important role in early signaling of chickpea roots during drought stress and subsequent tolerance.	De Domenico et al. 2012

Table 1 Contd.

Plant	Growth stage	Drought treatment	Water status	Techniques used	Root response observed	Reference
Arabidopsis thaliana	4 day old seedling	PEG treatment	-0.5 Mpa	Agrobacterium mediated transformation	. ABA modulates root adaptation to drought stress through up-regulation of miR393-targeted cleavage of auxin receptor transcripts.	Chen et al. 2012
Brassica napus	7 day old seedlings	1-7 days Water witholding	Not mentioned	Comparative proteomics	V-type H^+ ATPase, plasma membrane associated cation binding protein, HSP-90 and elongation factor (EF)-2 plays important role in drought tolerance of rapeseed.	Mohammadi et al. 2012a
Glycine max	3 day old seedlings	10 % PEG treatment or 4 days water withholding	Not mentioned	Comparative proteomics, qRT-PCR, Western Blotting	Roots are more responsive to drought stress than PEG treatment. Methionine synthase could be a target gene for developing drought tolerance in soybean.	Mohammadi et al 2012b
Triticum aestivum	Booting stage (shortly after flag leaf emergence)	50 to 60 % of the irrigation solution	Not mentioned	Various root morphological analyses	Root biomass was suggested to be a crucial character for drought resistance.	Ehdaie et al. 2012
Triticum aestivum	7 day old seedling	PEG treatment for 7 days	-0.976 Mpa	Biochemical analysis of different peroxidases and qRT-PCR	Abundance of two peroxidase sequences (TaPrx04 and TaPrx03) was enhanced in the apical root segments under osmotic stress and this correlated with the H_2O_2 levels.	Csiszár et al. 2012
Eucalyptus globulus	1 year old rooted cuttings	PEG treatment	-0.6 MPa	Phytohoromone (ABA and CK) analysis	ABA and pH dynamics can be seen in the short term response of *E. globulus*, where pH acts as an early signal and xylematic ABA becomes a later signal.	Granda et al. 2011

Table 1 Contd.

Plant	Growth stage	Drought treatment	Water status	Techniques used	Root response observed	Reference
Vitis berlandieri3V. rupestris	13 year old vines	Field experiment (seasonal drought)	-0.99MPa	Root hydraulic conductance analysis	Drought-tolerant root system had an enhanced ability to produce roots during summer drought and increased root water conductance (kr).	Alsina et al. 2011
Zea mays	Seedling (2^{nd} leaf fully expanded)	PEG treatment 6 h	-0.1 MPa	Comparative proteomics	Identification of candidate proteins (regulatory, ROS scavenging and detoxifying, energy production and metabolism) associated with drought stress.	Hu et al. 2011
Arachis hypogaea	Preflowering	25 days Water witholding	Not mentioned	Root growth and morphological analysis	Root dry weight and root length density (RLD) plays important role in pod yield under pre flowering drought stress in *A. hypogeae*.	Jongrungklang et al. 2011
Quercus pubescens	1 year old seedlings	14 days water witholding	Leaf RWC decreased by 75%	Analysis of rootmorphometric traits	Morphological adjustment in the fine roots plays a key role in the acclimation process to drought in *Q. pubescens*.	Di Iorio et al. 2011
Oryza sativa	4 weeks after transplantation	72 to 82 days after sowing	soil moisture 42 to 53 %	Root morphological analyses	Genetic differences in root architecture and deep root growth among genotypes in response to drought in lowland rice. Variation for lateral root production under both drought stress and non stress conditions.	Henry et al. 2011
Nicotiana tabacum	6 week old plants	1-6 days Water witholding	Leaf RWC declined from 87 to 61 %	Biochemical analysis and qRT-PCR	Free proline concentration, P5CS A gene expression was significantly higher in leaves compared to roots under drought. During 24-h recovery from drought, P5CS A and PDH transcript levels reached control levels in roots, but not in leaves. ABA content was highest in upper leaves and the lowest in roots.	Dobrá et al. 2011

Table 1 Contd.

Plant	Growth stage	Drought treatment	Water status	Techniques used	Root response observed	Reference
Kentucky bluegrass	60 day old plants	5 days Water witholding	Leaf RWC declined from 95 to 68 %	Biochemical analysis and RT-PCR	Drought stress caused ROS production and lipid peroxidation of roots in Kentucky bluegrass. The differential responses of ROS production, antioxidant enzyme activities and gene expression in response to drought stress between leaves and roots.	Bian and Jiang 2009
Zea mays	6 visible leaf stage	20 to 60 h Water witholding	Leaf RWC declined from 85 to 65 %	cDNA library construction, EST clustering and sequence analysis	Identification of candidate genes up-regulated in response to drought stress in maize roots. .	Hui-Yong et al. 2009
Quercus rubra	Seedlings	27 to 71 days Irrigation witholding	-0.9 MPa / -1.8 MPa	Physiological analysis	Large initial root system size does not confer drought avoidance in bareroot northern red oak seedlings. Greater growth allocation to roots relative to shoots, increased root growth and stomatal regulation are effective mechanisms of drought tolerance in oak.	Jacobs et al. 2009
Oryza sativa	Seedlings	4 weeks Water witholding	8-10 % soil moisture content	Physiological and root morphological fractal analysis	Fractal values decreased indicating lesser exploration of the soil by whole root system. Fractal values significantly correlated with the total root length that represents root system size in respective genotypes.	Wang et al. 2009
Vitis vinifers	3 months old plants	8 days Water withholding	Ψ_{stem} -0.5 to -1.15 MPa	Root hydraulic conductance analysis, qRT-PCR and immunolocalization.	Root water transport is closely coupled to shoot transpiration. Aquaporins are important contributors to the overall hydraulic conductance of the root system.	Vandeleur et al. 2009

Table 1 Contd.

Plant	Growth stage	Drought treatment	Water status	Techniques used	Root response observed	Reference
Cicer arietinum	7 days after emergence (DAE)	Gradual water drainage to maintain soil moisture at 1/3 of available water for 40 DAE.	Leaf RWC declined from 95 to 65 %	Physiological measurements including transpiration analysis, plant water staus, soil moisture content and root dry weight estimations.	Peanut genotypes with larger root systems maintained high transpiration efficiencies (TE) under drought conditions. It was demonstrated that root dry weight is an important trait related to TE during early season drought. RDW should be useful as selection criteria for drought-tolerance.	Puangbut et al. 2009
Triticum durum	Seedlings	20 % PEG 4000 treatment	-0.5 MPa	Biochemical analysis of cell wall polysaccharides of roots	Amount of side chains of rhamnogalacturonans I and/or rhamnogalacturonans II significantly increased in response to water stress in roots of drought tolerant cultivar of wheat.	Leucci et al. 2008
Arachis hypogaea	14 day after sowing (DAS)	28-35 DAS Water witholding	2/3 and 1/3 of available soil water (AW)	Root growth and morphological analysis	Smaller reductions in pod yield and harvest index were related to the increased root distribution into deeper soil regions, especially under 1/3 AW.	Songsri et al.2008
Norway Spruce	Mature 140 year old trees	Plot study: Rainfall exclusion usingplastic roof panel for a period of 45 days	Soil metric potential declined from -300 hPa to -500 hPa (approx)	Quantitaive analysis of fine root dynamics including fine root biomass, necromass, turn over and decomposition during drought period.	Drought leads to a decrease in root necromass decomposition rate and hence delayscarbon and nutrient transfer from dead roots to soil. Drought-induced increase in fine root turnover reduces above ground productivity of Spruce.	Gaul et al. 2008

which are synthesized in the roots in response to water stress, and the consecutive root-to-shoot signaling is also highly important for targeting crop improvement under drought stress. Among these signals, phytohormones are one of the important controllers of plant metabolism under limited water availability (Weyers and Paterson 2001) and such phytohormone-mediated developmental as well as root system plasticity could provide benefits through growth and architectural alterations, finally leading to an optimized response against drought. In root to shoot signaling, abscisic acid (ABA), cytokinins and ethylene are the major phytohormones which play an active role in drought-induced plant response and ROS is known to mediate this long distance signaling through hormones (Lake et al. 2002). It has been shown that increased cytokinin concentration in the xylem sap promotes stomatal opening directly and decreases stomatal sensitivity to ABA. Importance of ABA during drought stress has been extensively reviewed including its biosynthesis, compartmentalization within the cell and tissue, its modulation by various factors and also co-ordination of the responses at the whole plant level (Hartung et al. 2002, Wilkinson and Davies 2002). Such information has enabled us to understand how some plants respond to soil drying, sometimes even without significant changes in the shoot water status as evident in the case of 'isohydric' plants where they are able to buffer their leaf water potential by controlling stomatal aperture via root-shoot communication through feed-forward mechanisms (Maseda and Fernández 2006).

Discussion on root functionality under drought conditions will remain incomplete without mentioning the importance of root hydraulic conductivity (L_{p_r}) and plant aquaporins. L_{p_r} is a measure of the efficiency of bulk water flow through the root system and can be defined as flow rate per unit pressure driving force and is strongly influenced by soil water fluctuations and aquaporins, which play a major role in water transport across membranes, being the proteinaceous water channels. Thus, both L_{p_r} and aquaporin activities must be highly crucial during water-deficit conditions.

Root hydraulic conductance and role of aquaporins during drought

Along with reduction in stomatal conductance, soil water deficit limits Lp_r as well, which compromises the overall plant water status. Though mechanisms underlying stomatal conductance under drought is quite well characterized, factors responsible for changes in Lp_r still remains unknown (Mahdieh et al. 2008). Usually, hydraulic conductance of roots is highly variable in both time and space, affecting soil water extraction and consecutively shoot water status (Steudle 2000) and during drought stress, changes in Lp_r depend on intensity and duration of stress as well as plant genotype (Siemens and Zwiazeck 2004). It was suggested that variation in root hydraulic conductivity could be related to root anatomy as radial movement of water towards the xylem usually follows three pathways: the apoplastic, symplastic, and transcellular. Due to close similarity, sometimes the symplastic and transcellular pathways are together called as the cell-to-cell pathway (Steudle 2000). The apoplastic water flow can be irreversibly altered by several anatomical changes such as casparian bands and suberin lamellae whereas; the conductance of the cell-to-cell pathway is highly dependent on the activity of aquaporins (Mahdieh et al. 2008). Water conducting pathways through roots were illustrated graphically in **Fig. 5**.

Aquaporins are small integral tetrameric membrane proteins, belonging to the family of major intrinsic proteins (MIPs) and are known to facilitate permeation of water across membranes, driven by water potential gradient (Maurel et al. 2008). Apart from its usual role of water conductance, aquaporins are also known to mediate the transport of small non charged molecules, including glycerol, urea CO_2, formaldehyde, silica and boron and also considered as a putative osmotic stress or turgor sensor in plants (Mahdieh et al. 2008). Plant aquaporins have been classified into four subfamilies based on amino acid sequence comparison which includes plasma membrane intrinsic proteins (PIPs), tonoplast intrinsic proteins (TIPs), NOD-26 like intrinsic proteins (NIPs) and small basic intrinsic proteins (SIPs). PIPs were then further divided into PIP1 and PIP2 isoforms, based on sequence homology. However, not all aquaporins show significant increase in water conductance

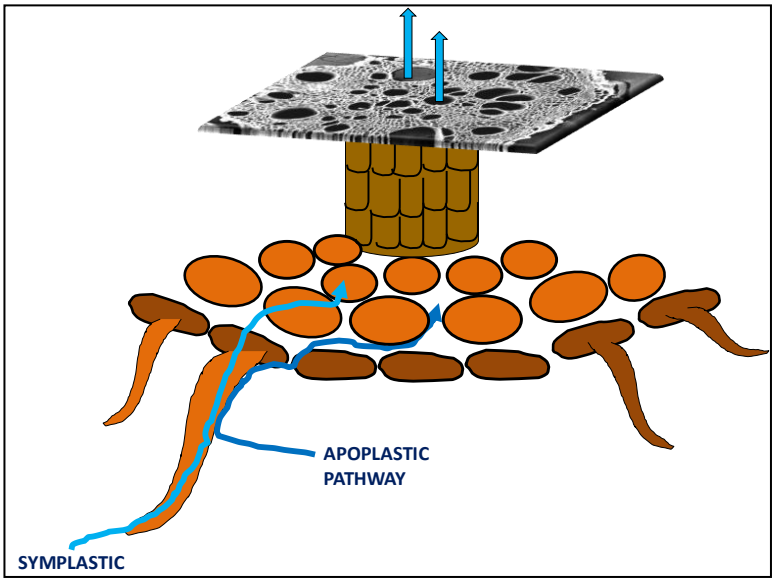

Fig 5. Root hydraulic conductivity. Diagrammatic representation of a root cross section showing cell to cell symplastic and the extracellular apoplastic routes of water conductance.

during drought stress. Water deficiency is assumed to evoke transcriptional and post-translational regulation of aquaporin activity, as it has been shown that aquaporin activity is regulated by phosphorylation (Luu and Maurel 2005). However, functional role of aquaporins in plants during drought stress has not been completely understood yet. In transgenic tobacco plants, the overexpression of AtPIP-1 from *Arabidopsis thaliana,* increased the growth rate of the plant during non stress conditions but, contrastingly under drought, the transgenic tobacco plants wilted faster when compared to wild types (Aharon et al. 2003). However, complete reverse was observed by knocking down the NtAQP1 (*Nicotiana tabacum* aquaporin 1) gene using NtAQP1 antisense constructs, wherein transgenic tobacco plants (sileneced NtAQP1) became more susceptible to water stress (Siefritz et al. 2002).

It is clear from the above discussion that crop performance under drought stress conditions is closely related to root system modulations, root to shoot signaling and changes in Lp_r. Now, among different food crops, grain legumes are highly renowned for

their nutritional values and agricultural importance as nitrogen-fixing 'rotational crop'. However, their productivity is usually low, since they are majorly grown under adverse soil and climatic conditions. So, now we will narrow down our discussion on drought-induced responses of food legumes with special emphasis on roots as it was reported that drought-tolerance of food legume species is also closely related to root system distribution and rooting patterns in the soil (Gaur et al. 2008). Hence, knowledge of root characteristics and genotypic variations within each species, under drought stress is essential to select suitable crop species to be grown in a particular environment.

Effect of drought on legume roots

Analyses of drought-induced responses in legume roots deserves separate discussion as apart from Lp_r and other morpho-physiological traits for drought tolerance, legume roots are also considerably significant owing to their distinct metabolic ability to fix atmospheric nitrogen. However, due to this specific ability of symbiotic association with soil bacteria, research on legume root responses during drought stress becomes an interesting as well as complex area of stress biology research since it requires understanding of nodule responses along with whole root response. As expected, various reports on legume root response during drought indicated a wide range of differential response patterns which varies within species, stress intensity and developmental stage of the plant. Based on rooting characteristics, Benjamin and Nielsen (2006) reported that chickpea and field pea are better suited to dryland cropping systems in the semi-arid western United States when compared to soybean. It was shown that both species have a greater portion of their root systems deeper in the soil than soybean and they respond to water stress by shifting their roots to deeper soil layers. Analyses of soluble protein composition of primary roots of soybean during drought stress suggested that under well watered conditions, the region of the root which exhibited maximum elongation showed a progressive deceleration of growth during drought conditions, even though the elongation rates of apical region remained same. They also observed an increase in isoflavonoid biosynthetic enzymes in the root apical regions and up-regulation of proteins involved in lignin biosynthesis which

were considered to have some role in growth inhibition, especially in the elongation region of roots under drought stress conditions. Several proteins involved in growth maintenance, inhibition, and protection against oxidative damage and protein degradation were identified that were translocated to different regions of the root under water stress (Yamaguchi et al. 2010).

Drought also affects the process of symbiotic nitrogen fixation and nodule formation in legumes. Thus, it is equally important to look into the nodular changes under water deficit conditions. Root nodule proteome of the model legume, *Medicago truncatula* in response to drought stress was reported along with an insight on the associated bacteroid proteome. Overall decrease in nodule metabolism was observed with down-regulation of proteins including methionine synthase, asparagine synthase, sucrose synthase, and leghemoglobin which controls the internal oxygen concentration within the nodule, in response to drought stress. It has been reported that isoforms of sucrose synthase are strongly induced in root nodules, and the reduction of enzymatic activity is associated with significant inhibition of symbiotic nitrogen fixation. Though most of the proteins declined significantly at approximately three days of drought stress treatment, there was only 30 % reduction in the corresponding nitrogen fixation (Larrainzar et al. 2007, Larrainzar et al. 2009). In another study on *Phaseolus vulgaris* (common bean) roots, twenty early- and four late dehydration-responsive genes were identified in response to drought stress. Among the identified genes, 14 encoded proteins had functions related to drought stress response and tolerance capacity. Analysis of the expression patterns of these genes opens interesting perspectives to understand the functional role of these genes in *P. vulgaris* roots and their subsequent involvement in drought response and tolerance mechanisms (Torres et al. 2006).

Importance of identifying root traits for drought avoidance is now well recognized and a considerable amount of work has been dedicated towards unraveling such root based mechanisms in food legumes during drought stress. However, many aspects of varying root responses in different economically important food legumes, which are usually grown under rainfed conditions are yet to be explored.

Impact of drought on mungbean cultivation

In the Indian agricultural system, food legumes (pulses) constitute an important segment immediately following cereals and oilseeds. Apart from being an excellent source of high quality protein, essential amino and fatty acids, fibres, minerals and vitamins, they also enrich soil fertility by compensating up to 80% of the soil nitrogen requirement through symbiotic fixation of atmospheric nitrogen. Moreover, intercropping of pulses between two cereal crops provides substantial amount of residual nitrogen and organic matter for the latter. Among the major pulse producing countries of the world, India ranks first followed by China, Brazil, Canada, Myanmar and Australia.

Mungbean (*Vigna radiata* L. Wilczek) has number of synonyms including mung, moong and greengram in India and mungo in the Phillippines, is a leguminous pulse crop which is highly recognized for its seeds which are high in protein, easily digested and consumed as food. As other legumes, in a symbiotic relationship with specific soil rhizobia, root nodules develop on mungbeans in which atmospheric nitrogen is converted to biologically available forms. Mungbean is known to be native of the Northeastern India-Burma region of Asia. Though, its progenitor species is unknown, the closest wild relative is believed to be *Vigna radiata* var. *sublobata* (Roxburgh) Verdcourt, which are widely distributed in Western Ghats andsporadic distribution in Rajasthan, Madhya Pradesh and NorthWestern Himalayas (Bisht et al. 2005). Mungbean is cultivated most extensively in the India-Burma-Thailand region of Southeastern Asia, but it is also grown in Iran, Pakistan, Vietnam, Peoples Republic of China, the Philippines, Republic of China, Malaysia, Indonesia, and adjacent countries and islands of south eastern Asia and the South Pacific. It is a short season crop adapted to multiple cropping systems in the drier and warmer climates of the lowland tropics and subtropics. Flowering in mungbean is photoperiod and temperature sensitive which is known to be delayed by long photoperiods and low temperatures and it grows best on a deep loam or sandy soil. Economic yields are frequently low due to disease and insect damage, low genetic yield potential of the varieties grown, unfavorable cultural practices or a combination of these factors.

Apart from its high protein-rich seeds which are used as human food, mungbean plant can also be utilized as fodder for livestock, or the crop may be incorporated into the soil for soil improvement purposes. Among pulses, mungbean is favored for children and older people due to its easy digestibility and low production of flatulence. Protein content of seeds averages around 22 to 24 %. Mungbean protein is comparatively rich in lysine, an amino acid deficient in cereal grains and deficient in methionine and cystine. A diet combining mungbeans and cereal grains compensates for the deficiencies in protein quality found in either grain alone and provides balanced amino acid content. Despite its multiple benefits, mungbean is given lower priority than the cereals in allocation of irrigation water or fertilizer, and cultural practices are inferior to those used with the staple cereals in spite of its economic and agricultural importance. Research on mungbean was also neglected in the past, but has expanded rapidly in the past 10 to 15 years (Kim et al. 2004, Oo et al. 2005, Webber et al. 2006, Song et al. 2007, Ranawake et al. 2011, Mahmoodian et al. 2012).

Mungbean (*Vigna radiata* L. Wilczek) is one of the important food legumes qualifying all the desired traits of an agriculturally and economically important crop. It is considered to be superior to other plants for second culture due to its shorter life cycle, nitrogen fixing capability, prevention of soil erosion and soil reinforcement. The yield of paddy in Punjab was enhanced by introducing mungbean in rice rotation (Weinberger 2003). Further, the seeds, sprouts and young pods of mungbean are consumed as source of protein, amino acid, vitamin and minerals while other plant parts are used as fodder or green manure. The production area of mungbean in the world is around 5.5 million ha[3] annually of which Asia alone contributes 90% of the total area and India is the biggest producer of mungbean where aroung 2.99 million ha[3] are cultivated. However, more than 87% of the area under pulse cultivation in India, is presently rainfed with annual rainfall of about 1000 mm. Mungbean is a warm season crop and adequate rainfall is highly essential, especially from flowering to late pod fill stage to in order to ensure good yield. It is reported that due to rapid expansion of drought-prone areas worldwide, mungbean production is highly affected as among other environmental restraints, limitation of water supply primarily

influences its yield (Ranawake et al. 2011). Soil water deficit inhibits vegetative growth, initiation and retention of floral buds as well as seed yield. As evident in rain-fed systems, plants experience cycles of water deficit rather than continuous drought. Thus, to have a proper understanding of stress responses of crop plants, analyses should be focused at different levels of stress intensity as well stress recovery rather than at a single stress treatment period.

OBJECTIVES

Based on the above background on drought-induced stress responses in crop plants and importance of root system during drought conditions, following four objectives were framed for the present research work:

1. **Analysis of progressive drought-induced changes in photosynthetic performance of *Vigna radiata* (L.)Wilczek.**

2. **Characterization of dynamic root protein modulation in response to progressive drought and recovery through comparative proteomics approaches.**

3. **Functional analyses of drought-induced ROS detoxifying NADPH -aldehyde reductase (VrALR) to understand its protective role in *V. radiata* roots.**

4. **Molecular characterization of key enzymes associated with proline and glutathione biosynthesis in *V. radiata* roots under progressive drought stress and recovery.**

PLANT MATERIAL AND EXPERIMENTAL DESIGN

Plant material

Cultivar Vamban-2 of *V. radiata* (L.) Wilczek was used for our experimental purpose which was procured from Tamil Nadu Agricultural University (TNAU), Coimbatore, India. It is a high yielding variety developed by National Pulse Research Centre (TNAU) at Vamban, Tamil Nadu by crossing two existing varieties, VGG4 and MH309. The new variety has registered a higher seed yield over other ruling varieties namely CO5, CO6 and vamban-1. It is a short duration crop (65-70 days) having moderate resistance to Yellow mosaic virus disease and pod borers. Lobed margins of the leaves are a distinct character of this variety **(Fig 6a, b).**

Experimental design

Seeds of *Vigna radiata* cv. vamban-2 were surface sterilized using 0.1 % sodium hypochlorite (15 min) and subsequently washed in running tap water for 5-6 times. Germination was carried out in pots (12 L cement pots filled with mixture of red soil and sand) inside in glasshouse, with an average of 15 seeds per pot at Botanical gardens of University of Hyderabad, Hyderabad. Pots were arranged in a completely randomized block design (CRBD) with three to eight replications, varying according to experimental requirement **(Fig 6c)**. Seedlings were grown for 30 days till they attained vegetative maturity to allow development of well established root systems in all the plants. During the complete growth period, pot water holding capacity (PC) was maintained at 80-90 % which was measured according to Ennahli and Earl (2005). Before planting, pot water holding capacity was determined by watering two similar volume pots in excess and then allowed to drain till constant weight (Saturated pot weight, W_S) was observed. Possibility of evaporative water loss was excluded by covering the soil surface with plastic cover. Thereafter, soil was dried at 80 °C in a hot air oven till constant weight was observed, which was considered as pot dry weight (W_D) and includes soil dry weight, pot weight and lid weight. PC was calculated as: (Current pot weight – W_D –W_P)/ (W_S – W_D) where W_P is the plant fresh weight which was measured by destructive harvest of roots and shoots of

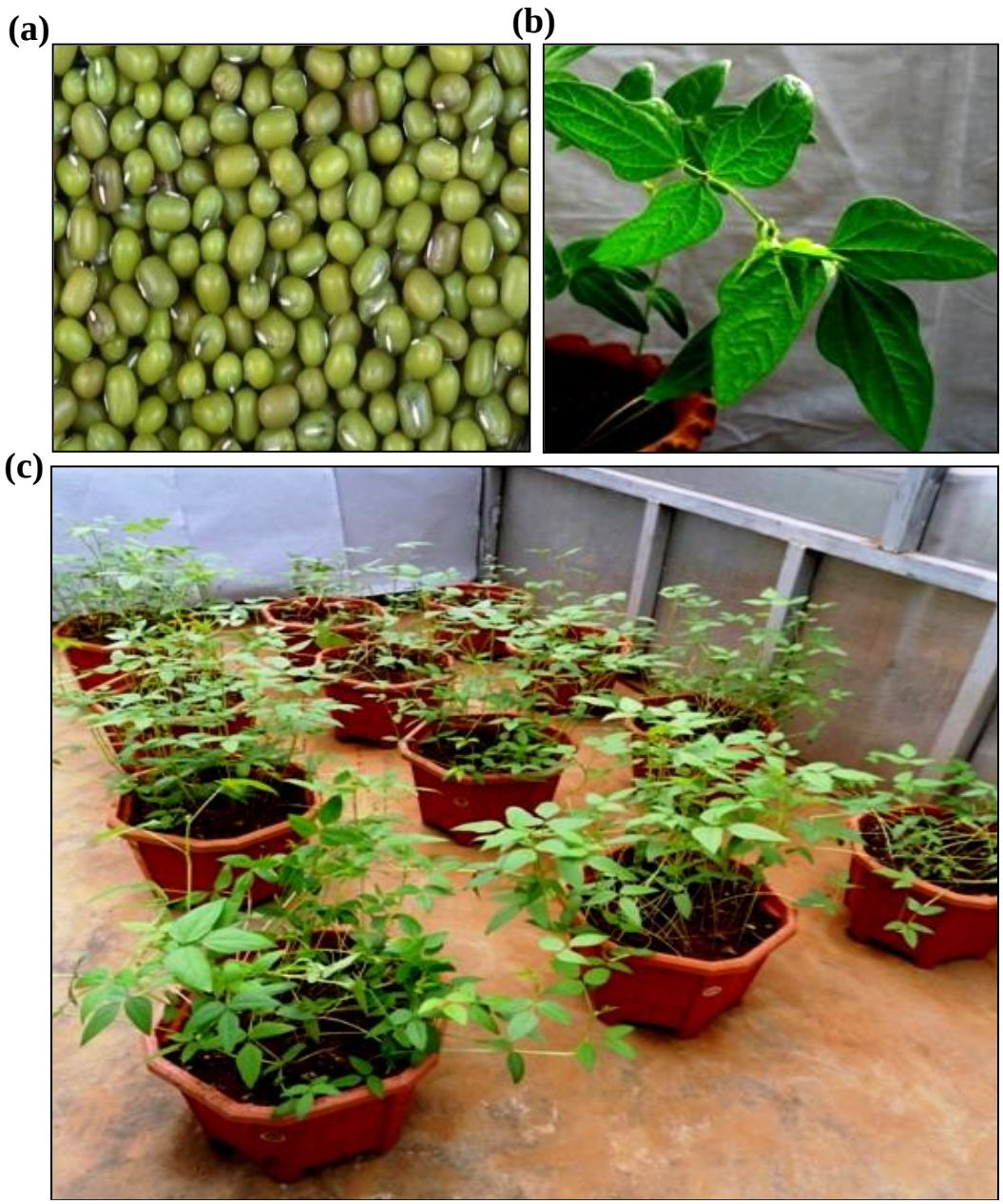

Fig 6. Seeds of *V. radiata* cv. vamban-2 (**a**), typical leaf morphology of vamban-2 cultivar of *V. radiata*, showing distinct lobed margins (**b**), completely randomized block design arrangement (CRBD) of pots inside glasshouse at University of Hyderabad Botanical garden (**c**).

three extra plants per experiment just before initiating drought stress treatment.

After 30 days, plants were subjected to two different watering treatments: well-watered (control) and water-stressed (drought). Control plants were maintained at PC of 80-90 % throughout the experiment and the stressed plants were subjected to progressive water stress by withholding of water for a period of three days (short-term, D3) and six days (long-term, D6) and then re-watered for the next six days for recovery (6R). As *V. radiata* is a nitrogen fixing plant, substantial dose of nitrogenous fertilizer was not applied. However, a meagre quantity (8 g) of standard slow release fertilizer (NPK) (10% N, 10% P, 14% K) was added to each pot in both the treatments only once during 15th day of the plant's vegetative growth. For all experiments, samples (whole roots) were collected from plants having similar morphology and leaf gas exchange characteristics during D3, D6 and 6R. All readings for the root growth and leaf gas exchange studies were done in fifteen replication (n=15). The photosynthetic photon flux density (PPFD) inside the glasshouse ranged from 900-1200 $\mu molm^{-2} s^{-1}$, air temperature varied from 23 ± 1 ºC (early morning) to 34 ± 4 ºC (early afternoon) and relative humidity ranged from 36 ± 5% to 48 ± 2%.

CHAPTER 2

Analysis of progressive drought-induced changes in photosynthetic performance of *Vigna radiata* (L.) Wilczek.

INTRODUCTION

Drought stress is primarily perceived by plant roots and its most conspicuous impact is on the photosynthesis process (Davies and Zhang 1991, Flexas and Medrano 2002, Reddy et al. 2004). Thus, it is equally important to understand both drought-induced root responses and factors affecting photosynthetic performance of crop plants. Available literature shows wide range of variations in drought-induced root responses (reviewed in **Table 1**) and photosynthetic physiology of plants under drought stress (Chaves et al. 2009, Chen et al. 2010, Sicher et al. 2012). However, studies involving a coherent insight on both root and leaf-level responses together under drought are quite rare. Moreover, with increasing evidences of dynamic root to shoot signaling including chemical and hydraulic signals during drought stress, investigating both root and shoot response is highly interesting as well as essential in order to have a comprehensive drought-response picture of crop plants (Schachtman and Goodger 2008). There were few interesting inputs from such integrated root-shoot research involving different abiotic stress factors including drought, in the recent past. Drought-induced modulation in the growth response sensitivity of root verses leaf with an insight on water transport mechanism was reported by Hsiao and Xu (2000). An integrated study on root morphology and photosynthetic performance of maize under low temperature stress was reported by Hund et al. (2007). A possible root to shoot communication in terms of internal CO_2 concentrations (C_i) and impact of aerated adventitious roots in flooded tomato plants on the physiological responses including stomatal closure and photosynthetic gas exchange patterns was reported in a recent study by Else et al. (2009).

Here, we will briefly describe the drought-induced changes in photosynthetic performance of crop plants along with the underlying stomatal as well as non-stomatal inhibitory factors and also the importance of root defense responses including antioxidant system and protective osmolytes during water deficit conditions.

Photosynthesis during drought: stomatal and non-stomatal limitations

Immediate drought-induced stress symptom in plants is the partial or complete stomatal closure, which is the primary cause of decreased net CO_2 assimilation or photosynthetic rate (P_n) due to reduced uptake of CO_2 (Yordanov et al. 2000). However, stomatal control of transpirational water loss by stomatal closure, during drought stress is an essential adaptive strategy to maintain plant water status. As a result, the rate of CO_2 fixation and stomatal conductance (g_s), declines almost parallel to each other during drought stress and hence, it was initially assumed that stomatal limitation to CO_2 conductance is the major factor responsible for decline in P_n. However, as more in-depth research was carried out, it was observed that stomatal limitations were not always the dominant factors responsible for decreased photosynthetic efficiency and thus, the concept of non-stomatal limitations developed which along with stomatal factors, may also play a dominant role in decreasing P_n during drought conditions. Non-stomatal limitation includes reduced carboxylation efficiency due to mesophyll resistance, non photochemical quenching or inhibited functional activity of PSII. Major factors responsible for decline in photosynthesis during drought stress, could be either stomatal, non-stomatal or both and differ from plant to plant. Some reports considered stomatal limitation to be the major factor contributing for decrease in P_n (Yin et al. 2005). While, in grapevine, decrease in P_n was found to be associated with decline in the effective quantum yield of PSII photochemistry and with increase in leaf to air vapour pressure deficit (Yu et al. 2009). Moreover, moderate to severe drought causes significant inhibition of Calvin cycle enzymes which was considered as metabolic impairment and act as non-stomatal limitation for photosynthetic CO_2 assimilation (Dias and Brüggemann 2007).

Importance of Photosystem II (PSII) efficiency during drought stress

Among various non-stomatal limitations, drought-induced injury to the photosynthetic apparatus due to generation of highly energetic ROS is one of the crucial factors inhibiting P_n. Though plants have developed efficient mechanisms such as consumption of the excess

energy *via* Mehler reaction and photorespiration, to protect the photosynthetic apparatus from drought-induced injury, severe drought stress still causes significant damage (Foyer and Noctor 2000, Valladares and Pearcy 2002, Foyer and Noctor 2003). However, tolerance capacity of the photosynthetic apparatus including PSII varies from plant to plant depending upon their respective drought-tolerance capacity and also on the existence of other alternative sinks for dissipating the excess energy. Thus, it is essential to assess the extent of damage to photosynthetic apparatus (PSI and PSII) during drought stress. Among the various analytical methods used to screen photosynthetic performance and stability of photosystems during abiotic stress conditions including drought, use of Chl fluorescence represent an efficient and reliable method owing to its non-destructive nature and high sensitivity (Naumann et al. 2007, Oukarroum et al. 2009). Moreover, with development of new fluorescence recording systems such as PAM (Pulse Amplitude Modulation)-fluorimeter and PEA (Plant Efficiency Analyzer)-fluorimeter, analyzing Chl *a* fluorescence for screening drought-induced damage to photosynthetic apparatus have become extensively convenient and time conserving.

There exists a strong correlation between Chl fluorescence and rate of photosynthetic electron transport (PET), as a part of the absorbed light energy by the photosynthetic pigments was used for photochemical reactions including PET and the rest was re-emitted as Chl a fluorescence or released as thermal dissipation (Non photochemical quenching, NPQ). It was found that most of the Chl fluorescence at room temperature was emitted by Chl *a* of PSII. Thus, changes in the fluorescence intensity (Chl fluorescence yield) indicate the degree of utilization of the absorbed energy by PSII and other complexes within the thylakoid membrane. Under normal (non-stress) conditions, maximum fluorescence (F_M) yield was observed when all reaction centres (RC) of PSII are "closed" or in a reduced state, while when all RC are "open" (oxidized state), minimum fluorescence yield (F_O) was recorded. Fluorescence emission kinetics constitute a transient or polyphasic increase in fluorescence intensity from initial (F_O) to the maximum (F_M), including the intermediate steps (fluorescence rise) and together theses phases were termed alphabetically as O, J, I

and P phases (OJIP curve). Since drought-induced damage to PSII will be depicted through deviation from the typical OJIP curve, analyzing fluorescence transients will provide significant information regarding PSII stability index during drought conditions (Strasser et al. 2010). Thus, the OJIP transient proves to be highly potential for the characterization of the photochemical quantum yield of PSII photochemistry, and the electron transport activity under normal as well as drought stress conditions.

Importance of root defense responses during drought stress: Antioxidant system and protective osmolytes

Immediately after drought perception through roots, accumulation of reactive oxygen species (ROS) in cells occurs due to disturbance in the delicate "oxidant-antioxidant" balance existing under normal physiological conditions (Apel and Hirt, 2004). Though ROS was found to be useful as second messengers in the stress signal transduction pathway, excessive ROS is able to cause significant damage by inducing oxidative stress to the photosynthetic apparatus and also impair normal cell functioning. Damaging consequences of ROS upon practically all important macromolecules *i.e* proteins, nucleic acids and lipids are well-characterized. Apart from proteolysis and protein oxidation, ROS can damage nucleic acids, lipids, terpenoids, and carbohydrates (Møller et al. 2007, Foyer and Noctor 2009). For proper metabolic functioning of the cells during drought stress, plants need to regain the redox homoeostasis and in order to do so, they respond through a number of interconnected morpho-physiological, biochemical and molecular alterations, which differ from plant to plant depending on their ability to either tolerate, adapt or succumb to the existing water-limiting conditions (Waseem et al. 2011). Among various plant defense responses, most efficient as well as predominant is the dynamic modulations in the enzymatic and non-enzymatic antioxidant pool. Non-enzymatic or low molecular-weight antioxidants are molecules that are able to reduce oxidants without themselves having significant pro-oxidant action. These include ascorbate, glutathione, tocopherols, carotenoids, flavonoids, and related phenylpropanoid derivatives. Among enzymatic antioxidants, there are three categories: proteins which act as primary antioxidative enzyme

(i.e., uses superoxide, H_2O_2 or organic peroxide as substrates) include superoxide dismutase (SOD), Catalase (CAT) and ascorbate peroxidase (APX). The second category consists of proteins that supply or maintain reductant which includes dehydroascorbate reductase (DHAR), glutathione reductase (GR) and glutaredoxins and thioredoxins, while the third category consists of enzymes which function to control secondarily released metabolite signals including glyoxylases, aldo-keto reductases and glutathione transferases (Foyer and Noctor 2009).

In addition to the antioxidative system, accumulation of compatible solutes such as proline and glycine betaine have been demonstrated to be involved in protection and/or repairing processes of some molecules and structures damaged by ROS and also in ROS sequestration (Møller et al. 2007). Thus osmotic adjustment (OA) has become one of the potentially important mechanisms of drought tolerance, which can be achieved from the accumulation of compatible solutes (such as amino acids, sugars or sugar alcohols) in protoplasm (Chaves et al. 2003, Bartels and Sunkar 2005). Additionally, OA allows cell enlargement and plant growth during severe drought stress and also helps stomata to remain partially open to facilitate CO_2 assimilation to continue during drought stress. Structural integrity of the membranes was also maintained through OA, in order to provide resistance against drought and cellular dehydration (Ramanjulu and Bartels 2002). One of the most important protective osmolyte is proline, which is considered as a multifunctional amino acid. Rapid accumulation of proline in various plant species in response to different types of abiotic stress factors including drought is quite well known. Apart from its osmoprotective role, it was known to be involved in maintaining cellular homeostasis, as a signaling molecule to modulate mitochondrial functions, role in cell proliferation or cell death and also it was known to contribute in triggering specific gene expression which was considered to be essential for plant recovery after stress conditions. However, regulation and actual mechanism behind proline accumulation in plants is not yet completely unraveled and requires further in-depth analysis for targeting proline metabolism in plants to improve their stress-tolerance index.

Though, a considerable amount of research was dedicated towards unraveling such defense responses of plants including antioxidants and protective osmolytes, under various abiotic stress factors including drought, majority of such studies were based on foliar responses with comparatively fewer reports on root antioxidative defense (Haberer et al. 2008, Selote and Khanna-Chopra 2010). However, in contrast the significance of studying root antioxidants for understanding the overall plant response to drought stress is quite higher, as the root tissue senses soil drought much prior to the leaves. Further, it is now well established from previous reports that photosynthesis is also directly and/or indirectly interlinked to the corresponding root metabolisms under drought stress (Zhao et al. 2001, Flexas and Medrano 2002, Wilkinson and Davies 2002). Since soil drought is considered to be a root-borne stress, any change in photosynthetic responses including stomatal conductance, PET, Chl *a* fluorescence or rate of CO_2 assimilation under drought stress could be directly or indirectly correlated to root-level alterations.

In the present chapter, we aim to understand the progressive drought-induced alterations in the photosynthetic gas exchange characteristics of mungbean with an insight on the contributing factors for the observed changes. We also look into the PSII efficiency of mungbean during progressive drought. Simultaneously, analysis of the pattern of response of important antioxidants (ascorbic acid; ASA, glutathione; GSH, guaiacol peroxidase; GPOX) and protective osmolyte (proline) in roots of *V. radiata* under progressive drought and recovery was investigated.

Plant water status

Plant water status was estimated in terms of its leaf relative water content (LRWC %) as well as leaf and root moisture contents (LMC and RMC %, respectively). For measuring LRWC %, fresh leaves from control and drought stressed groups were collected from three individual plants grown in three different pots and immediately weighed to get the leaf fresh weight (Lfw) value. Then leaves were immersed in double distilled water at 4°C for 24 hours for complete rehydration and weighed next day to obtain the leaf turgid weight (Ltw). Further, leaves were oven dried at 80 °C for 24 hours and weighed to give the leaf dry weight value (Ldw). From the above obtained values, LRWC was calculated as: LRWC (%) = [(Lfw-Ldw)/(Ltw-Ldw)] × 100 where, Lfw is leaf fresh weight, Ltw is the leaf turgid weight (obtained after rehydration of leaf samples in distilled water for 24 h) and Ldw is the leaf dry weight after oven drying (80 °C). Leaf moisture content (LMC %) was calculated as: LMC (%) = [(Lfw-Ldw)/ Lfw]. To obtain root moisture content, root fresh weight was taken immediately after harvest by washing the roots thoroughly to remove soil particles and then for obtaining root dry weight, roots were oven dried under similar conditions as for leaves and RMC % was calculated as: [Rfw-Rdw/Rfw] where Rfw is root fresh weight and Rdw is root dry weight.

Measurement of leaf gas exchange parameters

The rate of leaf gas exchange was measured using a portable infrared CO_2/H_2O gas analyzer, IRGA (LCpro-32 070, ADC Bioscientific Ltd., Great Amwell, U.K.) equipped with a broad leaf chamber (**Fig 7a**). Using the gas analyzer, photosynthetic rate or net CO_2 assimilation rate (P_n), stomatal conductance (g_s), transpiration rate (E) and internal CO_2 (sub-stomatal CO_2) concentration (C_i) were measured at a saturating photosynthetically active radiation (PAR) of 1800 µmol m^{-2} s^{-1}, 60 % air humidity inside leaf chamber, 360 µmol mol^{-1} CO_2 concentration and air temperature of 25 ± 2 °C. Measurements were recorded after 1-2 minutes of incubation time for leaf acclimation inside the chamber and stabilization of the observed readings. Instantaneous water use efficiency (WUE_i) was calculated as the ratio of P_n/E. All photosynthetic measurements were done in situ on clear sunny days, between 10:00 and 11:00AM. Fully expanded, non- detached and light exposed

young leaves (3^{rd}-4^{th} positions from the apex) were chosen for all photosynthetic measurements.

Photosystem II (PSII) efficiency

Chlorophyll *a* fluorescence was measured at room temperature on mature, intact leaves which were previously used for gas exchange studies, using a portable Handy PEA (Plant Efficiency Analyzer-2126) fluorimeter (Hansatech Instruments Ltd., kings Lynn Norfolk, UK) (**Fig 7b**). Tagged leaves were dark-adapted for 30 min using leaf-clips and the fluorescence intensities were recorded after illuminating with a saturating light intensity of 3000 μmol m^{-2} s^{-1} (an excitation intensity sufficient to ensure closure of all PSII reaction centers) provided by an array of three light emitting diodes, for 1s. Saturating light pulse-induced Chl *a* fluorescence was measured and digitized between 50 μs and 1s by the instrument. The fluorescence intensities at 50 μs (F_O), 150 μs(L), 300 μs (K), 2 ms (J), 30 ms (I) and 500 ms-1s (P or F_M) were recorded and used for all analyses. The different steps of the polyphasic fluorescence transient are labelled in alphabetical order from the slower to the faster part of the transient. The most prominent step at 2 ms is called the J-step. The fluorescence rise up to the J-step provides information about single turnover events of the primary reactions of photochemistry which includes primarily QA reduction. The different phases of this process show up in the fluorescence rise as the steps J, I and P. The step with the highest fluorescence intensity is called P (peak). In the single turnover range Fo (measured at 50 μs) to F_J (measured at 2 ms), the bands L (at about 100–200 μs) and K (at about 200–400 μs) can often be visualized by subtraction or by calculation of differences between fluorescence transients (Strasser et al. 2004). Analysis of Chl *a* fluorescence transients for O-K, O-J, O-I and I-P phases of *V.radiata* leaves under progressive drought and recovery was done by double normalization of variable fluorescence between phase O and K (F_O to F_K) from 50 μs to 300 μs [V_{OK}= (F_t-F_O)/ (F_K-F_O)] and the kinetic difference of V_{OK} (ΔV_{OK}) was calculated with respect to control (D0) to visualize the L-band. Similarly, double normalized variable fluorescence between phase O and J (F_O to F_J) from 50 μs to 2 ms [V_{OJ} = (F_t-F_O)/(F_J-F_O)] and its corresponding kinetic difference of V_{OJ} (ΔV_{OJ}) with

(a)

(b)

Fig 7. Portable infrared CO_2/H_2O gas analyzer, IRGA (LCpro-32 070, ADC Bioscientific Ltd., Great Amwell, UK used for all photosynthetic gas exchange measurements (**a**). Portable Handy PEA (Plant Efficiency Analyzer-2126) fluorimeter (Hansatech Instruments Ltd., kings Lynn Norfolk, UK used for chlorophyll *a* fluorescence measurements (**b**).

respect to D0 was calculated. Double normalized variable fluorescence between O and I [$V_{OI} = (F_t-F_O)/(F_I-F_O)$] between time interval of 50 µs to 30 ms ($V_{OI} < 1$); (F) variable fluorescence V_{OI} between time interval of 30 ms to 300 ms ($V_{OI} \geq 1$) was used to calculate the kinetic difference of V_{OI} (ΔV_{OI}) with respect to D0 and subsequently the variable fluorescence between I and P phases [$V_{IP} = (F_t-F_I)/(F_P-F_I)$] was done which showed a

hyperbolic curve and the kinetic difference of V_{IP} (ΔV_{IP}) was also calculated with respect to D0 values. Values are average of four independent replicates.

Measurement of chlorophyll pigments

Circular leaf discs of 1 cm^2 area were punched using a cork borer and used for pigments' extraction by following dimethyl sulpoxide (DMSO) method, described by Hiscox and Israelstam (1979) with minor modifications. Each individual leaf disc was kept in an eppendorf and 2 mL DMSO was added to each vial. Eppendorfs were kept at room temperature under dark conditions for 2 days. When leaf discs became visibly devoid of green pigment (after 2 days), supernatant was removed through centrifugation. Absorbance of the supernatant was measured at 663.2 and 646.8nm using UV-Visible 160A spectrophotometer (Shimadzu, Tokyo, Japan) and chlorophyll contents were calculated according to Lichtenthaler (1987) using the following formula and the results were expressed as µg cm^{-2} basis.

Chl *a* : $12.25 \times A_{663.2} - 2.79 \times A_{646.8}$

Chl *b*: $21.5 \times A_{646.8} - 5.1 \times A_{663.2}$

In-situ localization and quantification of hydrogen peroxide (H_2O_2)

For in-situ localization of H_2O_2, freshly harvested roots from control and stressed groups were submerged in 5 µM dichlorodihydrofluorescein diacetate (H_2DCF-DA) in 5 mM DMSO for 2 h in dark. Roots were then washed with 50 mM phosphate buffer (pH 7.4) twice and then subjected to microscopic analysis. Image acquisition was made on a confocal microscope ((Leica TCS SP2 AOBS Microscope, Germany, with a filter # 10) with excitation and emission wavelength of 475 and 520 nm, respectively.

Quantification of H_2O_2 was done according to the method described by Velikova et al. (2000) with minor modifications. Fresh roots (0.5g) were homogenized in 5 mL of 0.1% (w/v) trichloroacetic acid (TCA) at 4°C and the homogenate was centrifuged at 1200 *g* for

15 min. Supernatant was separated and a 0.5 mL aliquot was mixed with 0.5 mL of 10 mM potassium phosphate buffer (pH 7.0) and 1 mL of 1M potassium iodide (KI) solution. The absorbance of the supernatant was measured spectrophotometrically using a UV-Visible spectrophotometer (Shimadzu) at 390 nm. The actual H_2O_2 concentration in the root tissue was determined from the H_2O_2 standard graph prepared under similar conditions.

Determination of malondialdehyde (MDA) content (Lipid peroxidation assay)

Lipid peroxidation was estimated by determining the MDA content, a degradation product of peroxidized polyunsaturated fatty acids (PUFA) component of membrane lipids according to the method given by Fu and Huang (2001) with slight changes. Root tissue (200 mg) was homogenized in 2 mL of 0.1% TCA and the homogenate was centrifuged at 10,000*g* for 5 min at 4°C. An aliquot of 0.3 mL supernatant was mixed with 1.2 mL of 0.5 % thiobarbituric acid (TBA) prepared in 20% TCA, and incubated at 95°C for 30 min. Reaction was terminated by keeping the tubes in ice-bath for 5 min. Samples were then centrifuged at 10,000*g* for 10 min at 25 °C. The absorbance of the supernatant was measured at 532nm and was corrected for non specific absorbance at 600 nm. MDA concentration was determined using the extinction coefficient of MDA, 155 mM^{-1} cm^{-1} at 532 nm.

Estimation of free proline

Extraction and estimation of free proline were conducted according to Bates et al. (1973). Root tissue (0.5g) was homogenized in 10 mL of 3% (w/v) aqueous sulphosalicylic acid and centrifuged at 12000*g* for 30 min. The supernatant was further used for free proline estimation. From the supernatant, 2 mL aliquot was mixed with 2 mL of "acid ninhydrin" solution (acid ninhydrin solution was prepared freshly by dissolving 1.25 g ninhydrin in a mixture of 30 mL glacial acetic acid and 20 mL 6M orthophosphoric acid) and 2 mL of glacial acetic acid. The reaction mixture was then incubated at 100 °C for 1 h and reaction was terminated by placing the tubes on ice bath. Then, the red coloured free proline-acid

ninhydrin complex was extracted using 4 mL toluene and the chromophore phase was separated from the aqueous phase. Absorbance of the extracted organic phase was measured at 520 nm using a UV-Visible spectrophotometer. Concentration of free proline in the root tissue was calculated from the L-proline standard graph prepared under similar reaction conditions.

Estimation of ascorbic acid (ASA)

Ascorbic acid content in the roots of *V. radiata* was determined according to Mukherjee and Choudhuri (1983) with minor changes. Root tissue (100 mg) was homogenized in 10% trichloroacetic acid (TCA) solution (1:5 w/v) and centrifuged at 3500 rpm for 20 min. The supernatant was used to estimate ASA content. From the supernatant, 4 mL aliquot was mixed with 2 mL of a 2% solution of dinitrophenylhydrazine (DNPH) and then, a drop of 10 % thiourea solution in 70 % ethanol was added. The reaction mixture was boiled in water bath for 15 min and after cooling at room temperature, 5 mL of 80 % sulphuric acid (H_2SO_4) solution was added to the reaction mixture at 0 °C. Absorption of the reaction mixture containing the hydrazone complex was measured at 530 nm using a UV-Visible spectrophotometer. Exact ASA content in the root tissue was calculated from the ASA standard graph.

Guaiacol peroxidase (GPOX) assay

Guaiacol peroxidase activity was assayed in root tissue of *V. radiata* according to the method described by Zhang and Kirkham (1994) with minor modifications. Frozen root tissue (1 g) was homogenized in 50mM potassium phosphate buffer (pH 7.0, adjusted with KOH) and the homogenate was centrifuged at 15000*g* at 4°C for 30 min. The supernatant was used for the GPOX enzyme assay. The enzyme activity was assayed in a reaction mixture containing 60 mM phosphate buffer (pH 6.1), 28 µM guaiacol, 5µM H_2O_2 and 50 µg protein extract. Increase in absorbance at 470 nm due to oxidation of guaiacol was observed with respect to time. Enzyme activity was calculated as µmol guaiacol oxidized

min^{-1} mg^{-1} protein using extinction coefficient of guaiacol as 26.6 $mM^{-1}cm^{-1}$. Protein content was determined according to Bradford (1976).

Determination of oxidized and reduced glutathione (GSH-GSSG)

Oxidized and reduced glutathione was measured using a fluorometric method according to Hissin and Hilf (1976) with slight modifications. Root tissue (1 g) was homogenized in 25% H_3PO_3/ 0.1 M sodium phosphate EDTA buffer (pH 8.0) in 1:3 ratios (v/v), centrifuged for 30 min at 10,000*g* and the resulting clear supernatant was used for analysis of oxidized (GSSG) and reduced (GSH) glutathione content. For GSH, the supernatant was diluted further to 1:4 ratios with 0.1 M sodium phosphate EDTA (pH 8.0) buffer. From this diluted supernatant, 100 µL of sample was added to 1.8 mL of phosphate-EDTA buffer and 100 µL of O-phthalaldehyde (OPT) from a 1 mg mL^{-1} stock to make a final reaction mixture of 2 mL. Reaction mixture was thoroughly mixed and incubated at room temperature for 15 min. Fluoroscence was measured at 420 nm after 350 nm excitation using a Hitachi spectrofluorimeter F-3010. For estimating GSSG, 500 µl supernatant was incubated with 200 µL of 0.04M N-ethyl maleimide for 30 min in order to block all the reduced GSH present. After incubation, the final volume of the mixture was made up to 5 mL by adding 4.3 ml of 0.1 N NaOH. A 100µL aliquot from the above mixture was then added to 1.8 ml of 0.1N NaOH and 100 µL OPT to make the final reaction mixture which was further analysed similar to GSH assay as described above.

Statistical analysis

All data on physiological (LRWC, LMC, RMC and leaf gas exchange) and biochemical (H_2O_2, MDA, Proline, ASA, GPOX and GSH) measurements are represented as mean ± standard deviations (n = 5). For Chl *a* fluorescence, measurements were taken in 4 replications and a single leaf per plant constituted each replicate. All fluorescence data were analyzed using the software Biolyzer versions vl 30-31 and SigmaPlot 11.0. One way ANOVA and Tukey test were used to determine the significant difference.

RESULTS

Changes in plant water status

Progressive water-deficit affected the overall plant water status. Leaf relative water content decreased from 80 % (D0) to 69 and 56 % during D3 and D6, respectively while upon recovery, LRWC regained to 74 %. Leaf moisture content also declined gradually from 86% during D0 to 70% during D6 and again increased to 85% during 6R. Similarly in roots, RMC % dropped from 93 to 65 % with progressive water deficit but increased to 87% upon re-watering (6R) (Table 2). One way ANOVA showed significant time by treatment ($T \times T_m$) interactions for LMC, LRWC and RMC %. Regression analysis between LRWC and RMC % showed a linear and positive correlation with each other with a R^2 value of 0.912 **(Fig. 8**).

Photosynthetic performance: Leaf gas exchange characteristics

Changes in leaf gas exchange parameters and the level of photosynthetic pigments recorded during progressive drought and recovery were presented in **Fig 9.** P_n declined significantly by 54 and 74 % during D3 and D6, respectively (from 6.08 to 2.8 and 1.6 $\mu molm^{-2}s^{-1}$on D3 and D6, respectively) and upon 6 days re-watering treatment for recovery, P_n recovered significantly (67% increase when compared to D6) (**Fig 9a**). A similar concomitant decline in g_s was observed, where it declined by 59 % during D3 and 80% during D6 and upon recovery, stomatal conductance increased by 77 % when compared to D6 (**Fig 9b**). We also observed a significant reduction in transpiration rate (E), which declined by 66 % during D3 and 87% during D6 and recovered significantly by showing 77% increase during 6R when compared to D6 (**Fig 9c**). Though, both P_n and E declined significantly with progressive drought stress, the decrease in P_n was lesser when compared to the corresponding decline in E values and hence, the WUEi in the stressed plants showed 27 and 49 % increase on D3 and D6, respectively when compared to D0 plants. While on recovery, WUEi showed a marginal 17 % reduction when compared to the D6 plants; however WUEi values remained higher in comparison to D0 plants (**Fig 9d**). Subsequent regression analysis between P_n with g_s and E with g_s showed a strong linear and positive correlation with each other with a R^2 value of 0.791and 0.733, respectively (**Fig 9e and f**).

Table 2. Leaf relative water content (LRWC %), leaf moisture content (LMC %) and root moisture content (RMC %) of *V. radiata* during gradual water deficit and recovery period. Values represent mean ± SD (n = 5). Significance of drought treatment was tested by one way ANOVA and the significance level was denoted as: s; significant, (F value)* $P < 0.001$

Sampling stages	LRWC (%)	LMC (%)	RMC (%)
D0	80.4 ± 3.1^{a}	86.3 ± 2.3^{a}	93.2 ± 1.2^{a}
D3	69.2 ± 2.8^{b}	81 ± 2.0^{b}	74.5 ± 2.1^{b}
D6	56 ± 3.4^{c}	70 ± 2.8^{c}	65.4 ± 1.8^{c}
6R	74.1 ± 2.7^{d}	84.7 ± 1.5^{d}	87.6 ± 1.5^{d}
T X T_m (F value)	s (190^{*})	s (65.9^{*})	s (305.5^{*})

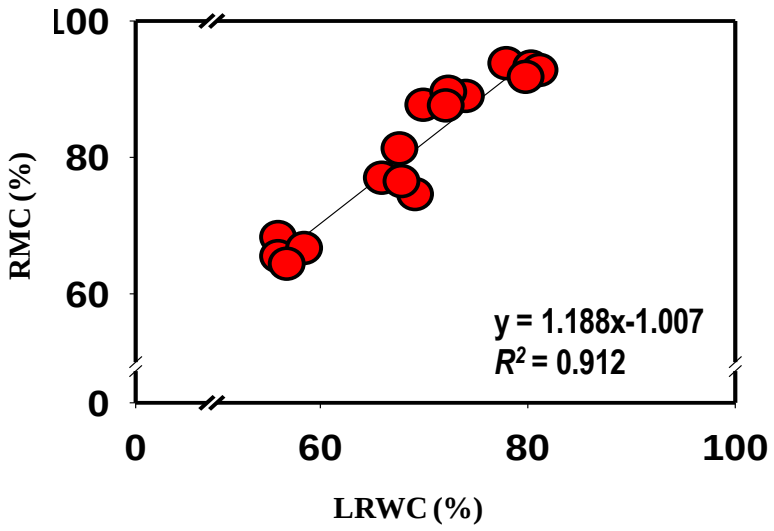

Fig 8. Regression analysis between leaf relative water content (LRWC %) and root moisture content (RMC %) using Sigma plot 11.0 software, showed a linear and positive correlation with each other with a R^2 value of 0.912.

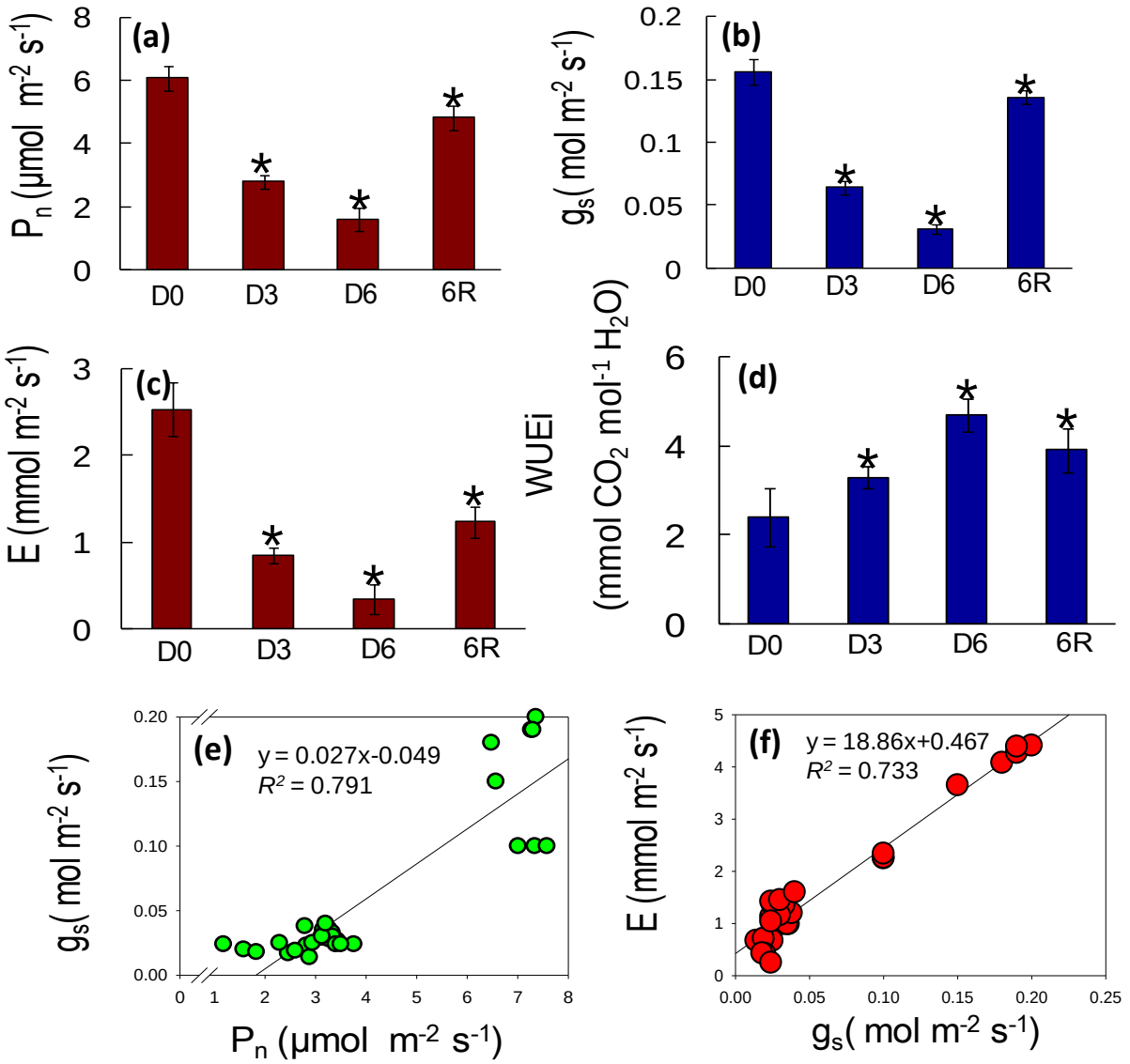

Fig 9. Photosynthetic leaf gas exchange parameters of *V. radiata* under progressive drought stress and recovery and their interrelationship. (**a**) Net CO_2 assimilation rate (P_n); (**b**) stomatal conductance (g_s); (**c**) transpiration rate (E); (**d**) instantaneous water use efficiency (WUEi); (**e**) regression analysis between gs and P_n; (**f**) regression analysis between E and g_s. Values represents mean ± SD with n = 5. P* (<0.001) indicates significant difference (one way ANOVA).

However, a comparatively lesser decline was observed in the internal CO_2 (sub-stomatal) concentration (Ci) of *V. radiata* during progressive drought stress which declined by 33 and 32% during D3 and D6, respectively and increased marginally by 7 % when compared to D6 during 6R (**Fig 10a**). The observed drought-induced changes in the P_n, g_s, E and C_i indicates that both stomatal and non-stomatal limitations are responsible for the observed depression in photosynthetic efficiency during progressive drought stress. Mechanisms of stomatal and non-stomatal limitations during drought stress were illustrated diagrammatically in **Fig 10b**.

Chlorophyll *a*, *b* and total chlorophyll content per unit area was consistently ($P < 0.001$) enhanced with progressive water deficit and was maintained even after recovery treatment. Chl *a* content increased by 22 and 34 % during D3 and D6, respectively when compared to D0 and even upon re-watering, Chl *a* content increased by 2 % when compared to D6 values. Similarly Chl *b* content increased by 17% on D3, 30 % on D6 and during recovery a marginal 4 % increase was observed when compared to D6 values. A corresponding 22 and 33% increase was observed in total Chl content during D3 and D6, respectively as compared to D0 and a slight increase of 2 % was observed upon re-watering the plants, when compared to D6 values (**Fig 10c**).

Photosynthetic performance: Fast kinetics of Chl a fluorescence

A typical polyphasic Chl *a* fluorescence rise was observed during 1s of illumination after 30 min dark adaptation. The fluorescence intensity (F_t) transients (raw fluorescence curves) from 50 µs to 1s during D0, D3, D6 and 6R were depicted in **Fig. 11a**. Slight decline in initial fluorescence (F_O) was recorded during D3 and D6 when compared to D0, while during 6R the F_O levels were almost similar to D0. Maximum fluorescence (F_M) showed significant decline during D3 when compared to D0, however, with extended water deficit (D6), F_M levels increased when compared to D3 but still remained lower than D0. Upon recovery, a slight decline in F_M values was observed in comparison to D6. The variable relative fluorescence between O and P phase (V_{OP} normalized) declined on D3. However, during D6 and 6R, the V_{OP} values were higher than D0 (**Fig. 11b**).

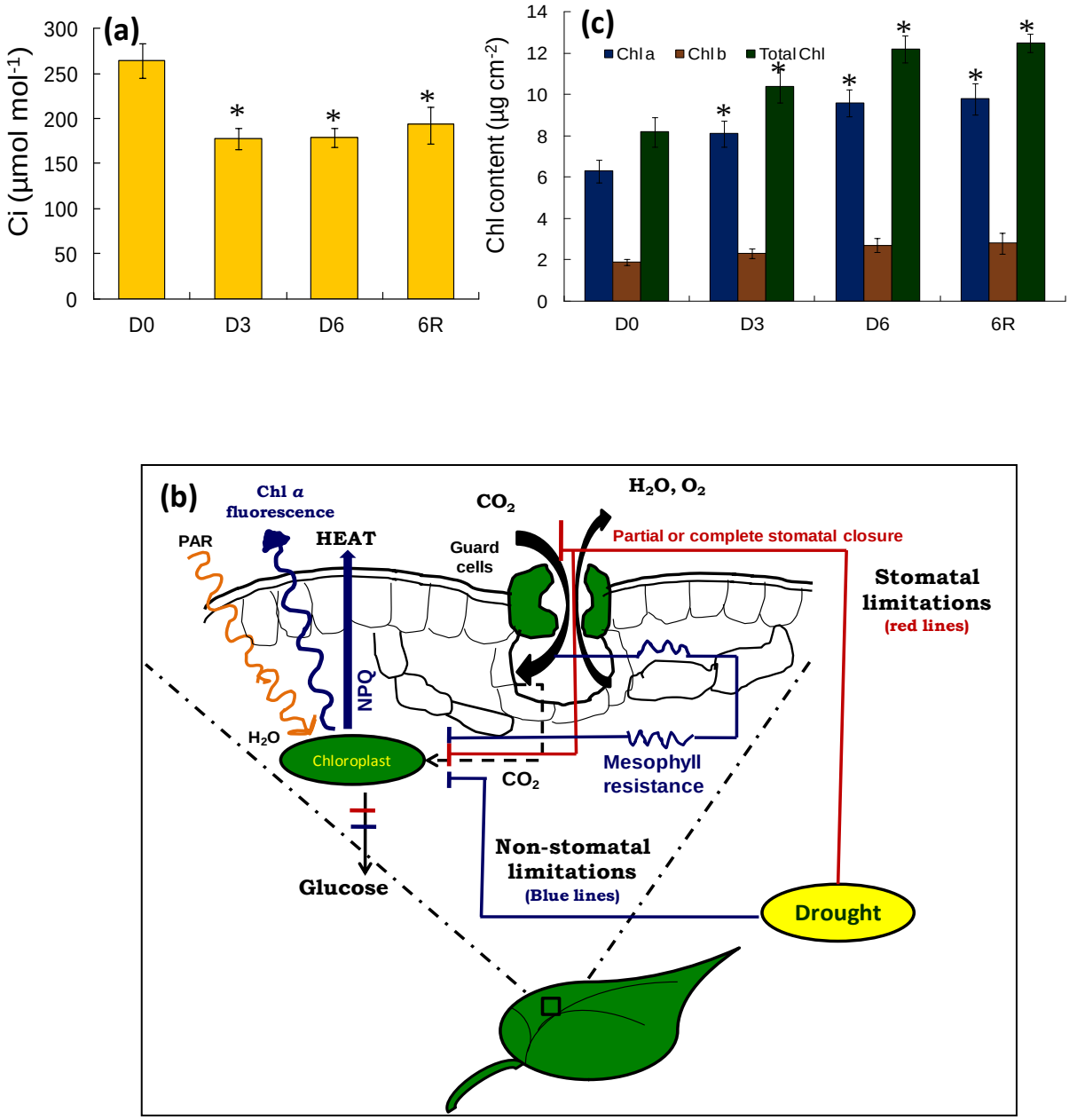

Fig 10. Changes in the sub-stomatal CO_2 concentration (C_i) of *V. radiata* during progressive drought stress and recovery (**a**). Values represents mean ± SD with $n = 5$. P^* (<0.001) indicates significant difference (one way ANOVA).Diagrammatic representation of drought-induced stomatal (red bars) and non-stomatal limitation (blue bars) to normal (Black lines) photosynthetic carbon assimilation(**b**). Chlorophyll a, b and total chlorophyll content during drought and recovery (**c**).

The kinetic differences of transient fluorescence at periodic stages of progressive drought calculated as relative to D0 [$\Delta V_{OP(D0)} = V_{OP(D0)} - V_{OP(D0)}$; $\Delta V_{OP(D3)} = V_{OP(D3)} - V_{OP(D0)}$; $\Delta V_{OP(D6)} = V_{OP(D6)} - V_{OP(D0)}$; $\Delta V_{OP(6R)} = V_{OP(6R)} - V_{OP(D0)}$] showed negative peaks during D3 in respect to D0 during the OJ and JI phases, while during D6, negative peak occurred only during OJ phase and JI phase showed a slightly positive peak. Upon recovery treatment (6R), the ΔV_{OP} plot showed significant positive peak (**Fig. 11c**). The normalized relative fluorescence between O and K phase (50µs to 300µs) expressed as V_{OK} for D0, D3 and D6 were depicted in **Fig.12a** and the corresponding kinetic differences (ΔV_{OK} calculated in a similar way like ΔV_{OP}) are presented in **Fig. 12b**. A positive L-band with a peak around 150 µs appeared during D3 and its amplitude significantly elevated with extended water-deficit (D6) and declined on 6R but still remained higher than D0. The normalized relative fluorescence between the O (50µs) and J (2 ms) phases (expressed as V_{OJ}) and the respective kinetic differences (ΔV_{OJ}) were illustrated in **Fig. 12c and d**, respectively. For the OI phase, relative fluorescence was normalized between 50µs – 1s ($V_{OI} < 1$) (**Fig. 12e**) and 30-300µs ($V_{OI} \geq 1$) (**Fig. 12f**). V_{OI} declined gradually under progressive drought stress showing the lowest value on D6 which thereafter increased again upon re-watering (6R). The ΔV_{OI} showed a negative band (with a peak around 800 µs) on D3 which declined further on D6, but became less negative on 6R (**Fig. 12g**). The normalized variable relative fluorescence between I and P phase (V_{IP}: 30 ms to 180 ms) showed a typical hyperbolic curve (**Fig. 12h**) which when fitted to Michaelis-Menten equation, elucidated the time taken to attain $V_{IP} = 0.5$ (K_m value) which became gradually higher (i.e higher K_m values) under increasing water-deficit conditions when compared to D0. However, upon recovery the K_m value was almost similar to that of D0. Kinetic difference curves between I-P phases (ΔV_{IP}) were illustrated in **Fig.12i**, which showed a similar pattern as that of ΔV_{OI}. The corresponding parameter plots for the major phenomenological fluxes per cross section area basis, such as absorption (ABS) (**Fig 13a**), electron transport (ET_O) (**Fig 13b**) and trapping energy (TR_O) (**Fig 13c**) showed insignificant changes and consecutively PHI (P_O) (**Fig 13d**) was also found to be more or less stable during the entire drought treatment procedure.

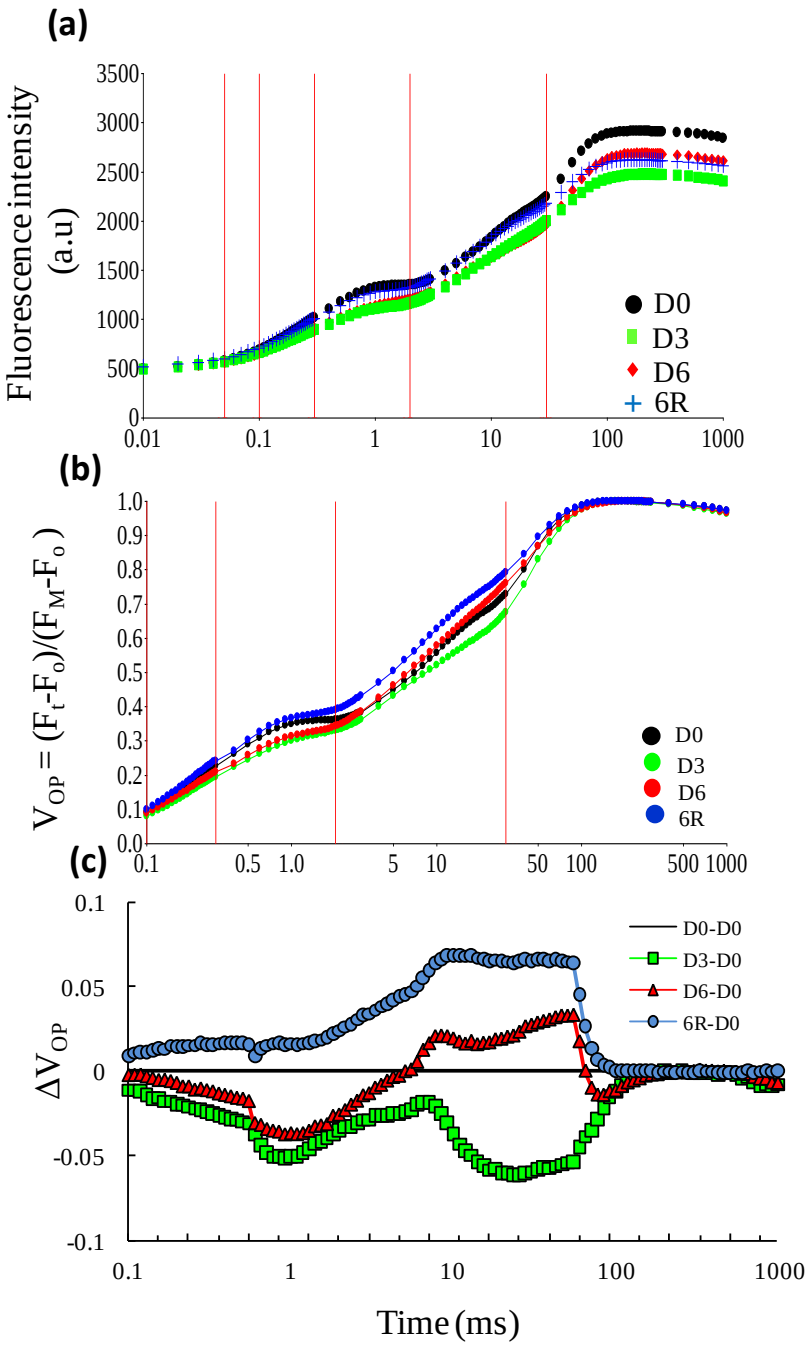

Fig 11. Chl *a* fluorescence transients after normalization from O to P (F_O to F_M) phase in dark adapted leaves of *V. radiata* under progressive drought (D3 and D6) and recovery (6R). Fluorescence intensity (F_t) (**a**); relative variable fluorescence, $V_{OP} = (F_t-F_o)/(F_M-F_O)$ (**b**); kinetic difference of V_{OP} (ΔV_{OP}) with respect to D0 (**c**). Values are average of four independent replicates.

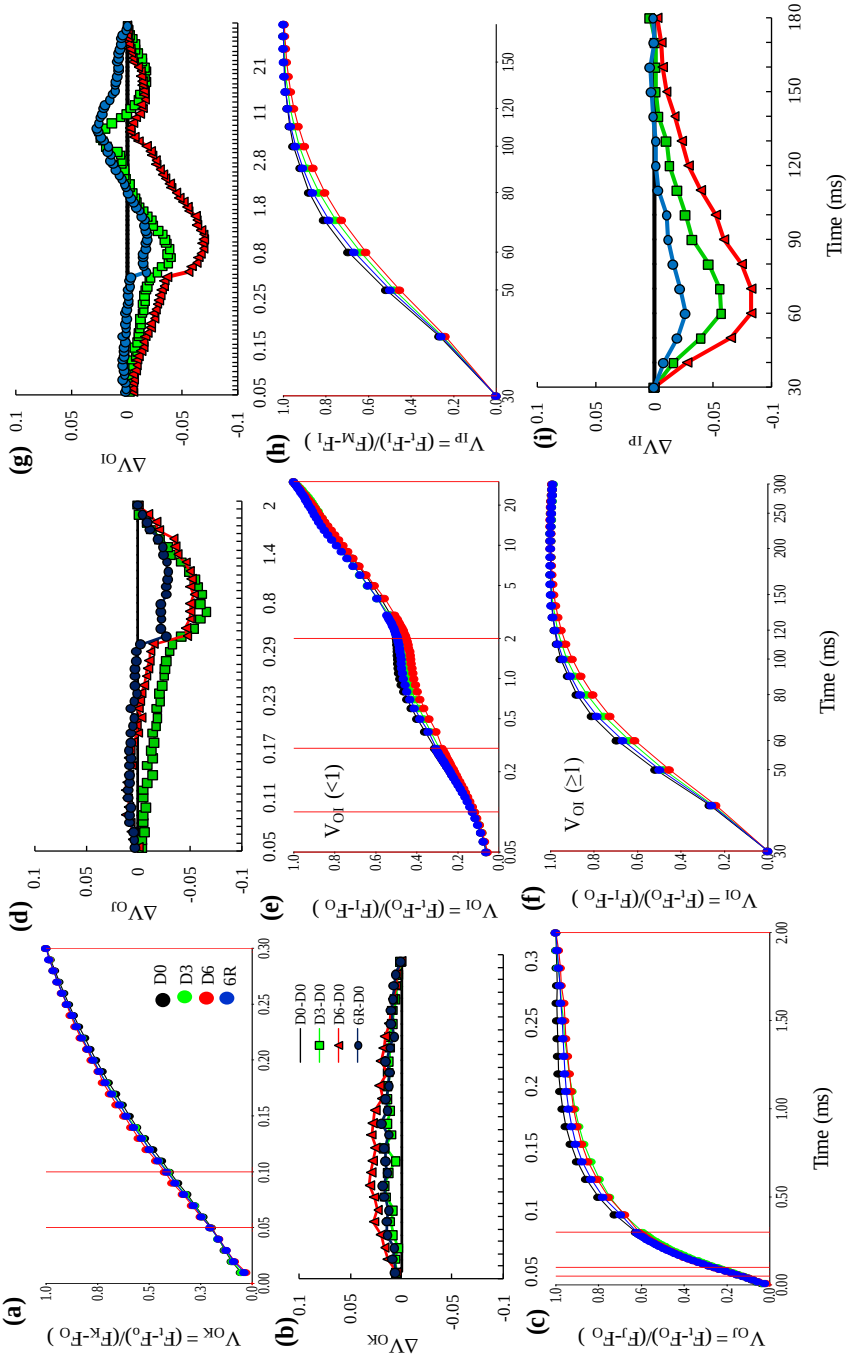

Fig 12. Analysis of chl *a* fluorescence transients for O-K, O-J, O-I and I-P phases of *V. radiata* leaves under progressive drought and recovery. Doube normalized variable fluorescence between phase O and K (F_o to F_K) from 50 µs to 300 µs [V_{OK}= (F_t-F_O)/ (F_K-F_O)](**a**); kinetic difference of V_{OK} (ΔV_{OK}) with respect to control showing prominent L-band (**b**); double normalized variable fluorescence between phase O and J (F_O to F_J) from 50 µs to 2 ms [V_{OJ} = (F_t-F_O)/(F_J-F_O)] (**c**); kinetic difference of V_{OJ} (ΔV_{OJ}) with respect to control (**d**);Double normalized variable fluorescence between O and I [V_{OI} = (F_t-F_O)/(F_I-F_O)] between time interval of 50 µs to 30 ms (V_{OI} < 1) (**e**); variable fluorescence V_{OI} between time interval of 30 ms to 300 ms (V_{OI} ≥ 1) (**f**); kinetic difference of V_{OI} (ΔV_{OI}) with respect to control (**g**); variable fluorescence between I and P phases [V_{IP} = (F_t-F_I)/(F_P-F_I)] showing a hyperbolic curve, shift in the K_m values (time required to attain V_{IP} = 0.5) is indicated with broken line (**h**); kinetic difference of V_{IP} (ΔV_{IP}) calculated with respect to control values (**i**). Values are average of four independent replicates

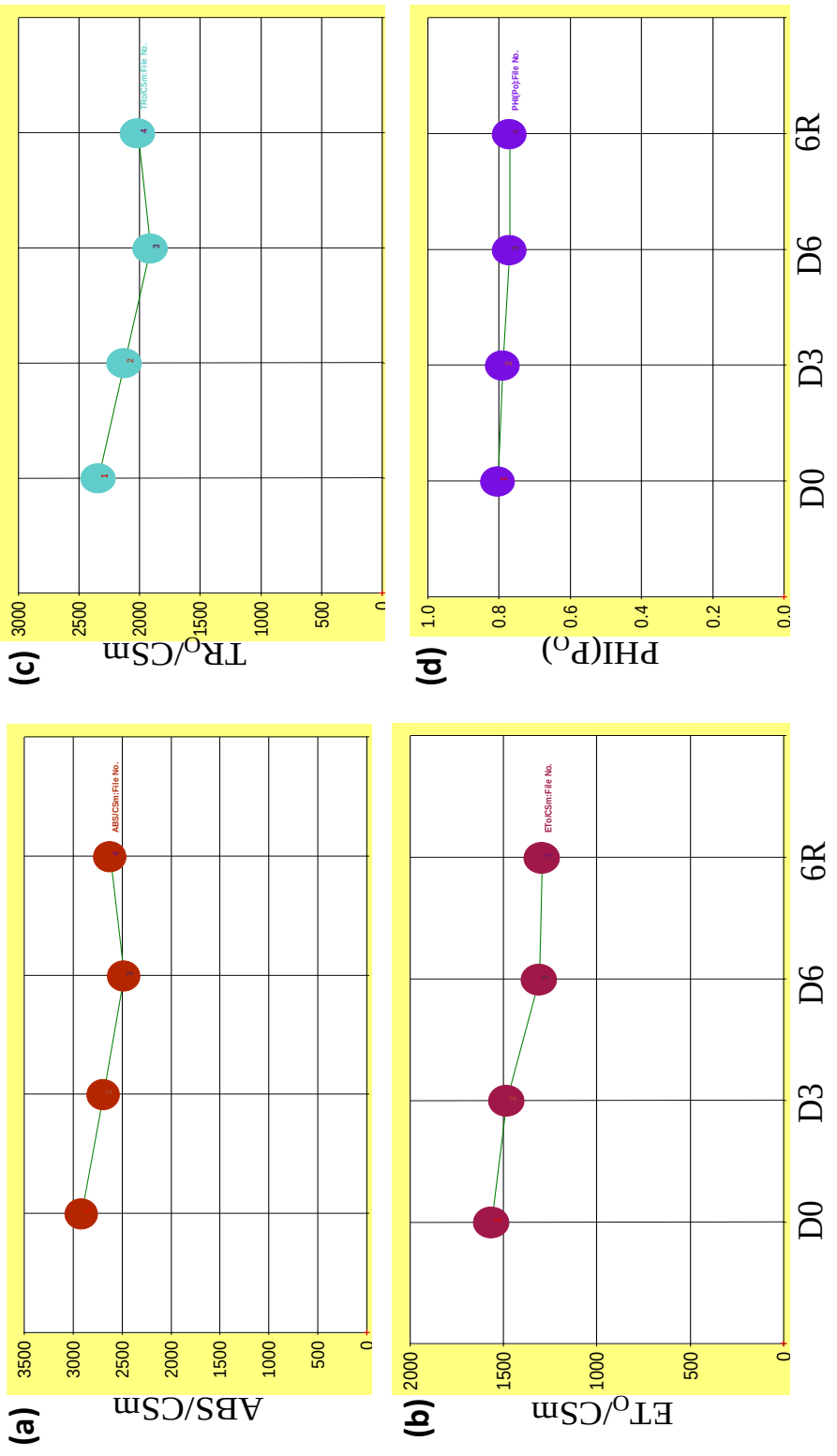

Fig 13. Phenomenological fluxes of *V. radiata* Chl *a* fluorescence under progressive drought stress and recovery. Absorption per cross section area (ABS/ CSm) (**a**); electron transport per cross section area (ET_O/ CSm) (**b**); Trapping energy per cross section area (TR_O/CSm) (**c**); highest quantum yield of PSII (PHI (P_O) (**d**). Value are average of four independent replicates.

Root defense responses: Antioxidant system and protective osmolytes

Drought-induced oxidative stress in *V. radiata* roots was estimated in terms of H_2O_2 content and the corresponding lipid peroxidation levels. Hydrogen peroxide levels were measured qualitatively through localization using H_2DCFDA dye. Confocal microscopic images of the root tips showed a gradual accumulation of H_2O_2 shown as green fluorescence produced by DCDHF-DA dye after reacting with H_2O_2 associated with increasing water limitation which subsequently reduced upon re-watering (**Fig.14a**). The H_2O_2 content in the roots and the corresponding MDA levels also showed a similar pattern of gradual increase and subsequent decrease during progressive stress and recovery period, respectively (**Fig. 14b).** Regression analysis between H_2O_2 and MDA levels depicted a strong positive correlation with each other with a R^2 value of 0.907 (**Fig 14c**). Oxidative stress related non-enzymatic antioxidants; including ascorbic acid (ASA) and glutathione (GSH) showed different patterns of accumulation with progressive drought and recovery. Ascorbic acid content increased slightly on D3, but was significantly higher (2 folds) on D6 and declined again upon re-watering (**Fig. 15a**). On the other hand, reduced GSH content and the ratio of reduced to oxidized GSH was enhanced significantly on D3 but remained stable and almost similar to D0 levels on D6 as well as on 6R. However, the concentrations of the oxidized form (GSSG) remained more or less stable throughout the experimental period (**Fig. 15b**). Guaiacol peroxidase (GPOX) showed significant increase in the activity with gradual water-limitation, with slight decline during recovery period (**Fig. 15c**).

Important protective osmolyte proline, accumulated rapidly at a significantly high level (approximately 5 fold higher) during medium stress (D3) itself. Proline content was similar during D6 and thereafter rapidly decreased upon re-watering. To understand the expression pattern of proline in roots of *V. radiata*, we analyzed the mRNA expression pattern and the corresponding enzyme activity levels of pyrroline-5-carboxylate synthetase (*VrP5CS*), the key regulatory enzyme of proline biosynthetic pathway and the details are shown in chapter 5, hence, the data on proline content was represented along with the corresponding *VrP5CS* mRNA and enzyme activity data in **Fig 37**.

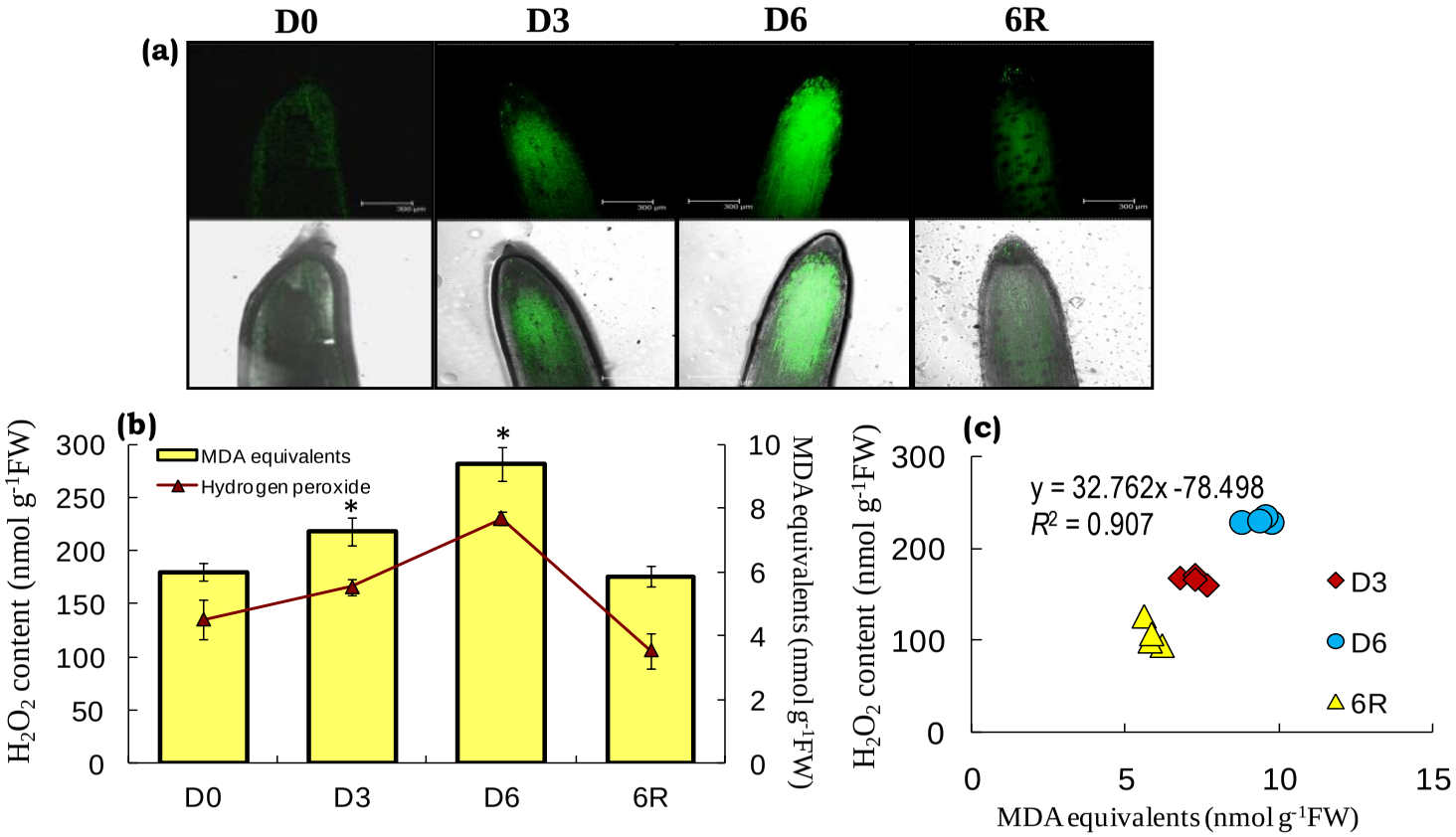

Fig 14. Oxidative stress induction in roots of *V. radiata* with progressive drought stress. Confocal microscopic image of the H_2DCFDA stained hydrogen peroxide (H_2O_2) accumulation pattern in the root tips of *V.radiata* subjected to gradual water deficit and consecutive re-watering treatment (**a**); quantification of H_2O_2 and lipid peroxidation in roots of *V. radiata* under progressive drought and recovery (**b**); Regression analysis between H_2O_2 content and lipid peroxidation levels (**c**).Values represents mean ± SD with n = 5. P* (<0.01) indicates significant difference (one way ANOVA.

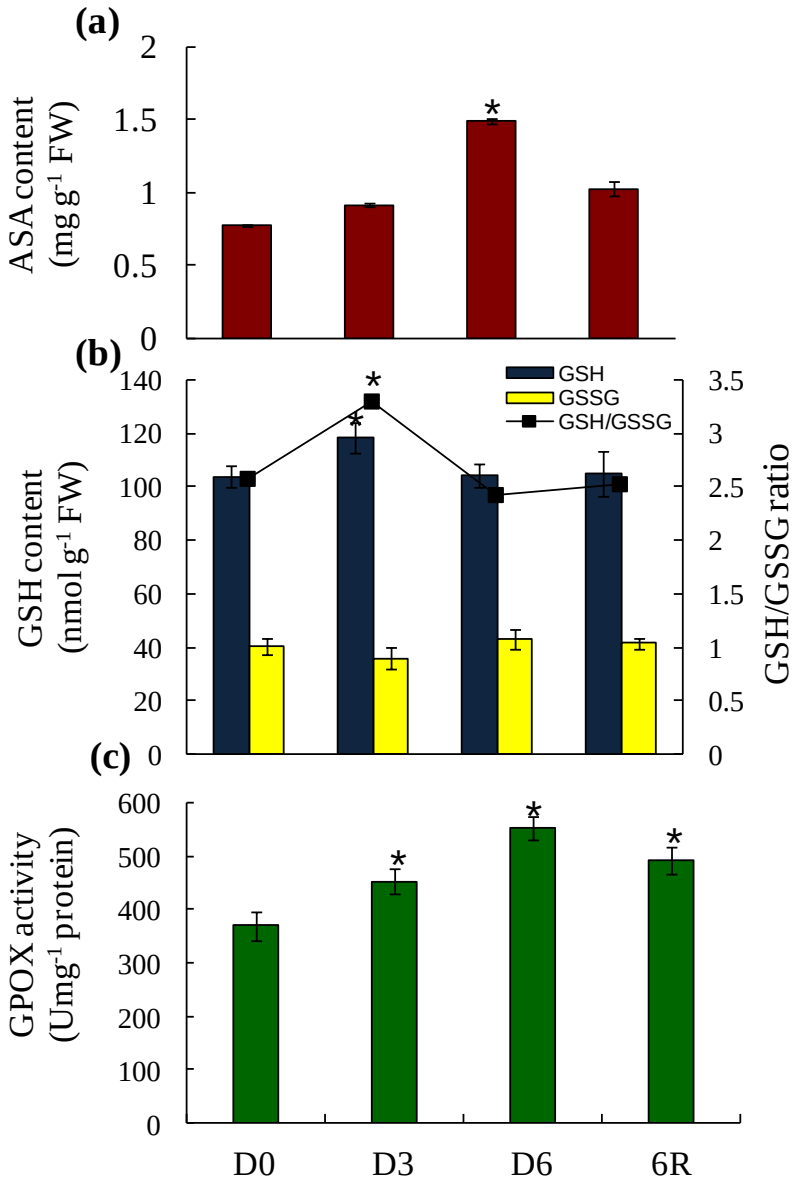

Fig 15. Root defense responses of *V.radiata* against progressive drought induced oxidative stress. Ascorbic acid (ASA) content in roots of *V. radiata* under progressive drought and recovery (**a**);Reduced (GSH) and oxidized glutathione (GSSG) levels and the ratio between the two (**b**); guaiacol peroxidase (GPOX) enzyme activity (**c**). Values represents mean ± SD with $n = 5$. $P^* < 0.001$ indicate significant difference (one way ANOVA).

DISCUSSION

Drought has been reported to inhibit photosynthesis through stomatal limitations (Yin et al. 2005) as well as non-stomatal limitations (Jia et al. 2008). Drought-induced decline in photosynthetic rates could be correlated with decrease in the demand for reducing power including ATP and NADPH, resulting in reduced utilization of absorbed photonic energy (Ort and Baker 2002). Thus, drought-stressed plants encounter the risk of light-induced photo-inhibition or even damage in the photosynthetic apparatus, especially during high irradiance when absorbed light energy exceeds the demand of CO_2 fixation. However, plants utilize different mechanisms to protect itself from photo-damage by dissipating the excess energy through photorespiration, cyclic electron transport, Mehler reaction, chlorophyll fluorescence or heat dissipation (NPQ) (Hu et al. 2013).

Changes in photosynthetic responses and the major underlying limiting factors still continue to remain as important areas to be analyzed during all drought-related studies. In *V. radiata*, we observed a gradual decline in g_s and E with increasing water deficit (D3 and D6), which later recovered upon re-watering (6R) and as a result, P_n also declined. Though, it is well established that decline of P_n could be either due to stomatal or non-stomatal limitations, it is important to analyze which of the two factors dominate for the observed changes in P_n. In case of *V. radiata*, we observed a decline in C_i during progressive drought which could be the direct consequence of stomatal closure and absence of limitations in mesophyll conductance but the extent of decline (32%) was not comparable to the huge drop observed for P_n, g_s and E (74, 80 and 87%, respectively) indicating the involvement of other non-stomatal factors. It was reported that inhibition of CO_2 assimilation along with changes in PSII activities and photosynthetic electron transfer (PET) capacity, causes ROS generation through Mehler reaction inside chloroplast (Asada 2006). To analyze such ROS-induced damages which were crucial indicators for screening drought-tolerance in plants, use of Chl fluorescence measurements as well as malondialdehyde (MDA) contents were considered as highly efficient and informative techniques (Molinari et al. 2007, Moustakas et al. 2011). Thus, for further insight on photosynthetic physiology of *V. radiata* under water deficit conditions, we analyzed the drought-induced effect on PSII efficiency.

Different phases of the OJIP curve (Chl *a* fuorescence) signify different electron transport chain reactions. The photochemical reduction of Q_A in PSII was represented by the O-J phase, while the kinetic properties representing the oxidation and reduction of the plastoquinone (PQ) pool and the alterations in the electron flux from reduced plastoquinone (PQH_2) to the final electron acceptor of PSI was revealed by the J-I and the I-P phases, respectively (Adamski et al. 2011, Gomes et al. 2012). A typical OJIP curve as described by Strasser and Strasser (1995) was observed for *V. radiata* during all the drought stress regimes as well as recovery period which signifies functional photosynthetic systems (Yusuf et al. 2010). Maximum quantum yield of primary photochemistry of *V .radiata* declined gradually with increasing water deficit with D0 showing a F_v/F_M ratio of 0.840 which declined to 0.822, 0.803 during D3 and D6, respectively which increased marginally to 0.809 upon recovery. However, the observed differences in F_V/F_M ratio were not highly significant indicating that F_V/F_M is not a useful indicator of drought tolerance and susceptibility (Oukarroum et al. 2007). A slight but consistent increase in the initial fluorescence (F_O) was observed with increasing water limitation as well as after re-watering. The size of the PSII chlorophyll antenna and the integrity of the PSII reaction centres (RC) determine the value of F_O and it is reported that heat stress induces uncoupling of antenna proteins and thus increases F_O (Strasser 1997). In the present study, we hypothesize that the observed increase in F_O could be due to the drought-induced increase in the chlorophyll index per unit area. Drought-induced modulation in the variable fluorescence between O to P phase (V_{OP}) indicates the actual site of disturbance to the electron transport chain on PSII acceptor side. We observed a negative ΔV_{OP} curve for OJ ,JI as well as IP phases during D3 indicating a decline in the photochemical reduction of Q_A and PQ pool and also a diminished pool of final electron acceptors of PSI. However, during D6, the OJ phase became slightly less negative, JI phase completely recovered and subsequently a positive IP phase also became apparent.

While upon recovery treatment, all phases showed positive peaks. The observed increase in the IP phase signifies increased size of PSI final electron acceptors or increase in electron transfer efficiency to PSI acceptor side which could be due to enhanced photosynthetic machinery to generate either NADPH (non-cyclic electron flow) or ATP through the cyclic electron flow (Adamski et al. 2011, Redillas et al. 2011, Gomes et al. 2012). We observed an increased reduction of the PQ pool with concomitant enhancement in the electron transfer efficiency to during 6R while the electron transfer to Q_A remained normal *i.e* almost equal to that of D0.

The connectivity among the PSII units in terms of the excitation energy transfer was represented by the L-band which was determined through kinetic difference of the double normalized variable fluorescence between O and K phase (50 to 300µs). A positive L-band depicts lower energetic connectivity among PSII units suggesting reduced utilization of the excitation energy due to the changes in the structural organizations of thylakoid membrane (Oukarrom et al. 2007). In *V. radiata,* D6 showed highest amplitude of L-band with respect to D0 while during D3 a positive L-band with comparatively lower amplitude appeared which was almost equal to 6R. Drought-induced decrease in the grouping among PSII units has been well characterized (Strasser and Stirbet 1998, Strasser et al. 2004). Pattern of L-band in *V. radiata* reflects that though high water deficit disrupts the energy connectivity among PSII units, it does not cause an irreversible damage and after re-watering, the plant effectively regained the efficiency of energy utilization through PSII units. The appearance of prominent K-band under various stress conditions is attributed to the disruption of electron transfer between the donor and acceptor side of PSII due to dissociation of the oxygen evolving complex (OEC) and utilization of alternate electron donors (Yusuf et al. 2010). The results from the present study on mungbean excludes the possibility of discrepancy in electron transfer to Q_A as no pronounced K-band was visible and moreover the kinetic differences in the variable fluorescence from O to P phase also suggested similar phenomenon as discussed earlier. Hence, it is clear that increasing water-deficit has no effect on the OEC complex of PSII in *V. radiata*. Negative ΔV_{OI} as well as ΔV_{IP} peaks were apparent in *V. radiata* from D3 itself, which declined further on D6 and recovered

significantly during 6R indicating that the process of exciton capture to reduction of PQ. The electron transport from PQH_2 to PSI final electron acceptor were affected gradually with increasing water-deficit but the systems were not irreversibly damaged as upon re-watering, both the processes recovered and became almost similar to that of D0 plants.

Roots are known to be the initial perceivers of drought stress signal, rather than leaves and also the fact that ascorbic acid (ASA) induced abscisic acid (ABA) production in roots, and transported to leaves causing stomatal closure. Analyses of drought induced modulations in root antioxidants for understanding overall plant responses to drought deserves primary importance (Haberer et al. 2008). In plants, the low molecular weight antioxidant, ASA occurs in millimolar concentrations in both photosynthetic (shoot) as well as non-photosynthetic (roots) tissues. ASA reacts directly with hydroxyl radicals, superoxide and singlet oxygen (Buettner and Jurkiewicz 1996). Apart from its role in photo-protection and regulation of photosynthesis, ASA is also known to preserve activities of enzymes containing transition metal ions as prosthetic groups (Padh 1990, Foyer and Harbinson 1994, Forti and Elli1995). We observed a gradual accumulation of ASA with progressive drought stress which was inversely proportional to the stomatal conductance and one among other causes for this could be ASA induced production of ABA in the roots and its subsequent translocation to the leaves. However the assumption requires confirmation with more in-depth translocation related experiments on ABA production. Ironically, ABA is also needed for maintenance of normal root growth under water deficit (Sharp et al. 2004).

Glutathione is a multifunctional tripeptide (γ-L-glutamyl-L-cysteinyl-glycine) known to be an important redox buffer and a non-enzymatic antioxidant. However, the alteration in the glutathione pool and the redox states under drought stress conditions were not consistent and shows different responses in different plant systems (Tausz et al. 2004). In the present study, GSH followed the general ecophysiological stress response concept given by Tausz et al. (2004), wherein GSH (reduced) concentration increased initially during D3 presenting a more reduced redox state (higher GSH/GSSG ratio) indicating acclimation response. Upon extended water deficit (D6), GSH concentrations declined when compared to D3.

However, the redox status was maintained almost similar to that of D0 which could be due to higher regeneration of reduced GSH under stress conditions. Further analysis on regulation of GSH biosynthesis and the rate-limiting enzyme γECS was discussed in chapter 5. In response to progressive drought, GPOX activity in *V. radiata* roots gradually enhanced and subsequently declined upon recovery indicating a positive correlation with the drought-induced H_2O_2 and lipid peroxidation levels. As peroxidases are known to be bifunctional enzymes which can reduce H_2O_2 as well as generate ROS under abiotic stress conditions (Passardi et al. 2005), the observed increase in GPOX activity could be either due to the corresponding drought-induced H_2O_2 generation or vice versa. The multifaceted protective role of proline under drought stress is well documented (Szabados and Savouré, 2010). In the present study, *V. radiata* drastically enhanced proline biosynthesis under water-deficit conditions which was also degraded rapidly upon re-watering. Further analysis on proline biosynthesis in *V. radiata* during drought was discussed in detail in Chapter 5.

In conclusion, *V.radiata* cv. Vamban-2 adapts to gradual decline in soil water potential through an integrated and dynamic root-shoot response. Stomatal closure and reduced CO_2 assimilation rates were a part of the adaptive mechanism of the plant under drought, rather than permanent damage as the parameters recovered significantly upon re-watering. Drought differentially affected various PSII reactions and the electron flux. However, drought-induced damage on the PSII quantum yield and the stability of PSII complex was insignificant. Simultaneously, the antioxidative root defense against the drought-induced oxidative stress complemented the observed photosynthetic performance of *V. radiata* under progressive drought and recovery. ASA and POX were found to be directly proportional to induced water-deficit conditions in *V. radiata* roots while GSH concentrations were not altered significantly. Our data provide crucial inputs associated with time course-dependent drought responses in an economically important food legume, *Vigna radiata* with detailed insights including PSII reactions, photosynthetic physiology and root defense patterns which could be highly beneficial for developing better performing cultivars under water limiting regimes.

CHAPTER 3

Characterization of dynamic root protein modulation in response to progressive drought and recovery through comparative proteomics approaches

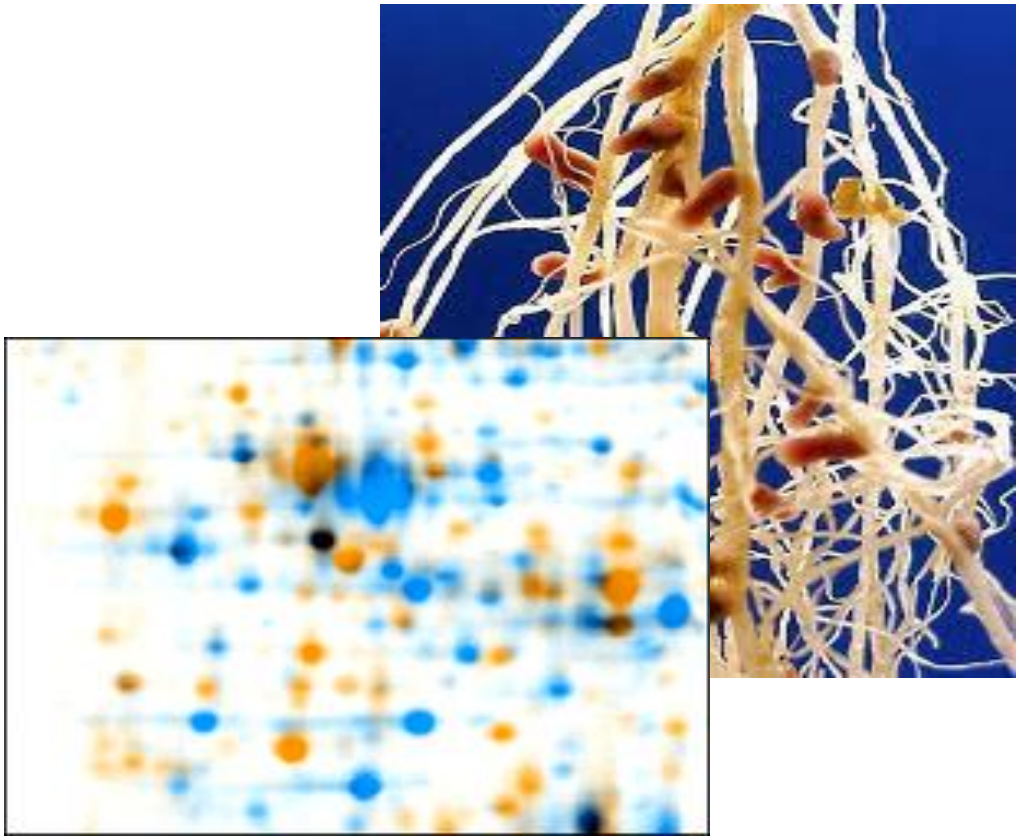

INTRODUCTION

Roots are highly important but intrinsically complex structures required for proper plant growth and development. Previous studies on root responses mostly focused on the developmental aspects of roots and later several genes responsible for cell growth, cell-cycle regulation as well as abiotic stress responses were identified (Kohler et al. 2003, Jiang and Deyholos 2006, Mouchel et al. 2006). To elucidate various mechanisms of plant root responses under adverse environmental conditions, it is highly essential to carry out a comprehensive expression analysis of candidate genes or proteins, as plants usually encounters more than a single abiotic stress factor during its life cycle and responds dynamically which includes either specific or more complex cross-talk responses. As it is now well established that there is little correspondence between mRNA expression and protein levels, study of protein expression patterns became progressively more important. Therefore, to analyze complicated stress-responses, utilization of proteomic-based approaches were found to be highly informative and convenient for both overall analyses of the plant response to various stresses to understand protein dynamics as a whole and also for dissecting various stress responsive pathways.

Importance of comparative proteomic approach for stress response studies

For global expression analysis and protein identification, utilization of proteomic-based approaches have proved highly efficient and useful in the field of protein research. With considerable improvements in mass spectrometry and two dimensional gel electrophoresis (2DGE) techniques, proteomics-based approaches were widely used in various aspects of biological processes including protein identification, analysis of post-translational modifications, protein-protein interactions and protein expression profiling during stress conditions or developmental stages. Though in animal systems proteomic research was highly developed, plant proteomics has not explored many of the aspects of plant-environment interaction yet. Several proteins involved in abiotic stress response and signalling are present in low abundance and hence, become undetectable in crude extracts. Moreover, frequent occurrence of post-translational modifications including phosphorylation, signal peptide excision, ubiquitination, glycosylation and other processes

could not be accounted with gene expression studies alone. Hence, proteomics has an increasingly important and complementary role in stress biology research in the post-genomic era. Owing to its increasing usefulness, in recent past, proteomics-based approaches were applied for dissecting different plant-responses under different abiotic stress conditions including drought, cold, heat, ozone, UV light, heavy metals, nutrient deficiency and elevated CO_2 conditions (Agrawal et al. 2002, Salekdah et al. 2002, Bae and Sicher 2004, Kang et al. 2004, Ingle et al. 2005, Amme et al. 2006, Ferreira et al. 2006, Hashiguchi et al 2010), To give few examples, a single guard cell proteome analysis revealed 336 different proteins which were not identified earlier (Zhao et al. 2008). Similarly, drought-induced modulations in the proteome profile of important crops including rice, wheat, maize and watermelon were reported (Rabello et al. 2008, Hajheidari et al. 2007, Alvarez et al. 2008, Yoshimura et al. 2008). Proteomic-based research was also carried out to analyze various sub-cellular proteomes including chloroplast, mitochondria, cell wall, nuclear envelope and plasma membranes (Peltier et al. 2002, Bae et al. 2003, Bordereis et al. 2003, Zolla et al. 2004). Further, proteomic analysis of individual tissues other than leaves, including seeds, roots, root tips were also carried out to elucidate differential developmental responses (Chang et al. 2000, Gallardo et al. 2001, Mathesius et al. 2001).

Root proteomics-based approaches in plant stress response studies

A recent review on plant proteomics emphasized the importance of undertaking root proteomics-based analyses under various stress conditions (Mehta et al. 2008). Despite extensive work on proteomics-based dissection of stress-tolerance mechanisms of plants, root proteomic analysis is still insipient in comparison to other plant tissues. Major factors responsible for comparatively slower progress in root proteomics were difficulties in isolation of good quality protein from root tissue due to mechanical impedance, low concentrations of proteins and low tissue amounts as starting material. Moreover, presence of proteases and contaminating materials including, polyphenols, polysaccharides, lipids and secondary metabolites in roots, pose further hindrance to efficient protein extraction

(Tsugita and Kamo 1999). Also, successful identification of all the proteins becomes almost impossible due to dominance of the most abundant proteins in the proteomic profile of root extracts. Thus, sample preparation becomes the most crucial step in any root proteomics-based analysis and usually all protein extraction protocols include a protein precipitation step to ensure extraction of maximum number of proteins (including low abundant proteins) and high purity (free from non-protein contaminants). Most widely accepted protein extraction methods include TCA/ acetone precipitation and phenol/ammonium acetate in methanol (Damerval et al. 1986, Hurkman and Tanaka 1986). Thus, together with improved protein extraction techniques, 2DGE and MS analysis makes implementation of root proteomics-based approaches quite convenient as well as highly informative for identifying novel protein targets for abiotic stress-tolerance.

Proteomics-based analysis of legume roots

It is known that during drought conditions, declining water-potential of the soil is primarily perceived through plant roots due to their direct proximity with the drying soil. In fact, a plant's susceptibility or tolerance capacity under drought is actually correlated to its root development modulation and to the corresponding stress response mechanisms (Smucker 1993). Moreover, as legume roots are able to form symbiotic association with nitrogen fixing soil bacteria (*Rhizobia*), study on legume root responses under drought in terms of proteome profiling becomes highly complex. Earlier reports have shown interesting data on legume root responses to drought with respect to antioxidants and osmolytes synthesis (Porcel et al. 2002; Jain et al. 2006; Akcay et al. 2010). However, studies on legume roots protein dynamics under drought were quite rare and some studies focused mainly on root nodules proteomes (Pedersen et al. 1996; Larrainzar et al. 2007). Recently, proteomic studies of *M. trunculata* root nodules infected with *Agrobacterium tumefaciens* has been demonstrated (Valot et al. 2004). Also, root nodules of other legumes including *Glycine max, Pisum sativum* and *Lotus japonicus* infected by *Bradyrhizobium japonicum*, *Rhizobium leguminosarum* and *Mesorhizobium loti*, respectively were reported (Panter et al. 2000, Saalbach et al. 2002, Wienkoop and Saalbach 2003).

Furthermore, membrane associated proteins were characterized in *Glomus intraradices* infected *M. truncatula* roots by using an additional chloroform/methanol extraction step in the comparative proteomic study (Valot et al. 2005).

Also, as evident in natural conditions (rainfed systems), plants often experience cycles of water-deficit rather than continuous drought. In order to have a proper understanding of stress response mechanisms of crop plants, analyses should be focused at different levels of stress intensity as well as stress recovery rather than at a single stress treatment period. Hence, a systematic analysis of the root protein expression patterns during progressive drought stress and recovery is quite important for a comprehensive understanding of the dynamic regulatory mechanisms of plants under water-deficit conditions. For such studies, comparative proteomics proves to be the best approach as it has emerged as a promising tool for global analyses of protein expression levels in the recent past (Cánovas et al. 2004). To our knowledge, only one report on comparative proteomic analysis in mungbean exists till date, which focused on involvement of brassinosteroid during chilling stress (Huang et al. 2006). Moreover, drought responses of legumes at the molecular level were based on foliar proteins only and a focused analysis, involving root protein expression patterns at different levels of stress intensity and recovery period, were not yet reported. In the present study, we aim to analyze the root responses of mature *V. radiata* with respect to its root protein expression dynamics during progressive drought stress as well as recovery period, employing a comparative proteomics approach.

Root growth measurements

Primary root length was measured using a cm scale and the number of lateral roots and root nodules/ plant were manually counted for D0, D3 and D6 as well as 6R groups of plants (n= 15). Nodule dry weight/plant and root dry weight were taken after completely drying the tissue samples inside a hot air oven at 80°C for 2 days.

Protein extraction and two-dimensional gel electrophoresis (2DGE)

Whole roots from both control and stressed group of plants were collected, washed thoroughly and immediately frozen in liquid nitrogen and stored at -80 ºC till protein extraction. Total root proteins were extracted as described by Sarvanan and Rose (2004) with minor modifications. Frozen root tissue (1g) was ground to fine powder in liquid nitrogen and suspended in 4 ml of the extraction buffer containing 0.5 M Tris-HCl (pH 7.5), 0.7 M sucrose, 0.1 M KCl, 50 mM EDTA, 2% β mercaptoethanol and 1 mM PMSF. After thorough mixing, equal volume of Tris-saturated phenol (pH 7.5) was added to the extract suspension and further mixed for 30 min at 4 ºC using a rotospin cyclomixer. Tris-saturated phenol was prepared by mixing 100 mL Tris-HCl (pH 7.5) to equal volume of phenol for 3-4 h with continuous stirring. Then, the phenolic layer was separated from the aqueous layer using a separating funnel. Further, to the separated phenolic phase equal volume of Tris-HCl (pH 7.5) was added and mixed for another 2-3 h. While using, the phenolic phase was separated or else stored under Tris buffer at 4°C.

The Tris-saturated phenol added sample suspension was centrifuged at 5000 *g* for 30 min at 4 ºC.The upper phenolic phase was collected carefully with the help of pipette and an equal volume of extraction buffer was added to it. The above step was repeated and the upper phenolic phase was re-extracted. To the final collected phenolic phase, four volumes of 0.1 M ammonium acetate in methanol was added and incubated overnight at -20 ºC for protein precipitation. The samples were then centrifuged at 10000 *g* at 4 ºC for 30 min and the precipitate was washed thrice in ice cold methanol, twice in ice cold

acetone and air dried for few minutes. The final pellet was solubilized in 200 µL of the rehydration solution containing 8 M (w/v) urea, 2M (w/v) thiourea, 4% (w/v) CHAPS, 30 mM DTT, 0.8% (v/v) IPG buffer of pH range 4-7 (GE, Healthcare) and the protein concentration was determined by using RC-DC protein assay kit (Bio-Rad, Hercules, CA,USA) using BSA as standard.

Aliquots of 600 µg protein were mixed with rehydration solution (8 M urea, 2 M thiourea, 4% CHAPS, 30 mM DTT, 0.8% IPG buffer pH range 4-7 and 0.004% bromophenol blue) to a final volume of 320 µL and used for 2DGE which was done according to Rasineni et al. (2010). Active rehydration of protein (600 µg) was done on immobilized pH gradient (IPG) strips (18 cm, 4-7 pH linear gradient; Amersham, GE) for 12 h at 50 V. Rehydration and focusing was carried out in Ettan IPGphor II (GE Healthcare) at 20 ºC, using the following program: 30 minutes at 500 V, 3 h to increase from 500 to 10000 V and 6 h at 10000 V (a total of 60000 Vh). After IEF, strips were equilibrated twice for 30 min with gentle rocking at room temperature (25 ± 2 ºC) in equilibration buffers. The first equilibration was performed in a solution containing 6 M urea, 50 mM Tris-HCl buffer (pH 8.8), 30% (w/v) glycerol, 2% (w/v) SDS and 2% DTT and the second equilibration was performed by using 2.5% (w/v) iodoacetamide instead of DTT. Proteins were separated in the second dimension SDS-PAGE (12% vertical polyacrylamide slab gels) at 10 mA gel^{-1} for1 h and then 38 mA gel^{-1} for 6 h, using an EttanDalt6 chamber (GE Healthcare). Gels were stained with modified colloidal coomassie staining (Wang et al. 2007a). Protein patterns in the gels were recorded as digitized images using a calibrated densitometric scanner (GE, Healthcare) and analyzed (normalization, spot matching, expression analyses, and statistics) using Image Master 2-D Platinum version 6 image analysis software (GE, Healthcare).

In gel trypsin digestion and mass spectrometry (MS)

In gel digestion and matrix- assisted laser desorption/ionization time of flight mass spectrometric (MALDI-TOF MS) analysis was conducted with a MALDI- TOF/TOF mass spectrometer (Bruker Autoflex III smartbeam, Bruker Daltonics, Germany) according to

the method described by Shevchenko et al. (1996) with slight modifications. Colloidal coomassie stained protein spots were manually excised from three reproducible gels. The excised gel pieces were first washed with 200 µL of 25 mM ammonium bicarbonate (NH_4HCO_3) solution to remove ammonium acetate. Then, the gel pieces were destained with 100 µL of 50% acetonitrile (ACN) in 25 mM NH_4HCO_3 for five times and then, treated with 10 mM DTT in 25 mM NH_4HCO_3 and incubated at 56 ºC for 1 h. This is followed by treatment with 55 mM iodoacetamide in 25 mM NH_4HCO_3 for 45 min at room temperature (25 ± 2 ºC), washed with 25 mM NH_4HCO_3 and ACN, dried in speed vac and rehydrated in 20 µL of 25 mM NH_4HCO_3 solution containing 12.5 ng μL^{-1} trypsin (sequencing grade, Promega). The above mixture was incubated on ice for 10 min and kept overnight for digestion at 37 ºC. After digestion, a short spin for 10 min was given and the supernatant was collected in a fresh eppendorf tube. The gel pieces were re-extracted with 50 µL of 0.1% trifluoroacetic acid (TFA) and ACN (1:1) for 15 min with frequent vortexing. The supernatants were pooled together and dried using speed vac and were reconstituted in 5 µL of 1:1 ACN and 0.1 % TFA. An aliquot (2 µL) of the above sample was mixed with 2 µL of freshly prepared α-cyano-4-hydroxycinnamic acid (CHCA) matrix in 50% ACN and 1% TFA (1:1) and 1 µL was spotted on target plate for MALDI analysis.

Peptide mass fingerprinting and MS/MS analysis

Protein identification was performed by database searches (PMF and MS/MS) using MASCOT program (http://www.matrixscience.com) employing biotools software (Bruker Daltonics, Germany).The similarity search for mass values was done with existing digests and sequence information from NCBInr and Swiss Prot database. Taxonomic category was set to *Viridiplantae* (green plants) and other search parameters were fixed modification of carbamidomethyl (C), variable modification of oxidation (M), enzyme trypsin, peptide charge of 1^+ and monoisotropic. According to the MASCOT probability analysis ($P < 0.05$), only significant hits were accepted for protein identification.

Statistical analysis

Results of the root morphological parameters were represented as mean ± standard deviations (n = 15). The significance of the differences between mean values of well watered and water-stressed plants was determined using one way ANOVA and Student's *t*-test. All the statistical analyses were performed using the statistical package Sigma Plot 11.0. For proteomic analysis, three independent experiments with three replications of both control and stressed samples of each time point with each replication comprising of ten to fifteen pooled plants were considered and the spots were analyzed using Image Master 2-D Platinum image analysis software (GE, Healthcare) and statistical one-way factor ANOVA ($p<0.05$) was performed considering the values (n = 6) of the best matched replicate gels from the three independent experiments. The normalized volume (% vol) of each spot was automatically calculated by the software as a ratio of the volume of a particular spot to the total volume of all the spots present on the gel.

Root growth parameters under progressive drought stress

The exposure of mature mungbean plants to progressive water-deficit conditions inhibited the growth of primary root and induced abscission of longer lateral roots. In the present analysis, abscised longer lateral roots were replaced by the short-roots which could possibly be either pre-existing or newly-induced. During D0, both control and stressed group of plants showed similar root morphology (**Fig. 16a**). During D3, control group of plants maintained similar morphology with the presence of long lateral roots (red arrows) while in stressed populations, most of the longer lateral roots were abscised and few short-roots were visible (**Fig. 16b**). With subsequent water withdrawal (D6), even the number of short-roots declined and only the primary root was visible (**Fig. 16c**). Upon re-watering (6R), induction of small lateral roots was observed (**Fig. 16d**).

Primary root exhibited an average growth of 0.35 cm per day under well-watered conditions, whereas the growth rate declined to 0.12 and 0.04 cm per day during D3 and D6, respectively (**Fig. 17a**). Root dry weight declined by 50 % on D3 when compared to D0. However, the alterations in the root dry weight during D6 and 6R were not significant when compared to D3, but were found to be significantly lesser when compared with control populations (**Fig. 17b**). Similarly, number of lateral roots declined by almost 70 and 84 % during D3 and D6, respectively and recovered marginally upon recovery (**Fig. 17c**). As expected, we also observed a reduction in root nodule number (**Fig. 17d**) and nodule dry weight/ plant (**Fig. 17e**) in response to progressive drought stress. Overall, we observed that upon re-watering (6R), all the above root growth parameters showed slight recovery trend but did not come back to the control values immediately.

2DGE and protein expression profiling

To investigate the root protein expression patterns in response to progressive water-stress treatment and recovery, root protein profiles of *V. radiata* were examined. Triplicate gels were obtained from three independent experiments and the representative gels D0, D3, D6 and 6R were illustrated in **Fig. 18 a, b, c** and **d**. More than 500 spots were reproducibly

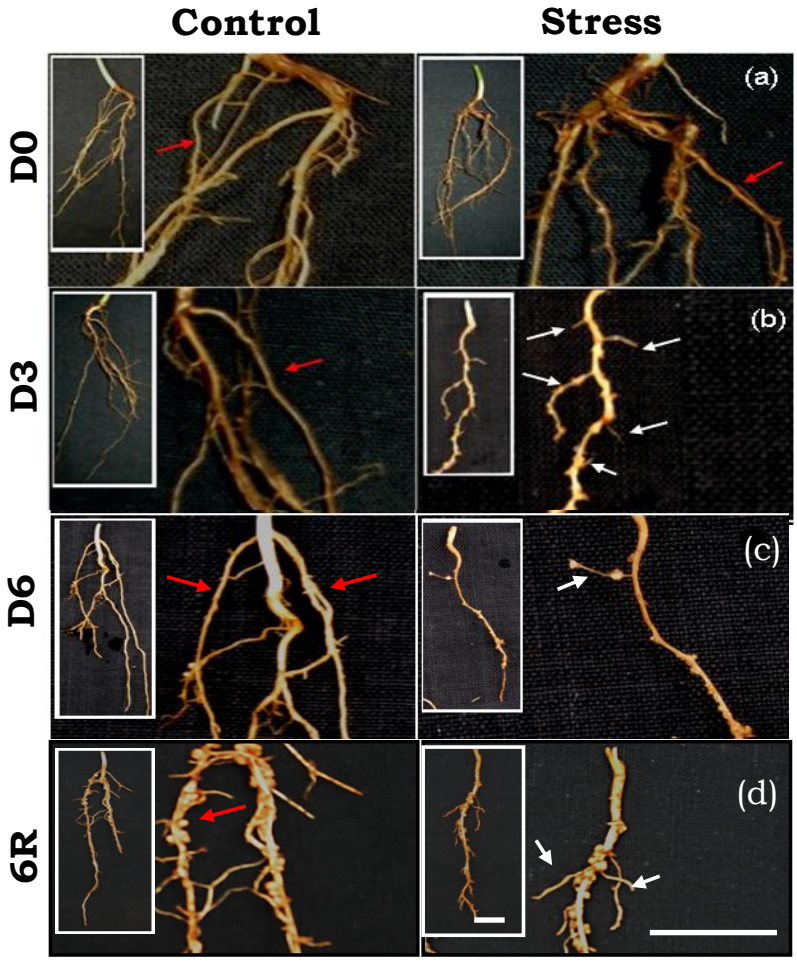

Fig 16. Root growth patterns of control and drought-stressed plants of *V. radiata* during D0 **(a),** D3 **(b)** D6 **(c)** and 6R **(d).** Abscission of longer lateral roots (indicated by red lines) is clearly visible at D3 and D6 of drought treatment. The arrows (white) indicate the short-roots (either pre-existing or newly-induced) visible in the drought stressed populations during D3, D6 and 6R.

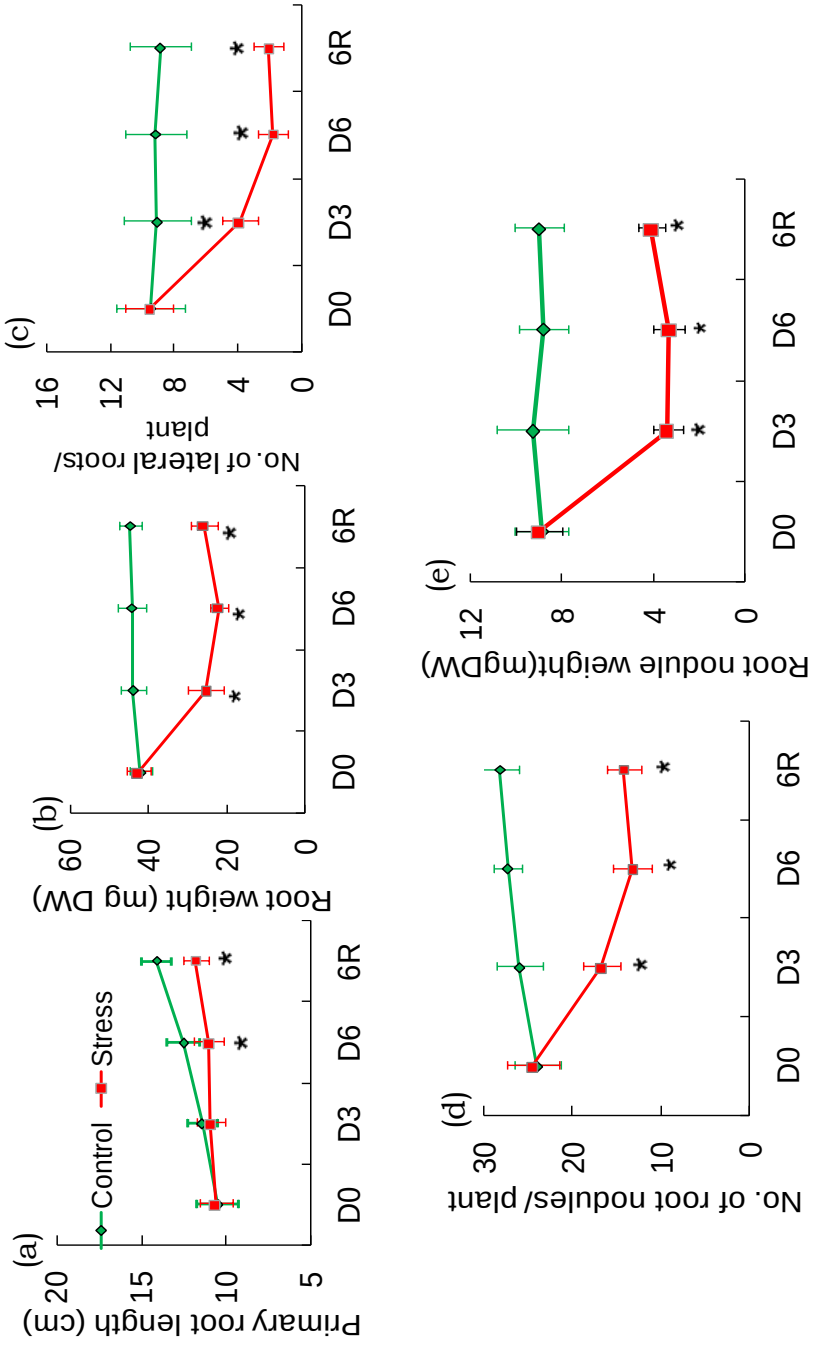

Fig 17. Root growth parameters of *V. radiata* before onset (D0), three days (D3), six days (D6) after onset of drought stress treatment and six days after re-watering (6R). Primary root length (cm) **(a),** root dry weight(mg DW) **(b),** number of lateral roots **(c),** number of root nodules/plant **(d)** and root nodule dry weight/ plant **(e).** Results are mean ± SD (n = 15). Vertical bars represent ± SD, significant difference at * $p<0.05$.

detected in the colloidal coomassie stained gels with Image Master 2D Platinum software and all gels showed highly similar distribution patterns in 2D image. Overall analysis of all the gels revealed that out of the matched spots between D0 and D3 stress, 4.2 % were significantly up-regulated (> 1.5 fold) and 6.2 % were down-regulated while during D6 , 3.8 % up-regulated and 3.2 % were down-regulated (**Fig. 18 e, f**). A Venn diagram analysis of the quantitative expression patterns of all the up and down-regulated proteins from *V. radiata* roots during short (D3) and long (D6) term water-deficit and recovery was illustrated in **Fig. 18g** and **Fig. 18h**, respectively. A total of 34 major spots which were distinct, well-separated but not in complexes and of considerable intensity were selected for protein identification by MALDI-TOF analysis. Selected spots showed differential expression during progressive stress treatment and recovery, out of which 26 proteins were successfully identified. Positions of the 26 identified proteins were numbered and depicted accordingly in the master gel (**Fig. 19a**) and the rest eight did not show any significant hits in the database and hence not considered. Few of the identified spots were enlarged in **Fig. 19b** and **19c** to visualize their expression patterns during progressive water-deficit and recovery.

Identification of differentially expressed proteins during progressive drought stress and recovery

In order to avoid complexity, we first grouped the 26 identified proteins as up-regulated, down-regulated, highly down-regulated (which is beyond detection level of the software) and unchanged based on their expression patterns during short-term drought (D3) and then the subsequent changes in the expression patterns of these proteins during long-term stress treatment and recovery period was analyzed. The relative spot intensities during progressive drought stress and recovery (0d, 3d, 6d, R), matched peptide sequence, accession number, source organism, sequence coverage, experimental and theoretical molecular weight and pI and the MS/MS score of each individual proteins were shown in **Table 3**. In some cases, more than one spot were identified as the same protein. For example, lectin (spot 1 and 2) and actin (spot 15 and 16).

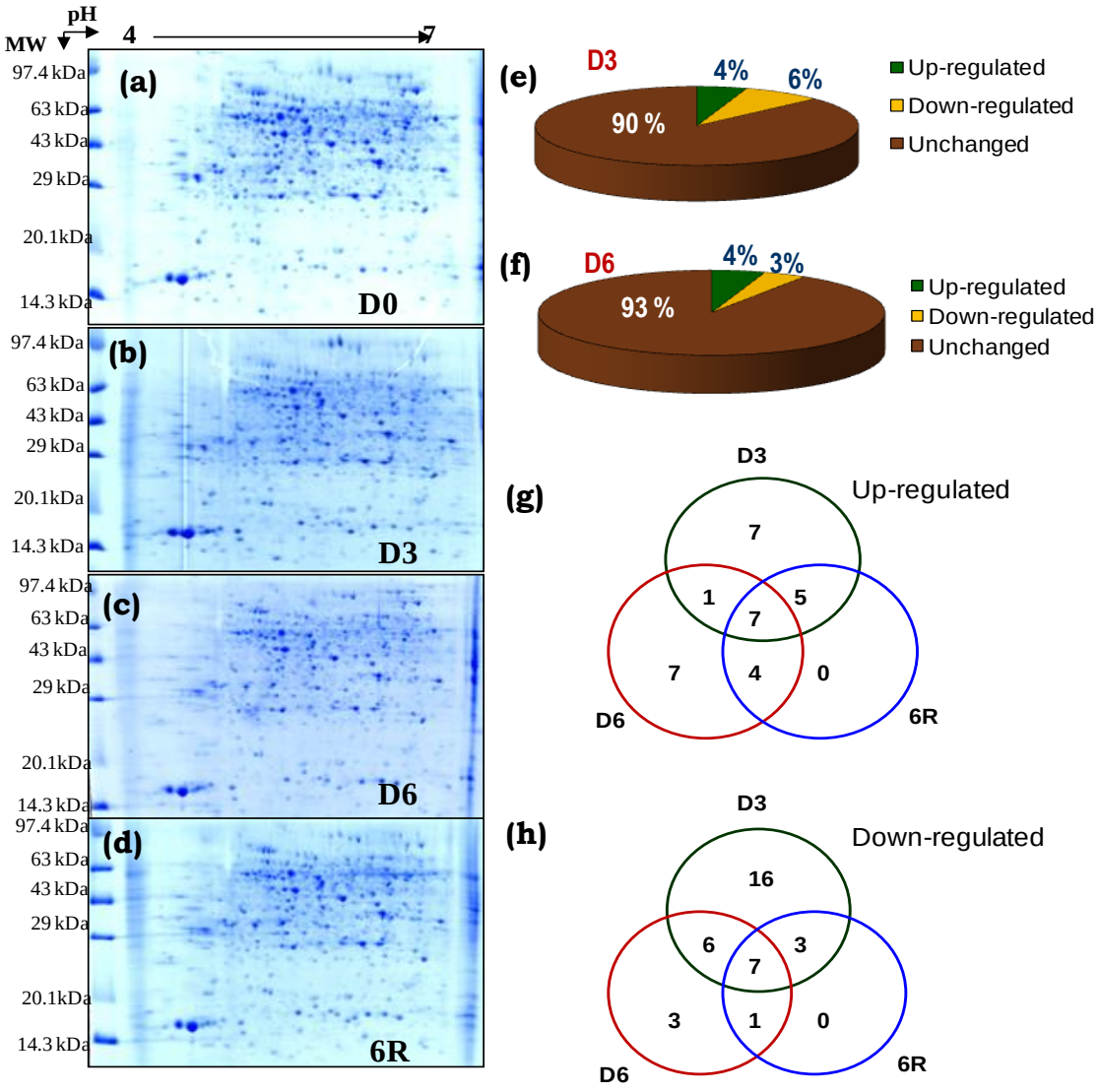

Fig 18. 2-D protein profile of *V. radiata* roots grown under well watered D0 **(a)**, short term D3 **(b)**, long term D6 **(c)** water withdrawal and recovery 6R **(d)**. Diagrammatic representation of *Vigna* root protein expression patterns during D3 **(e)** and D6 **(f)**. Venn diagram analysis of the expression patterns of up-regulated **(g)** and down-regulated **(h)** root proteins under progressive drought and recovery. The numbers of differentially expressed spots at different time points are shown in different segments.

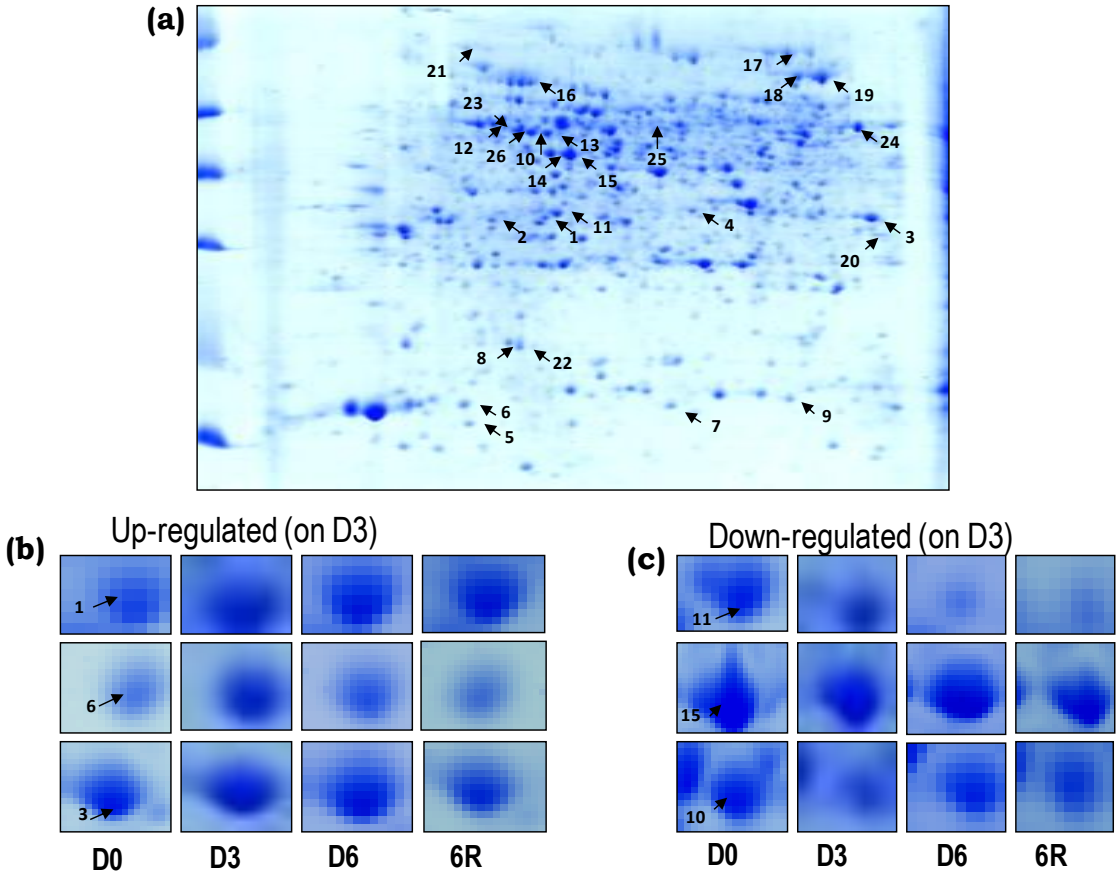

Fig 19. 2-DE master gel from the control root sample illustrating twenty-six identified proteins **(a)**. The spot numbering in the master gel shown corresponds to the spot numbers given in **Table 3**. Enlarged view of the expression patterns of few up-regulated **(b)** and down-regulated **(c)** spots during short-term (D3), long-term (D6) drought stress and recovery period (6R).

Table 3. Identification of major root proteins of *Vigna radiata* differentially expressed during progressive drought stress and recovery. Relative spot volumes for each spot were expressed as % Spot Vol indicating the normalized values of the ratio of the individual spot to the total volume of all the spots in the gel. Significant difference between 3d, 6d and R when compared with C are analysed through one-way factor ANOVA and are indicated with "*"($p < 0.05$).

Groups	Spot No.	Relative spot volumes (C, 3d, 6d, R)[a]	Protein identified	Peptide Sequences matched	Observed Mr/ pI on the gel	Theoretical Mr/ pI	Accession no.	S C (%)[b]	Reference organism	MS / MS Score
Up-regulated	1	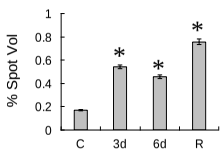	Lectin precursor	LLVASLVHPSR HIGIDVNSIESIR	33 kDa / 5.1	29.4 kDa / 5.32	gi /54019701	8	*Phaseolus filiformis*	205
	2	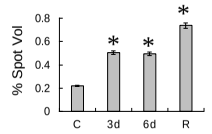	Lectin precursor	LLVASLVHPSR HIGIDVNSIQSIR	32 kDa / 6.1	30 kDa / 5.14	gi /22208832	8	*Vigna linearis var. latifolia*	130
	3	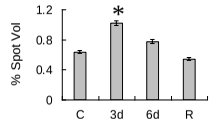	Aldehyde reductase	VVLTSSIAAVAFSDRPK DVALAHILAYENASANG R NPDVVVDETWYSDPEY CK NASLGWVDVKDVALAH ILAYENNASANGR	34 kDa / 5.2	35.7 kDa / 6.33	gi / 5852203	19	*Vigna radiata*	315
	4	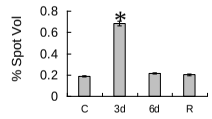	V-type proton ATPase subunit E 1	DLIVQCLLR LKEPSVLLR	38 kDa / 6.0	26.2 kDa / 6.04	VATE1_A RATH	7	*Arabidopsis thaliana*	49

Table 2 (Contd)

5		Unknown protein	SAAVGENYK HSWSINEFGDLTR	14.4 kDa / 4.8	14.67 kDa / 4.9	gi / 217073006	9	*Medicago truncatula*	62
6		Predicted protein	IDQFDGRNISR GVLEERILNALVL	16 kDa / 4.9	44.5 kDa / 5.58	gi|168031802	6	*Physcomitrella patens subsp. patens*	45
7		Xyloglucan endotransglucosylase precursor	KATAGALLAVVVAAVL LR IYLWFDPTK	16 kDa / 5.7	33.6 kDa / 6.5	gi / 38605539	8	*Triticum aestivum*	43
8		Cu/Zn Superoxide dismutase	KEHGAPEDENR RAVVVHADPDDLGK	21 kDa / 5.1	15.2 kDa / 5.64	gi /134598	15	*Zea mays*	97
9		Oxidoreductase	ISRAMLMLPPGAATIAA VGSR TQVVLDAVKASIDK	16.5 kDa / 6.3	40.4 kDa / 5.8	gi / 195629692	9	*Zea mays*	56

Table 2 (Contd)

Down-regulated	10	Enolase 1	KVNQIGSVTESIEAVR RIEEELGDAAVYAGAKF R	56 kDa / 5.2	48.2 kDa / 5.3	ENO1_MAIZE	7		*Zea mays*	54
	11	Chalcone isomerase	VNFPPGASVFYR AVSAAVLETMIGEHAVS PDLKR	34 kDa / 5.3	21.9 kDa / 6.02	gi / 81864	16		*Phaseolus vulgaris*	226
	12	Beta- Tubulin	INVYYNEASGGR LAVNLIPFPR	64 kDa / 4.9	50.4 kDa / 4.7	gi/303842	4		*Oyza sativa*	127
	13	Tubulin alpha -2 chain	EIVDLCLDR AVCMISNNTAVAEVFSR	62 kDa / 5.3	40.6 kDa / 5.06	gi / 464841	7		*Anemia phyllitidid*	139
	14	Actin	AVFPSIVGRPR SYELDGQLITIGDER TTGIVLDSGDGVSHTVPI YEGYALPHAILR	55 kDa / 5.3	42.9 kDa / 5.31	gi / 1666234	14		*Pisum sativum*	235

Table 2 (Contd.)

	16	Heat shock protein 90-1	ITYLKEDQLEYLEER RAPFDLFDTR	90 kDa / 4.9	80.7 KDa / 4.94	gi / 208964724	3	*Glycine max*	74
	17	Mitochondrial translational initiation factor, putative	DMVKMICK TLKSVWR	97 kDa / 6.3	110.6 kDa / 6.86	gi/ 255584176	1	*Ricinus communis*	43
	18	Methionine synthase	ALAGQKDEAYFAANAAA QASR YGAGIGPGVYDIHSPR	85 kDa / 6.4	47 kDa / 5.73	gi /17017263	4	*Zea mays*	60
	19	Cobalamine independent methionine synthase	YLFAGVVDGR AGITVIQIDEAALR YGAGIGPGVYDIHSPR	84 kda / 6.5	84.4 kDa / 6.17	gi /33325957	5	*Glycine max*	255
Highly Down-regulated	20	Unnamed protein product	IATIHNVFAIIRGSEEPDR KIATIHNVFAIIR	32 kDa / 6.5	32.3 kDa / 5.82	gi / 270234876	11	*Vitis vnfera*	62

Table 2 (Contd)

	21	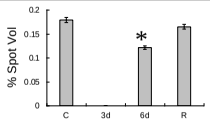	Penta tricopeptide repeat contaning protein	GCEPNEFTFGILVR RDSTITIMKNLR	110 kDa / 4.5	99.2 kDa / 6.62	gi / 255572426	2	*Ricinus communis*	45
Unchanged	22	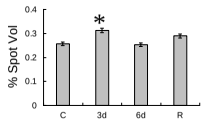	ATP synthase subunit d	FSQEPEPIDWDYYR EAYDSIEIPK	20 kDa / 5.2	19.5 kDa / 5.09	ATP5H_ARATH	14	*Arabidopsis thaliana*	64
	23	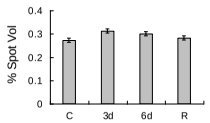	Vacuolar H+ ATPase B subunit	TVLFLNLANDPTIER GYPGYMYTDLATIYER	65 kDa / 5.1	54.5 kDa / 5.24	gi / 134133942	6	*Medicago truncatula*	129
	24	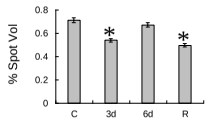	ATP synthase alpha subunit	VVDALGVPIDGR EAFPGDVFYLHSR EVAAFAQFGSDLDAATQA LLDR	60 kda / 6.7	27 kDa / 6.2	gi / 20146580	11	*Heliamorpha sp.Anderberg s.n.*	224
	25	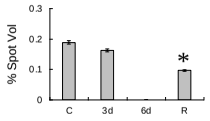	Hypothetical protein	HAYEGITLATPAIPR GVLLEALYK	66 kDa / 5.7	64.1 kDa / 9.03	gi / 147820779	4	*Vitis vinifera*	60
	26	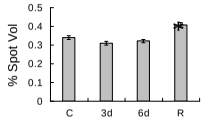	UDP glucose pyrophosphorylase	YQNSNIEIHTFNQSQYPR VLQLETAAGAAIR	63 kDa / 5.2	51.6 kDa / 5.9	gi / 12585472	6	*Astragalus penduliflorus*	115

[a] C: Control, 3d: 3 days after onset of stress treatment, 6d: 6 days after onset of stress treatment, R: 6 days after re-watering;
[b] SC: Sequence coverage

Based on their biological function, the 26 identified proteins could be categorized into 5 major groups i.e 1) ROS-detoxification: Cu-Zn SOD and aldheyde reductase; 2) Root morphology related proteins: actin, tubulin and Xyloglucan endotransglucosylase (XET); 3) Sulphur metabolism: methionine synthase and cobalamine-independent methionine synthase ; 4) Protein synthesis /Energy metabolism: ATPase E subunit, Enolase, translational inititation factor (tIF) and Heat Shock Protein-90 (HSP 90) and finally 5) Cell signalling related proteins: lectins, oxidoreductase and chalcone isomerise (**Fig. 20a**).

The analysis of the expression patterns of these proteins highlight their possible role in the plant's overall drought-response mechanisms. We observed that an inter-relationship and coherence exist among the identified groups of proteins and a schematic representation of such interactions with medium and high water stress as the master regulatory switch for these complex networks was depicted in **Fig. 20b**. We analyzed the effects of medium and high water-deficit on each of the five groups of proteins for a better understanding of the regulatory mechanisms which will be discussed in the next section.

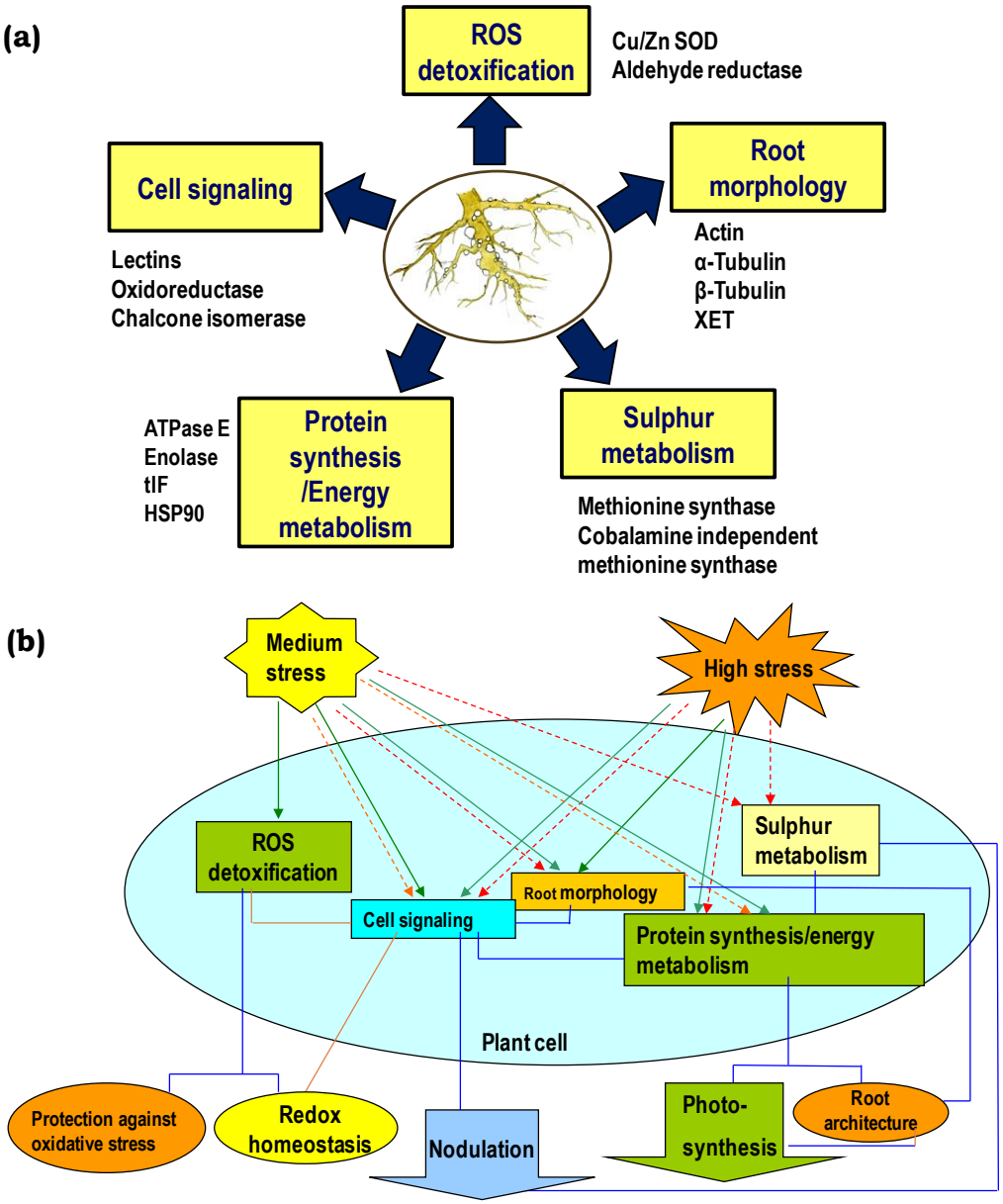

Fig 20. Grouping of differentially expressed identified proteins based on their functional roles (**a**); Schematic representation of the inter-relationship and networking between the identified group of proteins and overall plant metabolism in response to medium and high water-deficit. Solid arrows indicate up-regulation and broken arrows indicate down-regulation. Solid lines signify inter-relationship between two different functions (**b**).

DISCUSSION

Plant growth and survival depend upon the rooting vigour and root architecture in response to the varied soil environments. Molecular mechanisms underlying the complex drought response networks in legume roots have been well documented in the present study through comparative proteomic analysis which showed a dynamic regulation of the root proteins involved in different cellular functions of *V. radiata* under progressive drought conditions and recovery period. Identification and analyses of the expression patterns of the proteins differentially expressed during short and long term drought stress and recovery can contribute significantly to our present understanding of drought response mechanism of legume roots and also help to identify the key regulators of drought tolerance in crop plants.

Previous studies have supported the fact that drought-tolerance in crops including food legumes is closely associated with its rooting pattern in the soil or its root system distribution (Silim and Saxena 1993, Gaur et al. 2008, Jiang et al. 2012). It was a common observation that in drought-stressed plants, total root configuration reduces which in most cases was directly proportional to the severity of the drought conditions. For example, significantly slower rates of root elongation were observed in cereals under severe drought stress when compared to control plants (Pardales and Kono 1990). Due to inhibition of root growth as well as abscission of lateral roots in dry soil, the overall root hydraulic conductivity could also be affected. Inhibition in the rate of primary root elongation could be due to the significant reduction in the cell supply rate to the cortical layers of the primary root which is present just behind the root apex, as limited soil moisture supply primarily affects the process of cell growth (Abdelhamid 2010). Our results on *V. radiata* root system showed that the primary root growth slowed down considerably with progressive water-deficit, but was not inhibited completely and upon recovery treatment. Thus, we can assume that with progressive drought intensity, primary root growth elongation of *V. radiata* was affected due to inhibition of cell growth and proliferation. However, there were other reports showing negligible effect of drought on root system or

even promotion of root growth during mild water deficit conditions (Weerathaworn et al. 1992, Mia et al. 1996), Moreover, increase in root: shoot ratio was usually considered as drought-tolerant selective trait of crop plants. However, as drought often interacts mutually with other soil (physical and biological impedance) as well as environmental factors (heat and light), root architectural responses during drought stress could not be attributed to water-limitation alone. Also, the ability to modulate root architecture in order to adapt or avoid water deficit conditions varies from plant to plant depending on their drought-tolerance capacities as well as on the severity and time of drought induction.

Maximum resistance to liquid water flow through soil-plant-atmosphere continuum was known to be imposed by roots and thus root hydraulic conductivity (Lp_r) plays an indirect but crucial role in determining root metabolism and architectural changes during water limitations (Huang and Nobel 1992). Drought stress is known to cause abscission of lateral roots in dry soil due to reduced Lp_r, and induces secondary lateral roots in regions of soil containing higher soil water content (Smucker 1993). Our data on *V. radiata* depicts abscission of the longer lateral roots while less number of short-roots were observed in the drought-stressed populations. Since the same root was not observed during progressive drought stress treatment, it could not be predicted whether these short-roots were pre-existing or newly induced. It was reported earlier that rapid growth of functional roots into unoccupied regions of the soil provides better survival chances to the plant, due to their greater acquisition rates of the biogeochemical resources (Eissenstat & Caldwell 1989). However, with increase in stress intensity (D6), the number of the lateral roots further declined indicating higher rate of abscission of these roots with gradual drying up of soil, while upon re-watering (6R). We also observed induction of new lateral roots. Newly induced lateral roots were known to have comparatively higher Lp_r than main roots. Our results clearly demonstrate plant's innate ability to regulate the root morphology towards maximum water up-take strategies depending on the availability of water in the soil (Nobel and Huang 1992, Huang and Nobel 1992, Rieger and Litvin 1999). Our data also suggested that *V. radiata* was able to tolerate medium level drought stress intensity

(D3) but gets susceptible under subsequent enhancement of the drought treatment (D6). Though we have observed different patterns of root architectural alterations in *V. radiata* under progressive drought as well as recovery period, the question remains that what actually happens at the protein level inside the roots? To answer this question, we analyzed the differentially regulated root proteins of *V. radiata* during progressive water deficit and recovery period. Our results depicted that root morphology related proteins including actin (spot 14, 15), α-tubulin (spot 13) and β-tubulin (spot 12) were significantly down-regulated during D3 but consecutively enhanced their expression under long term water-deficit which declines again on re-watering. Actin and tubulins are the subunits of cellular microfilament and microtubule, respectively whose major function is to impart mechanical strength to the cell and assist in cell wall synthesis and direction of cell expansion, apart from involving in cytokinesis, mitosis and intracellular localization of organelles and vesicles (Niini et al. 1996, Sheahan et al. 2007, Takagi et al. 2009, Gutierrez et al. 2009). Actin was also reported to be involved in K^+- channel activity in guard cells (Eun and Lee 1997). Yoshimura et al. (2008) have also found induction of actin and tubulin proteins in roots of wild watermelon during water-deficit conditions, though the induction was at earlier stages of drought stress in their case, which could be due to differences in drought tolerance capacity of the two plants as wild watermelon is a xerophyte. Also, it was reported that actin contributes in regulation of root-hair tip growth of soybean (Brechenmacher et al. 2009). Induction of actin isoform B in leaf, hypocotyls and roots of drought-stressed soybean seedlings was recently reported wherein it was hypothesized that actin was involved in repairing drought-induced injuries to plant membranes (Mohammadi et al. 2012). Nevertheless, the results observed in the present study, demonstrate that regulation of cytoskeleton related proteins are essential during drought stress adaptation in crop plants.

In contrast to actin and tubulin, expression levels of another important enzyme responsible for cell structure modification, xyloglucan endotransglucosylase (XET) (spot7)

was enhanced during D3 and subsequently was suppressed during D6 (when compared to D3) but remained higher than the D0 values and even enhanced further upon re-watering. Previous studies on root growth patterns during drought stress have indicated that changes in the cell wall properties play a crucial role in maintenance of root growth in low soil water potentials (Bracale et al. 1997, Wu and Cosgrove 2000, Shimazaki et al. 2005, Leucci et al. 2008). Xyloglucans form the primary cell walls of most seed plants along with cellulose microfibrils and pectin (Campbell and Braam 1999, Rose et al. 2002). Xyloglucan domains interact specifically with cellulose microfibrils through hydrogen bonds and this interaction requires a conformation change in the xloglucan chain from twisted to flat ribbons so that its surface becomes complementary to the cellulose microfibrils (O'Neill and York 2003). The enzyme XET catalyzes transglycosylation or hydrolysis of xyloglucan molecules during cell growth and thus considered as the primary mechanical determinant of cell wall extension in dicots which is particularly important in case of roots as they have to maintain their growth and elongation to maximize water uptake in drying soil (Van Sandt et al. 2007, Thompson and Fry 2001). XET was found to be induced in response to different environmental stimuli including heat shock and cold stress (Xu et al. 1995, Wu et al. 1996). However a recent study on soybean seedlings, grown under low water potentials, showed decreased XET activity in the hypocotyls elongation region (Wu et al. 2005). There were strong evidences in support of additional role of XET in cell wall biogenesis and reinforcement apart from its traditional function of wall loosening and extensibility (Thompson et al. 1997, Bourquin et al. 2002). Moreover, transgenic studies demonstrated that over-expression of XET imparts tolerance in transgenic plants under various abiotic stress conditions which could be attributed to its involvement in cell wall strengthening and subsequent protection of mesophyll cells against water deficit conditions (Wu and Cosgrove 2000, Cho et al. 2006). The expression patterns of the root growth and morphology-related proteins describes that actin, tubulin expression and XET activity were probably complementing each other at different levels of stress intensity to alter the root growth rate under different stress intensities.

However, the exact mechanism on how these proteins affects the root growth rate during progressive drought needs further investigation.

Plants synthesize well-defined carbohydrate-binding proteins (lectins) in response to biotic and abiotic stress conditions (Lannoo and Van Damme 2010). Plant lectins are a heterogeneous group of proteins classified together on the basis of their ability to bind in a reversible way to well-defined simple sugars and/or complex carbohydrates. There are evidences to support that plants respond to specific biotic or abiotic stimuli through the expression of cytoplasmic and/or nuclear plant lectins which were involved in specific endogenous protein-carbohydrate interactions, leading to the idea that lectins might be involved in cellular regulation and signaling (Shakirova et al. 1998, Van Damme et al. 2004). In *O. Sativa*, a mannose-specific jacalin-related lectin was induced in roots and sheaths in response to salt and drought stress (Claes et al. 1990). Lectins were also found to be expressed in response to jasmonic acid, ABA and fungal infections (Zhang et al. 2000). In banana and maize proteome analysis, up-regulation of euonymus lectin domain was observed in response to osmotic stress (Riccardi et al. 2004, Carpentier et al. 2007). All these observations suggest that lectins play an important role in stress-related physiological processes. However, the actual role of lectins under drought stress is not yet completely established. In our study, we found a very interesting expression pattern of the legume lectin (spot 1, 2) which were significantly up-regulated on D3, maintained the same levels during D6 and continued to increase their expressions during recovery period. Based on our observations, we hypothesize that under drought stress, lectins were over-expressed due to their possible involvement in the endogenous cellular regulation and signaling pathways which may assist in imparting adaptive advantages to the plant under low water regimes and also helps in normal growth and development of the plant.

Flavonoids are a group of plant polyphenolic secondary metabolites, known to be involved in various plant growth and developmental processes, including pollen tube

germination, UV light protection and pathogen resistance. An important enzyme involved in the flavonoid biosynthetic pathway, chalcone isomerise (CHI) (spot 11) which isomerizes chalcone to form the flavonone naringenin, was highly down-regulated under drought stress conditions and failed to recover completely even on re-watering. Flavanoids are also known to mediate communication between soil bacteria and plant roots and thus assist in the formation of root nodules (Stafford 1997). Drought stress is known to affect nitrogen fixation and root nodule activity through various complex mechanisms (Abdel-Waheb et al. 2002; Marino et al. 2007). CHI might play an important role in the overall process of nitrogen fixation and a decrease in the activity of this enzyme may interrupt the initial signal communication between the host (legume) and the symbiont (*Rhizobium*) for establishing a successful association which is required for proper nodule formation and nitrogen fixation. Interestingly, in the present analysis, we also observed a significant reduction in the root nodule number and mass in response to progressive drought stress.

Drought stress is known to imbalance the cellular redox homeostasis and thus leads to formation of reactive oxygen species (ROS) and reactive aldehydes such as 4-hydroxy nonenal (HNE) and methylglyoxal, causing oxidative damage to cellular structures (membrane lipids and proteins). In response, plants develop ROS scavenging mechanisms to cope with the oxidative stress. SOD is an essential antioxidative enzyme which dismutates two superoxide radicals to produce hydrogen peroxide and oxygen. Over-expression of different types of SODs was shown to confer protection against oxidative stress (Bowler et al. 1992, McKersey et al. 1996). In this study, we observed up-regulation of Cu/Zn SOD (Spot 8) during D3, which slightly declined during further continuation of the stress treatment (D6) and maintained the same expression levels even after re-watering (6R). Another enzyme aldehyde reductase (spot 3) showed up-regulation during the initial stress period (D3) but its expression levels were suppressed during later stages of water withdrawal. Ectopic over-expression of aldehyde reductase was known to detoxify the highly toxic lipid peroxide degradation products, such as HNE in transgenic tobacco plants under low temperature and cadmium stress (Hegedus et al. 2004).

Hideg et al. (2003) have demonstrated the role of aldehyde reductase during drought and UV-B stress in transgenic tobacco. The results indicate that endogenous aldehyde reductase could provide protection against oxidative stress only up-to a certain level of stress intensity but if the protein is over-expressed, it could possibly enhance the drought tolerance level to a significant extent. From the expression patterns of the above enzymes we can assume that *V. radiata's* defense strategy against oxidative stress through over-expression of antioxidative enzymes was limited only to moderate drought stress levels (D3). Expression levels were not further enhanced upon severe drought stress (D6) which could be due to the inhibitory effects of the higher oxidant levels.

Oxidoreductases represents a superfamily of enzymes which primarily catalyze any reaction involving redox changes of the substrates including signal transduction, metabolic pathways as well as stress defense mechanisms (Jacquot et al. 2009). Here, we observed that the expression patterns of a particular oxidoreductase which contains two domains namely NADB Rossmann (NADP + binding dehydrogenase) superfamily and Gfo_IDH_MocA_C (Glucose fructose oxidorectase, myo-inositol dehydrogenases superfamily (spot 9) was up-regulated under progressive drought stress.The presence of the above two domains in the identified protein indicates its possible role in the plant metabolic pathways. The expression pattern of this enzyme under progressive drought stress signifies its importance in the maintenance of primary metabolism in plants during stress conditions.

Protein synthesis is one of the major metabolic pathways to be affected by drought stress. We observed that a mitochondrial translational initiation factor (spot 17) is initially down-regulated (D3) but later its expression levels were enhanced on subsequent water withdrawal (D6). However, upon re-watering, the expression levels declined again and were almost equivalent to D3 expression value. Interestingly, similar expression patterns were observed for heat shock protein-90 (spot 16), except that upon re-watering the expression levels became almost equal to the control. HSP-90 is known to be associated with protein folding by acting as a chaperone under different abiotic stress

conditions (Wang et al. 2004). The present study reveals that drought susceptible food legumes induce these proteins only at a later stage of drought stress period. The V-ATPase at the tonoplast of higher plants is a complex multi-subunit enzyme that establishes and maintains an electrochemical proton gradient across the membrane which is the driving force for various transport processes of electrically charged as well as neutral solutes. Apart from being the essential housekeeping enzyme, it also performs certain special turgor-dependent mechanisms such as extension, growth and movements like that of stomatal guard cells and pulvini. It is also known to have dynamic plasticity with respect to its structure under different abiotic stress conditions (Lüttge et al. 2001). In the present study only one subunit *i.e* subunit E of V-ATPase (spot 4) was highly up-regulated exclusively during short term water-deficit conditions (D3). Enolase is an essential glycolytic enzyme that catalyzes the dehydration of 2-phosphoglycerate (2-PGA) to phosphoenolpyruvate. This enzyme has been known to have various isoforms and was expressed more in roots than in leaves. It was reported to be up-regulated under hypoxic conditions when the plants shift their carbohydrate metabolism from oxidative pathway to fermentative pathway (Van Der Straeten et al. 1991). Up-regulation of this enzyme under PEG treatment and salt stress in rice root was also reported (Yan et al. 2005, Wang et al. 2007b). However, we recorded down-regulation of enolase (spot 10) during D3, which enhanced its expression level on D6 when compared to D3. Enolase quantity remained lower than the control which might be due to the susceptible nature of *V. radiata* towards drought or the protein identified here could be a different isoform of enolase. However, nature of the initial down-regulation of this enzyme as observed in our study, needs further investigation.

Methionine is a sulfur-containing amino acid which serves as the building block of proteins and also as a component of the universal activated methyl donor, S-adenosyl methionine. The enzyme, methionine synthase (MS) catalyzes the last step of methionine synthesis pathway (Ravanel et al. 2004). Induction of MS under various abiotic stresses in certain plants has been previously reported (Narita et al. 2004). In the present study, there

was significant down-regulation of the MS (spot 18) on D3 but the expression levels enhanced upon D6. Similarly, another spot which corresponds to cobalamine-independent MS (spot 19), which catalyzes the same step but does not require the intermediary methyl donor (vitamin B_{12}) was also highly down-regulated during the D6. But on subsequent water-withdrawal for 6 days, expression levels of this protein enhanced considerably. Increased activities of this enzyme might be required for maintaining the methionine biosynthetic rates during severe stress conditions as it serves the substrate for many essential metabolic reactions during plant growth and development.

In conclusion, the above proteomics-based study of the dynamic expression patterns of the root proteins of *V. radiata* provides an insight into the regulatory mechanisms of the plant under different levels of drought stress intensity. Our results clearly demonstrate that under different levels of drought stress intensity, components of both primary and secondary metabolic pathways of the plant were dynamically regulated and these responses are highly complex and inter-related. Primarily, the root proteins involved in the root architectural changes, energy metabolism, ROS detoxification, primary as well as secondary metabolite biosynthetic pathways and cell signaling were differentially regulated during progressive drought stress. The present data also provide a snapshot of the root responses of *Vigna* under varying water-deficit levels, which could be beneficial for further research to have a comprehensive understanding of highly complex drought stress-induced responses, involving an array of signaling pathways.

CHAPTER 4

Functional analyses of drought-induced ROS detoxifying NADPH-aldehyde reductase (VrALR) to understand its protective role in *V. radiata* roots

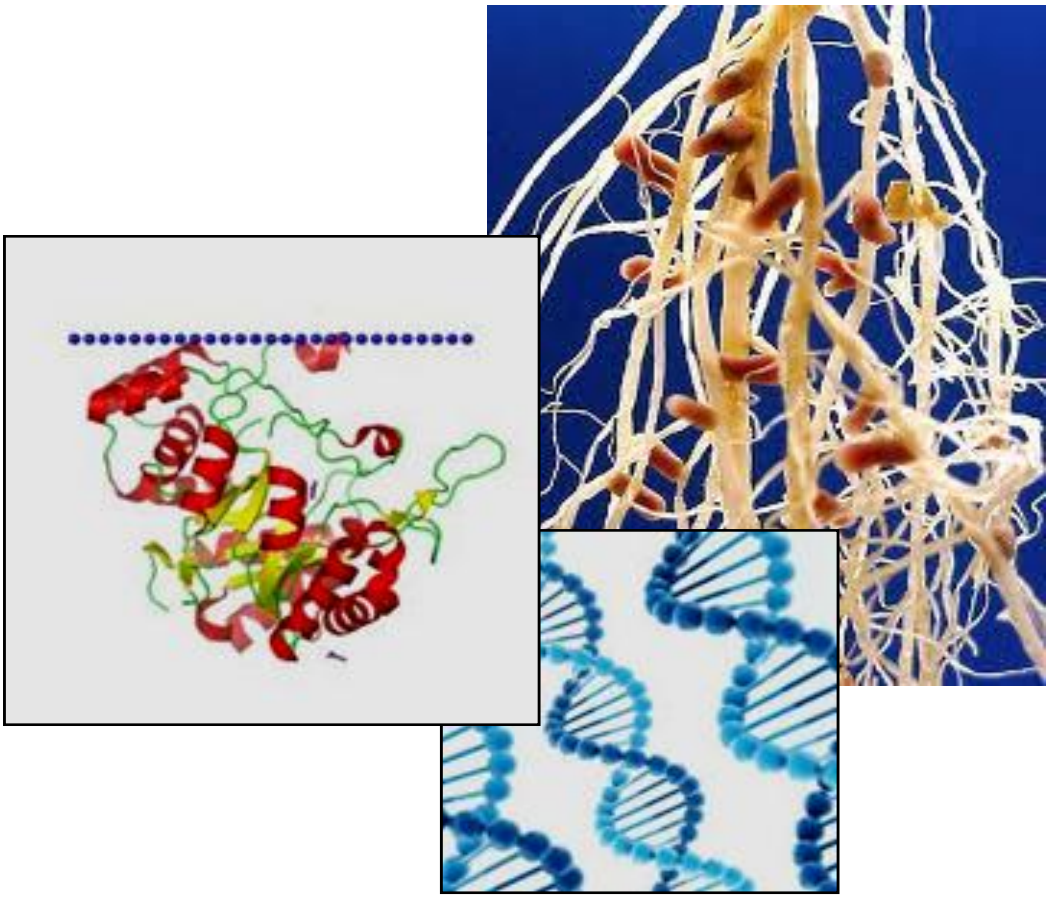

Oxidative stress due to elevated levels of ROS is an inevitable consequence of drought stress which was frequently encountered by plants. It is therefore widely accepted that prevention or decline in ROS accumulation during abiotic stress conditions, is a promising strategy for engineering stress-tolerance in plants. Primary targets of ROS are the polyunsaturated fatty acids (PUFA) present in the membrane phospholipids of plants which gets peroxidised by ROS (lipid-peroxidation) and subsequently a self propagating chain of free radical reactions are produced giving rise to several alkenals, hydroxyalkenals and reactive aldehydes (Winger et al. 2007). Previous studies reported that lipid peroxidation-derived reactive aldehydes were usually more stable than ROS and causes significant damage to proteins and other sub-cellular compounds (Skibbe et al. 2002). Among different reactive aldehydes produced, 4-hydroxy-2-nonenal (HNE) was considered to be the most abundant and toxic aldehyde which was generated through oxidation of linoleic acid of plant membranes. Another common by-product of lipid-peroxidation is malondialdehyde (MDA), which was usually considered as as a highly toxic indicator of ROS-induced membrane damage. In mammalian systems, a group of enzymes belonging to the aldo-keto reductase superfamily detoxifies HNE and also reduces the cytotoxic methylglyoxal to acetol and subsequently to propane-di-ol (Vander Jagt et al. 1995). Apart from detoxifying reactive aldehydes, this group of enzymes are known to catalyze the production of sorbitol from D-glucose and thus can also act as potential osmoregulators during drought-induced osmotic stress conditions.

Aldo- keto reductase superfamily: General characteristics

Aldo-keto reductase (AKR) superfamily possesses a total of around 42 oxidoreductases as its members including, seven 3α-hydroxysteroid dehydrogenase (HSDs), seven aldose reductases (ADRs), six aldehyde reductases (ALRs), three plant chalcone reductases (CHR), apple sorbitol-6-phosphate reductase, two 2,5-diketo-gulonate reductases, a putative reductase from *Leishmania*, human liver bile acid binding protein, bovine lung prostaglandin F synthase, bovine dihydrodiol dehydrogenases, frog lens crystallin, a mouse vas deferens protein, two xylose reductases from yeast, 4- dihydromet-

-hyltrisporate dehydrogenase from *Mucor mucedo,* yeast GCY protein, an inducible protein from Chinese hamster ovary cells, a murine protein induced by fibrobroblast growth factor-1, and an ethoxyquin-inducible aflatoxin B1 aldehyde reductase (reviewed by Jez et al. 1997). These proteins were found to form six distinct groups within the AKR superfamily through Cluster analysis and among them the largest and most studied group comprises of plant ALRs apart from mammalian ALRs, HSDs and ADRs. It was reported that members of AKR superfamily retain a common three dimensional fold in their protein structure and X-ray crystallographic studies confirmed the presence of an identical $(\alpha/\beta)_8$ barrel-fold in the protein structure. ALRs reduce a range of substrates using NADPH as cofactor and the reduction mechanism involves 4-pro-R-hydride transfer from NADPH to the substrate carbonyl and protonation of the oxygen by a general acid residue of the enzyme. In plants, members of ALR and ADR gene families were found to be induced during several abiotic stress conditions (Kirch et al. 2001). For example, in cultured bromegrass cells, freezing-tolerance was found to be associated with induction of high levels of aldose reductase gene (Lee and Chen 1993), while during the dessication phase of embryogenesis in mature embryos of barley, aldose reductase gene was expressed (Bartels et al. 1991). Though a wide range of aldehyde compounds were identified as putative substrates for these enzymes, actual physiological targets for most of the members still remain unknown.

Plant aldehyde reductases (ALRs)

Plant ALRs (EC 1.1.1.21) are cytoplasmic, monomeric proteins which share high sequence similarity with aldose reductases, belonging to the same superfamily. Although both are known to catalyze the NADPH-depedent reduction of aldehydes, ketones and trioses, the former is preferential towards aromatic aldehydic substrates (Colrat et al. 1999a, 1999b; Simpson et al. 2009). It was reported that *ALR* gene from the model legume *Medicago sativa,* was accumulated to higher levels in response to ABA treatment, osmotic stress, cadmium and also by ROS generating chemicals. Biochemically, MsALR enzyme was reported to show comparatively higher resemblance with human aldose reductase in

several aspects, than barley aldose reductase (Olsen et al. 2008). Moreover, recombinant MsALR protein was found to metabolize HNE efficiently like mammalian homologues. However, the activity was comparatively lesser. Nevertheless, MsALR enzyme was considered to possess ROS-detoxification potential. The recognition of the creditable role of this enzyme in plants under abiotic stress conditions was further enlightened by different researchers during the last decade, wherein they have ectopically overexpressed the aldehyde reductase (*ALR)* gene in different plants and analysed their tolerance capacity in response to various abiotic stress factors (Oberschall et al. 2000, Kotchoni and Bartels 2003, Sunkar et al. 2003, Rodrigues et al. 2006, Wen et al. 2012). The encouraging results from the above investigations remarkably enhanced our present understanding on plant aldehyde reductases and further re-inforced the assumption, which considers that ALRs could act as a potential targets for generating stress-tolerance in crop plants (Bartels 2001).

Importance of using heterologous systems for plant gene characterization

The functional analysis of plant genes usually involves the use of mutant of the gene of interest and/or through complementation of the loss of function mutant. However, when this approach is not feasible because of the lack of an appropriate mutant, a heterologous system can be adopted (Yesilirmak and Sayers 2009; Farhi et al. 2010). Heterologous expression system includes transfer of plant genes to other host systems for protein synthesis and subsequent functional analysis as it is highly inconvenient as well as cost expensive to isolate protein from plant sources. Among prokaryotic expression systems, *E. coli* is the first and most extensively used heterologous system for protein production owing to its simplicity, rapid growth and relatively lesser cost (Frommer and Ninnemann 1995). Functional expression of plant proteins in *E. coli* was demonstrated mostly through studies on membrane proteins. For example, functional characterization of chloroplast ATP/ADP transporter from *A. Thaliana* was performed in *E. coli* C43 strain which was suitable for membrane protein expression (Tjaden et al. 1998). Low K^+ uptake mutant strains of *E. coli* were used as host for studies on *Arabidopsis* K^+ transporters including AKT2, AtKUp1-2, and AtHKT1 (Uozumi et al. 1998, Kim et al. 1998, Uozumi et al. 2000)

Use of eukaryotic expression system offers additional benefits over prokaryotic system by providing the possibility of post-translational modification of expressed proteins. Being single cell eukaryotic organisms with molecular, genetic and biochemical characteristics almost similar to higher eukaryotes, yeast (*Sachharomyces cerevisiae*) system was widely considered as highly useful heterologous expression system for plant proteins. Thus, a wide range of plant proteins were characterized through functional complementation in different yeast mutant strains (Dreyer et al. 1999, Howarth et al. 2003, Sancenón et al. 2003, Hayes et al. 2007). Hence, for an overall functional assessment of any stress-responsive genes, utilization of heterologous expression system has been highly informative and crucial.

Reports from our earlier study (Chapter 3) using a proteomics approach showed a significant up-regulation of aldehyde reductase protein in roots of *V. radiata* during short-term water deprivation (D3) and its expression levels declined upon extended water-deficit (D6). Our analysis of this protein through MASCOT search showed high sequence similarity with the already reported novel NADPH-dependent aldehyde reductase protein from *V. radiata* which was shown to detoxify a grapevine fungal toxin eutypine (4-hydroxy-3-(3-methyl-3-butene-1-ynyl) benzyl aldehyde). It was reported that the tolerance capcity of different grape genotypes against eutypine-induced toxicity was related to their capacity to detoxify eutypine to its corresponding alcohol, eutypinol (Guillén et al. 1998). However, a detailed study focussing on the comparison of the protective function of this enzyme in heterologous system as well as its actual role in endogenous plant system during abiotic stress conditions has not yet been elucidated. In the present study, we aim to analyse the protective role of VrALR in heterologous as well as endogenous plant system by over-expressing the protein in bacteria and yeast system under different oxidative conditions and simultaneously investigating its endogenous mRNA expression levels and enzyme activities in roots of *V. radiata* during progressive drought stress and re-watering. Our main target through this study was to conceptualize the stress tolerance ability of VrALR by correlative and comparative analysis of the degree of detoxification capacity of this protein using different concentrations of oxidizing agents and varying levels of water-deficit conditions.

Cloning of full length VrALR cDNA from V. radiata roots

Total RNA was isolated from 100 mg of *V. radiata* root tissue using column-based Plant Spectrum RNA isolation kit (Sigma-Aldrich) following manufacturer's instructions. Isolated total RNA (4 µg) was used as template for synthesizing the first strand of cDNA using Revert Aid^{TM} First Strand cDNA synthesis kit (Fermentas life Sciences, St Leon-Rot, Germany). For cDNA synthesis, a 20µL reaction was set up consisting of the RNA template, reaction buffer, oligodT primers, riboinhibitor (RNAse inhibitor), dNTP mix and reverse transcriptase enzyme and incubated at 37°C for 1 h to allow cDNA strand synthesis, followed by 10 min incubation at 70°C to degrade the RNA template in the RNA-DNA hybrid formed. In order to amplify the *VrALR* gene, we designed primers based on the available sequence of *V. radiata* aldehyde reductase in the NCBI GenBank database (Accession no. gi| 5852203|gb|AAD53967.1). In forward and reverse primers, restriction sites BamHI and XhoI were included, respectively (Forward Primer: 5'GTAGGATCCATGAGCACCGCCGCTGGAAAA 3'; Reverse primer: 5'GTACTCGAGTTA AACTTTCAGAAACTTCTTTTC 3'). at the 5' ends based on the multiple cloning sites of pGEX-4T-1 vector (vector map given in **Fig. 25c**). Before selecting the appropriate restriction enzyme, we ensured that there are no internal restrictions sites present within the ORF region of VrALR using the NEB-Cutter software. Upstream to the restriction sites 3 nucleotide overhangs were added for proper enzyme binding respectively. Using these primers, a 978bp long full length cDNA sequence of *VrALR* which consists of the complete ORF region is amplified in a 35 cycles PCR reaction. The PCR program includes initial template denaturation at 94°C for 4 min, followed by denaturation at 94°C for 30 s and annealing at 60 °C for 45 s. Primer extension was done at 72 °C for 1 min 30 s and the final extension at 72°C for 10 min.

The PCR amplified product was eluted from agarose gel using Sigma GenElute Gel Extraction kit following manufacturer's instruction and the gel eluted product was quantified using a Nanodrop ND1000 Spectrophotometer (JL Technologies). Eluted PCR product was then ligated to pTZ57RT vector using TA cloning strategy and transformed

into *E. coli* DH5α. Selection of recombinant colonies were done based on the principle of α-complementation using LB media containing IPTG, X-Gal and 50 µg ampicillin. White recombinant colonies were initially screened using colony PCR with gene specific primers for the presence of insert and plasmid was isolated from the respective positive colonies which were further confirmed through restriction double digestion using BamHI and XhoI to release the insert. Confirmed plasmids were then sent for sequencing. To confirm the identity of the gene, we compared the obtained sequence with the available sequence at NCBI database using Multalin software (Corpet 1988). A three dimensional putative protein model for VrALR was predicted through Geno3D software (www.expasy.com) tool (Combet et al. 2002).

VrALR protein expression and purification

Recombinant plasmid (pTZ57RT + *VrALR*) and the expression vector pGEX-4T-1 were double digested using BamHI and XhoI restriction enzymes and separated on agarose gel. The released *VrALR* insert and the pGEX-4T-1 vector were gel eluted (Sigma GenElute Gel extraction kit), quantified using NanodropND1000 spectrophotometer and then ligated to each other. The ligation reaction was carried out overnight at 4°C. Ligated product was initially transformed into *E. coli* DH5α cells and selected on LB media plates containing 50µg ampicillin. Observed colonies were first screened using colony PCR, with gene specific primers and then the respective plasmids from positive colonies were subjected to restriction digestion confirmation using BamHI and XhoI. Confirmed plasmids were then transformed into *E.coli*BL21 cells for protein expression and positive colonies were screened through colony PCR.

Overnight primary culture containing the recombinant plasmid (pGEX-4T-1+ VrALR) was inoculated (1%) to 250 mL LB broth with 50µg ampicillin as the selection marker and incubated at 37°C with shaking till the OD at 600 nm reached 0.5-0.6. At the appropriate OD_{600}, secondary culture was induced using 1 mM IPTG and incubated further at 30 °C for 5-6 h. A similar un-induced (without IPTG) culture was maintained as control. After the incubation period, both cultures were sonicated at 50% amplitude with 1 min pulse for 3

min giving 1 min gap period and then the sonicated culture was centrifuged at 12,000*g* for 30 min to separate the soluble protein containing supernatant from the insoluble aggregate containing pellet fraction.

Purification of the recombinant protein was carried out using Genei^{TM} GST-Fusion protein purification kit (Bangalore Genei, Bangalore, India). CL-agarose column (provided in the kit) was first equilibrated with 10 mL of 1X equilibration buffer and then the culture supernatant was passed through the column to facilitate binding of the GST-tagged fusion protein. Column was then washed with 1X equilibration buffer till the eluted fraction showed no significant absorbance at 280 nm. Fusion protein was eluted with 10 mL of 1X elution buffer containing reduced glutathione (amount as mentioned in the manufacturer's protocol) and ten aliquots of 1 mL each were collected in eppendorf tubes. All aliquots were separated on 12 % SDS-PAGE gels to check for the presence of the purified fusion protein. Recombinant fusion protein was then subjected to thrombin digestion for 4 h at room temperature to remove the GST tag using Thrombin CleanCleave kit (Sigma-Aldrich) following manufacturer's instructions. An aliquot (100 µL) of the thrombin containing slurry was taken in an eppendorf and centrifuged at 2500*g* for 5 min to get the thrombin attached beads to settle down at the bottom. After removing the above supernatant, pellet was washed twice with 500 µL of 1X washing solution (provided with the kit). Then the thrombin beads pellet was suspended gently in 100 µL of 10X washing solution and the purified protein fraction containing 1 mg protein was added and the final volume was made up to 1 mL. The reaction mix was incubated at 37 °C with gentle shaking to keep the thrombin attached beads in continuous circulation for 4 h and the supernatant was separated by centrifugation at 2500*g* for 5 min. All fractions were analyzed through 12 % SDS-PAGE. Protein estimation was done according to Bradford (1976).

Analysis of the oxidative stress protective role of VrALR *in bacteria*

For determining the oxidative stress protective role of VrALR protein in bacteria, cultures containing the plasmid construct pGEX-4T-1+*VrALR* were allowed to grow at 37°C with shaking till 0.5-0.6 OD_{600} was attained, followed by induction with 1mM IPTG and incubated at 37°C for next 10 h. Another culture containing pGEX-4T-1 vector which can express only GST protein was also simultaneously induced under similar conditions. The point of induction with IPTG was considered as 0 h and simultaneously both cultures were supplemented with different concentrations of H_2O_2 and p-nitrobenzaldehyde (p-NB) as oxidative stress factors. The growth patterns of both GST and GST+ VrALR protein expressing cultures were then observed periodically at 1 h intervals by measuring the respective absorbance at 600 nm till stationary growth was observed. A graph was plotted based on the growth rate ($\Delta A_{600}\, h^{-1}$) of GST and GST+ VrALR expressing *E.coli* cultures in order to visualize the effect of each individual oxidative stress factor and the protective role of VrALR in bacterial system.

VrALR aldehyde reducing activity: Enzyme kinetics

The enzyme activity of VrALR was measured according to Guillén et al. (1998) with minor modifications. The decrease in absorbance of the co-factor NADPH at 340 nm at 25 °C was observed for 5 min in a 1mL reaction mixture containing 25 mM Tris-HCl (pH 7.0),100µM NADPH and 100µM aldehyde substrate (cinnamaldehyde, benzaldehyde, *p*-nitrobenzaldehyde). One unit enzyme activity (U) was defined as the amount of NADPH (µM) utilized in 1 min. A constant protein concentration of 50 µg was used for all reactions. Substrate (aldehydes) and cofactor (NADPH) concentrations were varied from 100-500 µM and the initial reaction velocities were used for determination of K_m values. Assuming Michaelis-Menten type performance of the enzyme, other kinetic parameters (V_{max} ,K_{cat} and K_{cat}/K_m) were calculated. For the expressed VrALR protein, no significant change was observed in aldehyde reducing activity of recombinant fusion protein and

thrombin cleaved pure protein as GST has no role in reducing the given aldehyde substrates.

For determining the aldehyde reducing activity in crude root extracts, we followed the extraction method described by Negm (1986) with minor modifications. Frozen root tissue (1g) was homogenized in 3 mL of extraction buffer containing 0.2M Tris-HCl buffer (pH 8.0), 1 mM DTT, 10 mM isoascorbate and 1% PVP. Homogenate was centrifuged at 12,000*g* for 45 min at 4 °C and the supernatant was used for analysis of enzyme activity by observing the rate of oxidation of NADPH at 340 nm using p-NB as substrate and 50 µg of crude root protein extract as the enzyme source.

Yeast transformation and analysis of detoxification potential of VrALR in yeast

Recombinant plasmid pGEX4T-1+ *VrALR* and the yeast expression vector p424 containing the glyceraldehydes-3-phosphate dehydrogenase (GAPDH) promoter, were double digested with BamHI and XhoI restriction enzymes and separated on agarose gel. Digested vector (p424) and insert (*VrALR*) were eluted from the gel using Sigma GenElute Gel extraction kit and ligated to each other using T4 DNA ligase for overnight at 4 °C. Ligated product was subsequently transformed into *E.coli* DH5α cells and positive colonies were selected based on ampicillin resistance and further confirmed through restriction digestion using BamHI and XhoI. Confirmed clones containing the recombinant plasmid construct (p424+ *VrALR*) were used for transformation of yeast (*Saccharaomyces cerevisiae*) strain W3O3-1-A [MATa(leu2-3,112 trp1-1 can1-100 ura3-1 ade2-1 his3-11,15)] which possesses a ybp1-1 mutation that abolishes the function of Ybp1p (Yap1-p binding protein) and thus makes the strain sensitive to oxidative stress. Yeast transformation was done using frozen EZ-yeast transformation II™ kit (Zymo Research, http://www.zymoresearch.com) following manufacturer's instructions. Transformants were selected on complete synthetic medium (SD) lacking tryptophan (SD-Trp) which is the selection marker for p424 vector.

For the functional analysis, yeast cultures in SD-Trp media containing only p424 vector and the p424+*VrALR* plasmid construct were grown overnight at 30°C and the OD_{600} was observed. Considering presence of 2×10^7 cells for 1.0 OD_{600}, numbers of cells in both the cultures were adjusted to 5×10^5 cells and were serially diluted at 1:2 ratios till 5^{th} concentration. From each diluted series, 5µl aliquot was spotted on SD-Trp plates (without any supplements) which served as control and SD-Trp plates supplemented with 200µM H_2O_2 and 100µM p-nitrobenzaldehyde (p-NB) as test samples. As p-NB was dissolved in ethanol, we have also spotted transformed cultures on SD-Trp plates supplemented with equal amounts of ethanol as used for preparation of 100µM p-NB to exclude the possibility of ethanol-induced effect on the yeast growth.

Quantitaive RT-PCR of VrALR expression during progressive drought stress and recovery

Real time qRT-PCR analysis was done on Eppendorf Realplex MasterCycler (Eppendorf, Hamburg, Germany) using the KAPA SYBR FAST (Mastermix (2X) Universal) (KAPA Biosystems, Woburn, USA) real time PCR kit using SYBR green as the fluorescence dye following the manufacturer's instructions. Primers (Forward primer: 5' TGGTTACAATGAACCCAGCA 3'; Reverse primer: 5' AATATGGGCCAATGCAACAT 3') were designed based on the obtained *VrALR* cDNA sequence to amplify a 158 bp product using Primer3 software. Total RNA (1 µg) was extracted from *V. radiata* root tissue at different stages of drought stress (D0, D3, D6) and recovery treatment (6R) and quantified using Nanodrop ND1000 spectrophotometer. From all the test samples, 1 µg RNA was taken as template for synthesizing the first strand of cDNA using Revert Aid^{TM} First Strand cDNA synthesis kit (Fermentas life Sciences).

For real time PCR, triplicate reactions for each stress point were kept with 50 ng of cDNA as template. Background calibration was done using AxyGen real time PCR strip tubes with domed caps. Amplification of the 158 bp *VrALR* gene fragment was done using a qPCR program which included one cycle of 2 min at 95°C for initial denaturation, followed by 40 cycles of 15 sec at 95°C for denaturation, 30 sec at 55°C for primer

annealing and 20 sec at 72 °C for extension, followed by the dissociation (melting) curve to ensure absence of any primer dimers which can give false fluorescence with SYBR green dye. Fluorescence readings were captured using the Realplex software (Eppendorf). Alterations in the mRNA expression levels of *VrALR* gene in *V. radiata* (relative quantification) during progressive drought stress and recovery in comparison to the well-watered D0 plants was calculated according to the $2^{-\Delta\Delta Ct}$ formula as explained by Livak and Schmittgen (2001). Experiment was repeated thrice with mRNA isolated from different sets of plants subjected to similar stress conditions. Actin (ACT) gene from *V.radiata* was used as the internal control and a validation experiment was performed to ensure equal efficiency amplification for target and reference genes, using different concentrations of template DNA according to Applied Biosystems User Bulletin No. 2(P/N 4303859).

Two-dimensional gel electrophoresis (2DGE) and protein identification (MALDI-TOF-TOF)

Total root proteins from *V. radiata* were isolated and analyzed using 2DGE and MALDI-TOF-TOF mass spectrometry. Among the identified proteins, one spot corresponds to NADPH-dependent aldehyde reductase from *V. radiata* as per the NCBI GenBAnk database which showed significant up-regulation during medium (D3) drought stress. Methods used for 2DGE and identification of the proteins through MALDI-TOF-TOF and Mascot search engine was described in detail in the previous chapter (Chapter 3).

Statistical analysis

All quantitative values for VrALR enzyme kinetics, crude enzyme activity and real time qPCR analysis were represented as mean ± standard deviations with sample sizes of *n* = 3. For enzyme kinetics, non linear regression analysis using global curve fit model for Michaelis-Menten equation (y = a*x/b+x) was used for determination of V_{max} and K_m values, where "y" is the initial reaction velocity, "x" is substrate concentration and the coefficients "a" and "b" correspond to V_{max} and K_m, respectively.

RESULTS

Cloning and sequence analysis of full length cDNA sequence of VrALR from V. radiata roots

Using direct primers, a 978 bp long *VrALR* fragment was PCR amplified by using *V. radiata* root cDNA (**Fig. 21a**). PCR product was further cloned to pTZ57RT vector and transformed into *E. coli* DH5α. Positive colonies showing the presence of the insert (*VrALR*) in colony-PCR screening with gene specific primers were selected for plasmid isolation (**Fig. 21b**). Isolated plasmids were further confirmed through restriction digestion with BamHI and XhoI and the digestion products showing two clear bands of the plasmid vector (pTZ57RT) and the insert (*VrALR*) were finally sent for sequencing (**Fig 21c**). The obtained VrALR cDNA sequence (978 bp) containing the complete open reading frame (ORF) sequence from *V. radiata* roots showed 100% sequence similarity with the available *ALR* gene sequence (gi| 5852202|gb|AF033851.1) at NCBI GenBank database (http://www.ncbi.nlm.nih.gov). The *VrALR* ORF encodes a 325 amino acid long protein, having a theoretical molecular weight of 35.6 kDa and 6.3 pI. The protein BLAST analysis of our protein sequence showed 100% sequence similarity with the available sequence from *Vigna radiata* (gi|5852202|gb|AAD53967.1), 99% with CPRD14 protein (*V.unguiculata*), dihydroflavanol-4-reductase like protein (*Glycine max*) and cinnamamoyl CoA reductase like protein (*Populus trichocarpa*) and 98% with phenylacetaldehyde reductase (*Rosa X damascena*). The protein belongs to the NADB-Rossmann superfamily, having conserved NADPH binding, substrate binding and active sites.

VrALR protein expression and enzyme kinetics

Through sequence analysis, identity of the cloned 978 bp PCR-fragment (*VrALR*) was confirmed as NADPH-dependent aldehyde reductase and then excised from the TA vector (pTZ57RT) and re-cloned into expression vector pGEX-4T-1 and transformed into *E. coli* BL21 cells. Double digested pGEX-4T-1 vector was shown in **Fig. 22a**. Positive recombinant colonies, showing the presence of insert (*VrALR*) were selected for protein induction (**Fig. 22b**). Under control of the Lac promoter of pGEX-4T-1 vector, VrALR

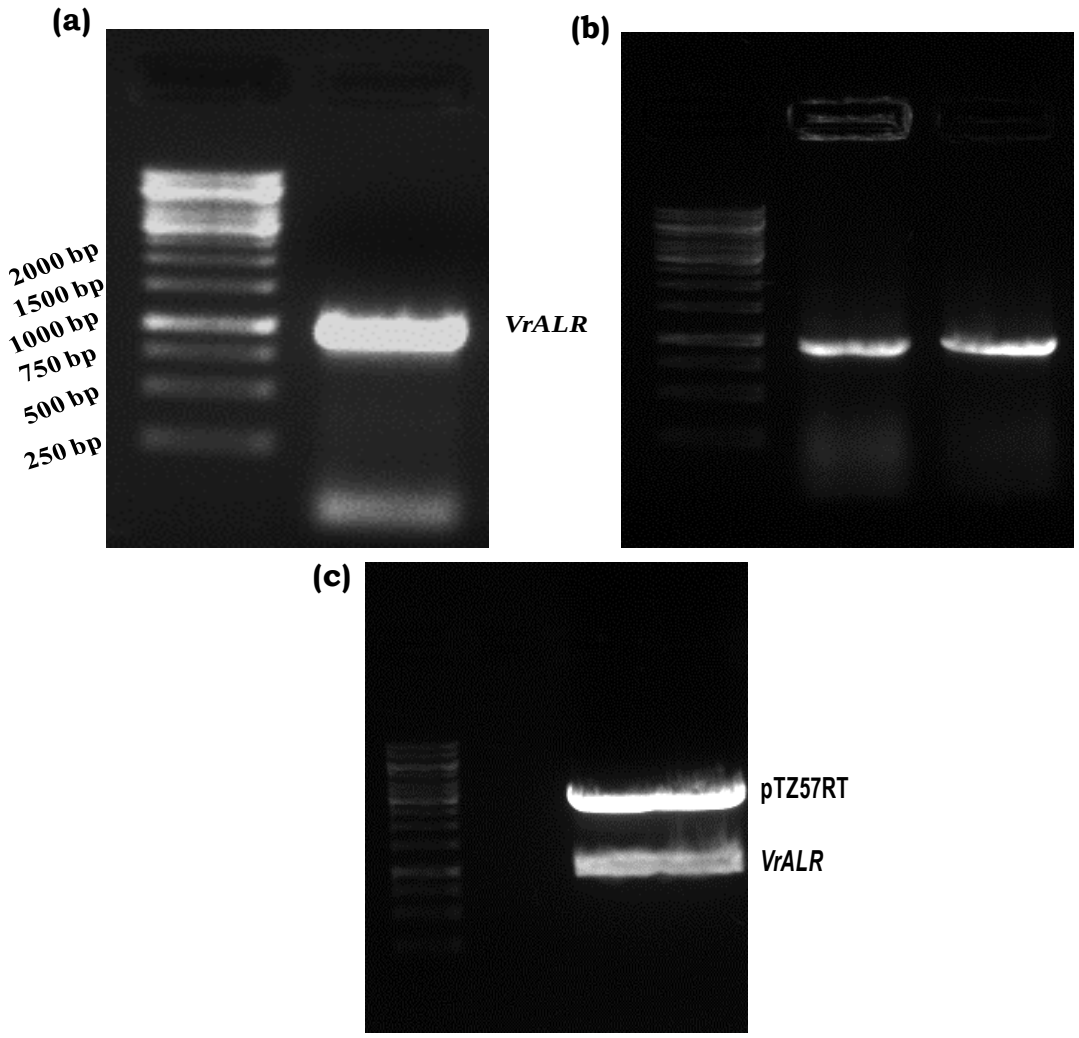

Fig 21. PCR amplification of the complete ORF region of VrALR (978 bp) from roots of *V. radiata* (**a**). Colony PCR result with gene specific primers for *VrALR* (**b**). Restriction digestion with BamHI and XhoI showing two distinct bands of pTZ 57RT vector and the insert, *VrALR* (**c**).

protein was expressed as a fusion protein along with a N-terminal GST-tag. The combined molecular weight of the induced recombinant protein was approximately 62 kDa (26 kDa GST and 36 kDa VrALR). The subsequent purified protein also showed a single band at the same molecular weight range. Further, thrombin digestion of the recombinant protein produced two bands at around 36 kDa (VrALR) and 26 kDa (GST) ranges (**Fig. 22c**).

Aldehyde reducing activity of the purified VrALR protein was analysed by using three randomly chosen aldehydic substrates, p-NB, benzaldehyde and cinnamaldehyde. Purified VrALR showed maximum catalytic efficiency (K_{cat}/K_m) of 38.6 $\times 10^5$ min^{-1} M^{-1} with p-NB as substrate, while a considerably lesser K_{cat}/K_m of 2.6 and 0.8 $\times$ 10^5 $min^{-1}M^{-1}$ was observed with benzaldehyde and cinnamaldehyde as substrates, respectively. Similarly, highest V_{max} of 8.9 µM NADPH utilized min^{-1} and lowest K_m of 4.5 min^{-1} was recorded with p-NB as substrate. Respective values for V_{max} , K_m and K_{cat} for all three aldehyde substrates were given in **Table 4**. Thus, for all functional analysis and enzyme activity from crude extract, p-NB was used as the substrate. The three dimensional model predictions for VrALR showed the presence of 6 parallel β-sheets alternating with 7 α-helices forming a barrel structure with 2 distinct helices being outside this barrel (**Fig. 23**).

Oxidative stress protective role of VrALR in bacterial system

Bacterial (*E.coli* BL21) growth curve response for the culture, expressing the VrALR protein reveals an efficient and significant protective role by maintaining the growth rate to normal levels when compared to the culture expressing only GST. Under non-stress conditions, both GST as well as GST+ VrALR expressing cultures showed almost equal growth rate patterns (**Fig. 24a**). However, in presence of 500 µM H_2O_2 and p-NB, growth rate of GST expressing culture (red line) declined significantly when compared to the VrALR expressing cultures (green line) (**Fig. 24b and c**). Effect of both stressors (H_2O_2 and p-NB) was visible from 3rd h after induction and thus, the overall growth rate during the period of 3-8 h was chosen for analyzing the extent of growth reduction (shaded portion in **Fig. 24b** and **c**). By assuming the growth rate value of the

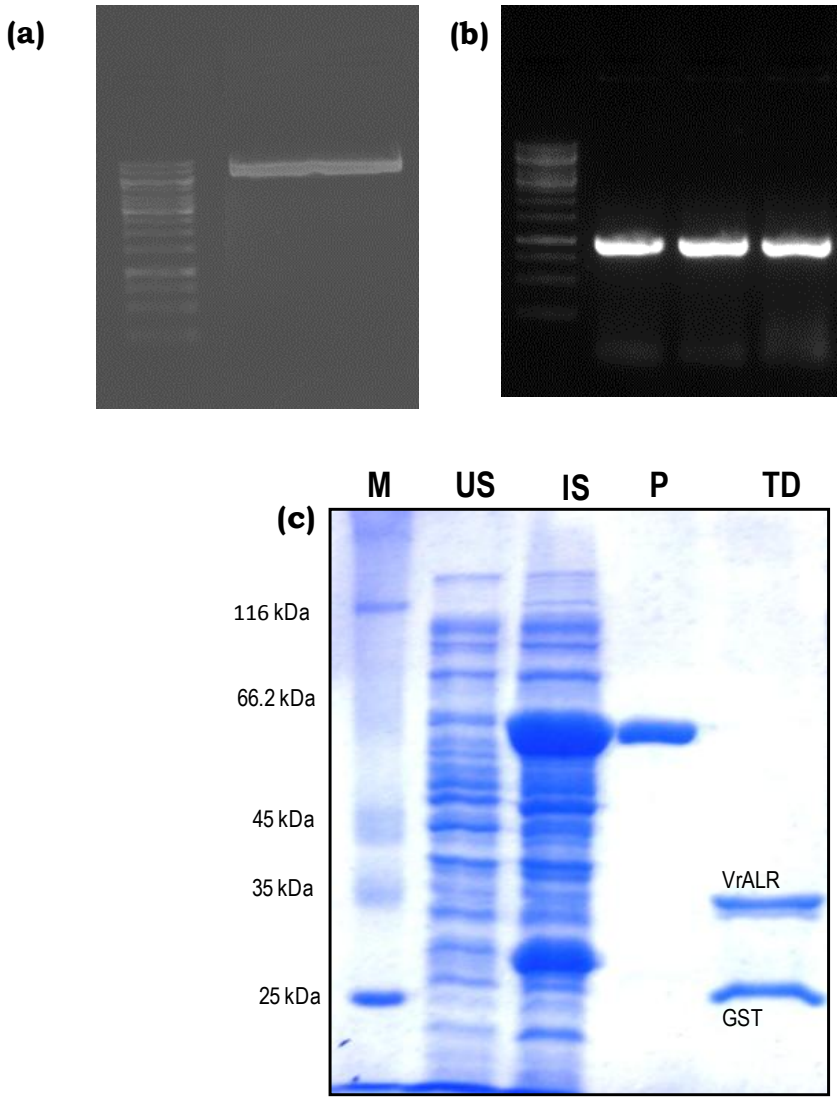

Fig 22. Double digested (with BamHI and XhoI) pGEX4T-1 vector for gel elution (**a**). Colony PCR confirmation result with gene specific primers for screening pGEX-4T-1 + *VrALR* transformed *E. coli* DH5α (**b**). Recombinant GST-tagged fusion protein expression in *E.coli* BL21 cells; M, Protein molecular weight marker (medium range); US, Uninduced sonicate; IS, Induced sonicate; P, purified recombinant fusion protein; TD, Thrombin digested fraction. Arrows indicate the position of the purified VrALR protein (36 kDa) and the cleaved GST tag (26 kDa) (**c**)

Table 4 Enzyme kinetic parameters and catalytic efficiency of VrALR towards different aldehydic substrates. Mean values from three independent experiments were used for analyzing the kinetic parameters through global curve fit method in a non-linear regression analysis using the Michaelis-Menten equation (y = a*x/b+c), where coefficients a and b corresponds to V_{max} and K_m, respectively.

Substrate	V_{max} (µM NADPH utilized min^{-1})	K_m (µM)	K_{cat} (min^{-1})	Catalytic efficiency (K_{cat}/K_m) (10^5 $min^{-1}M^{-1}$)
Benzaldehyde	3.43	25.1	6.7	2.6
p-nitrobenzaldehyde	8.88	4.5	17.4	38.6
Cinnamaldehyde	1.66	121	3.3	0.3

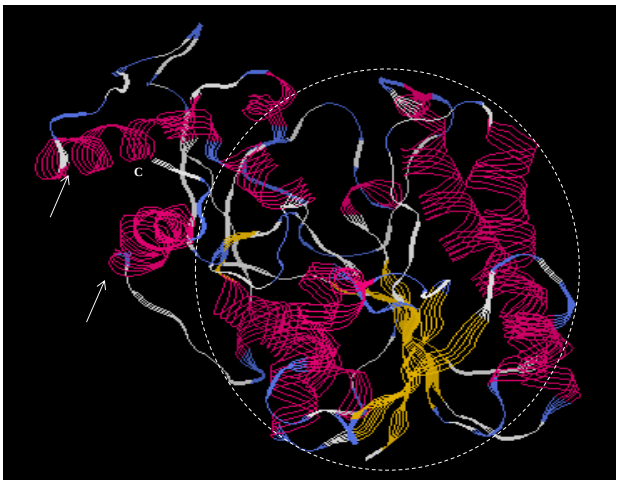

Fig 23. Putative three dimensional VrALR protein model generated using Geno3D software (www.expasy.com) showing the typical structural features of aldo-keto reductase family members. The circle indicates the core barrel type structure made of parallel β-sheets and alternate α-helices with C-terminal end at the top (indicated by C). The two helices present outside the barrel were indicated by arrows.

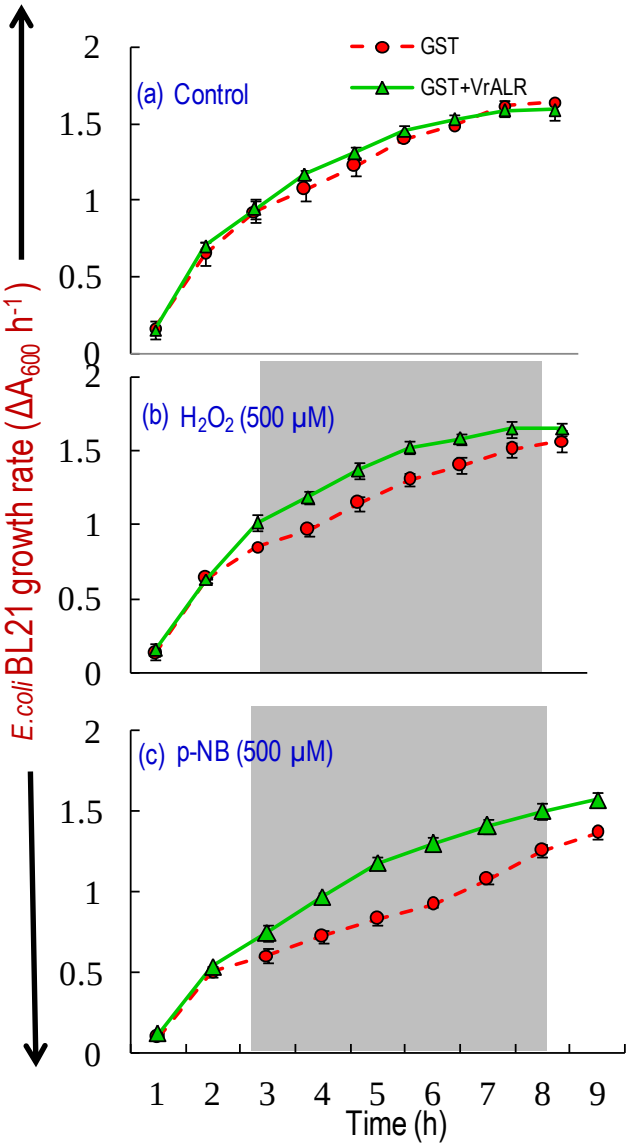

Fig 24. Detoxifying potential of VrALR in *E.coli* BL21 in presence of externally added oxidative stress factors. Bacterial growth rate pattern in absence of stressors, *i.e* control **(a)**, in presence of 500 µM H_2O_2 **(b)** 500 µM p-NB **(c)**. Shaded region indicates the time span (3-8 h) chosen for calculation of the extent of growth reduction.

control (in the absence of stressors) as 100%, we have calculated the relative growth rate percentages (%) for test samples (in presence of stressors). In presence of H_2O_2 and p-NB, the growth rate of GST expressing cultures declined to 85 and 84%, respectively when compared to controls. While the cultures expressing the recombinant protein (GST + VrALR), maintained their growth rates at 95 and 116% when compared to controls in the presence of H_2O_2 and p-NB, respectively. However, at higher concentrations (1mM) of H_2O_2, VrALR failed to detoxify the ROS-induced effects and bacterial growth was inhibited.

Stress response analysis of VrALR expressed in yeast system

The plasmid (p424) carrying the gene of interest (*VrALR*), which was used for W3O3-1-A transformation, was confirmed through restriction digestion with BamHI and XhoI (**Fig. 25a**). In yeast system, VrALR protein was expressed under the control of glyceraldehyde-3-phosphate dehydrogenase (GAPDH) promoter of p424 yeast expression vector. The p424 vector map was shown in **Fig. 25b** and the vector map of pGEX-4T-1 was given in **Fig 25c.** We used the *S. cerevisiae* strain W3O3-1-A [MATa (leu2-3,112 trp1-1 can1-100 ura3-1 ade2-1 his3-11,15)] which possesses a *ybp1-1* mutation that abolishes the function of Ybp1p (Yap1p-binding protein) and thus makes the strain sensitive to oxidative stress. VrALR expressing yeast culture exhibited enhanced tolerance levels in the presence of 200µM of H_2O_2 and 100µM of p-NB when compared to the culture containing only p424 vector. Under control conditions, growth was visible in all the six dilutions in both p424 and p424+VrALR expressing cultures (**Fig. 26a**). In presence of 200 µM H_2O_2 in the culture media, p424 containing culture could grow only up to 4^{th} dilution while VrALR expressing culture continued to grow till the 6^{th} dilution (**Fig. 26b**). Similarly, in media supplemented with 100 µM p-NB, empty vector containing culture failed to grow beyond 4^{th} dilution, while VrALR expressing culture maintained a normal growth trend similar to ethanol controls (**Fig. 26c and d**). However, at higher concentrations of H_2O_2 and p-NB, no growth was observed for both the cultures (p424 and p424+*VrALR*) and hence the results for these concentrations were not included.

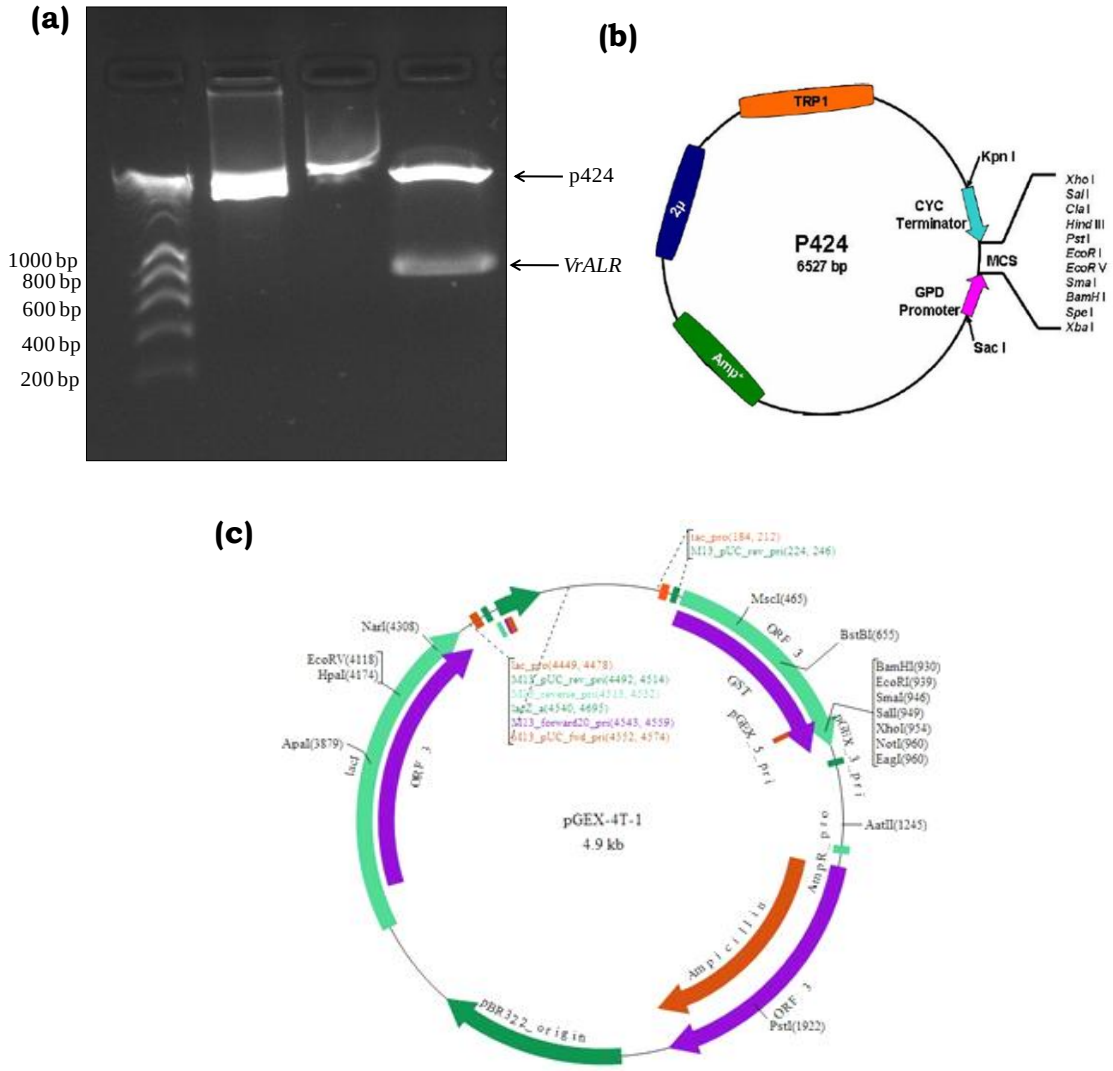

Fig 25. Confirmation of recombinant p424 vector carrying the *VrALR* gene with restriction digestion using BamHI and XhoI enzymes. Lane 1: 1 kb DNA ladder; lane 2: p424 (empty vector); lane 3: p424 vector + *VrALR* (uncut recombinant plasmid); lane 4: digested recombinant plasmid showing p424 vector and the released insert *VrALR*. (**a**); Vector map of yeast expression vector p424 (**b**); Vector map of bacterial expression vector pGEX-4T-1(**c**).

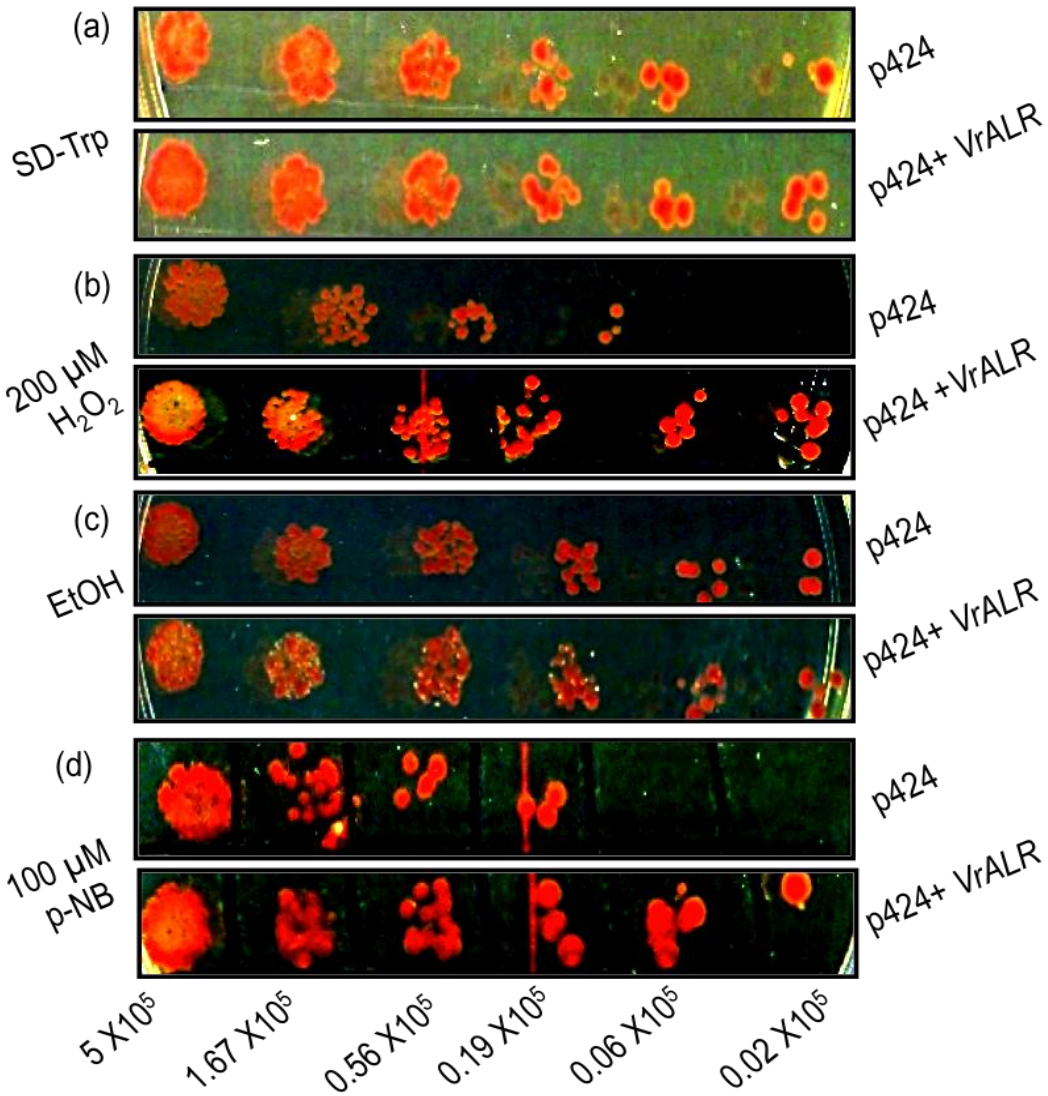

Fig 26. Growth pattern of W3O3-1-A strains harboring only p424 vector and p424+VrALR construct under normal SD-Trp media **(a)**. SD-Trp supplemented with 200 µM H_2O_2 **(b)**, ethanol control (as p-NB was dissolved in ethanol **(c)**, 100µM p-NB **(d)**

Enzyme activity and mRNA expression pattern of VrALR under progressive drought stress and recovery in V.radiata roots

In the 2D profile of whole root proteins of *V.radiata* under similar progressive water-deprivation and re-watering conditions (Chapter 3), we identified a protein spot showing extensive homology with NADPH-aldehyde reductase enzyme and the expression of this protein was found to be significantly induced during D3. The magnified spot image of this protein and the corresponding spot volume (%) with induction factors during different intensities of drought as well as recovery period was shown in **Fig. 27 a** and **b**, respectively. To maintain the continuity in the present study, we observed the enzyme activity and mRNA expression patterns of *VrALR* gene during similar watering regimes. *VrALR* mRNA expression levels showed 1.5 fold up-regulation during D3. However, the expression was down-regulated during higher stress intensity (D6) and recovered only partially upon re-watering (6R) (**Fig. 27c**). With gradual increase in water-deficit (D3 and D6), we observed a concomitant enhancement in the ALR activity levels in roots of *V. radiata*. During D3, ALR enzyme activity increased by more than 1.5 fold and upon subsequent water-withdrawal (D6), the activity levels were enhanced up to 2.6 fold. However, upon re-watering (6R) aldehyde reducing activity declined by around 1.8 fold (**Fig. 27d**).

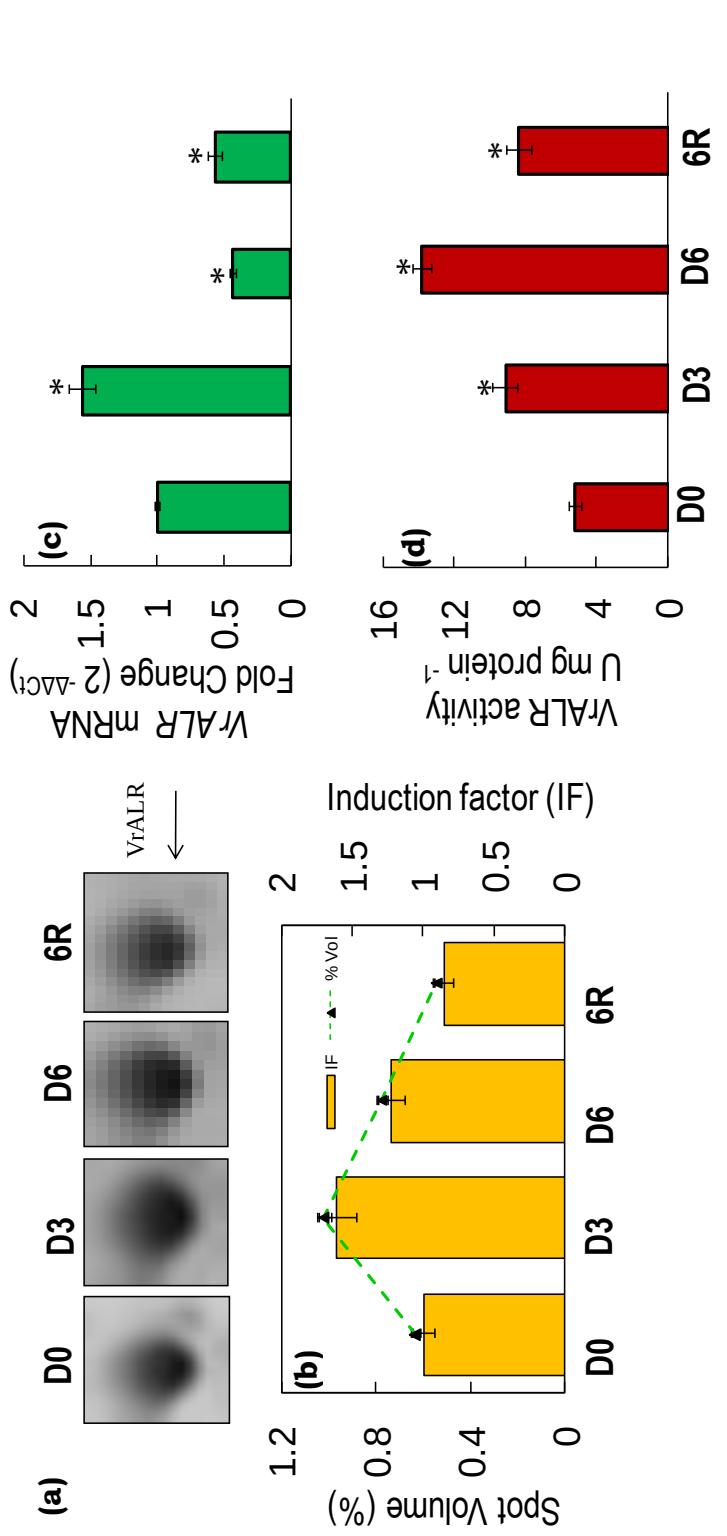

Fig 27. Regulation of endogenous ALR in *V.radiata* during gradual water-defiict and recovery treatment. ALR protein spot in 2DGE from *V.radiata* roots and its expression pattern in terms of spot volume (%) and relative induction factor (IF) during progressive drought and recovery **(a, b)**. Relative fold expression ($2^{-\Delta\Delta C_t}$) of *VrALR* mRNA in *V.radiata* roots under similar progressive drought stress conditions and recovery period **(c)**. Enzyme activity pattern of VrALR in the roots of *V.radiata* under gradual water-deficit (D3 and D6) and recovery period (6R) **(d).** Vertical bars represents mean ± SD with $n = 3$. Significant difference at $^*P < 0.05$ (Student's *t*-test)

DISCUSSION

Majority of the drought-induced damage was implicated through ROS generation and its downstream interactions with major cellular macromolecules. Particularly, lipid membrane oxidation magnifies cellular toxicity through generation of highly toxic aldehyde degradation products and lipid hydroperoxides. Thus, recent upsurge in identifying potential target genes involved in ROS-detoxification pathway in plants, grown under challenging environmental conditions such as drought, proved highly encouraging for plant biologists. In the present study, we analysed the detoxification potential of NADPH-dependent aldehyde reductase from *V. radiata* roots (VrALR) in heterologous systems (bacteria and yeast), challenged with oxidative stress factors. Further, we have also compared the detoxification potential with the endogenous role of *VrALR* gene under progressive drought stress as well as recovery period in roots of *V. radiata*. Results from our study provide a clear and informative picture about the detoxifying potential of this protein and its regulation in crop plants during water deficit regimes.

Various members of the aldo-keto reductase superfamily have been cloned and characterized from different plant species (Bartels 2001, Blanco-Portales et al. 2002). This specific NADPH-dependent aldehyde reductase chosen for the present study was initially identified by Guillén et al. (1998) from *V. radiata* hypocotyls, where they found that it can effectively detoxify the grapevine fungal toxin eutypine which is a complex aldehyde. Subsequently, this protein was purified from mungbean hypocotyls and characterized by Colrat et al. (1999a) where they showed that it was a 36 kDa monomeric protein with a wide range of substrate specificity. The role and possible involvement of this protein during drought stress response of *V. radiata* became evident from our proteomics based study (Chapter 3) during progressive drought stress and recovery period where we observed a significant induction of this protein during D3. In the present study, we cloned and expressed the *VrALR* gene isolated specifically from mungbean root tissue and the identity of the protein was confirmed through BLAST analysis, wherein the expressed protein showed similar homology with the already available sequences of aldehyde reductases from different plant species as reported by Guillén et al. (1998).

Also, the predicted 3-D model for the protein showed more or less a similar basic pattern with a barrel consisting of parallel β-sheets with alternating α-helices, as commonly displayed by the members of aldo-keto reductase superfamily (Jez et al. 1997; Olsen et al. 2008). Based on the K_m values reported by Colrat et al. (1999a), we also checked the aldehyde reducing activity of the expressed protein using three different randomly chosen aldehydic substrates such as benzaldehyde, cinnamaldehyde and p-nitrobenzaldehyde. Our results revealed that purified VrALR showed highest rate of NADPH oxidation (enzyme activity) in the presence of p-NB and the least with cinnamaldehyde, with benzaldehyde being in between. The present kinetic parameters and catalytic efficiencies of the purified VrALR protein with K_m values 121, 25.1 and 4.5 µM for cinnamaldehyde, benzaldehyde and p-NB, respectively were almost similar to the aldehyde reducing activity patterns of the earlier report by Colrat et al. 1999a. Similarity in the kinetic parameters further confirms the identity of the expressed protein in the present study.

Generation of reactive oxygen species (ROS) such as superoxide anion radical (O_2^-), hydrogen peroxide (H_2O_2), and the extremely unstable hydroxyl radical ($^{\bullet}OH$) is inevitable for any aerobic organism. In addition to different potential targets of these highly unstable ROS, including DNA, RNA and protein, oxidation of polyunsaturated fatty acids (PUFA) in membranes resulting in lipid peroxidation is highly damaging for the viability of the cell in both prokaryotes and eukaryotes. Moreover, the reactive aldehydes formed during degradation of oxidized PUFA causes further damage to the cellular proteins and also act as "second toxic messengers" by diffusing to distant cellular targets owing to their comparatively higher stability (Cabiscol et al. 2000). There is evidence for accumulation of reactive aldehydes in bacteria in response to H_2O_2 and thus, it is extremely crucial for the cell to detoxify these highly cytotoxic aldehydes (Semchyshyn et al. 2005). Also, it was reported that oxidative stress-induced lipid peroxidation of bacterial membranes produce toxic aldehydes which were readily diffusible and were able to

inactivate key metabolic enzymes and form DNA adducts resulting in enhanced mutation rates and inhibits DNA replication (Szweda et al. 1993, Chen et al. 1998, Yang et al. 2001). To counteract such deleterious effects, bacteria are known to induce production of a variety of antioxidative enzymes such as catalases, peroxidase and superoxide dimutases (Imlay 2003; Cha et al. 2004). Recently, ALR and SDR group of enzymes belonging to AKR superfamily, have been reported to provide protection against harmful lipid peroxidation-derived aldehydes in bacteria including *E. coli* and *Gluconobacter oxydans* (Pérez et al. 2008; Schweiger and Deppenmeier 2010). In the present study, we observed that *E. coli* cells, expressing VrALR, were able to tolerate externally applied H_2O_2 (500 µM) and maintained their normal growth pattern while for the *E.coli* BL21cultures expressing only GST, growth was inhibited in presence of similar H_2O_2 concentration. However, at higher concentrations (1 mM) VrALR fails to cope up with the given oxidizing stress factor and growth. Our results demonstrate that VrALR expression has successfully complemented the endogenous defence mechanism of *E.coli* BL21 against oxidative stress conditions upto a certain threshold (500 µM H_2O_2), indicating the effective detoxification of the H_2O_2 -induced toxic aldehydes through membrane lipid oxidation. It was reported that an *E. coli* enzyme YqhD, was able to reduce various lipid-peroxidation derived aldehydes including, acrolein, malondialdehyde, and butyraldehyde and overexpression of YqhD protein imparted enhanced cellular tolerance against such toxic aldehydes derived from lipid peroxidation due to H_2O_2, tert-butylhydroperoxide, potassium tellurite, or titanium oxide (Yoon et al. 2002, Semchyshyn et al. 2005, Pérez et al. 2007, Pérez et al. 2008). Our present data further demonstrate that the direct substrate of the purified enzyme, p-NB also inculcates a cell multiplication inhibitory effect on *E. coli* BL21 cells wherein endogenous aldehyde reducing systems were not able to detoxify completely. However, the induced expression of the VrALR protein effectively reduced the cell growth inhibiting aldehyde p-NB, most probably to its less toxic alcoholic form and thus allowing the cells to maintain their normal growth response patterns.

Yeasts (*S. cerevisiae*), owing to their close proximity in metabolic pathways with the multicellular eukaryotic organisms (plants and animals), were often exploited as experimental models for functional characterization of genes from other higher plant or animal systems. Previous reports demonstrated the use of *S. cerevisiae* null mutants for fuctional characterization of plant proteins, especially membrane transporters (Frommer and Ninnemann 1995). In *S. cerevisiae*, oxidative stress response was mediated through transcriptional induction of a variety of antioxidant genes which reduces the toxic levels of ROS and the key regulator of transcriptional induction is the leucine zipper containing-transcription factor Yap1p (Jamieson 1998, Estruch 2000). The specific yeast mutant W3O3-1-A lacks the H_2O_2-specific regulator of Yap1p, known as Yap1p-binding protein (Ybp1p). Thus, in response to H_2O_2, the mutant strain was unable to form the oxidized form of Yap1p and translocation of Yap1p from cytoplasm to nucleus was inhibited. Hence, W3O3 mutant strain could not activate its antioxidant genes and becomes susceptible to oxidative stress (Gulshan et al. 2004). There are several reports on identification and characterization of AKR members from yeast genomes itself, some of which were shown to be up-regulated during stress conditions and more interestingly one of such stress responsive yeast proteins showed similarity with plant dihydroflavonol reductases as well (Garay-Arroyo and Covarrubias 1999; Larroy et al. 2002; Liu et al. 2008; Liu and Moon 2009). Also, *S. cerevisiae* aldehyde dehydrogenase (ADHVI) enzyme showed high catalytic efficiency for aldehyde reduction in the presence of NADPH (Larroy et al. 2002). In the present study, we have induced the expression of cloned *VrALR* gene in this mutant strain to analyze whether the detoxifying ability of this protein (VrALR) is able to complement the mutant phenotype to regain its tolerance against oxidative stress factors, especially H_2O_2 and the aldehydic substrates. Our data clearly showed that VrALR expressing mutant strain displays slightly higher tolerance against H_2O_2 as well as p-NB, when compared to the control strain (without VrALR). Uninhibited growth in control rows (containing only p424 vector) at higher cell concentrations (5×10^5 to 0.19×10^5) could be attributed to the detoxifying ability of the strain's endogenous aldehyde reducing system. However, in comparison with the bacterial system, yeast has shown lower detoxifying

capacity, being able to detoxify only upto 100 and 200 µM concentrations of p-NB and H_2O_2, respectively while bacterial growth pattern was maintained even upto 500 µM concentrations.

Crops usually experience cycles of dry seasons rather than prolonged drought conditions under rain-fed systems. Thus, studies related to drought response mechanisms under varying water deficit conditions are highly crucial (Bogeat-Triboulot et al. 2007; Harb et al. 2010). Reactive aldehydes, formed as a consequence of lipid peroxidation during drought-induced oxidative stress, have been known to act as potential toxic agents causing cellular injury and nucleic acid modifications (Gill and Tuteja 2010; Yin et al. 2010). Thus, a wide range of research initiatives including molecular studies showed novel resistance mechanisms as well as candidate genes responsible for providing tolerance to plants against oxidative stress. However, no real diagnostic marker for stress-tolerance has been reported yet as oxidative stress-tolerance was believed to be a complex quantitative trait. Hence, continuous identification of newer molecular targets for oxidative stress-tolerance becomes highly essential for devising efficient strategies to obtain plants with multiple stress tolerance.

The crucial role of AKR superfamily members, both endogenously as well as in ectopically overexpressed transgenic plants during abiotic stress conditions was well documented. Some AKR members have been described as part of detoxification process while others play a direct role in cellular osmoregulation through osmolyte biosynthesis (Oberschall et al. 2000; Ramanjulu and Bartels 2002; Kotchoni and Bartels 2003; Sunkar et al. 2003; Rodrigues et al. 2006; Huang et al. 2008). In our earlier proteomics-based analysis of the *V. radiata* root proteins under progressive drought and recovery, we observed significant up-regulation of a 34 kDa protein spot with a pI of 5.2 in the 2D-gel during medium water-deficit (D3) condition. This protein was identified as NADPH-dependent aldehyde reductase (*V. radiata*) by MASCOT search engine. In the present study, the importance of the same protein during water-limiting regimes has been investigated further with a concomitant analysis of its detoxifying potential in two

heterologous systems as well as in *V. radiata*. Our results demonstrate that during medium water deficit conditions (D3), *VrALR* gene expression, protein levels as well as enzyme activity displayed a positive correlation with a significant 1.5 to 2 fold up-regulation. Further decline in the soil water content (D6) resulted in a significant down-regulation in the mRNA expression of the gene with a slight decline in the protein content. However, the corresponding enzyme activity showed significant enhancement with increasing water deprivation (D6) and declined upon re-watering. We hypothesize that, *V. radiata* effectively regulates the *VrALR* gene expression in response to short-term water deficit by up regulating its mRNA expression and consecutively the protein content as well as the aldehyde reducing activity. However, higher oxidizing conditions inhibited the gene expression and thus the protein content as well. The continued enhancement in the aldehyde reducing activity of the *V. radiata* root extract during D6 could be due to some other stable proteins with aldehyde reducing enzymatic properties as the possibility of existence of other members of the aldo-keto reductase superfamily in the crude root extract cannot be ruled out.

In conclusion, the present comparative analysis of the detoxifying potential of VrALR in two heterologous systems as well as the progressive drought-induced regulation of this crucial ROS-detoxifying enzyme not only provided an evidence for its differential oxidative stress alleviation capacity but also highlighted the endogenous regulation of *VrALR* in crop plants during gradual water deprivation as well as recovery period. It is established that preventing oxidative stress or reducing the levels of toxic aldehydes proves to be an efficient approach to engineer oxidative stress-tolerant plants which could have be highly beneficial for our present agricultural system. Thus, our data in the present study significantly contribute to the present understanding on ROS detoxifying systems as well as their genetic regulation in crop plants grown under unfavourable environmental regimes and suggest that targeting such detoxification pathways could contribute greatly in plant genetic engineering for abiotic stress-tolerance.

CHAPTER 5

Molecular characterization of key enzymes associated with proline and glutathione biosynthesis in *V. radiata* roots under progressive drought stress and recovery

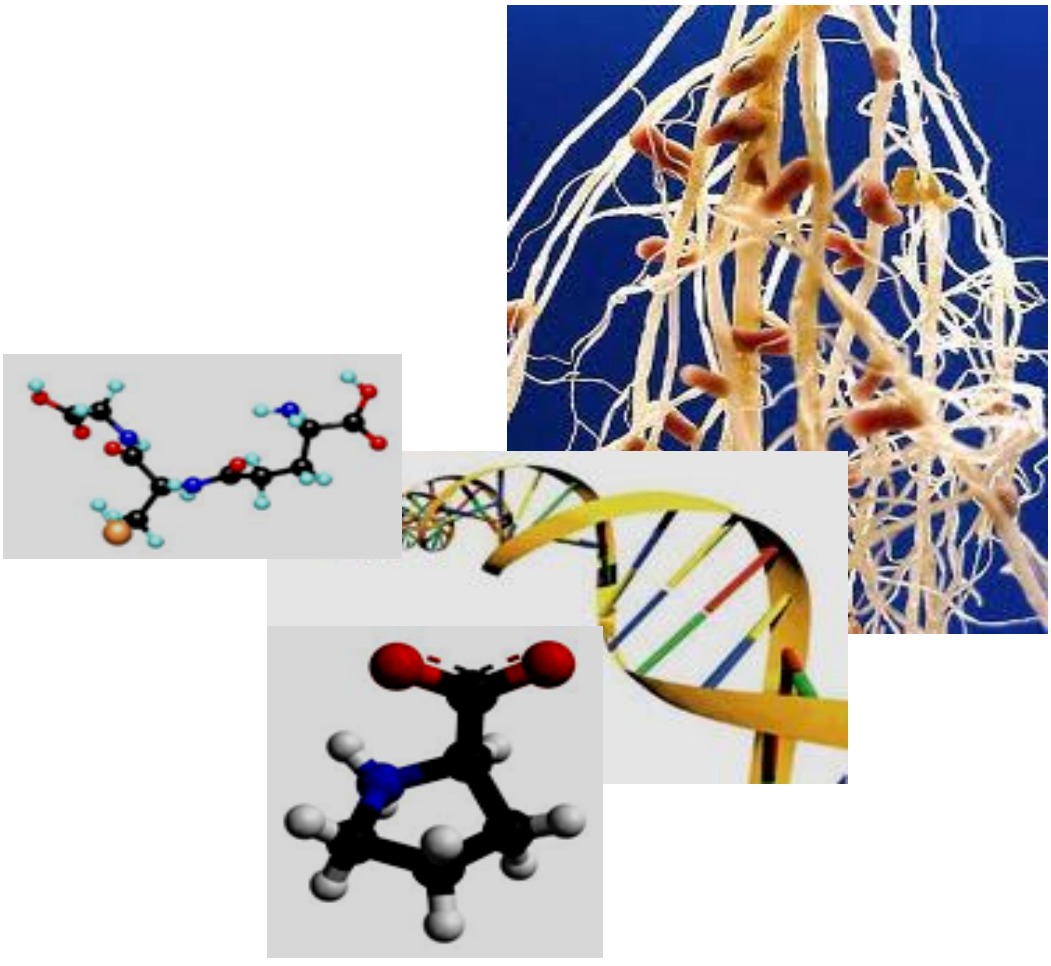

During drought stress, ROS production is enhanced through disruption of electron transport system and oxidation of different metabolic reactions occurring inside chloroplasts, mitochondria and microbodies resulting in oxidative stress conditions (Van Breusegem et al. 2001). Though redox adjustments are central for any drought-induced plant response, the extent of enhancement in the intra-cellular ROS concentrations varies greatly from plant to plant depending on their drought tolerance capacities. Under normal (non-stress) conditions ROS are promptly detoxified by non-enzymatic and enzymatic antioxidants as well as protective osmolytes.

Non-enzymatic antioxidants include low molecular weight compounds such as ascorbate, glutathione and tocopherols which also constitute the pool of redox buffers apart from playing a crucial role in defense against oxidative stress. In plants, the tripeptide glutathione (γ-L-glutamyl-L-cysteinyl-glycine) is well known for its multipurpose role as an efficient xenobiotic detoxifier (Cummins et al. 2011), sulphur assimilator (Kopriva 2006), heavy metal detoxifier (Cobbett 2000), cell signalling component (Foyer and Noctor 2005), antioxidant (Mittova et al. 2003) and also a key component of various plant developmental processes (Vernoux et al. 2000). Moreover, through different observations, it was suggested that alterations in the status of intra-cellular glutathione levels is equally important as enhanced ROS levels, in redox signalling for activation of plant defense response against drought-induced oxidative stress (Ball et al. 2004, Gomez et al. 2004, Evans et al. 2005). It was shown that in *Arabidopsis* mutant, *root meristem less 1* (*rml1*) where root development is inhibited, glutathione concentrations were significantly low due to decreased activity of the key enzyme, γ-glutamyl cysteine synthetase (γECS) of glutathione biosynthetic pathway (Vernoux et al 2000). Also, high accumulation of oxidized glutathione (GSSG) was often associated with tissue quiessense or death (Foyer and Noctor 2005).

Regulation of glutathione (GSH) biosynthesis: Role of γECS

Owing to its diversified importance, the biosynthesis, recycling, degradation and regulation of glutathione during adverse environmental conditions have been actively

investigated (Xiang et al. 2001, Ball et al. 2004, Chen et al. 2004, Aravind and Prasad 2005). Cellular concentration of reduced GSH is maintained through reduction of GSSG to GSH by glutathione reductase (GR; EC 1.6.4.2). Glutathione is synthesized in two ATP dependent steps involving two different enzymes: γ-glutamyl cysteine synthetase or γECS (EC 6.3.2.2) and glutathione synthetase or GS (EC 6.3.2.3) (**Fig. 28a**). The first enzyme, γECS ligates glutamate and cysteine to form γ-glutamyl cysteine while GS catalyzes the formation of GSH by addition of glycine to the C terminal end of γ-glutamyl cysteine. It was reported that GSH biosynthesis is regulated by cysteine availability, feedback inhibition of γECS by GSH, transcriptional control of γECS as well as redox regulation of translated γECS (May et al. 1998, Xiang and Oliver 1998, Foyer and Noctor 2005). Through different mutant analyses, it was confirmed that GSH cannot be functionally replaced by any other metabolite except their homologues including homoglutathione and hydroxymethylglutathione. For example, in few plant families, glutathione GSH is replaced either partially or completely by its homologs where the terminal glycine is replcaed by other amino acids such as β-alanine (hGSH; Homoglutathione, *Fabaceae*) or serine (hmGSH; hydroxymethylglutathione, *Gramineae*) (Klapheck 1988, Klapheck et al. 1992). However, the first step of GSH biosynthetic pathway is common in all higher plants and the first enzyme, γECS serves as the rate limiting enzyme and also plays an important role in regulating the intracellular redox environment. Moreover, this enzyme is known to be the major control point during adverse conditions such as biotic or abiotic stresses when the demand for GSH enhances (Noctor et al. 1998).

Plant γECS is structurally dissimar to its animal and fungal counterparts (May and Leaver 1994) and the first plant γECS structure was reported recently by Hothorn et al. (2006) from *Brassica juncea*. There are reports indicating the presence of mutiple regulatory factors for γECS activity, which starts from the preliminary concept of the negative feedback regulation by glutathione and continues with the much recent concepts on redox regulation via disulphide bridges present in the enzyme to assist the monomer-dimer transition (Hicks et al. 2007, Innocenti et al. 2007, Gromes et al. 2008).

Comprehending specific mechanisms regulating γECS activity, when demand for GSH in the plant enhances, is crucial to develop stress-tolerant varieties of important crop plants. Thus, a systematic analysis focussing on the dynamic changes in the γECS at both transcript and enzyme activity levels under stress conditions is required for developing a conceptual basis regarding the role of such key enzymes under different abiotic stresses. Several interesting reports on different aspects of glutathione metabolism under various abiotic stress conditions including drought has broadened our perspectives to understand the abiotic stress biology (Dhindsa 1991, Chen and Goldsbrough 1994, Kocsy et al. 2001, Chen et al. 2004, Loscos et al. 2008, Diao et al. 2011). Earlier studies on the role of *γECS* in plant roots were mostly based on heavy metal stress as GSH is the the precursor for the metal binding phytochelatin proteins (Schäfer et al. 1998, Rivera-Becerril 2005).

Regulation of proline biosynthesis: Role of Δ^1-pyrroline-5-carboxylate synthase (P5CS)

In addition to antioxidative systems, many plants also enhances their cellular osmotic potentials through accumulation of various protective osmolytes including proline, glycine betaine, mannitol and trehalose (Zhu 2002, Wang et al. 2007c). Proline is a multifunctional amino acid which was found to accumulate in many organisms including bacteria and fungi other than plants during adverese environmental conditions such as drought and salinity (Claussen 2005). Drought-induced accumulation of proline in higher plants is usually associated with increasing osmotic potential, stabilizing proteins, membranes and subcellular structures and also protecting cells against oxidative damage by ROS (Verslues et al. 2006, Vendruscolo et al. 2007). However, the correlation between abiotic stress tolerance in higher plants with the observed accumulation of proline was not always apparent. For example, high proline content was found in drought-tolerant rice varieties (Choudhary et al. 2005), while the proline content could not be correlated to salt tolerance capacity in *Hordeum vulgare* (Widodo et al. 2009). Inspite of such variations, a wide range of studies involving transgenic palnts or mutant analysis have proved the fact that proline metabolism affects plants developmental processes, stress-response patterns and

its accumulation proves highly beneficial for tolerating certain abiotic stress factors (Mattioli et al. 2008, Székely et al. 2008, Miller et al. 2009).

In higher plants, glutamate or arginine/ornithine act as the precursor for proline biosynthesis. However, it was reported that the pathway via arginine/ornithine does not play an important role during drought (osmotic stress) (Hu et al. 1992). Proline biosyntheic pathway with glutamate as the precursor was illustrated in **Fig. 28b**. Precursor glutamate is first reduced to glutamate semialdehyde (GSA) by the bifunctional, rate-limiting enzyme Δ^1-Pyrroline-5-carboxylate synthase (P5CS). P5CS functions as both γ-glutamyl kinase (γ-GK) and glutamic-γ-semialdehyde dehydrogenase (GSA-DH). Intermediate product GSA was spontaneously converted to Δ^1-Pyrroline-5-Carboxylate (P5C). Further, with the help of another enzyme, P5C reductase, (P5CR EC 1.5.1.2) P5C is reduced to form proline. Usually in most of the plants, P5CS is encoded by two genes while P5CR is encoded by a single gene. Proline catabolism takes place inside mitochondria where proline dehydrogenase/proline oxidase (PDH/POX) oxidizes proline to form P5C which was then converted to glutamate by the enzyme P5C dehydrogenase (P5CDH). Levels of intra-cellular proline were usually regulated through its biosynthesis, catabolism as well as transport between cells and different cellular compartments (Szabados and Savouré 2010).

The expression pattern of the gene coding for the rate-limiting enzyme P5CS have been studied previously in different plants under various abiotic stress factors and it was observed that it's regulation pattern varies greatly with plant as well as the type and duration of the stress factor. In salt-stressed *V. aconitifolia*, the gene *VaP5CS* was highly expressed in leaves and roots (Hu et al. 1992). Similarly, in *A. thaliana* and *O. Sativa,* corresponding *AtP5CS1* and *OsPVCS1* genes were up-regulated during drought, high salinity, cold and ABA treatments (Strizhov et al. 1997, Igarashi et al. 1997). However, the other isoform *OsP5CS2* transcript was found to be present in reproductive organs, especially in stamens is evident through RT-PCR analysis (Hur et al. 2004). However in case of *M. truncatula*, two P5CS genes showed developmental and environment-specific responses where *MtP5CS1* showed steady-state transcript levels that were well correlated with proline level in different

organs while *MtP5CS2* transcripts were accumulated only in shoots of salt stressed plants (Armengaud et al. 2004). It was hypothesized that *MtP5CS1* might be acting as a developmental housekeeping enzyme which is responsible for supplying proline to the reproductive organs while *MtP5CS2* isoform was responsible for shoot-specific osmoregulation.

Apart from proline's osmotic functions which were directly related to its actual cellular concentrations, it was postulated that the interconversion of proline and glutamate via P5C, could shuttle redox equivalents between cellular compartments, couple the oxidation of NADPH to mitochondrial electron transfer and thus, serve as a mechanism for energy production. Moreover it also maintains the balance of NADPH/$NADP^+$ redox pool, which is highly essential to ensure proper metabolic functioning (DeRonde et al. 2004). Both the process of proline synthesis and catabolism as well as the absolute concentration of proline are important in the adaptation of plants to drought stress through various metabolic adjustments.

In the present study, we aim to analyse the role of γECS as well as P5CS in *V. radiata* roots under progressive drought stress as well as recovery period through cloning and subsequent exression analysis of the corresponding genes and putative proteins with an insight on their possible regulations during drought stress.

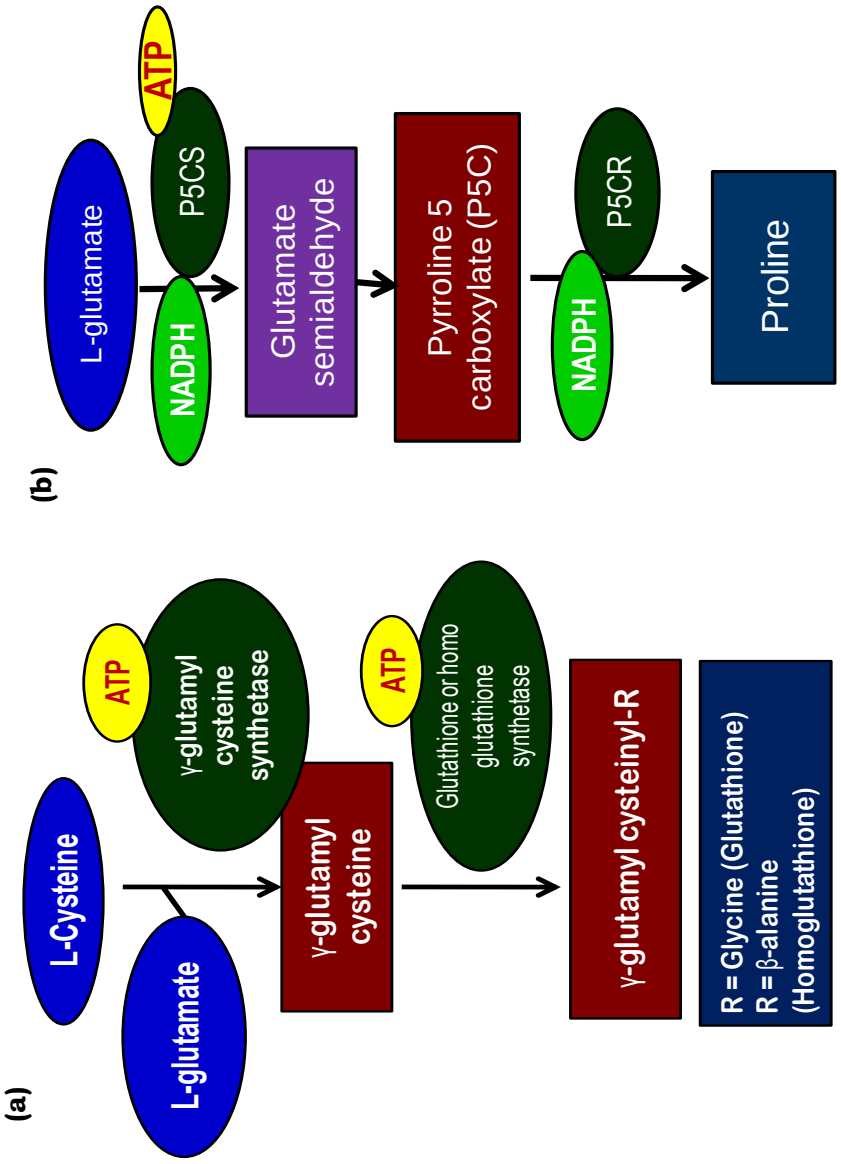

Fig 28. Diagrammatic representation of the biosynthetic pathways of glutathione (homoglutathione) (**a**) and L-proline (**b**) in higher plants

MATERIALS AND METHODS

Cloning of a fragment of VrγECS

Total RNA was isolated from 100 mg of *V. radiata* root tissue using column based Plant Spectrum RNA isolation kit (Sigma-Aldrich) following manufacturer's instructions. Total RNA was used as template for the synthesis of first strand of cDNA using Revert Aid^{TM} First Strand cDNA synthesis kit (Fermentas life Sciences, St Leon-Rot, Germany). For cDNA synthesis, a 20µL reaction was set up consisting of the RNA template, reaction buffer, oligodT primers, riboinhibitor (RNAse inhibitor), dNTP mix and reverse transcriptase enzyme and incubated at 37°C for 1 h to allow cDNA strand synthesis, followed by 10 min incubation at 70°C to degrade the RNA template in the RNA-DNA hybrid formed. Primers [Forward primer: 5'CTAAGCTGTGACCCACCGAGTG 3'; reverse primer: 5'CTTCAGCACAAGTCTGGTGCAA 3'] were designed based on the conserved region of γECS from available sequences of *Phaseolus vulgaris, Medicago truncatula* and a clone of *Vigna unguiculata* at NCBI GenBank (http://www.ncbi.nlm.nih.gov) and the synthesized cDNA was used as template to amplify a 706 bp fragment of *VrγECS*. PCR amplification was performed in a 25 µL reaction mixture for 35 cycles where initial denaturation was carried out at 94°C for 3 min, followed by 1 min denaturation at 94°C, 45 s annealing at 62°C, 1 min primer extension at 72°C and final extension at 72°C for 10 min.

Amplified PCR product was eluted from agarose gel using GenElute Gel extraction kit (Sigma) and ligated to TA vector, pTZ57RT (Fermentas, Germany) at 4°C overnight. Ligated product was subsequently transformed into *E. coli* DH5α and recombinant plasmid containing white colonies were selected on LB agar media supplemented with 50 µg ampicillin, X-Gal and IPTG through blue-white screening. Presence of insert in the selected white colonies was confirmed through colony PCR with gene specific primers and plasmid was isolated from confirmed colonies using column based MiniPrep Plasmid isolation kit (Sigma) following manufacturer's protocol, quantified using Nanodrop ND1000 spectrophotometer and sent for sequencing. The obtained sequence was compared with the available full length cDNA sequence of *P. vulgaris γECS* using Multalin software (Corpet 1988).

3' Rapid amplification of cDNA ends (RACE) of VrγECS

Since the obtained sequence consists of the 5' end of the *VrγECS* gene with "ATG" and its upstream sequence, only 3' RACE-PCR was performed to deduce the full length cDNA sequence using 5'/3' RACE kit (Roche Applied Sciences, Germany) following manufacturer's instructions. By comparing the obtained sequence with the available full length cDNA sequence of *PvγECS*, the approximate size of the 3' end PCR product which was expected on agarose gel was deduced (**Fig. 31a**). Three internal gene specific forward primers were designed based on the partial cDNA sequence obtained [GSP1: 5'CTAAGCTGTGACCCACCGAGTG 3'; GSP2: 5'CCACTTATCCCGACGACACT 3'; GSP3: 5'TTTGGAAGTTTGCGTCCTATG 3']. Total RNA (4 µg) was reverse transcribed using Transcriptor Reverse Transcriptase which was provided with the kit. For 3' RACE-PCR oligo dT-anchor primers were used in reverse transcription reaction for the synthesis of first strand cDNA. The 3' RACE PCR was performed first (primary reaction) with GSP1 as the forward primer and universal anchor primer as the reverse primer. Secondary PCR reaction was carried out with the product of the primary reaction as template and GSP2 as the forward primer and similarly tertiary PCR reaction was carried out with GSP3 as the forward primer and PCR product of secondary reaction as template. After comparing all the PCR products on gel, the correct 3' fragment was identified and eluted from agarose gel using GenElute Gel Extraction kit (Sigma). Gel eluted PCR product was cloned into pTZ57RT vector (Fermentas, Germany), screened using blue-white screening technique, plasmid was isolated from confirmed positive colonies and sent for sequencing. The obtained sequence was trimmed and compared by aligning with the earlier fragment sequence to obtain the full-length cDNA sequence of *VrγECS*. The full length *VrγECS* was subsequently characterized at the molecular level, such as the putative protein sequence and sequence homology. The ChloroP software (Emanuelsson et al. 1999) is used to predict the presence of a putative plastidic transit peptide in the VrγECS putative protein sequence. A putative three dimensional protein model for VrγECS was generated using Geno3D software (www.expasy.com) tool (Combet et al. 2002).

Quantitative Real time RT-PCR analysis of VrγECS

Based on the obtained *VrγECS* sequence, direct primers for real time PCR (Forward primer: 5'CCACTTATCCCGACGACACT3' and reverse primer: 5'CCACGTGTGACAATCCTCTG 3') were designed to amplify a 120 bp product. Real time qPCR analysis was done on Eppendorf Realplex MasterCycler (Eppendorf, Germany) using the KAPA SYBR FAST (Mastermix (2X) Universal) (KAPA Biosystems) real time PCR kit following manufacturer's instructions. Total RNA was isolated from *V. radiata* root tissue at different stages of drought stress and recovery period using column based Plant Spectrum RNA isolation kit (Sigma) and quantified using Nanodrop ND1000 spectrophotometer. Equal concentrations (1µg) of total RNA was used as template to synthesize first strand cDNA using M-MuLV reverse transcriptase enzyme and oligo dT primers (Reverse Aid cDNA synthesis kit, Fermentas). Each reaction was carried out in triplicate with 50 ng of cDNA as template. The qPCR program included one cycle of 2 min at 95°C for template denaturation, followed by 40 cycles of 15 sec at 95°C for template denaturation, 30 sec at 55°C for primer annealing and 20 sec at 72 °C for primer elongation, followed by the dissociation (melting) curve to ensure that no primer dimers were formed during the reaction. Fluorescence was detected using the Realplex software (Eppendorf, Germany).

The relative fold differences in expression of *VrγECS* during progressive drought stress and recovery when compared to the well-watered D0 plants was determined using the $2^{-\Delta\Delta Ct}$ formula as explained by Livak and Schmittgen (2001). For each sample a qPCR was performed in triplicate on three independent RNA extracts as described above. The *V. radiata* actin (ACT) gene was used as the internal control. A validation experiment, with different concentrations of template DNA was performed for both target and reference genes according to Applied Biosystems User Bulletin No. 2(P/N 4303859) to ensure that both the genes amplify with approximately equal efficiency.

VrγECS enzyme activity

The enzyme activity of VrγECS protein was assayed according to Rüeggsegger and Brunold (1992). Fresh root tissue was homogenized with 100 mM Tris-HCl (pH 8.0), 10 mM $MgCl_2$, 1 mM EDTA and centrifuged for 15 min at 10,000*g* (0 °C). For VrγECS activity, the reaction was started by addition of the enzyme extract (140 µL) to give 500 µL assay mix containing 100 mM Hepes (pH 8.0), 50 mM $MgCl_2$, 20 mM glutamate, 1 mM cysteine, 5 mM ATP, 5 mM phosphoenolpyruvate (PEP), 5 mM DTT and 10 units mL^{-1} pyruvate kinase. The reaction mixture was incubated at 37 °C for 45 min and the reaction was stopped by addition of 100 µL of 50% TCA. The mixture was centrifuged and the supernatant was used for estimation of phosphate content by phosphomolybdate method. Mixed reagent was prepared by adding 125 mL of 5 N H_2SO_4 and 37.5 mL of 4 % ammonium molybdate solution. To this mixture, 75 mL of ascorbic acid was added and the final volume was made up to 250 mL. From the enzyme reaction mixture, 4 mL aliquot was mixed with 0.8 mL of mixed reagent and 0. 2 mL of double distilled water (DDW) to make the final volume 5 mL and the reaction mix was incubated at 60°C for 30 min. Absorbance of the blue colour formed was measured at 827 nm. A standard graph was prepared for inorganic phosphate concentrations ranging from 2-20 µg using KH_2PO_4 as standard and the amount of phosphate released in the reaction mixture was calculated. Protein content of the extracts was measured according to Bradford (1976) with BSA as the standard.

Real time qPCR analysis of Pyrroline 5-carboxylate synthetase (P5CS) gene

Total RNA was isolated from *V. radiata* root tissue during different sampling points (D0, D3, D6 and 6R) using column based RNA isolation kit (Sigma) and equal amounts (1µg) of RNA was converted to cDNA using Revert Aid First strand cDNA synthesis kit (Fermentas, St Leon Road, Germany). Synthesized cDNA was used as template for amplification of a 1.48 kb fragment of *VrP5CS* gene using forward and reverse primers (Fwd: ACATCGGCTCAGCTTCTTGT and Rev: CGTCATCCACAATTTCAACG) which were designed based on the available full length sequence of *P5CS* cDNA from *Phaseolus vulgaris*

at NCBI GenBank (gi|164564393|gb|EU340347.1|). Gel-purified PCR product was directly sent for sequencing (without TA cloning) and the obtained sequence was compared with the available *PvP5CS* sequence using Multalin software for confirming the product identity. Within the obtained sequence, internal primers (Fwd: CTTCATTGGCAATCCGAAGT; Rev: TCCCTTGAGGTCACAAGTCC) were designed to amplify a 148 bp product for real time qPCR analysis using KAPA SYBR FAST (Mastermix (2X) Universal) (KAPA Biosystems, Woburn, USA) real time PCR kit in an Eppendorf Realplex MasterCycler (Eppendorf, Hamburg, Germany). Equal amounts (1 µg) of RNA, extracted during different sampling stages, were converted to cDNA and triplicate reactions were kept with 50 ng of cDNA as template following the program: 2 min at 95°C, followed by 40 cycles of 15 sec at 95°C, 30 sec at 55°C annealing temperature and 20 sec at 72 °C, followed by the dissociation (melting) curve. Fold change in *VrP5CS* was calculated according to the $2^{-\Delta\Delta Ct}$ formula (Livak and Schmittgen 2001). Experiment was repeated thrice. Actin (*ACT*) gene from *V. radiata* was used as the internal control and a validation experiment was performed to ensure equal efficiency amplification for target and reference genes, using different concentrations of template DNA according to Applied Biosystems User Bulletin No. 2(P/N 4303859).

VrP5CS enzyme assay

The VrP5CS enzyme assay was carried out according to the method described by Garcia-Rios et al. (1997). Enzyme activity was determined based on the rate of consumption of NADPH, during the ATP and NADPH-dependent reduction of glutamate to γ-glutamic semialdehyde (GSA). Enzyme was extracted from root tissue (1g) in 2 mL of extraction buffer containing 0.05M Tris-HCl buffer (pH7.2), 1 mM β-mercaptoethanol, 10mM $MgCl_2$. Homogenate was centrifuged at 15,000*g* for 20 min at 4°C. The assay was carried out in 100 mM Tris-HCl (pH 7.2), 25mM $MgCl_2$, 75 mM Na-glutamate, 5 mM ATP, 0.4 mM NADPH and 50 µg of crude extract protein at 25°C in a total volume of 1mL reaction mixture. The decrease in absorbance at 340 nm was recorded using a UV-visible spectrophotometer as a function of time.

Statistical analysis

Results of the biochemical parameters were represented as mean ± standard deviations (n = 3). The significance of the differences between mean values of well watered and water-stressed plants was determined using one way ANOVA (tukey-test) and Student's *t*-test. All the statistical and linear regression analyses were performed using the statistical package Sigma Plot 11.0. For qPCR analysis, three independent RNA samples were used for each sample and each reaction was run in triplicate for both control and stressed samples of each time point.

RESULTS

Cloning and sequence analysis of VrγECS cDNA

Primers were designed based on the conserved region of available sequences of γECS from *P. vulgaris*, *M. truncatula* and a clone of *V. unguiculata* for the amplification of fragment of *γECS* like cDNA from *V. radiata* (**Fig. 29**). The PCR amplified 706 bp fragment of *VrγECS* (**Fig. 30a**) was further cloned and sequenced. The obtained sequence was aligned with the known sequence of *P. vulgaris* to verify its identity (**Fig. 30b**). It was observed that the obtained sequence includes the translation start site (ATG) along with 186 bp of 5'UTR sequence and thus, we designed internal gene specific primers (GSP1, GSP2 and GSP3) which were used as forward primer in 3' RACE-PCR. Based on *PvγECS* sequence, expected sizes of the 3' RACE-PCR fragments of *VrγECS* according to the position of the corresponding internal GSP forward primers were determined (**Fig. 31a**). After three consecutive PCR amplifications, we obtained a single and specific fragment of about 1.6 kb, which was cloned to TA vector and transformed into *E. coli* DH5α (**Fig. 31b**). Colonies showing the bands of interest after colony-PCR-analysis were selected for plasmid isolation and the isolated recombinant plasmids were sequenced (**Fig. 31c**). Obtained sequence showed the presence of a 209 bp 3'UTR region downstream to the stop codon. Based on the earlier sequence and the 3'RACE sequence, we were able to deduce the full length cDNA of *VrγECS*. The full length cDNA sequence with putative amino acid sequences was presented in **Fig. 32**. We have submitted this sequence to NCBI GenBank (GenBank accession no. HQ999996). A schematic representation of the full length cDNA sequence of *VrγECS* was illustrated in **Fig. 33a** which includes a 1527 bp open reading frame (ORF), encoding a predicted protein of 508 amino acids with a calculated molecular weight of 57.6 kDa and a pI of 6.18. The ChloroP software predicted the presence of a putative plastidic transit peptide of 60 amino acids in the VrγECS putative protein sequence followed by the conserved cleavage site Ile X Ala $^{\downarrow}$ Ala. In this case X is a Valine residue. For further sequence analyses, the putative oxidized GSH binding site from glutathione reductase (GR) of *P. sativum* was compared with ECS protein sequences from different plant species. **Fig. 33b** illustrates the conserved amino acids from the putative oxidized GSH binding site among the different plant species and their respective positions in

Fig 29. Multiple alignment of available *Phaseolus vulgaris* γECS cDNA sequence with two *Vigna unguiculata* clones (available in NCBI database) which showed high sequence similarity. Based on the highly conserved regions (shown with circles) primers were designed for amplifying a fragment of γECS gene from roots of *V. radiata*.

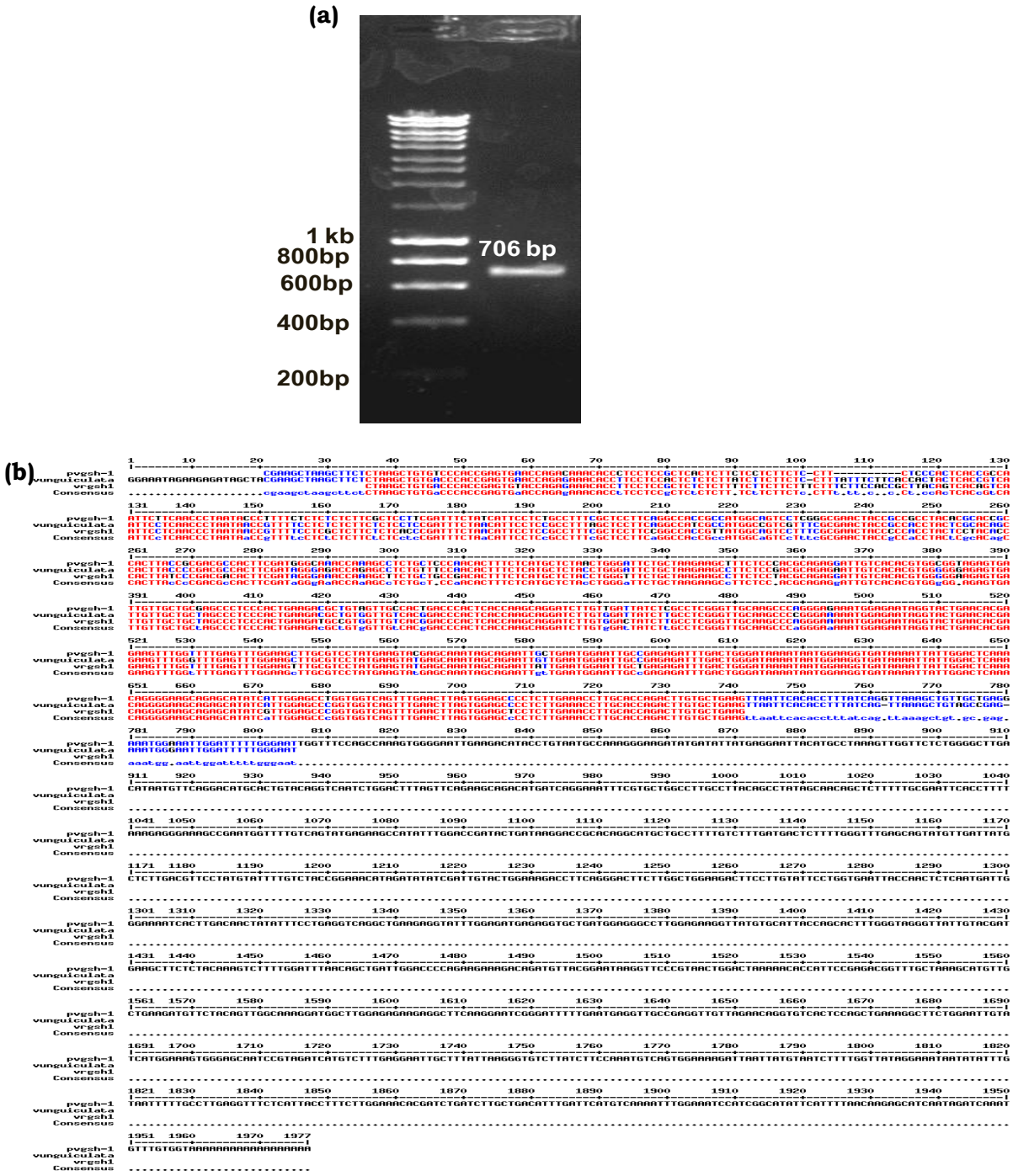

Fig 30. A 706 bp PCR amplified fragment of *VryECS* gene which was cloned to pTZ57RT vector and sequenced (**a**) Multiple alignment of the obtained *VryECS* partial sequence with the available full length cDNA sequence of *PvγECS* (**b**).

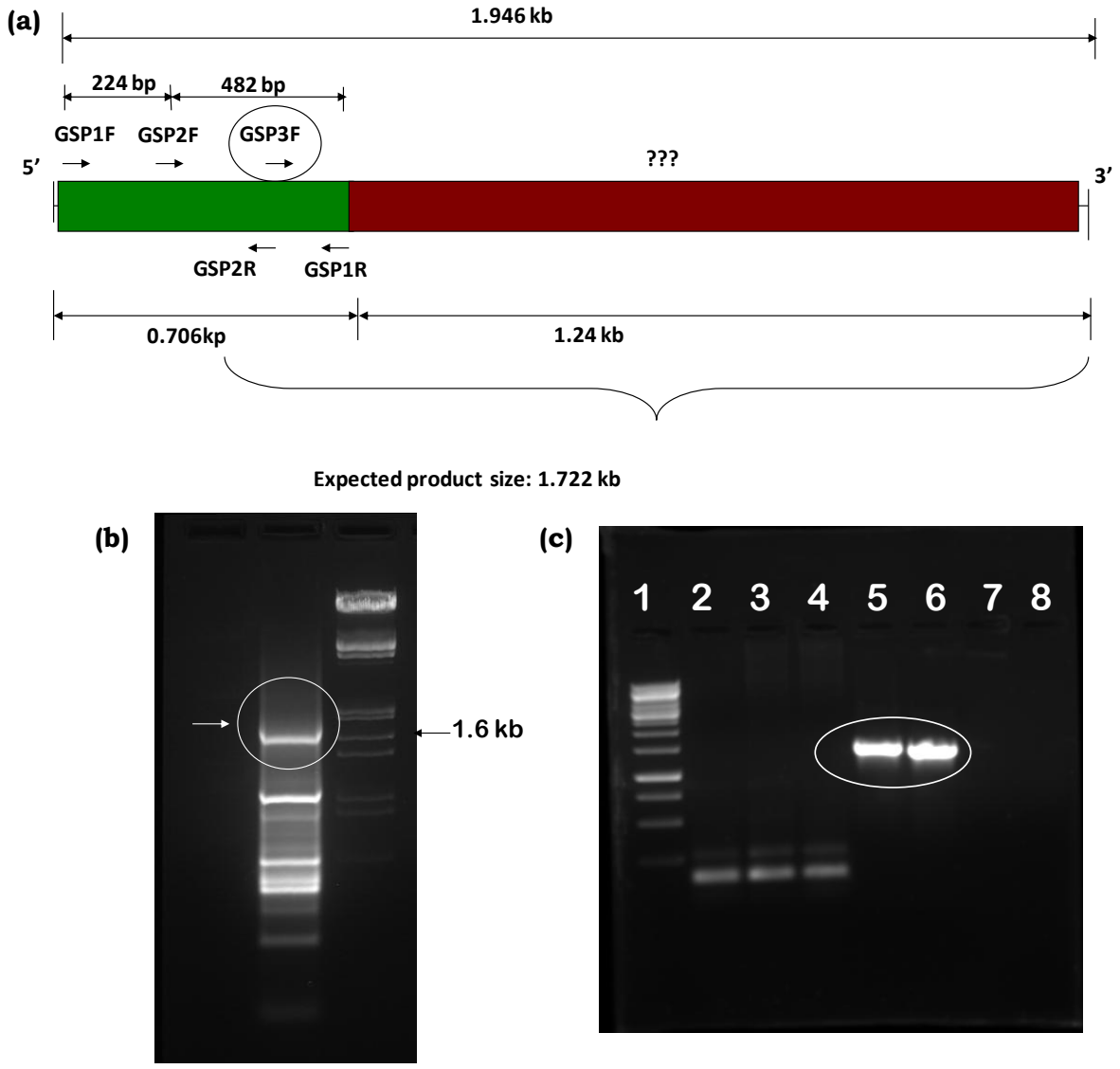

Fig 31. Schemmatic representation of the RACE-PCR strategy followed for deducing the full length cDNA sequence *VrγECS* by comparing with the available *PvγECS* sequence (**a**); Agarose gel for 3'RACE PCR products showing the presence of expected size fragment (circle) of 1.6 kb (**b**); Cloned 1.6 kb fragment was screened through colony PCR using gene specific primers (**c**).

```
CTAAGCTGTGACCCACCGAGTGTACCAGAGAAACACCTTCCTCCGCTCTCTCTTTTCTTCTTCTTTC 67

TTTCTTCCACCGCTTACAGTCACAGTCAATTCCTCAACCCTAATAACCGTTTTCCTCGCTCTTCTCT 134

CACCCGATTTCTAACATTCCTCCGCCTTTCGCTCCTTCCGGCCACCGTTATGGCAGTCCTTTCGCGA 201
                                                  M  A  V  L  S  R
ACTACCCCCACCTACTCCTACACCCACTTATCCCGACGACACTTCGATAGGGAAACCAAAGCTTCTG 268
 T  T  P  T  Y  S  Y  T  H  L  S  R  R  H  F  D  R  E  T  K  A  S
CTGCCGACACTTTCTCATGCTCTACCTGGGTTTCTGCTAAGAAGCCTTCTCCTACGCAGAGGATTGT 335
 A  A  D  T  F  S  C  S  T  W  V  S  A  K  K  P  S  P  T  Q  R  I
CACACGTGGGGGAAGAGTGATTGTTGCTGCTAGCCCTCCCACTGAAGATGCCGTGGTTGTCACGGAC 402
 V  T  R  G  G  R  V  I  V  A  A  S  P  P  T  E  D  A  V  V  V  T
CCACTCACCAAGCAGGATCTTGTGGACTATCTTGCCTCGGGTTGCAAGCCCAGGGAAAAATGGAGAA 469
 D  P  L  T  K  Q  D  L  V  D  Y  L  A  S  G  C  K  P  R  E  K  W
TAGGTACTGAACACGAGAAGTTTGGTTTTGAGTTTGGAAGTTTGCGTCCTATGAAGTATGAGCAAAT 536
 R  I  G  T  E  H  E  K  F  G  F  E  F  G  S  L  R  P  M  K  Y  E
AGCAGAATTATTGAATGGAATTGCTGAGAGATTTGACTGGGATAAAATAATGGAAGGTGATAAAATT 603
 Q  I  A  E  L  L  N  G  I  A  E  R  F  D  W  D  K  I  M  E  G  D
ATTGGACTCAAACAGGGGAAGCAGAGCATATCGTTGGAGCCCGGTGGTCAGTTTGAACTTAGTGGAG 670
 K  I  I  G  L  K  Q  G  K  Q  S  I  S  L  E  P  G  G  Q  F  E  L
CTCCTCTTGAAACCTTGCACCAGACTTGTGCTGAAGTCAATTCACACCTTTATCAGGTTAAAGCTGT 737
 S  G  A  P  L  E  T  L  H  Q  T  C  A  E  V  N  S  H  L  Y  Q  V
AGCTGAGGAAATGGGAATTGGATTTTTGGGAATTGGTTTCCAGCCAAAGTGGGGAATCAAAGACATA 804
 K  A  V  A  E  E  M  G  I  G  F  L  G  I  G  F  Q  P  K  W  G  I
CCTGTAATGCCAAAGGGAAGGTATGATATTATGAGGAATTACATGCCTAAAGTTGGTTCTCTGGGGC 871
 K  D  I  P  V  M  P  K  G  R  Y  D  I  M  R  N  Y  M  P  K  V  G
TTGACATGATGTTCAGGACATGCACTGTACAGGTCAATCTGGACTTTAGTTCAGAAGCAGACATGAT 938
 S  L  G  L  D  M  M  F  R  T  C  T  V  Q  V  N  L  D  F  S  S  E
CAGGAAATTTCGTGCTGGCCTTGCTCTACAGCCTATAGCAACGGCTCTTTTTGCGAATTCACCTTTT 1005
 A  D  M  I  R  K  F  R  A  G  L  A  L  Q  P  I  A  T  A  L  F  A
AAAGAGGGAAAGCCAAATGGTTTTGTCAGCATGAGAAGCCATATTTGGACCGATACTGACAAGGACC 1072
 N  S  P  F  K  E  G  K  P  N  G  F  V  S  M  R  S  H  I  W  T  D
GCACAGGCATGCTGCCTTTTGTCTTTGATGATTCTTTTGGGTTTGAGCAGTATGTTGATTATGCTCT 1139
 T  D  K  D  R  T  G  M  L  P  F  V  F  D  D  S  F  G  F  E  Q  Y
TGATGTTCCTATGTATTTTGTCTACCGGAAACATAGATATATTGATTGTACTGGAAAGACCTTCAGG 1206
 V  D  Y  A  L  D  V  P  M  Y  F  V  Y  R  K  H  R  Y  I  D  C  T
GACTTCTTGGATGGAAGACTTCCTTGTATTCCTGGGGAATTACCAACTCTCAATGATTGGGAAAATC 1273
 G  K  T  F  R  D  F  L  D  G  R  L  P  C  I  P  G  E  L  P  T  L
ACTTGACAACTATATTTCCTGAGGTCAGGCTGAAGAGGTATTTGGAGATGAGAGGTGCTGATGGAGG 1340
 N  D  W  E  N  H  L  T  T  I  F  P  E  V  R  L  K  R  Y  L  E  M
CCCTTGGAGAAGGTTATGTGCATTACCAGCACTCTGGGTAGGGTTATTGTACGATGATGCTTCTCTA 1407
 R  G  A  D  G  G  P  W  R  R  L  C  A  L  P  A  L  W  V  G  L  L
CAAAGTGTTTTGGATTTGACAGCTGATTGGACCCCAGAAGAAAGACTGATGTTAAGGAATAAGGTTC 1474
 Y  D  D  A  S  L  Q  S  V  L  D  L  T  A  D  W  T  P  E  E  R  L
CCGTAACTGGTCTAAAAACACCATTCCGAGATGGTTTGCTGAAGCATGTTGCTGAAGATGTTCTACA 1541
 M  L  R  N  K  V  P  V  T  G  L  K  T  P  F  R  D  G  L  L  K  H
GTTGGCAAAGGATGGCTTGGAGAGAAGAGGCTTCAAGGAATCGGGATTTTTGAATGAGGTCGCCGAG 1608
 V  A  E  D  V  L  Q  L  A  K  D  G  L  E  R  R  G  F  K  E  S  G
GTGGTTAGAACAGGCGTCACTCCAGNTGAGAAGCTTTTGGAATTGTATCATGGAAAGTGGGAGCAAT 1675
 F  L  N  E  V  A  E  V  V  R  T  G  V  T  P  X  E  K  L  L  E  L
CCGTAGATCATGTGTTTGAGGAATTGCTTTATTAAAGGTGTATTATCTTTCAAATGTCAGTGGAAGA 1742
 Y  H  G  K  W  E  Q  S  V  D  H  V  F  E  E  L  L  Y  *
TTAATTGTGTAATCTTTTGGTTATAGTCCTGGCTAGCTCATTTGAGCTCTCCATTTAGATATAGGAA 1809

ATAATGTATTTGTAATTTTTTCCATGAGGCTTCTCATATACCTTTCTTGGAAACACGATCTGATCTT 1876

GCTGACATTTAATTCATGTCATGCATTTGAAAAAAAAAAAAAA
```

Fig 32. Full length cDNA sequence of Vrγ*ECS* showing the ORF region with the encoded protein and the 5' and 3; UTRs

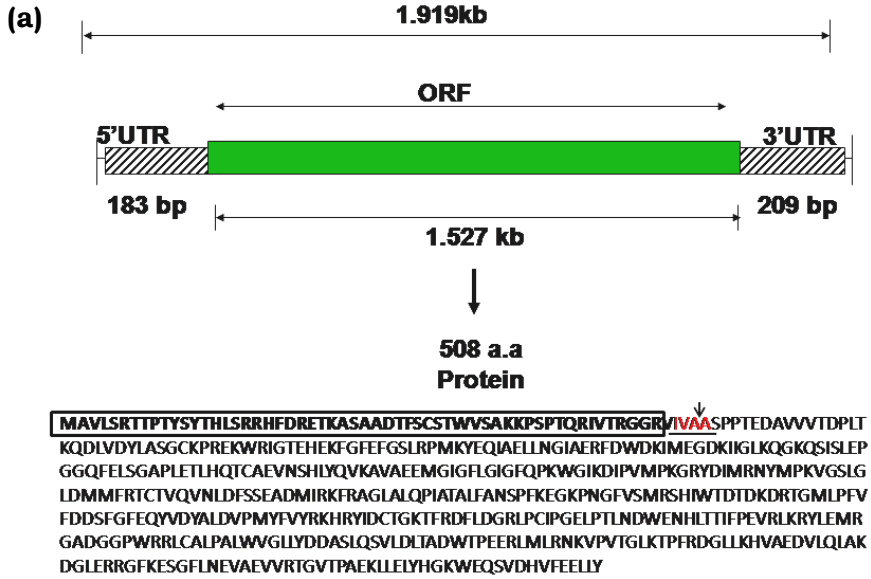

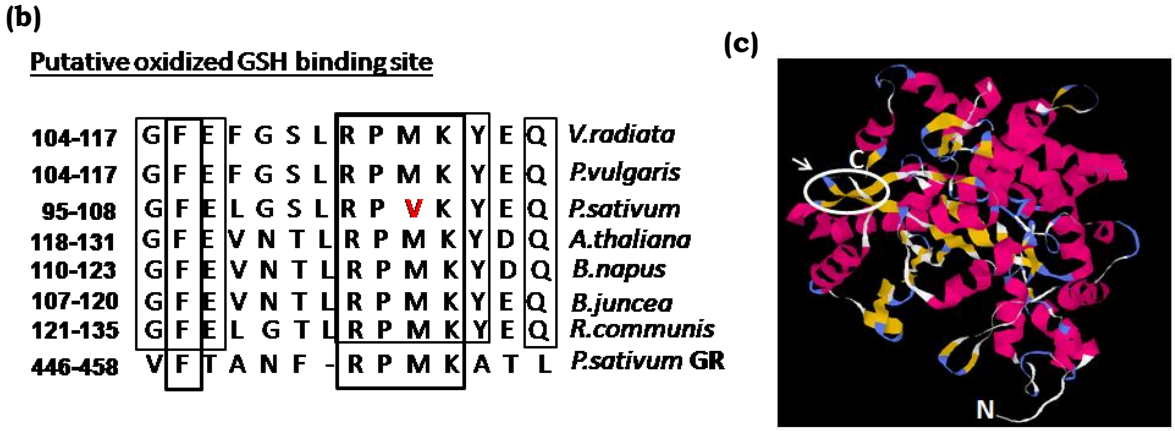

Fig 33. Schemmatic representation of the complete *VrγECS* cDNA including the 5' and 3'UTR's and 1.527 kb ORF region. The deduced amino acid sequence of *VrγECS*, showing the 60 bp long chloroplast target peptide and its putative cleavage site (IVAA) (**a**); Comparison of the deduced amino acid sequence of γECS from *V. radiata* and other plant sources with the putative oxidized GSH binding site of glutathione reductase (GR) from *P. sativum* (**b**). Three dimensional model of VrγECS protein. The circle and the arrow indicate the putative oxidized GSH binding site (**c**).

the protein sequence. The model depicts the monomeric protein including six antiparallel beta-sheets surrounded by alpha helices. The putative oxidized GSH binding site was highlighted in the protein 3D model (**Fig. 33c).** Further, according to the available literature, redox regulation of γECS protein was mediated through monomer-dimer transtitions via intermolecular disulphide bridges where the oxidized dimeric form of the protein was considered to be more active than the reduced monomeric form and it was assumed that conserved cysteine residues at particular positions within the protein sequence facilitate such disulphide bond formations (**Fig. 34a**). The putative VrγECS protein displayed 95, 85 and 82% sequence similarity with ECS protein sequence from *P. vulgaris, P. sativum* and *R. communis* respectively and *B. napus, B.juncea* and *A.thaliana* showed 78% sequence similarity with VrγECS. Upon multiple alignments of all the above sequences, we observed that the plastidic transit peptide cleavage site (IVAA) is conserved in all the above plant species. However, the transit peptide sequence was highly dissimilar with each other. The rest of the protein sequence (beyond the transit peptide cleavage site) showed high sequence similarity. Putative conserved Cysteine residues at 173rd, 338th , 352nd and 394th positions were highlighted which were predicted to participate in monomer-dimer trasitions through disulphide bond formation (**Fig. 34b**).

VrγECS mRNA expression and enzyme activity under progressive drought stress and recovery

A quantitative real time PCR analysis of *VrγECS* under progressive drought stress was performed with ACT as the internal control and the well-watered D0 plants as calibrator whose fold change in mRNA level was considered to be 1. The relative fold change was calculated according to the $2^{-\Delta\Delta Ct}$ method. Our results demonstrated a more or less constant expression (< 1.5 fold) levels during short-term and long-term water-deficit as well as during recovery period (**Fig. 35a**). However, VrγECS enzyme activity was significantly enhanced during medium stress (D3) when compared to D0 but declined upon consecutive severe stress (D6) and failed to recover even upon re-watering (**Fig. 35b**). As the *VrγECS* mRNA expression levels did not correspond to its activity, we correlated the endogenous H_2O_2 levels

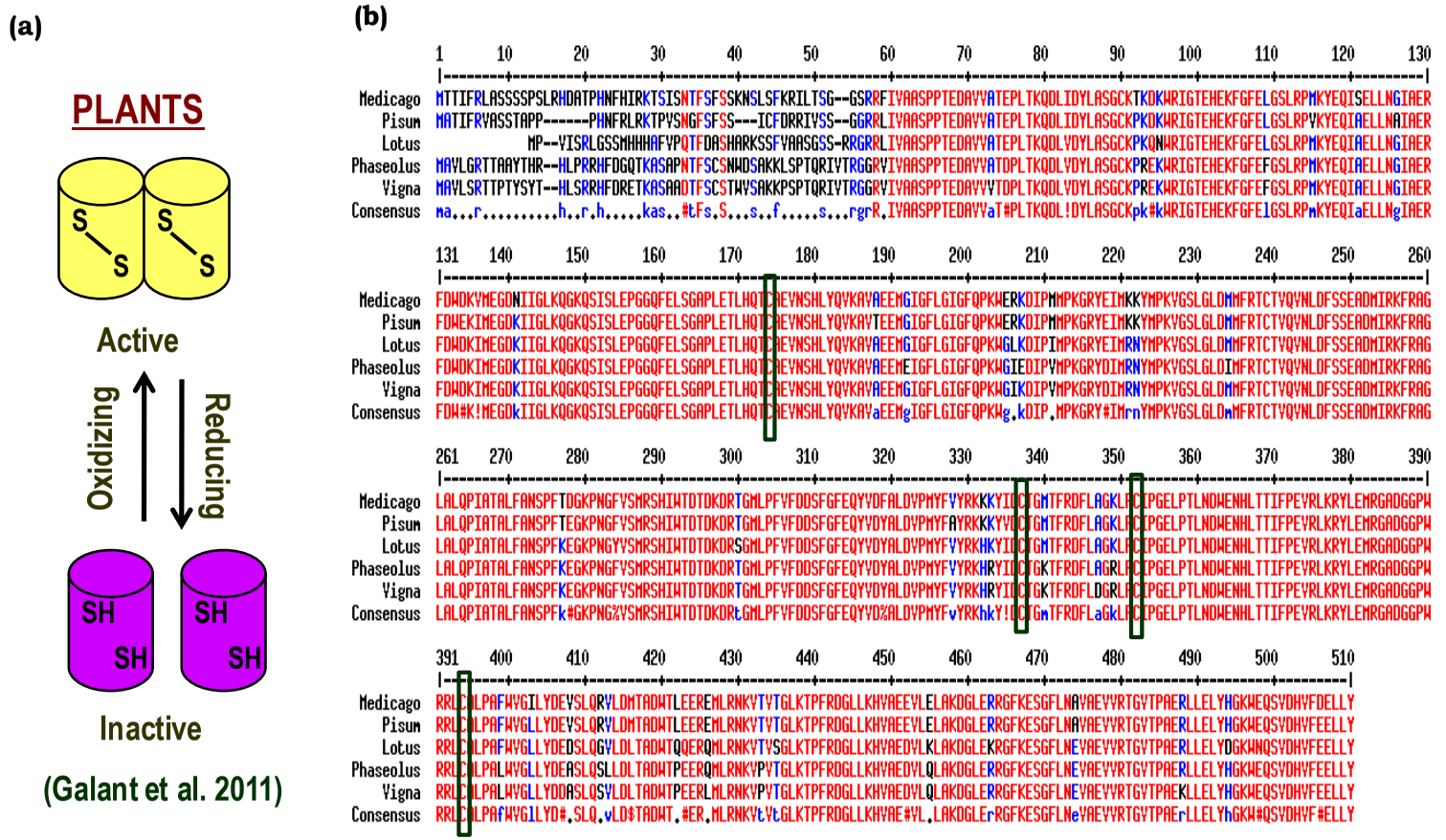

Fig 34. Mechanism of redox regulation of γECS through monomer-dimer transition in higher plants (**a**); Comparison of obtained VrγECS sequence with other legume γECS sequences to show the conserved cysteine residues which are proposed to be involved in forming inter-molecular and intra-molecular disulphide bonds to facilitate monomer-dimer transition (**b**).

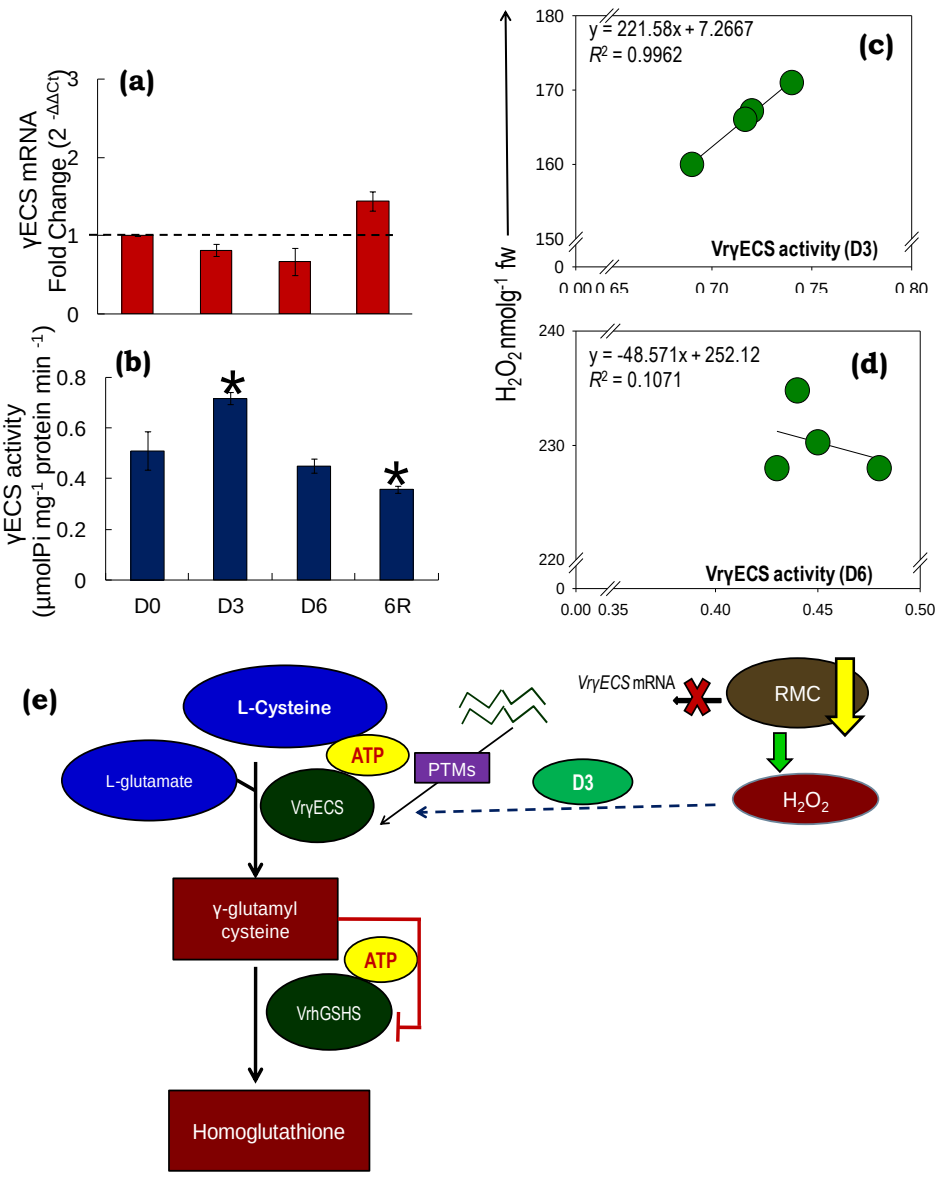

Fig 35. Real time qPCR analysis of *VrγECS* mRNA depicting the fold change ($2^{-\Delta\Delta Ct}$) during D3, D6 and 6R when compared to D0 (**a**). VrγECS enzyme activity during progressive drought stress and recovery (**b**). Values represents mean ± SD with n = 3. P* <0.001 indicate significant difference (one way ANOVA). Linear regression analysis between VrγECS enzyme activity (X-axis) and H_2O_2 content (Y-axis) during D3 (**c**)and D6 (**d**) indicating a positive and non-significant correlation, respectively. Schemmatic representation of the proposed hypothesis for VrγECS regulation during drought in *V. radiata* roots (**e**).

during D3 and D6 with the observed VrγECS activity patterns. Linear regression analysis between the VrγECS enzyme activity and H_2O_2 content during D3 showed a strong positive correlation between the two parameters with R^2 value of 0.9962 (**Fig. 35c**). However, during D6, the R^2 value was only 0.1071 indicating a non-significant correlation between these two parameters **(Fig. 35d**). Based on our observations, we hypothesized that low concentrations of H_2O_2 might be acting as a positive regulator of VrγECS enzyme activity in roots of *V. radiata* during drought stress conditions (**Fig. 35e**).

Changes in root-level proline accumulation, expression of VrP5CS mRNA and VrP5CS activity under progressive drought stress and recovery

Using primers based on *PvP5CS* sequence available at NCBI GenBank (gi|164564393|gb|EU340347.1|), a 1.48 kb fragment of *VrP5CS* was amplified from root cDNA and sequenced (**Fig 36a**). Deduced sequence was compared with the existing *PvP5CS* sequence for confirmation of the identity of the gene which showed 98 % sequence similarity (**Fig. 36b**). Proline accumulated rapidly at a significantly high level (approximately 5 fold higher) during medium stress (D3) itself. Proline content was similar during D6 (only a marginal decline was recorded) and thereafter rapidly catabolised upon re-watering (**Fig. 37a**). To understand the expression pattern of proline in roots of *V. radiata*, we analyzed the mRNA expression pattern and the corresponding enzyme activity levels of VrP5CS. The relative mRNA expression of *VrP5CS* gene showed 108 and 70 fold up-regulation on D3 and D6, respectively and the gene expression resumed to D0 levels during 6R (**Fig. 37b**). A similar pattern was recorded for VrP5CS enzyme activity levels, with approximately 7 and 6 fold enhancement in the activity levels on D3 and D6, respectively, whereas upon recovery the enzyme activity became equivalent to that of D0 (**Fig. 37c**). Linear regression analysis of RMC % versus proline concentrations, *VrP5CS* mRNA expression and VrP5CS enzyme activity elucidated positive linear correlations with R^2 values of 0.757, 0.646 and 0.830, respectively (**Fig.37d-f**).

Fig 36. PCR amplified 1.48 kb fragment of *VrP5CS* gene from *V. radiata* roots (**a**); Multiple alignment of the obtained VrP5CS sequence with the available sequence of *Phaseolus vulgaris* P5CS , showing 98 % sequence similarity (**b**).

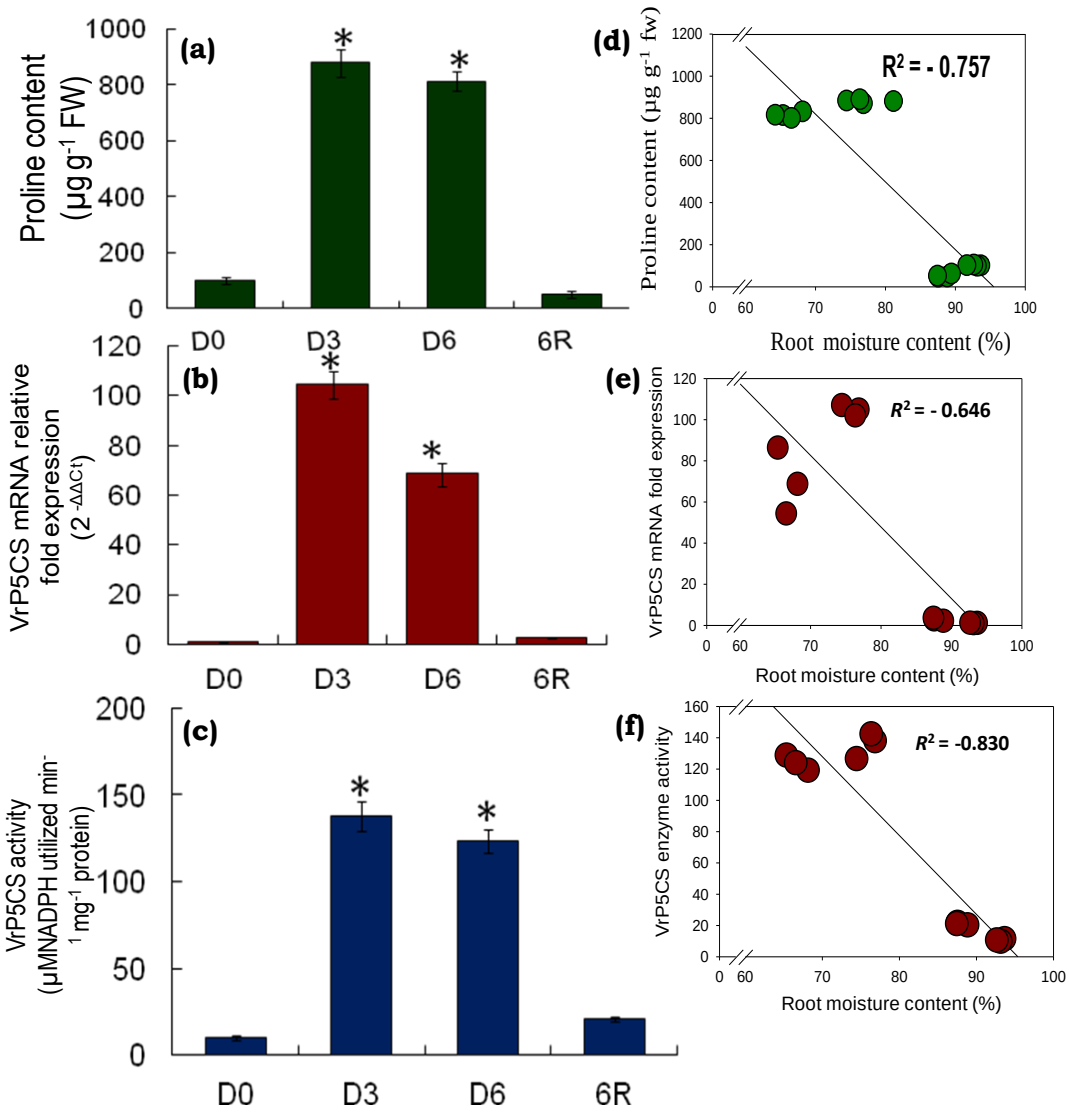

Fig 37. Changes in proline concentrations in *V.radiata* roots with gradual water deficit and re-watering (**a**); transcript level modulations in the proline biosynthetic enzyme, pyrroline 5 carboxylate synthetase (*VrP5CS*) (**b**); VrP5CS enzyme activity changes under progressive drought and recovery in mungbean roots (**c**). Values represents mean ± SD with $n = 3$. P* <0.001 indicate significant difference (one way ANOVA). Linear regression analysis between root moisture content and proline concentrations (**d**); *VrP5CS* mRNA expression levels (**e**); VrP5CS enzyme activity (**f**).

DISCUSSION

The protective mechanism of GSH and proline in higher plants has been conspicuously evident owing to their multifaceted functions inside plant cells (Ruiz and Blumwald 2002, Ogawa 2005, Szabados and Savouré 2010). However, analysis of the enzymes responsible for their synthesis as well as the factors regulating their activity during abiotic stress conditions, especially drought, has not been elucidated *in vivo*. Our results focused on the cloning and sequence analysis of the rate-limiting enzymes associated with GSH (*VrγECS*) and proline (*VrP5CS*) biosynthesis, and a subsequent insight into the regulation of these enzyme including mRNA expression levels and activity analysis under progressive drought stress and recovery.

Earlier reports demonstrated the catalytic properties and regulation of plant *γECS* in *Arabidopsis* and *B. juncea*, respectively (Jez et al 2004, Hothorn et al 2006). However, the relationship between the *γECS* mRNA levels and the corresponding enzyme activity of the γECS protein is still under debate. According to previous reports, the mRNA expression levels of γECS showed different patterns in response to various abiotic stresses in different plant as well as tissue systems. For example, in response to heavy metal stress and jasmonic acid, *γECS* mRNA levels increased in *Arabidopsis* leaves (Xiang and Oliver 1998). However, in *Arabidopsis* suspension cells, *AtγECS* levels remained constant upon heavy metal exposure (May et al. 1998). A recent report on cloning and characterization of γECS from a rare and typical alpine subnival plant, *Choriospora bungeana* which is a natural cold-resistant species, showed that both transcription and enzyme activities of γECS were enhanced in response to cold stress, indicating the probable existence of a different regulatory mechanism in that plant (Wu et al. 2009). In maize, a C_4 species of subtropical origin, it was reported that short term chilling stress increases γECS transcript levels in leaves, but the total γECS protein expression and enzyme activities remained unchanged (Gomez et al. 2004).

In the present study, we analysed the transcript levels of *VrγECS* in response to short-term (D3) and long-term (D6) water deficits as well as recovery period (6R). Our real time qPCR analysis clearly demonstrated that *VrγECS* transcript levels remained constant during varying water-deficit conditions as well as during recovery.

However, the enzyme activity patterns did not correlate with the corresponding transcript levels. Enzyme activity significantly enhanced during D3 but declined drastically during D6 and also failed to recover upon re-watering. Our data clearly indicate the existence of some posttranscriptional (or post-translational) regulation of *VrγECS* (May et al. 1998, Hicks et al. 2007). Also, enhancement of the enzyme activity during medium stress signifies the probable ability of *V. radiata* in regulating glutathione biosynthesis to tolerate moderate water-deficit regimes. Upon subsequent dehydration, it failed to enhance the levels of GSH. It was reported in *A. thaliana* that γECS undergoes reversible conformational changes that modulate the enzyme activity of the monomer in response to stress-induced redox environment (Jez et al. 2004). Moreover, there are circumstantial evidences indicating the influence of ROS, such as H_2O_2 and the redox states of antioxidants on the nuclear gene expression in plants (Creissen et al. 1999, Mittler et al. 2004). Also, there are several interesting reports demonstrating the direct or indirect induction of GSH biosynthesis by H_2O_2 (May and Leaver 1993, Queval et al. 2009). Apart from feedback inhibition by GSH (Hell and Bergman 1990), two mechanisms for activation of γECS enzyme activity have been proposed: (1) post-transcriptional oxidant-induced de-repression (Xiang and Oliver 1998, Xiang and Bertrand 2000) and (2) oxidation of enzyme thiol groups at post-translational level (Hicks et al. 2007). Further, it was recently shown that H_2O_2 induced changes in the cysteine biosynthetic enzymes may function in parallel with the proposed post-translational activation of γECS under oxidizing conditions (Queval et al. 2009). To further comprehend our findings towards the correlation of H_2O_2 and γECS activity in-vivo, we estimated H_2O_2 content in the roots of *V.radiata* during D3, D6 and 6R simultaneously and correlated the values with the VrγECS enzyme activity levels. The H_2O_2 levels increased gradually with gradual increase in the stress intensity and declined back to control levels upon re-watering. Individual linear regression analyses between H_2O_2 levels and VrγECS activity during D3 and D6 revealed an interesting and significant correlation between the two parameters. At medium level of water-deficit (D3), VrγECS activity was in positive and linear correlation with H_2O_2 levels ($R^2 = 0.9962$). However, during D6 there was no significant correlation between the two parameters ($R^2 = 0.1071$). It is known that at lower

concentrations, H_2O_2 can serve as a regulatory component in various signal transduction pathways whereas at higher concentrations it is able to act as a lethal ROS. From our data, we hypothesize that low concentrations of H_2O_2 could probably act as a positive regulator of VrγECS enzyme activity in-vivo, whereas at higher concentrations, this relationship is disrupted. It could be due to the fact that higher ROS levels become damaging to proteins, enzymes and other cellular metabolites (Smrinoff 1993). Direct interactive studies between H_2O_2 and VrγECS in-vitro, under similar oxidizing as well as osmotic conditions might provide further inputs in this regard. However, the present data provide an evidence for the possible regulation of VrγECS by H_2O_2 during progressive drought stress and recovery in *V. radiata*.

Further, based on the sequence analysis of putative VrγECS protein, we observed that the precursor protein consists of a 60-amino acid-long chloroplast target peptide. It has been reported that the encoded polypeptide in roots was targeted to the proplastids (Ruegsegger and Burnold 1993). The sequence analyses of the putative encoded protein indicate that the putative chloroplast target peptide cleavage sequence Ile Val Ala$^{\downarrow}$Ala is highly conserved among different plant species; however the target peptide itself is not conserved. The highly conserved nature of the whole sequence, rather than the catalytic site of the mature γECS polypeptide indicate that functions other than the catalytic activity which could be related to its post-translational regulation are also important for this enzyme (Noctor et al. 2002, Ball et al. 2004). Also, γECS from all sources were shown to bind oxidized GSH and a particular amino acid motif from *Arabidopsis* γECS (118-131) was known to share homology with putative oxidized GSH binding motif of glutathione reductase from *Pisum sativum* (May and Leaver 1994). We also observed similar homology between the putative oxidized GSH binding motif of γECS and the highly conserved Lys and Arg residues which facilitate GSH binding to a broad class of enzymes using GSH as their substrate.

In contrary to the popular belief of proline as an inert compatible osmolyte which protects subcellular structures and macromolecules during adverse environmental conditions, proline accumulation is now known to influence plant metabolism and stress-tolerance index

in multiple ways. Accumulation of proline in different plant species under certain abiotic stress condition is well documented (Szabados and Savouré 2010) and thus, understanding the regulation of proline biosynthesis, catabolism and inter- and intra-cellular transportation during adverse environmental conditions, including drought is quite essential (Kavi Kishor et al. 2005). Being an osmolyte, proline accumulation in cells during drought-induced osmotic stress prevents the damage from cellular dehydaration. As a molecular chaperone, proline protects protein structures and thus, maintains enzyme activity patterns during stress conditions (Sharma and Dubey 2005, Mishra and Dubey 2006) while as a ROS scavenger, it quenches singlet oxygen (Matysik et al. 2002). Thus, in general proline accumulation in higher plants is considered as a drought tolerance mechanism and proline biosynthesis is activated through enhanced activities of P5CS and P5CR enzymes while its catabolic pathway was inhibited during dehydration. However, during stress recovery (after re-watering), faster catabolism of proline was considered to be useful for better recovery from dehydration stress (Xue et al. 2009). In the present study, *V. radiata* drastically enhanced proline biosynthesis under water-deficit conditions which was also degraded rapidly upon re-watering. Now, proline biosynthesis is known to be regulated by the activity of two P5CS genes in higher plants, where one encodes a housekeeping protein while the other, a stress-specific isoform of P5CS. Both the P5CS genes show high degree of sequence homology in their coding regions, but differ in their transcriptional regulation patterns (Armengaud et al. 2004, Xue et al. 2009). In our study, elevated proline biosynthesis in *V. radiata* roots during progressive drought stress was highly correlated with the drastic increase in mRNA expression of *VrP5CS* gene which can be considered as the stress-specific isoform. Moreover, the corresponding enzyme activity of the VrP5CS enzyme also revealed a significant increase during D3 and D6 which indicates that rapid accumulation of proline might be a drought-resistance strategy of *V. radiata*. Moreover, as drought inhibits rate of photosynthesis, the cellular NADPH/$NADP^+$ ratio increases due to accumulation of NADPH, thus, higher rates of proline biosynthesis through glutamate which utilizes NADPH as cofactor, play an important role in balancing the cellular NADPH/ $NADP^+$ ratio which can be considered as an adaptive mechanism during drought stress.

It was also reported that proline biosynthesis might substitute for protein synthesis for ATP turnover as well as NADPH oxidation (DeRonde et al. 2000).

Proline biosynthesis was rapidly triggered during drought stress, while its catabolic pathway was activated during re-hydration or stress-relief and was controlled by the catabolic enzymes, PDH and P5CDH. In our study, we observed a rapid catabolism of proline during 6R associated with the corresponding *VrP5CS* gene expression and enzyme activity also declined rapidly upon re-watering. However, the observed proline degradation could be attributed to the induction of the catabolic enzymes PDH and P5CDH which we have not analyzed in our study. However, previous reports have confirmed that expression of these enzymes were significantly induced after stress-removal (stress recovery) (Rayapati and Stewart 1991, Nakashima et al. 1998). After rehydration, removal of the surplus proline levels appears to be quite significant for an efficient recovery from the stress as the rapid oxidation of proline to glutamate provides extra energy during recovery period. Thus, the actual amount and timing of proline accumulation were not the only factors responsible for stress-tolerance, but the ability of the plants to catabolise the accumulated proline also acts as an important strategy for plant stress-tolerance and subsequent recovery upon removal of the stress condition (DeRonde et al. 2004).

As we have seen earlier (Chapter 2) that progressive drought stress decreases RMC % in a dose-dependent manner. In order to correlate the observed modulations in root proline accumulation and the expression patterns of VrP5CS with drought, we performed three independent regression analyses between RMC % and proline content, *VrP5CS* mRNA expression pattern and VrP5CS enzyme activities as recorded during D0, D3, D6 and 6R. Pattern of proline accumulation, *VrP5CS* mRNA expression as well as enzyme activity showed negative correlation with declining RMC %. Hence, based on our present observations we could predict that drought-induced decline in the RMC % might be acting as a stress signal for roots to enhance proline biosynthesis by inducing the corresponding *VrP5CS* gene expression and associated enzyme activities

.

In this study, *VrγECS* and *VrP5CS* genes from *V. radiata* roots were sequenced and characterized. Sequence analysis of the putative VrγECS protein indicates that the identified gene codes for the chloroplastic and not cytosolic form, owing to the presence of an N-terminal chloroplast target peptide. Obtained VrP5CS cDNA sequence showed 98% sequence homology with *PvP5CS* and corresponds to the stress-specific isoform of the gene. In *V. radiata* roots, *VrγECS* was not induced at the transcript level during progressive drought stress but, the enzyme activity was significantly enhanced during D3. Thus, the existence of a post-transcriptional (or translational) regulatory mechanism was quite evident in this case. Dynamic correlation was also observed between the VrγECS activity and H_2O_2 concentrations in *V. radiata* roots under progressive drought and recovery, reflecting the possible concentration-dependent inter-relationship between the two parameters where low concentrations of H_2O_2 could be acting as positive regulator of VrγECS enzyme activity in-vivo. There was a rapid enhancement in proline biosynthesis in *V. radiata* roots during progressive drought (D3 and D6) and a rapid catabolism of the accumulated proline during recovery (6R). Expression patterns of the *VrP5CS* mRNA and the corresponding enzyme activities showed a strong positive correlation with the observed proline accumulation patterns, while a strong negative correlation was observed with the RMC % during similar watering regimes.

CHAPTER 6

Summary & Conclusions

SUMMARY AND CONCLUSIONS

Progressive drought caused a gradual and significant decline in the net CO_2 assimilation rate (P_n) in vegetatively mature *Vigna radiata* with a subsequent decline in the stomatal conductance (g_s) and transpiration rate (E). However, the observed decline in stomatal conductance and reduced CO_2 assimilation rates were a part of the adaptive mechanism of drought-stressed *Vigna*, rather than permanent damage, as the plants recovered significantly upon re-watering. It is known that decline of P_n could be either due to stomatal or non-stomatal limitations. In *V. radiata*, decline in P_n and g_s were not accompanied by a corresponding acute decline in the sub-stomatal CO_2 concentrations (Ci) which indicates involvement of non-stomatal factors along with stomatal limitations. For further insight on photosynthetic physiology of *V. radiata* under water deficit conditions, we analyzed the drought-induced effect on PSII efficiency by analyzing the modulations in chl *a* fluorescence. Drought differentially affected the various PSII reactions and the electron flux. However, drought-induced damage on the PSII quantum yields and the stability of PSII complex were insignificant and no alternate electron donors were utilized. As roots are known to be the initial perceivers of drought stress signal rather than leaves, we analyzed oxidative stress responses in *V. radiata* roots under progressive drought and recovery. Progressive drought stress induced a gradual accumulation of H_2O_2 and lipid peroxidation in *V. radiata* roots which declined upon re-watering. Ascorbic acid content and peroxidase activity in *V. radiata* roots showed a positive correlation with increasing drought stress intensity. However, glutathione content remained more or less stable except during D3. Root proline accumulation and its rapid catabolism upon re-watering indicate effective adaptive mechanisms in *V. radiata.*

Drought stress is known to cause abscission of most lateral roots in dry regions of soil and induces secondary lateral roots in regions of soil containing higher soil water content. Our data on *V. radiata*, depicts abscission of the longer lateral roots while short-roots were observed in the drought-stressed population which indicate that *V. radiata* can regulate its root morphology towards maximum water uptake strategies depending on the availability of water in the soil. Majority of the current understanding of drought responses

in legumes were based on foliar proteins only and a focused analysis involving root protein expression patterns at different levels of stress intensity and recovery period have not been reported. For a systematic analysis of the root protein expression patterns during progressive drought stress and recovery, we used comparative proteomics approach which has emerged as a promising tool for global analyses of protein expression levels in the recent past. Our proteomics-based study showed that *V. radiata* could express different sets of proteins at different stages of drought stress. Root proteins involved in root architecture, energy metabolism, ROS detoxification and cell signaling were differentially regulated during progressive drought stress. Expression patterns of proteins belonging to different functional groups were highly correlated and regulated by the soil water status in terms of medium and high stress intensity. Our data suggest that *V. radiata* could tolerate medium level drought stress intensity but gets susceptible under subsequent enhancement of drought treatment.

Drought stress-induced reactive oxygen species result in oxidation of lipids, resulting in unstable lipid peroxides which would degrade to form highly cytotoxic aldehydic products. Aldehyde reductases (ALRs), belonging to aldo-keto reductase superfamily, play important role in detoxifying the cytotoxic by-products of lipid peroxidation. Through proteomic approach, we observed a significant up-regulation of aldehyde reductase protein in roots of *V. radiata* (VrALR) during short term water deficit. Hence, in this objective we characterize the functional role of this enzyme in *V. radiata* under progressive drought. We cloned, expressed and purified the VrALR protein. The aldehyde reducing activity of the purified protein showed highest catalytic efficiency with p-NB and least with cinnamaldehyde. For analyzing the detoxification potential of VrALR, we expressed the protein in bacterial and yeast systems. VrALR expression has successfully complemented the endogenous defense mechanism of *E.coli* BL21 and yeast mutant W3O3-1A against oxidative stress conditions indicating the effective detoxification of the H_2O_2 and p-NB-induced toxicity. However, in comparison with the bacterial system, yeast has shown lower detoxifying capacity. For analyzing the protective role of endogeneous ALR, we observed the VrALR mRNA expression patterns and the

corresponding enzyme activity. We found that *V. radiata* effectively regulates the ALR gene in response to short term water defict by up-regulating its mRNA expression and consecutively the protein content as well as the aldehyde reducing activity. But higher oxidizing conditions inhibited the gene expression and thus the protein content. The continued enhancement of aldehyde reducing activity could be due to some other stable proteins in the root extract with aldehyde reducing enzymatic properties.

In glutathione biosynthesis, the rate limiting enzyme is γ-glutamyl cysteine synthetase (γECS) which serves as the control point during abiotic stresses when the demand for GSH enhances. γECS activity is usually influenced by multiple regulatory factors which include older concept of feedback regulation by glutathione and also the recent concept of redox regulation by H_2O_2 and disulphide bridges. In this study, we focused on the cloning, sequence analysis of *VrγECS* and a subsequent insight into the regulation of this enzyme including mRNA expression levels in *V. radiata* under progressive drought stress and recovery. We observed that declining root moisture content during progressive drought has no direct impact on *VrγECS* gene expression and under progressive drought stress; glutathione (GSH) biosynthesis in roots of *V. radiata* was directly dependent on the activity of VrγECS enzyme. Regression analysis with H_2O_2 concentrations showed that low concentrations of H_2O_2 could probably regulate VrγECS enzyme activity in vivo. The multifaceted protective role of proline under drought stress is well documented. In the present study, *V. radiata* significantly enhanced proline biosynthesis under water-deficit conditions which was also degraded rapidly upon re-watering. Elevated proline biosynthesis in *V. radiata* roots was highly correlated with a significant increase in its mRNA expression and catalytic activity of VrP5CS. Pattern of proline accumulation, *VrP5CS* mRNA expression as well as enzyme activity showed negative correlations with declining root moisture content which were possibly acting as stress signals in roots to enhance biosynthesis of protective osmolyte incuding proline.

CHAPTER 7

Literature cited

Literature cited

Abdelhamid MT (2010) Efficient root system in legume crops to stress environments. S.S. Yadav et al. (eds.), *Climate Change and Management of Cool Season Grain Legume Crops* pp 229-242.

Abdel-Waheb AM, Shabeb MSA, Younis MAM (2002) Studies on the effect of salinity, drought stress and soil type on nodule activities of *Lablab purpureus* (L.) sweet (Kashrangeeg). *Journal of Arid Environment* **51**: 587-602.

Adamski JM, Peters JA, Daniloski A, Bacarin MA (2011) Excess iron-induced changes in the photosynthetic characteristics of sweet potato. *Journal of Plant Physiology* **168**: 2056-2062.

Agrawal GK, Rakwal R,Yonekura M, Kubo A, Saji H (2002) Proteome analysis of differentially displayed proteins as a tool for investigating ozone stress in rice (*Oryza sativa* L.) seedlings. *Proteomics* 2: 947-959.

Aharon R, Shahak Y, Wininger S, Bendov R, Kapulnik Y, Galili G (2003). Overexpression of a plasma membrane aquaporin in transgenic tobacco improves plant vigor under favorable growth conditions but not under drought or salt stress. Plant Cell **15**: 439-47.

Akcay U.C, Eercan O, Kavas M, Yildiz L, Yilmaz C, Octem H.A, Yucel M (2010) Drought-induced oxidative damage and antioxidant responses in peanut (*Arachis hypogaea* L.) seedlings. *Plant Growth Regulation* **61**: 21-28.

Al-Kaisi MM, Broner I (2009) Crop Water Use and Growth Stages. *Colorado State University Extension publication, CO, USA* Publication number 4.715.

Alsina MM, Smart DR, Bauerle T, de Herralde F, Biel C, Stockert C, Negron C, Save R (2011) Seasonal changes of whole root system conductance by a drought-tolerant grape root system. *Journal of Experimental Botany* **62**: 99-109.

Alvarez S, Marsh EL, Schroeder SG, Schachtman DP (2008) Metabolomic and proteomic changes in the xylem sap of maize under drought. *Plant Cell and Environment* **31**: 325-340.

Amme S, Matros A, Schlesier, Hans-Peter M (2006) Proteome analysis of cold stress response in *Arabidopsis thaliana* using DIGE-technology. *Journal of Experimental Botany* **57**:1537-1546.

Annicchiarico P, Piano E (2004) Indirect selection for root development of white clover and implications for drought tolerance. *Journal Agronomy & Crop Science* **190**: 28-34.

Apel K, Hirt H (2004) Reactive oxygen species: metabolism, oxidative stress and signal transduction. *Annual Reviews in Plant Biology* **55**: 373-399.

Aravind P, Prasad MNV (2005) Modulation of cadmium-induced oxidative stress in Ceratophyllum demersum by zinc involves ascorbate-glutathione cycle and glutathione metabolism. *Plant Physiology and Biochemistry* **43**:107-116.

Armengaud P, Thiery L, Buhot N, Grenier-de March G, Savouré A (2004) Transcriptional regulation of proline biosynthesis in *Medicago truncatula* reveals developmental and environmental specific features. *Physiologia Plantarum* **120**: 442-450.

Asada K (2006) Production and scavenging of reactive oxygen species in chloroplasts and their functions. *Plant Physiology* **141**: 391-396.

Bae H, Sicher R (2004) Changes in soluble protein expression and leaf metabolite levels in *Arabidopsis thaliana* grown in elevated carbon dioxide. *Field Crop Research* **90**: 61-73.

Bae MS, Cho EJ, Choi E-Y, Park OK (2003) Analysis of the Arabidopsis nuclear proteome and its response to cold stress. *The Plant Journal* **36**: 652-663.

Ball L, Accotto G, Bechtold U, Creissen G, Funck D, Jimenez A, Kular B, Leyland N, Mejia-Carranza J, Reynolds H, Karpinski S, Mullineaux PM (2004) Evidence for a direct link between glutathione biosynthesis and stress defense gene expression in *Arabidopsis*. *The Plant Cell* **16**: 2448-2462.

Bartels D (2001) Targeting detoxification pathways: an efficient approach to obtain plants with multiple stress tolerance? *Trends in Plant Sciences* **6**: 284-286.

Bartels D, Engelhardt K, Roncarati R, Schneider K, Rotter M, Salamini F (1991) An ABA and GA modulated gene expressed in the barley embryo encodes an aldose reductase. *The EMBO Journal* **10**:1037-1043.

Bartels D, Sunkar R (2005) Drought and salt tolerance in plants. *Critical Reviews in Plant Sciences* **24**: 23-58.

Bates LS, Walderen RP, Teare ID (1973) Rapid determination of free proline for water stress studies. *Plant and Soil* **39**: 205-207

Bengough AG, McKenzie BM, Hallett PD, Valentine TA (2011) Root elongation, water stress, and mechanical impedance: a review of limiting stresses and beneficial root tip traits. *Journal of Experimental Botany* **62**: 59-68.

Benjamin JG, Nielsen DC (2006) Water deficit effects on root distribution of soybean, field pea and chickpea. *Field Crop Research* **97**: 248-253.

Bhattacharya E, Rajam MV (2006) Polyamine biosynthesis as a novel target for engineering crop plants for abiotic stress tolerance. *Journal of Plant Biology* **33**: 99-105.

Bian S, Jiang Y (2009) Reactive oxygen species, antioxidant enzyme activities and gene expression patterns in leaves and roots of Kentucky bluegrass in response to drought stress and recovery. *Scientia Horticulture* **120**: 264-270.

Bisht IS, Bhat KV, Lakhanpaul S, Latha M, Jayan PK, Biswas BK, Singh AK (2005) Diversity and genetic resources of wild *Vigna* species in India. *Genetic Resource and Crop Evolution* **52**: 53-68.

Blanco-Portales R, Medina-Escobar N, López-Ráez JA, González-Reyes JA, Villalba JM, Moyano E, Caballero JL, Muñoz-Blanco J (2002) Cloning, expression and immunolocalization pattern of a cinnamyl alcohol dehydrogenase gene from strawberry (*Fragaria X ananassa* cv. Chandler). *Journal of Experimental Botany* **53**: 1723-1734.

Blum A, Sinmena B, Mayer J, Golan G and Shpiler L (1994) Stem reserve mobilisation supports wheat grain filling under heat stress. *Australian Journal of Plant Physiology* **121**: 771-781.

Bogeat-Treboulot MB, Broché M, Renaut J, Jouve L, Thiec DL, Fayyaz P, Vinocur B, Witters E, Laukens K, Teichmann T, Altman A, Hausman JF, Polle A, Kangasjärvi J, Dreyer E (2007) Gradual soil water depletion results in reversible changes of gene expression, protein profiles, ecophysiology, and growth performance in *Populus euphrotica*, a poplar growing in arid regions. *Plant Physiology* **143**: 876-892.

Borderies G, Jamet E, Lafitte C, Rossignol M, Jauneau A, Boudart G, Monsarrat B, Esquerré-Tugayé MT, Boudet A, Pont-Lezica R (2003) Proteomics of loosely bound cell wall proteins of Arabidopsis thaliana cell suspension cultures: a critical analysis. *Electrophoresis* **24**: 3421-3432.

Bourquin V, Nishikubo N, Abe H, Brumer H, Denman S, Eklund M, Christiernin M, Teeri TT, Sundberg B, Mellerowicz EJ (2002) Xyloglucan endotransglycosylases have a function during the formation of secondary cell walls of vascular tissues. *The Plant Cell* **14**: 3073-3088.

Bowler C, Van Montagu M, Inzé D (1992) Superoxide dismutase and stress tolerance. *Annual Review of Plant Physiology and Plant Molecular Biology* **43**: 83-116.

Bracale M, Levi M, Savini C, Dicorato W, Galli MG (1997) Water deficit in pea root tips: effect on the cell cycle and on the production of Dehydrin-like proteins. *Annals of Botany* **79**: 593-600.

Bradford M (1976) A Rapid and sensitive method for the quantitation of microgram quantities of protein utilizing the principle of protein-dye binding. *Analytical Biochemistry* **72**: 248-254.

Brechenmacher L, Lee J, Sachdev S, Song Z, Nguyen THN, Joshi T, Oehrle N, Libault M, Mooney B, Xu D, Cooper B, Stacey G (2009) Establishment of a protein reference map for soybean root hair cells. *Plant Physiology* **149**: 670-682.

Buettner GR, Jurkiewicz BA (1996) Chemistry and biochemistry of ascorbic acid. *In Handbook of Antioxidants, ed.E Cadenas, L Packe*r, pp. 91–115. NewYork: Dekker

Cabiscol E, Tamarit J, Ros J (2000) Oxidative stress in bacteria and protein damage by reactive oxygen species. *International Microbiology* **3**: 3-8.

Campbell P, Braam J (1999) In vitro activities of four xyloglucan endotransglycosylases from Arabidopsis. *The Plant Journal* 18: 371-382.

Cánovas FM, Gaudot ED, Recorbet G, Jorrin J, Mock HP, Rossingol M (2004) Plant proteome analysis. *Proteomics* **4**: 285-298.

Carpentier SC, Witters E, Laukens K, Van Onckelen H, Swennen R, Panis B (2007) Banana (*Musa spp.*) as a model to study the meristem proteome: acclimation to osmotic stress. *Proteomics* **7**: 92-105.

Cattivelli L, Rizza F, Badeck FW, Mazzucotelli E, Mastrangelo AM, Francia E, Maré C, Tondelli A, Stanca AM (2008) Drought tolerance improvement in crop plants: An integrated view from breeding to genomics. *Field Crop Research* **105**: 1-14.

Cha MK, Kim WC, Lim CJ, Kim K, Kim IH (2004) *Escherichia coli* periplasmic thiol peroxidase acts as lipid hydroperoxide peroxidase and the principal antioxidative function during anaerobic growth. *Journal of Biological Chemistry* **279**: 8769-8778.

Chang WWP, Huang L, Shen M, Webster C, Burlingame AL, Roberts JKM (2000) Pattern of protein synthesis and tolerance of anoxia in root tips of maize seedlings acclimated to a low-oxygen environment, and identification of proteins by mass spectrometry. *Plant Physiology* **122**: 295-317.

Chaves MM, Flexas J, Pinheiro C (2009) Photosynthesis under drought and salt stress: regulation mechanisms from whole plant to cell. *Annals of Botany* **103**:551-60.

Chaves MM, Maroco JP, Pereira JS (2003) Understanding plant responses to drought from genes to the whole plant. *Functional Plant Biology* **30**: 239-264.

Chen H, Li Z, Xiong L (2012) A plant microRNA regulates the adaptation of roots to drought stress. *FEBS Letters* 1742-1747.

Chen J, Goldsborough PB (1994) Increased activity of γ-g]utamylcysteine synthetase in tomato cells selected for cadmium tolerance. *Plant Physiology* **106**: 233-239.

Chen J, Schenker S, Frosto T, Henderson G (1998) Inhiition of cytochrome C oxidase activity by 4-hydroxynonenal : role of HNE adduct formation with enzyme subunits. *Biochimica et Biophysica Acta* **1380**: 336-344.

Chen JW, Zhang Q, Li XS, Cao KF (2010) Gas exchange and hydraulics in seedlings of *Hevea brasiliensis* during water stress and recovery. *Tree Physiology* **30**: 876-885.

Chen KM, Gong HJ, Chen GC, Wang SM, Zhang CL (2004) Gradual drought under field conditions influences the glutathione metabolism, redox balance and energy supply in spring wheat. *Journal of Plant Growth and Regulation* **23**: 20-28.

Cho SK, Kim JE, Park JA, Eom TJ, KimWT (2006) Constitutive expression of abiotic stress-inducible hot pepper CaXTH3, which encodes a xyloglucan endo-transglucosylase/hydrolase homolog, improves drought and salt tolerance in transgenic Arabidopsis plants. *FEBS Letters* **580**: 3136-3144.

Choudhary NL, Sairam RK, Tyagi A (2005) Expression of delta1-pyrroline-5-carboxylate synthetase gene during drought in rice (*Oryza sativa* L.). *Indian Journal of Biochemistry and Biophysics* **42**: 366-370.

Claes B, Dekeyser R, Villaroel R, Van den Bulcke M, Bauw G, Van Montagu M, Caplan A (1990) Characterization of a rice gene showingorganspecific expression in response to salt stress and drought. *The Plant Cell* **2**: 19-27.

Claussen W (2005) Proline as a measure of stress in tomato plants. *Plant Science* **168**: 241-248.

Cobbett CS (2000) Phytochelatins and their roles in heavy metal detoxification. *Plant Physiology* **123**: 825-832.

Colrat S, Deswarte C, Latché A, Klaébé A, Bouzayen M, Fallot J, Roustan JP (1999b) Enzymatic detoxification of eutypine, a toxin from Eutypa lata, by Vitis vinifera cells: partial purification of an NADPH dependent aldehyde reductase. *Planta* **207**: 544-550.

Colrat S, Latché A, Guis M, Pech JC, Bouzayen M, Fallot J, Roustan JP (1999a) Purification and characterization of a NADPH-dependent aldehyde reductase from mungbean that detoxifies eutypine, a toxin from Eutypa lata. *Plant Physiology* **119**: 621-626.

Combet C, Jambon M, Deleage G, Geourjon C (2002) Geno3D: automatic comparative molecular modelling of protein. *Bioinformatics* **18**: 213-214.

Corpet F (1988) Multiple sequence alignment with hierarchical clustering. *Nucleic Acids Research* **16**: 10881-10890.

Creissen G, Firmin J, Fryer M, Kular B, Leyland N, Reynolds H, Pastori G, Wellburn F, Baker N, Wellburn A, Mullineaux P (1999) Elevated glutathione biosynthetic capacity in the chloroplasts of transgenic tobacco plants paradoxically causes increased oxidative stress. *The Plant Cell* **11**: 1277-1292.

Csiszár J, Gallé Á, Horváth E, Dancsó P, Gombos M, Váry Z, Erdei L, Györgyey J, Tari I (2012) Different peroxidase activities and expression of abiotic stress-related peroxidasesin apical root segments of wheat genotypes with different drought stress tolerance under osmotic stress. *Plant Physiology and Biochemistry* **52**: 119-129.

Cummins I, Dixon DP, Freitag-Pohl S, Skipsey M, Edwards R (2011) Multiple roles for plant glutathione transferases in xenobiotic detoxification. *Drug Metabolism Reviews* **43**: 266-280.

Damerval C, de Vienne D, Zivy M, Thiellement H (1986) Technical improvements in two-dimensional electrophoresis increase the level of genetic variation detected in wheat-seedling proteins. *Electrophoresis* **7**: 52-54.

Davies WJ, Zhang J (1991) Root signals and the regulation of growth and development of plant in dry soil. *Annual Review in Plant Physiology and Plant Molecular Biology* **42**: 55-76.

De Domenico S, Bonsegna S, Horres R, Pastor V, Taurino M, Poltronieri P, Imtiaz M, Kahl G, Flors V, Winter P, Snatino A (2012) Transcriptomic analysis of oxylipin biosynthesis genes and chemical profiling reveal an early induction of jasmonates in chickpea roots under drought stress. *Plant Physiology and biochemistry* **61**: 115-122.

De Ronde JA, Cress WA, Kruger GHJ, Strasser RJ, Van Staden J (2004) Photo-synthetic response of transgenic soybean plants, containing an *Arabidopsis* P5CR gene, during heat and drought stress. *Journal of Plant Physiology* **161**: 1211-1224.

Dhindsa RS (1991) Drought stress enzymes of glutathione metabolism, oxidation injury and protein synthesis in *Tortula ruralis*. *Plant Physiology* **83**: 816-819.

Di Iorio A, Montagnoli A, Scippa GS, Chiatante D (2011) Fine root growth of *Quercus pubescens* seedlings after drought stress and fire disturbance. *Environmental and Experimental Botany* **74**: 272-279.

Diao G, Wang Y, Wang C, Yang C (2011) Cloning and functional characterization of a novel glutathione-S-transferase gene from *Limonium bicolor*. *Plant Molecular Biology Reporter* **29**: 77-87.

Dias MC, Brüggemann W (2007) Limitation of photosynthesis in *Phaseolus vulgaris* under drought stress: gas exchange, chlorophyll fluorescence calvin cycle enzymes. *Photosynthetica* **48**: 96-102.

Dobrá J, Vanková R, Havlová M, Burman AJ, Libus J, Štorchová H (2011) Tobacco leaves and roots differ in the expression of proline metabolism-related genes in the course of drought stress and subsequent recovery. *Journal of Plant Physiology* **168**: 1588-1597.

Dreyer I, Horeau C, Lemaillet G, Zimmermann S, Bush DR, Rodriguez-Navarro A, Schachtman DP, Spalding EP, Sentenac H, Gaber RF (1999) Identification and characterization of plant transporters using heterologous expression systems. *Journal of Experimental Botany* **50**: 1073-1087.

Ehdaie B, Layne AP, Waines JG (2012) Root system plasticity to drought influences grain yield in bread wheat. *Euphytica* **186**: 219-232.

Eissenstat DM, Caldwell MM (1989) Invasive root growth into disturbed soil of two tussock grasses that differ in competitive effectiveness. *Functional Ecology* **3**: 345-353.

Else MA, Janowiak F, Atkinson CJ, Jackson MB (2009) Root signals and stomatal closure inrelation to photosynthesis, chlorophyll a fluorescence and adventitious rooting of flooded tomato plants. *Annals of Botany* **103**: 313-323.

Emanuelsson O, Nielsen H, von Heijne G (1999) ChloroP, a neural network-based method for predicting chloroplast transit peptides and their cleavage sites. *Protein Science* **8**: 978-984.

Ennahli S, Earl HJ (2005) Physiological limitations to photosynthetic carbon assimilation in cotton under water stress. *Crop Science* **45**: 2374-2382.

Estruch F (2000) Stress-controlled transcription factors, stress-induced genes and stress tolerance in budding yeast. *FEMS Microbiology Reviews* **24**:469-486.

Eun SO, Lee Y (1997) Actin filaments of guard cells are reorganized in response to light and abscisic acid. *Plant Physiology* **115**: 1491-1498.

Evans NH, McAinsh MR, Hetherington AM, Knight MR (2005) ROS perception in *Arabidopsis thaliana*: The ozone induced calcium response. *The Plant Journal* **41**: 615-626.

Farhi M, Lavie O, Masci T, Hendel-Rahmanim K, Weiss D, Abeliovich H, Vainstein A (2010) identification of rose phenylacetaldehyde synthase by functional complementation in yeast. *Plant Molecular Biology* **72**: 235-245.

Farooq M, Wahid A, Lee D, Ito O, Siddique KHM (2009) Advances in Drought Resistance of Rice. *Critical Reviews in Plant Sciences* **28**: 199–217.

Ferreira S, Hjerno K, Larsen M, Wingsle G, Larsen P, Fey S, Roepstroff P, Pais MS (2006) Proteome profiling of *Populus euphratica* Oliv. upon heat stress. *Annals of Botany* **98**: 361-377.

Flexas J, Medrano H (2002) Drought inhibition of photosynthesis in C3 plants: Stomatal and non stomatal limitations revisited. *Annals of Botany* **89**: 183-189.

Forti G, Elli G (1995) The function of ascorbic acid in photosynthetic phosphorylation. *Plant Physiology* **109**: 1207-1211.

Foyer CH, Harbinson J (1994) Oxygen metabolism and the regulation of photosynthetic electron transport. *In Causes of Photooxidative Stresses and Amelioration of Defense Systems in Plants, ed. CHFoyer, P Mullineaux*, pp. 1-42. BocaRaton, FL: CRC Press.

Foyer CH, Noctor G (2000) Oxygen processing in photosynthesis: regulation and signaling. *New Phytologist* **146**: 359-388.

Foyer CH, Noctor G (2003) Redox sensing and signaling associated with reactive oxygen in chloroplasts, peroxisomes and mitochondria. *Physiologia Plantarum* **119**: 355-364.

Foyer CH, Noctor G (2005) Redox homeostasis and antioxidant signaling: A metabolic interface between stress perception and physiological responses. *The Plant Cell* **17**: 1866-1875.

Foyer CH, Noctor G (2009) Redox regulation in photosynthetic organisms: signaling, acclimation and practical implications. *Antioxidant Redox signaling* **11**: 861-905.

Frommer WB, Ninnemann O (1995) Heterologous expression of genes in bacterial, fungal, animal and plant cell. *Annual Review of Plant Physiology and Plant Molecular Biology* **46**: 419-444.

Fu J, Huang B (2001) Involvement of antioxidants and lipid peroxidation in the adaptation of two cool-season grasses to localized drought stress. *Environmental and Experimental Botany* **45**:105-114.

Gallardo K, Job C, Groot SP, Puype M, Demol H, Vandekerckhove J, Job D (2001) Proteomic analysis of *Arabidopsis* seed germination and priming. *Plant Physiology* **126**: 835-848.

Garay-Arroyo A, Covarrubias AA (1999) Three genes whose expression is induced by stress in *Saccharomyces cerevisiae*. *Yeast* **15**: 879-892.

Garcia-Rios M, Fujita T, Christopher LP, Locy RD, Clithero JM, Bressan RA, Csonka LN (1997) Cloning of a polycistronic cDNA from tomato encoding γ-glutamyl kinase and γ-glutamyl phosphate reductase. *Proceedings of National Academy of Science, USA* **94**: 8249-8254.

Gaul D, Hertel D, Borken W, Matzner E, Leuschner C (2008) Effects of experimental drought on the fine root system of mature Norway Spruce. *Forest Ecology and Management* **256**: 1151-1159.

Gaur PM, Krishnamurthy L, Kashiwagi J (2008). Improving drought-avoidance root traits in chickpea (*Cicer arietinum* L.) -Current Status of Research at ICRISAT. *Plant Production Science* **11**: 3-11.

Gewin V (2010) Food: an underground revolution. *Nature* **466**: 552–553.

Gill SS, Tuteja N (2010) Reactive oxygen species and antioxidant machinery in abiotic stress tolerance in crop plants. *Plant Physiology and Biochemistry* **48**: 909-930.

Gomes MTG, daLuz AC, dosSantos MR, Batitucci MCP, Silva DM, Falqueto AR (2012) Drought tolerance of passion fruit plants assessed by the OJIP chlorophyll *a* fluorescence transient. *Scientia Horticulture* **142**: 49-56.

Gomez LD, Noctor G, Knight M, Foyer CH (2004) Regulation of calcium signaling and gene expression by glutathione. *Journal of Experimental Botany* **55**: 1851-1859.

Gowda VRP, Henry A, Yamauchi A, Shashidhar HE, Serraj R (2011) Root biology and genetic improvement for drought avoidance in rice. *Field Crop Research* **122**: 1-13.

Granda V, Cuesta C, Álvarez R, Ordás R, Centeno ML, Rodríguez A, Majada JP, Fernández B, Feito I (2011) Rapid responses of C14 clone of *Eucalyptus globulus* to root drought stress: Time course of hormonal and physiological signaling. *Journal of Plant Physiology* **168**: 661-670.

Gromes R, Hothorn M, Lenherr ED, Rybin V, Scheffzek K, Rausch T (2008) The redox switch of γ-glutamylcysteine ligase via a reversible monomer-dimer transition is a mechanism unique to plants. *The Plant Journal* **54**: 1063-1075.

Guillén P, Guis M, Martinez-Reina G, Colrat S, Dalmayrac S, Deswarte S, Bouzayen M, Roustan JP, Fallot J, Pech JC, Latché A (1998) A novel NADPH-dependent aldehyde reductase gene from *Vigna radiata* confers resistance to the grapevine fungal toxin eutypine. *The Plant Journal* **16**: 335-343.

Gulshan K, Rovinsky SA, Moye-Rowley WS (2004) YBP1 and its homologue YBP2/YBH1 inflence oxidative stress tolerance by non-identical mechanisms in *Saccharomyces cerevisiae*. *Eukaryotic Cell* **3**: 318-330.

Gutierrez R, Lindeboom JJV, Paredez AR, Emons AMC, Ehrhardt DW (2009) Arabidopsis cortical microtubules position cellulose synthase delivery to the plasma membrane and interact with cellulose synthase trafficking compartments. *Nature and Cell Biology* **11**: 797-806.

Haberer K, Herbinger K, Alexou M, Rennenberg H, Tausz M (2008) Effects of drought and canopy ozone exposure on antioxidants in fine roots of mature European Beech (*Fagus sylvatica*). *Tree Physiology* **28**: 713-719.

Hajheidari M, Eivazi A, Buchanan BB, Wong JH, Majidi I, Salekdeh GH (2007). Proteomics uncovers a role for redox in drought tolerance in wheat. *Journal of Proteome Research* **6**: 1451-1460.

Harb A, Krishnan A, Ambavaram MMR, Pereira A (2010) Molecular and physiological analysis of drought stress in *Arabidopsis* reveals early responses leading to acclimation in plant growth. *Plant Physiology* **154**:1254-1271.

Hartung W, Sauter A, Hose E (2002) Abscisic acid in the xylem: where does it come from, where does it go to? *Journal of Experimental Botany* **53**: 27-32.

Hashiguchi A, Ahsan N, Komatsu S (2010) Proteomics application of crops in the context of climate changes. *Food Research International* **43**: 1803-1813.

Hayes MA, Davies C, Dry IB (2007) Isolation, functional characterization, and expression analysis of grapevine (*Vitis vinifera* L.) hexose transporters: differential roles in sink and source tissues. *Journal of Experimental Botany* **58**: 1985-1997.

Hegedüs A, Erdei S, janda T, Tóth E, Horváth G, Dudits D (2004) Transgenic tobacco plants overproducing alfalfa aldose/aldehyde reductase show higher tolerance to low temperature and cadmium stress . *Plant Science* **166**: 1329-1333.

Hell R, Bergmann L (1990) γ-Glutamylcysteine synthetase in higher plants: catalytic properties and subcellular localization. *Planta* **180**: 603-612.

Henry A, Cal AJ, Batoto TC, Torres RO, Serraj R (2012) Root attributes affecting water uptake of rice (*Oryza sativa*) under drought. *Journal of Experimental Botany* **63**: 4751-4763.

Henry A, Gowda VRP, Torres RO, McNally KL, Serraj R (2011) Variation in root system architecture and drought response in rice (Oryza sativa): Phenotyping of the OryzaSNP panel in rainfed lowland fields. *Field Crop Research* **120**: 205-214.

Hicks LM, Cahoon RE, Bonner ER, Rivard RS, Sheffield J, Jez JM (2007) Thiol-based regulation of redox-active glutamtate cysteine ligase from *Arabidopsis thaliana*. *The Plant Cell* **19**: 2653-2661.

Hideg É, Nagy T, Oberschall A, Dudits D, Vass I (2003) Detoxification function of aldose/aldehyde reductase during drought and ultraviolet-B (280–320 nm) stresses. *Plant Cell and Environment* **26**: 513-522.

Hiscox JD, Israelstam, GF (1979) A method for the extraction of chlorophyll from leaf tissue without maceration. *Canadian Journal of Botany* **57**: 1332-1334.

Hissin PJ, Hilf R (1976) A fluorometric method for determination of oxidized and reduced glutathione in tissues. *Analytical Biochemistry* **74**: 214-226.

Hothorn M, Wachter A, Gromes R, Stuwe T, Rausch T, Scheffzek K (2006) Structural basis for the redox control of plant glutamate cysteine ligase. *Journal of Biological Chemistry* **281**: 27557-27565.

Howarth JR, Fourcroy P, Davidian JC, Smith FW, Hawkesford MJ (2003) Cloning of two contrasting high-affinity sulfate transporters from tomato induced by low sulfate and infection by the vascular pathogen *Verticillium dahlia*. *Planta* **218**: 58-64.

Hsiao TC, Xu LK (2000) Sensitivity of growth of roots versus leaves to water stress: biophysical analysis and relation to water transport. *Journal of Experimental Botany* **51**: 1595-1616.

Hu CA, Delauney AJ, Verma DP (1992) A bifunctional enzyme (Δ^1-pyrroline-5-carboxylate synthetase) catalyses the first two steps in proline biosynthesis in plants. *Proceedings of National Academy of Science, USA* **89**: 9354-9358.

Hu W, Yan X, Xiao Y, Zeng J, Qi H, Ogweno JO (2013) 24-Epibrassinosteroid alleviate drought-induced inhibition of photosynthesis in *Capsicum annum*. *Scientia Horticulturae* **150**: 232-237.

Hu X, Lu M, Li C, Liu T, Wang W, Wu J, Tai F, Li X, Zhang J (2011) Differential expression of proteins in maize roots in response to abscisic acid and drought. *Acta Physiologia Plantarum* **33**: 2437-2446.

Huang B, Chu CH, Chen SL, Juan HF, Chen YM (2006) A proteomics study of the mung bean epicotyl regulated by brassinosteroids under conditions of chilling stress. *Cell and Molecular Biology Letters* **11**: 264-278.

Huang B, Nobel PS (1992) Hydraulic conductivity and anatomy for lateral roots of *Agave deserti* during root growth and drought-induced abscission. *Journal of Experimental Botany* **43**: 1441-1449.

Huang W, Ma X, Wang Q, Gao Y, Xue Y, Niu X, Yu G, Liu Y (2008) Significant improvement of stress tolerance in tobacco plants by overexpressing a stress responsive aldehyde dehydrogenase gene from maize (*Zea mays*). *Plant Molecular Biology* **68**: 451-463.

Hui-yong L, Shu-hua H, Yun-su S, Yan-Chun S, Zhong-bao Z, Guo-ying W, Tian-yu W, Yu L (2009) Isolation and analysis of drought induced genes in maize roots. *Agricultural Sciences in China* **8**: 129-136.

Hund A, Richner W, Soldati A, Fracheboud YV, Stamp P (2007) Root morphology and photosynthetic performance of maize inbred lines at low temperature. *European Journal of Agronomy* **27**: 52-61.

Hur J, Jung KH, Lee CH, An G (2004) Stress-inducible OsP5CS2 gene is essential for salt and cold tolerance in rice. *Plant Science* **167**: 417-426.

Hurkman WJ, Tanaka CK (1986) Solubilization of plant membrane proteins for analysis by two-dimensional gel electrophoresis. *Plant Physiology* **81**: 802-806.

Igarashi Y, Yoshiba Y, Sanada Y, Yamaguchi-Shinozaki K, Wada K, Shinozaki K (1997) Characterization of the gene for delta1-pyrroline-5-carboxylate synthetase and correlation between the expression of the gene and salt tolerance in *Oryza sativa* L. *Plant Molecular Biology* **33**: 857-865.

Imlay JA (2003) Pathways of oxidative damage. *Annual Review of Microbiology* **57**: 395-418.

Ingle R, Smith J, Sweetlove L (2005) Responses to nickel in the proteome of the hyper accumulator plant *Alyssum lesbiacum*. *Biometals* **18**: 627-641.

Innocenti G, Pucciariello C, Gleuher ML, Hopkins J, de Stefano M, Delledonne M, Puppo A, Baudouin E, Frendo P (2007) Glutathione synthesis is regulated by nitric oxide in *Medicago truncatula* roots. *Planta* **225**: 1597-1602.

Intergovernmental Panel on Climate Change (IPCC) (2007) McCarthy JJ, Canziani OF, Leary NA, Dokken DJ, White KS eds. *Impacts, Adaptations and Vulnerability. Contribution of Working Group II to the Third Assesment Report of the Intergovernmental Panel on Climate Change.* Camridge, UK and New York, USA, Cambridge University Press.

Jacobs DF, Salifu KF, Davis AS (2009) Drought susceptibility and recovery of transplanted *Quercus rubra* seedlings in relation to root system morphology. *Annals of Forest Science* **66:** 504-512.

Jacquot JP, Eklund H, Rouhier N, Schürmann P (2009) Structural and evolutionary aspects of thioredoxin reductases in photosynthetic organisms. *Trends in Plant Sciences* **14**: 336-343.

Jain M, Nandwal A.S, Kundu B.S, Kumar B, Sheoran I.S, Kumar N, Mann A, Kukreja S (2006) Water relations, activities of antioxidants, ethylene evolution and membrane integrity of pigeonpea roots as affected by soil moisture. *Biologia Plantarum* **50**: 303-306.

Jamieson DJ (1998) Oxidative stress responses of the yeast *Saccharomyces cerevisiae*. *Yeast* **14**:1511-1527.

Jez JM, Bennett MJ, Schlegel BP, Lewis M, Prnning TM (1997) Comparative anatomy of the aldo-keto reductase superfamily. *Biochemical Journal* **326**: 625-636.

Jez JM, Cahoon RE, Chen S (2004) *Arabidopsis thaliana* Glutamate-Cysteine Ligase Functional properties, kinetic mechanisms and regulation of activity. *Journal of Biological Chemistry* **279**: 33463-33470.

Jia H, Oguchi R, Hope AB, Barber J, Chow WS (2008) Differential effects of severe water stress on linear and cyclic electron fluxes through Photosystem I in spinach leaf discs in CO_2-enriched air. *Planta* **228**: 803-812.

Jiang T, Fountain J, Davis G, Kemerait R, Scully B, Lee RD, Guo B (2012) Root morphology and gene expression analysis in response to drought stress in maize (*Zea mays*). *Plant Molecular Biology Reporter* **30**: 360-369.

Jiang YQ, Deyholos MK (2006) Comprehensive transcriptional profiling of NaCl-stressed *Arabidopsis* roots reveals novel classes of responsive genes. *BMC Plant Biology* **6**: 25.

Jongrungklang N, Toomsan B, Vorasoot N, Jogloy S, Boote KJ, Hoogenboom G, Patanothai A (2011) Rooting traits of peanut genotypes with different yield responses to pre-flowering drought stress. *Field Crop Research* **120**: 262-270.

Kang JG, Pyo YJ, Cho JW, Cho MH (2004) Comparative analysis of differentially expressed proteins induced by K^+ deficiency in *Arabidopsis thaliana*. *Proteomics* **4**: 3549-3559.

Kashiwagi J, Krishnamurthy L, Crouch JH, Serraj R (2006) Variability of root characteristics and their contribution to seed yield in chickpea (*Cicer arietinum* L.) under terminal drought stress. *Field Crops Research* **95**: 171-181.

Kavi Kishor PB, Sangam S, Amrutha RN, Sri Laxmi P, Naidu KR, Rao KRSS, Rao S, Reddy KJ, Theriappan P, Sreenivasulu N (2005) Regulation of proline biosynthesis, degradation, uptake and transport in higher plants: its implications in plant growth and abiotic stress tolerance. *Current Science* **88**: 424-438.

Kim EJ, Kwak JM, Uozumi N, Schroeder JI (1998) AtKUP1: an Arabidopsis gene encoding high-affinity potassium transport activity. *The Plant Cell* **10**: 51-62.

Kim YJ, Kim JE, Lee JH, Lee MH, Jung HW, Bahk YY, Hwang BK, Hwang I, Kim WT (2004) The *Vr-PLC3* gene encodes a putative plasma membrane-localized phosphoinositide-specific phospholipase C whose expression is induced by abiotic stress in mungbean (*Vigna radiata* L.). *FEBS Letters* **556**: 127-136.

Kirch HH, Nair A, Bartels D (2001) Novel ABA- and dehydration-inducible aldehyde dehydrogenase genes isolated from the resurrection plant *Craterostigma plantagineum* and *Arabidopsis thaliana*. *The Plant Journal* **28**: 555-567.

Klapheck S (1988) Homoglutathione: isolation, quantification and occurrence in legumes. *Physiologia Plantarum* **74**: 727-732.

Klapheck S, Chrost B, Starke J, Zimmermann H (1992) γ-glutamyl-cysteinylserine-a new homologue of glutathione in plants of the family *Poaceae*. *Botanica Acta* **105**: 174-179.

Kocsy G, Galiba G, Brunold C (2001) Role of glutathione in adaptation and signalling during chilling and cold acclimation in plants. *Physiologia Plantarum* **113**: 158-164.

Kohler A, Delaruelle C, Martin D, Encelot N, Martin F (2003) The poplar root transcriptome: analysis of 7000 expressed sequence tags. *FEBS Letters* **542**: 37-41.

Kopriva S (2006). Regulation of sulfate assimilation in *Arabidopsis* and beyond. *Annals of Botany* **97**: 479-495.

Kotchoni SO, Bartels D (2003) Water stress induces the up-regulation of a specific set of genes in plants: Aldehyde dehydrogenases as an example. *Bulgarian Journal of Plant Physiology* **special issue**: 37-51.

Krishnamurthy L, Zaman-Allah M, Marimuthu S, Wani SP, Kesava Rao AVR (2012) Root growth in *Jatropha* and its implications for drought adaptation. *Biomass and Bioenergy* **39**: 247-252.

Lake JA, Woodward I, Quick WP (2002) Long distance CO_2 signaling in plants. *Journal of Experimental Botany* **53**: 183-193.

Lannoo N, Van Damme EJM (2010) Nucleocytoplasmic plant lectins. *Biochimica et Biophysica Acta* **1800**: 190-201.

Larrainzar E, Wienkoop S, Scherling C, Kempa S, Ladrera R, Arrese-Igor C, Weckwerth W, Gonzalez EM (2009) Carbon metabolism and bacteroid functioning are involved in the regulation of nitrogen fixation in *Medicago truncatula* under drought and recovery. *Molecular Plant-Microbe Interactions* **22**: 1565-1576.

Larrainzar E, Wienkoop S, Weckwerth W, Ladrera R, Arrese-Igor C, Gonzalez EM (2007) *Medicago truncatula* root nodule proteome analysis reveals differential plant and bacteroid responses to drought stress. *Plant Physiology* **144**: 1495-1507.

Larroy C, Fernández MR, González E, Parés X, Biosca JA (2002) Characterization of the *Saccharomyces cerevisiae* YMR318C (ADH6) gene product as a broad specificity NADH-dependent alcohol dehydrogenase: relevance in aldehyde reduction. *The Biochemical Journal* **361**:163-172.

Lee PS, Chen HH (1993) Molecular cloning of abscisic acid-responsive mRNAs expressed during the induction of freezing tolerance in bromegrass (*Bromus inermis* Leyss) suspenson culture. *Plant Physiology* **101**: 1089-1096.

Leucci MR, Lenucci MS, Piro G, Dalessandro G (2008) Water stress and cell wall polysaccharides in the apical root zone of wheat cultivars varying in drought tolerance. *Journal of Plant Physiology* **165**: 1168-1180.

Lichtenthaler HK (1987) Chlorophylls and carotenoids: pigments of photosynthetic biomembranes. *Methods in Enzymology* **148**: 350-382.

Liu T, Zhang L, Yuan Z, Hu X, Lu M, Wang W, Wang Y (2013) Identification of proteins regulated by ABA in response to combined drought and heat stress in maize roots. *Acta Physiologia Plantarum* DOI 10. 1007/s11738-012-1092-x.

Liu ZL, Moon J (2009) A novel NADPH-dependent aldehyde reductase 1 gene from *Saccharomyces cerevisiae* NRRL Y-12632 involved in the detoxification of aldehyde inhibitors derived from lignocellulosic biomass conversion. *Gene* **446**: 1-10.

Liu ZL, Moon J, Andersh BJ, Slininger PJ, Weber S (2008) Multiple gene mediated NAD(P)H-dependent aldehyde reduction is a mechanism of in situ detoxification of furfural and 5-hydroxymethylfurfural by *Saccharomyces cerevisiae*. *Applied Microbiology and Biotechnology* **81**: 743-753.

Livak KJ, Schmittgen TD (2001) Analysis of relative gene expression data using real-time quantitative PCR and the $2^{-\Delta\Delta Ct}$ method. *Methods* **25**:402-408.

Loscos J, Matamoros MA, Becana M (2008) Ascorbate and homoglutathione metabolism in common bean nodules under stress conditions and during natural senescence. *Plant Physiology* 146: 1282-1292.

Lüttge U, Fischer-Schliebs E, Ratajczak R (2001) The H^+-pumping V-Atpase of higher plants: a versatile "eco-enzyme" in response to environmental stress. *Cell and Molecular Biology Letters* **6**: 356-361.

Luu DT, Maurel C (2005) Aquaporins in a challenging environment: molecular gears for adjusting plant water status. *Plant Cell and Environment* **28**: 85-96.

Mahdieh M, Mostajeran A, Horie T, Katsuhara M (2008) Drought stress alters water relations and expression of PIP-type aquaporin genes in *Nicotiana tabacum* plants. *Plant Cell and Physiology* **49**: 801–813.

Mahmoodian L, Naseri R, Mirzaei A (2012) Variability of grain yield and some important agronomic traits in mungbean (*Vigna radiata* L.) cultivars as affected by drought stress. *International Research Journal of Applied and Basic Sciences* **3**: 486-492.

Marino D, Frendo P, Ladrera R, Zabalza A, Puppo A, Arrese-Igor C, González EM (2007) Nitrogen fixation control under drought stress. Localized or systemic? *Plant Physiology* **143**: 1968-1974.

Maseda PH, Fernández RJ (2006) Stay wet or else: three ways in which plants can adjust hydraulically to their environment. *Journal of Experimental Botany* **57**: 3963-3977.

Mathesius U, Keijzers G, Natura SHA, Weinman JJ, Diordjevic MA, Rolfe BG (2001) Establishment of a root proteome reference map for the model legume *Medicago trancatula* using the expressed sequence tag database for peptide mass fingerprinting. *Proteomics* **1**: 1424-1440.

Matsui T, Singh BB (2003) Root characteristics in Cowpea related to drought tolerance at the seedling stage. *Experimental Agriculture* **39**: 29-38.

Mattioli R, Marchese D, D'Angeli S, Altamura MM, Constantino P, Trovato M (2008) Modulation of intracellular proline levels affects flowering time and inflorescence architecture in Arabidopsis. *Plant Molecular Biology* **66**: 277-288.

Matysik J, Alia BB, Mohanty P (2002) Molecular mechanisms of quenching of reactive oxygen species by proline under stress in plants. *Current Science* **82**: 525-532.

Maurel C, Verdoucq L, Luu DT, Santoni V (2008) Plant aquaporins: Membrane channels with multiple integrated fuctions. *Annual Reviews of Plant Biology* **59**: 595-624.

May M J, Leaver C J (1993) Oxidative stimulation of glutathione synthesis in Arabidopsis thaliana suspension cultures. *Plant Physiology* **103**: 621-627.

May MJ, Leaver CJ (1994) Arabidopsis thaliana γ-glutamyl cysteine synthetase is structurally unrelated to mammalian, yeast and Escherichia coli homologs. *Proceedings of National Academy of Science, USA* **91**: 10059-10063.

May MJ, Vernoux T, Sanchez-Fernandez R, Van Montagu M, Inze D (1998) Evidence for posttranscriptional activation of gammaglutamylcysteine synthetase during plant stress responses. *Proceeding of National Academy of Science, USA* **95**: 12049-12054.

Mckersie BD, Bowley SR, Harjanto E, Leprince O (1996) Water-Deficit Tolerance and Field Performance of Transgenic Alfalfa Overexpressing Superoxide Dismutase. *Plant Physiology* **111**: 1177-1181.

Mehta A, Magalhães BS, Souza DSL, Vasconcelos1 EAR, Silva LP, Grossi-de-Sa MF, Franco OL, da Costa PHA, Rocha TL (2008) Rooteomics: The Challenge of Discovering Plant Defense-Related Proteins in Roots. *Current Protein and Peptide Science* **9**: 108-116.

Mia MW, Yamauchi A, Kono Y (1996). Root system structure of six food legume species: Inter- and intraspecific variations. *Japanese Journal of Crop Science* **65**: 131-140.

Miller G, Honig A, Stein H, Suzuki N, Mittler R, Zilberstein A (2009) Unraveling delta1-pyrroline-5-carboxylate proline cycle in plants by uncoupled expression of proline oxidation enzymes. *Journal of Biological Chemistry* **284**: 26482–26492.

Miller G, Shulaev V, Mittler R (2008) Reactive oxygen signaling and abiotic stress. *Physiologia Plantarum* **133**: 481-489.

Mishra S, Dubey RS (2006) Inhibition of ribonuclease and protease activities in arsenic exposed rice seedlings: role of proline as enzyme protectant. *Journal of Plant Physiology* **163**: 927-936.

Mittler R, Blumwald E (2010) Genetic engineering for modern agriculture: challenges and perspectives. *Annual Review in Plant Biology* **61**: 443-462.

Mittler R, Vanderauwera S, Gollery M, Van Breusegem F (2004) Reactive oxygen gene network of plants. *Trends in Plant Sciences* **9**: 490-498.

Mittova V, Theodoulou FL, Kiddle G, Gomez L, Volokita M, Tal M, Foyer CH, Guy M (2003) Coordinate induction of glutathione biosynthesis and glutathione-metabolizing enzymes is correlated with salt tolerance in tomato. *FEBS Letters* **554**: 417-421.

Mohammadi PP, Moieni A, Hiraga S, Komatsu S (2012b) Organ-specific proteomic analysis of drought-stressed soybean seedlings. *Journal of proteomics* **75**: 1906-1923.

Mohammadi PP, Moieni A, Komatsu S (2012a) Comparative proteome analysis of drought sensitive and drought-tolerant rapeseed roots and their hybrid F1 line under drought stress. *Amino Acids* **43**: 2137-2152.

Molinari HBC, Marur CJ, Daros E, de Campos MKF, de Carvalho J, Filho JCB, Pereira LFP, Vieira LGE (2007) Evaluation of the stress-inducible production of proline in transgenic sugarcane (*Saccharum spp.*): osmotic adjustment, chlorophyll fluorescence and oxidative stress. *Physiologia Plantarum* **130**: 218-229.

Møller IM, Jensen PE, Hansson A (2007) Oxidative modifications to cellular components in plants. *Annual Review in Plant Biology* **58**: 459-481.

Mouchel CF, Osmont KS, Hardtke CS (2006) BRX mediates feedback between brassinosteroid levels and auxin signalling in root growth. *Nature* **443**: 458-461.

Moustakas M, Sperdouli I, Kouna T, Antonopoulou CI, Therios I (2011) Exogenous proline induces soluble sugar accumulation and alleviates drought stress effects on photosystem II functioning of *Arabidopsis thaliana* leaves. *Plant Growth Regulation* **65**: 315-325.

Mukherjee SP, Choudhury MA (1983) Implications of water stress induced changes in the levels of endogenous ascorbic acid and hydrogen peroxide in Vigna seedlings. *Physiologia Plantarum* **58**: 166-170.

Nakashima K, Satoh R, Kiyosue T, Yamaguchi-Shinozaki K, Shinozaki K (1998) A gene encoding proline dehydrogenase is not only induced by proline and hypo-osmolarity, but is also developmentally regulated in the reproductive organs of *Arabidopsis*. *Plant Physiology* **118**: 1233-1241.

Narita Y, Taguchi H, Nakamura T, Ueda A, Shi W, Takabe T (2004) Characterization of the salt-inducible methionine synthase from barley leaves. *Plant Science* **167**: 1009-1016.

National Science Foundation's, NSF (2010) Drought May Threaten Much of Globe Within Decades. http://www.nsf.gov/news/news summ.jsp?cntn id=117866&WT.mc id=USNSF51&WT.mc ev=click

Naumann JC, Young DR, Anderson J E (2007). Linking leaf chlorophyll fluorescence properties to physiological responses for detection of salt and drought stress in coastal plant species. *Physiologia Plantarum* **131**: 422-433.

Negm FB (1986) Purification and properties of an NADPH-aldose reductase (aldehyde reductase) from Euonymus japonica leaves. *Plant Physiology* **80**: 972-977.

Niini SS, Tarkka MK, Raudaskoski M (1996) Tubulin and actin protein patterns in scot ipine(Pinus sylvestris) roots nad developing ectomycorrhiza with Suillas bovines. *Physiologia Plantarum* **96**: 186-192.

Nobel PS, Huang B (1992) Hydraulic and structural changes for lateral roots of two desert succulents in response to soil drying and rewetting. *International Journal of Plant Science* **153**: S163-S170.

Noctor G, Arisi ACM, Jouanin L, Kunert KJ, Rennenberg H, Foyer CH (1998) Glutathione: biosynthesis, metabolism and relationship to stress tolerance explored in transformed plants. *Journal of Experimental Botany* **49**: 623-647.

Noctor G, Gomez L, Vanacker H, and Foyer CH (2002) Interactions between biosynthesis, compartmentation and transport in the control of glutathione homeostasis and signalling. *Journal of Experimental Botany* **53**: 1283-1304.

O'Neill MA, York WS (2003) The composition and structure of plant primary cell walls. In: Rose JKC, editor. *The plant cell wall-annual plant reviews, Oxford, Boca Raton, FL: Blackwell Publishing, CRC Press* **8**: 1-54.

Oberschall A, Deák M, Török K, Sass L, Vass I, Kovács I, Fehér A, Dudits D, Horváth GV (2000) A novel aldose/aldehyde reductase protects transgenic plants against lipid peroxidation under chemical and drought stresses. *The Plant Journal* **24**: 437-446.

Ogawa K (2005) Glutathione-associated regulation of plant growth and stress responses. *Antioxidant Redox Signalling* **7**: 973-981.

Olsen JG, Pedersen J, Christensen CL, Olsen O, Henriksen A (2008) Barley aldose reductase: structure cofactor binding and substrate recognition in the aldo/keto reductase 4C family. *Proteins* **71**: 1572-1581.

Oo HH, Araki T, Kubota F (2005) Effects of drought and flooding stresses on growth and photosynthetic activity of mungbean, (*Vigna radiata* L. Wilczek), cultivars. *Journal of the Faculty of Agriculture, Kyushu University* **50**: 533-542.

Ort DR, Baker NR (2002) A photoprotective for O_2 as an alternative electron sink in photosynthesis. *Current Opinion in Plant Biology* **5**: 193-198.

Oukarroum A, Madidi SE, Schansker G, Strasser RJ (2007) Probing the responses of barley cultivars (Hordeum vulgare L.) by chlorophyll a fluorescence OLKJIP under drought stress and re-watering. *Environmental and Experimental Botany* **60**: 438-446.

Oukarroum A, Schansker G, Strasser RJ (2009) Drought stress effects on photosystem I content and photosystem II thermotolerance analyzed using Chl a fluorescence kinetics in barley varieties differing in their drought tolerance. *Physiologia Plantarum* **137**: 188-199.

Padh H (1990) Cellular functions of ascorbic acid. *Biochemistry and Cell Biology* **68**: 1166-73.

Panter S, Thomson R, de Bruxelles G, Laver D, Trevaskis B, Udvardi M (2000) Identification with proteomics of novel proteinsassociated with the peribacteroid membrane of soybean root nodules. *Molecular Plant- Microbe Interactions* **13**: 325-333.

Pardales JR (Jr), Kono Y (1990). Development of sorghum root system under increasing drought stress. *Japanese Journal of Crop Science* **59**: 752-761.

Passardi F, Cosio C, Penel C, Dunand C. (2005) Peroxidases have more functions than a swiss army knife. *Plant Cell Reports* **24**: 255-265.

Pederson A.L, Feldner H. C, Rosendahl L (1996) Effect of praline on nitrogenase activity in symbiosomes from root nodules of soybean (*Glycine max* L.) subjected to drought stress. *Journal of Experimental Botany* **47**: 1533-1539.

Peltier JB, Emanuelsson O, Kalume DE, Ytterberg J, Friso G, Rudella A, Liberles DA, Söderberg L, Roepstorff P, von Heijne G, van Wijk KJ (2002) Central functions of the lumenal and peripheral thylakoid proteome of *Arabidopsis* determined by experimentation and genome-wide prediction. *The Plant Cell* **14**: 211-236.

Pérez JM, Arenas FA, Pradenas GA, Sandoval JM, Vásquez CC (2008) *Escherichia coli* YqhD exhibits aldehyde reductase activity and protects from the harmful effect of lipid peroxidation derived aldehydes. *Journal of Biological Chemistry* **283**: 7346-7353.

Pérez JM, Calderón IL, Arenas FA, Fuentes DE, Pradenas GA, Fuentes EL, Sandoval JM, Castro ME, Elías AO, Vásquez CC (2007) Bacterial toxicity of potassium tellurite: unveiling an ancient enigma. *Plos One* **2(e211)**: 1-9.

Porcel R.S, Barea J.M, Ruiz-Lozano J.M (2003) Antioxidant activities in mycorhhizal soybean plants under drought stress and their possible relationship to the process of nodule senescense. *New Phytologists* **157**: 135-143.

Puangbut D, Jogloy S, Vorasoot N, Akkasaeng C, Kesmala T, Rachaputi RCN, Wright GC, Patanothai A (2009) Association of root dry weight and transpiration efficiency of peanut genotypes under early season drought. *Agricultural Water Management* **96**: 1460-1466.

Pujni D, Chaudhary A, Rajam MV (2007) Increased tolerance to salinity and drought in transgenic *indica* rice by mannitol accumulation. *Journal of Plant Biochemistry and Biotechnology* **16:** 1-7.

Queval G, Thominet D, Vanacker H, Miginiac-Maslow M, Gakière B, Noctor G (2009) H_2O_2-Activated up-regulation of glutathione in *Arabidopsis* involves induction of genes encoding enzymes involved in cysteine synthesis in the chloroplast. *Molecular Plant* **2**: 344-356.

Rabello AR., Guimarães CM, Rangel PH, da Silva FR, Seixas D, de Souza E, Brasileiro ACM, Spehar CR, Ferreira ME, Mehta Â (2008). Identification of drought-responsive genes in roots of upland rice (*Oryza sativa* L.). *BMC Genomics* **9**: 485-497

Ramanjulu S, Bartels D (2002) Drought- and desiccation-induced modulation of gene expression in plants. *Plant Cell and Environment* **25**: 141-151.

Ranawake AL, Amarasingha UGS, Rodrigo WDRJ, Rodrigo UTD and Dahanayaka N (2011) Effect of water stress on growth and yield of mung bean (*Vigna radiata* L.) *Tropical Agricultural Research & Extension* **14**: 76-79.

Rasineni G.K, Chinnaboina M., Reddy AR (2010) Proteomic approach to study leaf proteins in a fast-growing tree species, *Gmelina arborea* Linn. Roxb. *Trees* **24**: 129-138.

Ravanel S, Block MA, Rippert P, Jabrin S, Curien G, Rébeillé F, Douce R (2004) Methionine metabolism in plants. *The Journal of Biological Chemistry* **279**: 22548-22557.

Rayapati PJ, Stewart CR (1991) Solubilization of a proline dehydrogenase from maize (Zea mays L.) mitochondria. *Plant Physiology* **95**: 787-791.

Reddy AR, Chaitanya KV, Vivekanandan N (2004) Drought induced responses of photosynthesis and antioxidant metabolism in higher plants. *Journal of Plant Physiology* **161**: 1189-1202.

Redillas MCFR, Strasser RJ, Jeong JS, Kim YS, and Kim JK (2011) The use of JIP test to evaluate drought-tolerance of transgenic rice overexpressing OsNAC10. *Plant Biotechnology Reporter* **5**: 169-175.

Reiger M, Litvin P (1999) Root system hydraulic conductivity in species with contrasting root anatomy. *Journal of Experimental Botany* **50**: 201-209.

Riccardi F, Gazeau P, Jacquemot MP, Vincent D, Zivy M (2004) Deciphering genetic variations of proteome responses to water deficit in maize leaves. *Plant Physiology and Biochemistry* **42**: 1003-1011.

Rivera-Becerril F, van Tuinen D, Martin-Laurent F, Metwally A, Dietz KJ, Gianinazzi S, Gianinazzi-Pearson V (2005) Molecular changes in *Pisum sativum* L. roots during arbuscular mycorrhiza buffering of cadmium stress. *Mycorrhiza* **16**: 51-60.

Rodrigues SM, Andrade MO, Gomes APS, DaMatta FM, Baracat-Pereira MC, Fontes EPB (2006) Arabidopsis and Tobacco plants ectopically expressing the soybean antiquitin-like ALDH7 gene display enhanced tolerance to drought, salinity and oxidative stress. *Journal of Experimental Botany* **57**: 1909-1918.

Rose JKC, Braam J, Fry SC, Nishitani K (2002) The XTH family of enzymes involved in xyloglucan endo-transglucosylation and endohydrolysis: current perspectives and a new unifying nomenclature. *Plant Cell and Physiology* **43**: 1421-1435.

Roy A, Rushton PJ, Rohila JS (2011) The potential of proteomics technologies for crop improvement under drought conditions. *Critical reviews in Plant Sciences* **30**:471-490.

Rüeggsegger A, Brunold C (1992) Effect of cadmium on γ-glutamylcysteine synthesis in maize seedlings. *Plant Physiology* **99**: 428-433.

Ruiz JM, Blumwald E (2002) Salinity-induced glutathione synthesis in *Brassica napus*. *Planta* **214**: 965-969.

Saalbach G, Erik P, Wienkoop S (2002) Characterisation by proteomics of peribacteroid space and peribacteroid membrane preparations from pea (*Pisum sativum*) symbiosomes *Proteomics* **2**: 325-337.

Salekdeh GH, Siopongco G, Wade L J, Ghareyazie B, Bennett J (2002) Proteomic analysis of rice leaves during drought stress and recovery. *Proteomics* **2**: 1131-1145.

Sancenón V, Puig S, Mira H, Thiele DJ, Peñarrubia (2003) Identification of a copper transporter family in *Arabidopsis thaliana*. *Plant Molecular Biology* **51**: 577-587.

Sarvanan RS, Rose JKC (2004) A critical evaluation of sample extraction techniques for enhanced proteomic analysis of recalcitrant plant tissues. *Proteomics* **4**: 2522-2532.

Schachtman DP, Goodger JQD (2008) Chemical root to shoot signaling under drought. Trends *in Plant Science* **13**: 281-287.

Schãfer HJ, Haag-Kerwer A, Rausch T (1998). cDNA cloning and expression analysis of genes encoding GSH synthesis in roots of the heavy metal accumulator Brassica juncea L.: Evidence for Cd-induction of a putative mitochondrial γ-glutamylcysteine synthetase isoform. *Plant Molecular Biology* **37**: 87-97.

Schweiger P, Deppenmeier U (2010) Analysis of aldehyde reductases from *Gluconobacter oxydans* 621H. *Applied Microbiology and Biotechnology* **85**: 1025-1031.

Selote DS, Khanna-Chopra R (2010) Antioxidant response of wheat roots to drought acclimation. *Protoplasma* **245**: 153-163.

Semchyshyn H, Bagnyukova T, Storey K, Luschak V (2005) Hydrogen peroxide increases the activities of soxRS regulon enzymes and the levels of oxidized proteins and lipids in Escherichia coli. *Cell Biology International* **29**: 898-902.

Serraj R, Sinclair TR (2002). Osmolyte accumulation: can it really increase crop yield under drought conditions? *Plant Cell and Environment* **25**: 333-341.

Shakirova FM, Bezrukova MV (1998) Effect of 24-epibrassinolide and salinity on the levels of ABA and lectin. *Russian Journal of Plant Physiology* **45**: 451-455.

Sharma P, Dubey RS (2005) Modulation of nitrate reductase activity in rice seedlings under aluminium toxicity and water stress: role of osmolytes as enzyme protectant. *Journal of Plant Physiology* **162**: 854-864.

Sharp RE, Poroyko V., Hejlek LG, Spollen WG, Springer GK, Bohnert HJ, Nguyen HT (2004) Root growth maintenance during water deficits: physiology to functional genomics. *Jourrnal of Experimental Botany* **55**: 2343-2351.

Sheahan MB, Rose RJ, McCurdy DW (2007) Actin-filament dependent remodeling of the vacuole in cultured mesophyll protoplasts. *Protoplasma* **230**: 141-152.

Shevchenko A, Wilm A, Vorm O, Mann M (1996) Mass spectrometric sequencing of protein from silver-stained polyacrylamide gels. *Analytical Chemistry* **68**: 850-858.

Shimazaki Y, Ookawa T, Hirasawa T (2005) The root tip and accelerating region suppress elongation of the decelerating region without any effects on cell turgor in primary roots of maize under water stress. *Plant Physiology* **139**: 458-465.

Shinozaki K, Yamaguchi-Shinozaki K (2007) Gene networks involved in drought stress response and tolerance. *Journal of Experimental Botany* **58**: 221-227.

Sicher RC, Timlin D, Bailey B (2012) Responses of growth and primary metabolism of water stressed barley roots to rehydration. *Journal of Plant Physiology* **169**: 686-695

Siefritz F, Tyree MT, Lovisolo C, Schubert A, Kaldenhoff R (2002) PIP1 plasma membrane aquaporins in tobacco: from cellular effects to function in plants. *The Plant Cell* **14**: 869-876.

Siemens JA, Zwiazek JJ (2004) Changes in water flow properties of solution culture-grown trembling aspen (Populus tremuloides) seedlings under different intensities of water-deficit stress. *Physiologia Plantarum* **121**: 44-49.

Signorelli S, Corpas FJ, Borsani O, Barroso JB, Monza J (2013) Water stress induces a differential and spatially distributed nitro-oxidative stress response in roots and leaves of *Lotus japonicas*. *Plant Science* **201-202**: 137-146.

Silim SN, Saxena MC (1993). Adaptation of spring-sown chickpea to the Mediterranean basin. I. Response to moisture supply. *Field Crops Research* **34**: 121-136.

Simpson PJ, Tantitadapitak C, Reed AM, Mather OC, Bunce CM, White SA, Ride JP (2009) Characterization of two novel aldo-keto reductases from Arabidopsis: Exression patterns, broad substrate specificity and an open active site structure suggest a role in toxicant metabolism following stress. *Journal of Molecular Biology* **392**: 465-480.

Skibbe DS, Liu F, Wenn TJ, Yandeau MD, Cui X, Cao J, Simmons CR, Schnable PS (2002) Characterization of the aldehyde dehydrogenase gene families of *Zea mays* and *Arabidopsis*. *Plant Molecular Biology* **48**: 751-761.

Smirnoff N (1993) The role of active oxygen in the response of plants to water deficit and desiccation. *New Phytologist* **125**: 27-58.

Smucker A.J.M (1993) Soil environmental modifications of root dynamics and measurement. *Annual Reviews in Phytopathology* **31**: 191-216.

Song YJ, Joo JH, Ryu HY, Lee JS, Bae YS, Nam KH (2007) Reactive oxygen species mediate IAA-induced ethylene production in mungbean (*Vigna radiata* L.) hypocotyls. *Journal of Plant Biology* **50**: 18-23.

Songsri P, Jogloy S, Vorasoot N, Akkasaeng C, Patanothai A, Holbrook CC (2008) Root distribution of drought-resistant peanut genotypes in response to drought. *Journal of Agronomy and Crop Science* **194**: 92-103.

Stafford HA (1997) Role of flavonoids in symbiotic and defense functions in legume roots. *Botanical Review* **63**: 27-39.

Steudle E (2000) Water uptake by roots: effects of water deficit. *Journal of Experimental Botany* **51**: 1531-1542.

Strasser A, Tsimilli-Michael M, Srivastava A (2004) Analysis of the fluorescence transient.In: Papageorgiou GC, Govindjee, editors. Chlorophyll fluorescence: a signature of photosynthesis. *Advances in photosynthesis and respiration series* Dordrecht: Springer p. 321-62.

Strasser BJ (1997) Donor side capacity of photosystem II probed by chlorophyll *a* fluorescence transients. *Photosynthetic Research* **52**: 147-155.

Strasser BJ, Strasser RJ (1995) Measuring fast fluorescence transients to address environmental questions: the JIP-test. In: Mathis P, ed. Photosynthesis: from light to biosphere. *Dordrecht: Kluwer Academic Publishers* : 977-980.

Strasser RJ, Stirbet AD (1998) Heterogeneity of photosystem II probed by the numerically simulated chlorophyll a fluorescence rise (O–J–I–P). *Mathematical Computational Simulation* **48**: 3-9.

Strasser RJ, Tsimilli-Michael M, Qiang S, Goltsev V (2010) Simultaneous in vivo recording of prompt and delayed fluorescence and 820-nm reflection changes during drying and after rehydration of the resurrection plant Haberlea rhodopensis. *Biochimica et Biophysica Acta* **1797**: 1313-1326.

Strizhov N, Ábrahám E, Ökrész L, Blickling S, Zilberstein A, Schell J, Koncz C, Szabados L (1997) Differential expression of two P5CS genes controlling proline accumulation during salt-stress requires ABA and is regulated by ABA1, ABI1 and AXR2 in *Arabidopsis*. *The Plant Journal* **12**: 557-569.

Sunkar R, Bartels D, Kirch HH (2003) Overexpression of a stress inducible aldehyde dehydrogenase gene from *Arabidopsis thaliana* in transgenic plants improves stress tolerance. *The Plant Journal* **35**: 452-464.

Szabados L, Savouré A (2010) Proline: A multifunctional amino acid. *Trends in Plant Science* **15**: 89-97.

Székely G, Abrahám E, Cséplo A, Rigó G, Zsigmond L, Csiszár J, Ayaydin F, Strizhov N, Jásik J, Schmelzer E, Koncz C, Szabados L (2008) Duplicated P5CS genes of *Arabidopsis* play distinct roles in stress regulation and developmental control of proline biosynthesis. *The Plant Journal* **53**: 11-28.

Szweda L, Uchida K, Stadtman R (1993) Inactivation of glucose-6-phosphate dehydrogenase by 4-hydroxy-2-nonenal. Selective modification of an active-site lysine. *Journal of Biological Chemistry* **268**: 3342-3347.

Taiz L, Zeiger E (2006) Plant physiology, *4th edn. Sunderland, MA, USA: Sinauer*.

Takagi S, Takamatsu H, Sakurai-Ozato N (2009) Chloroplast anchoring: its implication for the regulation of intracellular chloroplast distribution. *Journal of Experimental Botany* **60**: 3301-3310.

Tardieu F (2012) Any trait or trait-related allele can confer drought tolerance: Just design the right drought scenario. *Journal of Experimental Botany* **63**: 25-31.

Tausz M, Šircelj H, Grill D (2004) The glutathione system as a stress marker in plant ecophysiology: is a stress- response concept valid? *Journal of Experimental Botany* **55**: 1955-1962.

Tester M, Bacic A (2005) Abiotic stress tolerance in grasses. From model plants to crop plants. *Plant Physiology* **137**: 791-793.

Thompson JE, Fry SC (2001) Re-structuring of wall-bound xyloglucan by transglycosylation in living plant cells. *The Plant Journal* **26**: 23-34.

Thompson JE, Smith RC, Fry SC (1997) Xyloglucan undergoes interpolymeric transglycosylation during binding to the plant cell wall in vivo: evidence from 13C/3H dual labelling and isopycnic centrifugation in caesium trifluoroacetate. *Biochemical Journal* **327**: 699-708.

Tjaden J, Schwöppe C, Möhlmann T, Quick PW, Neuhaus HE (1998) Expression of a plastidic ATP/ADP transporter gene in *Escherichia coli* leads to a functional adenine nucleotide transport system in the bacterial cytoplasmic membrane. *The Journal of Biological Chemistry* **273**: 9630-9636.

Torres GAM, Pflieger S, Corre-Menguy F, Mazubert C, Hartmann C, Lelandais-Briére C (2006) Identification of novel drought-related mRNAs in common bean roots by differential display RT-PCR. *Plant Science* **171**: 300-307.

Tsugita A, Kamo M (1999) 2D electrophoresis of plant proteins. *Methods in Molecular Biology* **112**: 95-97.

Umezawa T, Fujita M, Fujita Y,Yamaguchi-Shinozaki K, Shinozaki K (2006) Enginneering drought tolerance in plants: discovering and tailoring genes to unlock the future. *Current Opinion in Plant Biology* **17**: 113-122.

Uozumi N, Kim EJ, Rubio F, Yamaguchi T, Muto S, Tsuboi A, Bakker EP, Nakamura T, Schroeder JI (2000) The Arabidopsis HKT1 gene homolog mediates inward Na+ currents in *Xenopus laevis* oocytes and Na^+ uptake in *Saccharomyces cerevisiae*. *Plant Physiology* **122**: 1249-1259.

Uozumi N, Nakamura T, Schroeder JI, Muto S (1998) Determination of trans-membrane topology of an inward rectifying potassium channel from *Arabidopsis thaliana* based on functional expression in *Escherichia coli*. *Proceedings of the National Academy of Sciences,USA* **95**: 9773-9778.

Valladares F, Pearcy RW (2002) Drought can be more critical in the shade than in the sun: a field study of carbon gain and photoinhibition in a Californian shrub during a dry El Niño year. *Plant Cell and Environment* **25**: 749-759.

Valliyodan B, Nguyen HT (2006) Understanding regulatory networks and engineering for enhanced drought tolerance in plants. *Current Opinion in Plant Biology* **9**: 189-195.

Valot B, Dieu M, Recorbet G, Raes M, Gianinazzi S, Dumas-Gaudot E (2005) Identification of membrane-associated proteins regulated by the arbuscular mycorrhizal symbiosis. *Plant Molecular Biology* **59**: 565-580.

Valot B, Gianinazzi S, Eliane DG (2004) Sub-cellular proteomic analysis of a *Medicago truncatula* root microsomal fraction. *Phytochemistry* **65**: 1721-1732.

Van Breusegem F, Vranovà E, Dat JF, Inzé D (2001) The role of active oxygen species in plant signal transduction. *Plant Science* **161**:405-414.

Van Damme EJM, Barre A, Rougé P, Peumans WJ (2004) Cytoplasmic/ nuclear plant lectins: a new story. *Trends in Plant Sciences* **9**: 484-489.

Van der Straeten D, Rodrigues-Pousada RA, Goodman HM, van Montagu M (1991) Plant enolase: gene structure, expression, and evolution. *The Plant Cell* **3**: 719-735.

Van Sandt VST, Suslov D, Verbelen J P, Vissenberg K (2007) Xyloglucan endotransglucosylase activity loosens a plant cell wall. *Annals of Botany* **100**: 1467-1473.

Vandeleur RK, Mayo G, Shelden MC, Gilliham M, Kaiser BN, Tyerman SD (2009) The role of plasma membrane intrinsic protein aquaporins in watertransport through roots: Diurnal and drought stress responses reveal different strategies between isohydric and anisohydric cultivars of grapevine. *Plant Physiology* **149**: 445-460.

Vander Jagt DL, Kolb NS, Vander Jagt TJ, Chino J, Martinez FJ, Hunsaker LA, Royer RE (1995) Substrate specificity of human aldose reductase :Identification of 4-hydroxynonenal as an endogenous substrate. *Biochimica et Biophysica Acta* **1249**: 117-126.

Velikova V, Yordanov I, Edreva A (2000) Oxidative stress and some antioxidant systems in acid rain-treated bean plants. *Plant Science* **151**: 59-66.

Vendruscolo ECG, Schuster I, Pileggi M, Scapim CA, Molinari HBC, Marur CJ, Vieira LG (2007) Stress-induced synthesis of proline confers tolerance to water deficit in transgenic wheat. *Journal of Plant Physiology***164**: 1367-76.

Vernoux T, Wilson RC, Seeley KA, Reichheld JP, Muroy S, Brown S, Maughan SC, Cobbett CS, Montagu MV, Inze D, May MJ, Sung ZR (2000) The ROOT MERISTEMLESS1/CADMIUM SENSITIVE 2 gene defines a glutathione dependent pathway involved in initiation and maintenance of cell division during post embryonic cell development. *The Plant Cell* **12**: 97-109.

Verslues PE, Agarwal M, Katiyar-Agarwal S, Zhu JH, Zhu JK (2006) Methods and concepts in quantifying resistance to drought, salt and freezing abiotic stresses that affect plant water status. *The Plant Journal* **45**: 523-539.

Wang H, Siopongco J, Wade LJ, Yamauchi A (2009) Fractal analysis on root systems of rice plants in response to drought stress. *Environmental and Experimental Botany* **65**: 338-344.

Wang H, Zhang H, Li Z (2007b) Analysis of gene expression profile induced by water stress in upland rice (*Oryza sativa* L. var.IRAT109) seedlings using subtractive expressed SequenceTags Library. *Journal of Integrated Plant Biology* **49**: 1455-1463.

Wang W, Vinocur B, Shoseyov O, Altman A (2004) Role of plant heat-shock proteins and molecular chaperones in the abiotic stress response. *Trends in Plant Sciences* **9**: 244-252.

Wang X, Li X, Li Y (2007a) A modified Commassie Brilliant Blue staining method at nanogram sensitivity compatible with proteomic analysis. *Biotechnology Letters* **29**: 1599-1603.

Wang ZQ, Yuan YZ, Ou JQ, Lin QH, Zhang CF (2007c) Glutamine synthetase and glutamate dehydrogenase contribute differentially to proline accumulation in leaves of wheat (*Triticum aestivum*) seedlings exposed to different salinity. *Journal of Plant Physiology* **164**: 695-701.

Waseem M, Ali A, Tahir M, Nadeem MA, Ayub M, Tanveer A, Ahmad R, Hussain M (2011) Mechanism of drought tolerance in plant and its management through different methods. *Continental Journal of Agricultural Science* **5**: 10-25.

Webber HA, Madramootoo CA, Bourgault M, Horst MG, Stulina G, Smith DL (2006) Water use efficiency of common bean and green gram grown using alternate furrow and deficit irrigation. *Agricultural Water Management* **86**: 259-268.

Weerathaworn P, Soldati A, Stamp P (1992) Root growth of tropical maize seedling at low water supply. *In: Person, H. and Sobotiik, M., (eds.), Root ecology and its practical application*,pp. 109–112. Verein für Wurzelforschung, Lagenfurt, Austria.

Weinberger K (2003) Impact analysis of Mungbean research in South and Southeast Asia. *Final report of GTZ Project. The World Vegetable Center (AVRDC), Shanhua, Taiwan*

Wen Y, Wang X, Xiao S, Wang Y (2012) Ectopic expression of VpALDH2B4, a novel aldehyde dehydrogenase gene from Chinese wild grapevine (*Vitis pseudoreticulata*), enhances resistance to mildew pathogens and salt stress in Arabidopsis. *Planta* 236: 525-539.

Weyers JDB, Paterson NW (2001) Plant hormones and the control of physiological processes. New Phytologist **152**: 375-407.

Widodo, Patterson JH, Newbigin ED, Tester M, Bacic A, Roessner U (2009) Metabolic responses to salt stress of barley (*Hordeum vulgare* L.) cultivars, Sahara and Clipper, which differ in salinity tolerance. *Journal of Experimental Botany* **60**: 4089-4103.

Wienkoop S, Saalbach G (2003) Proteome Analysis. Novel Proteins Identified at the Peribacteroid Membrane from *Lotus japonicus* Root Nodules. *Plant Physiology* **131**: 1080-1090.

Wilkinson S, Davies WJ (2002) ABA-based chemical signaling: the co-ordination of responses to stress in plants. *Plant Cell and Environment* **25**: 195-210.

Winger AM, Taylor NL, Heazlewood JL, Day DA, Millar AH (2007) The cytotoxic lipid peroxidation product 4-hydroxy-2-nonenal covalently modifies a selective range of proteins linked to respiratory function in plant mitochondria. *Journal of Biological Chemistry* **282**: 37436-37447.

Wu J, Qu T, Chen S, Zhao Z, An L (2009) Molecular cloning and characterization of a γ-glutamylcysteine synthetase gene from *Choriospora bungeana*. *Protoplasma* **235**: 27-36.

Wu Y, Cosgrove D J (2000) Adaptation of roots to low water potentials by changes in cell wall extensibility and cell wall proteins. *Journal of Experimental Botany* **51**: 1543-1553.

Wu Y, Jeong BR, Fry SC, Boyer JS (2005) Change in XET activities, cell wall extensibility and hypocotyls elongation of soybean seedlings at low water potential. *Planta* **220**: 593-601.

Wu Y, Sharp RE, Durachko DM, Cosgrove DJ (1996) Growth maintenance of the maize primary root at low water potentials involves increases in cell wall extension properties, expansin activity, and wall susceptibility to expansin. *Plant Physiology* **111**: 765-772.

Xiang C, Bertrand D (2000) Glutathione synthesis in Arabidopsis, multilevel controls coordinate responses to stress. In Sulfur Nutrition and Sulphur Assimilation in Higher Plants, *Brunold C. Rennenberg H. De Kok L.J. Stulen I. and Davidian J.C., eds (Bern, Switzerland: Paul Haupt),* pp. 409-412.

Xiang C, Oliver DJ (1998) Glutathione metabolic genes coordinately respond to heavy metals and jasmonic acid in *Arabidopsis*. *The Plant Cell* **10**: 1539-1550.

Xiang C, Werner BL, Christensen EM, Oliver DJ (2001) The biological function of glutathione revisited in Arabidopsis transgenic plants with altered glutathione levels. *Plant Physiology* **126**: 564-574.

Xu W, Purugganan MM, Polisensky DH, Antosiewicz DM, Fry SC, Braam J (1995). Arabidopsis TCH4, regulated by hormones and the environment, encodes a xyloglucan endotransglycosylase. *The Plant Cell* **7**: 1555-1567.

Xue X, Liu A, Hua X (2009) Proline accumulation and transcriptional regulation of proline biosynthesis and degradation in *Brassica napus*. *BMB Reports* **42**: 28-34.

Yamaguchi M, Sharp RE (2010) Complexity and coordination of root growth at low water potentials: recent advances from transcriptomic and proteomic analyses. *Plant Cell and Environment* **33**: 590-603.

Yamaguchi M, Valliyodan B, Zhang J, Lenoble ME, Yu O, Rogers EE, Nguyen HT, Sharp RE. (2010) Regulation of growth response to water stress in the soybean primary root. I. Proteomic analysis reveals region-specific regulation of phenylpropanoid metabolism and control of free iron in the elongation zone. *Plant Cell and Environment* **33**: 223-243.

Yan S, Tang Z, Su W, Sun W (2005) Proteomic analysis of salt stress-responsive proteins in rice root. *Proteomics* **5**: 235-244.

Yang IY, Hossain M, Miller H, Khullar S, Johnson F, Grollam A, Moriya M (2001) Responses to the major acrolein-derived deoxyguanosine adduct in *Escherichia coli*. *Journal of Biological Chemistry* **276**: 9071-9076.

Yesilirmak F, Sayers Z (2009) Heterologous expression of plant genes. *International Journal of Plant Genomics* **2009**: 296482.

Yin C, Peng Y, Zang R, Zhu Y, Li C (2005) Adaptive responses of *Populus kangdingensis* to drought stress. *Physiologia Plantarum***123**: 445-451.

Yin L, Mano J,Wang S, Tsuji W, Tanaka K (2010) The involvement of lipid-peroxide derived aldehydes in aluminium toxicity of tobacco roots. *Plant Physiology* **152**: 1406-1417.

Yoon SJ, Park JE, Yang JH, Park JW (2002) *OxyR* Regulon controls lipid peroxidation-mediated oxidative stress in *Escherichia coli*. *Journal of Biochemistry and Molecular Biology* **35**: 297-301.

Yordanov I, Velikova V, Tsonev T (2000) Plant responses to drought, acclimation, and stress tolerance. *Photosynthetica* **38**: 171-186.

Yoshimura K, Masuda A, Kuwano M, Yokota A, Akashi K (2008) Programmed proteome response for drought avoidance/tolerance in the root of a C_3 xerophyte (wild watermelon) under water deficits. *Plant Cell and Physiology* **49**: 226-241.

Yu DJ, Kim SJ, Lee HJ (2009) Stomatal and non-stomatal limitations to photosynthesis in field-grown grapevine cultivars. *Biologia Plantarum* **53**: 133-137.

Yusuf MA, Kumar D, Rajwanshi R, Strasser RJ, Tsimilli Michael M, Govindjee, Sarin NB (2010) Overexpression of γ-tocopherol methyl transferase gene in transgenic Brassica juncea plants alleviates abiotic stress: physiological and chlorophyll fluorescence measurements. *Biochimica et Biophysica Acta* **1797**: 1428-1438.

Zhang J, Kirkham MP (1994) Drought stress induced changes in activities of superoxide dismutase, catalase and peroxidase in wheat species. *Plant Cell and Physiology* **35**: 785-791.

Zhang W, Peumans WJ, Barre A, Astoul CH, Rovira P, Rougé P, Proost P, Truffa-Bachi P, Jalali AA, Van Damme EJ (2000) Isolation and characterization of a jacalin-related mannose-binding lectin from salt-stressed rice (*Oryza sativa*) plants. *Planta* **210**: 970-978.

Zhao Z, Zhang W, Stanley BA, Assmann SM (2008). Functional proteomics of *Arabidopsis thaliana* guard cells uncovers new stomatal signaling pathways. *The Plant Cell* **20**: 3210-3226.

Zhao ZG, Chen GC, Zhang CL (2001) Interaction between reactive oxygen species and nitric oxide in drought-induced abscisic acid synthesis in root tips of wheat seedlings. *Australian Journal of Plant Physiology* **28**:1055–1061.

Zhu J K (2001) Cell signaling under salt, water and cold stresses. *Current Opinion in Plant Biology* **4**: 401- 406.

Zhu JK (2002) Salt and drought stress signal transduction in plants. *Annual Reviews in Plant Biology* **53**: 247-273.

Zolla L, Rinalducci S, Timperio AM, Huber CG, Righetti PG (2004) Intact mass measurements for unequivocal identification of hydrophobic photosynthetic photosystems I and II antenna proteins. *Electrophoresis* **25**:1353-1366.

Appendix

List of publications and accessions

Research papers published

1. **Debashree Sengupta**, M Shalini, Attipalli R Reddy (**2012**). Detoxification potential and expression analysis of eutypine reducing aldehyde reductase (VrALR) during progressive drought and recovery in *Vigna radiata* L. Wilczek roots. **Planta 236: 1339-1349.**
2. **Debashree Sengupta**, G Ramesh, M Shalini, KR Rajesh Kumar, PB Kirti, Attipalli R Reddy (**2012**). Molecular cloning and characterization of γ-glutamyl cysteine synthetase (VrγECS) from roots of *Vigna radiata* L. Wilczek under progressive drought stress and recovery. **Plant Molecular Biology Reporter 30: 894-903**.
3. **Debashree Sengupta**, Monica Kannan, Attipalli R Reddy (**2011**).A root proteomics-based insight reveals dynamic regulation of root proteins under progressive drought stress and recovery in *Vigna radiata* L. Wilczek. **Planta 233: 1111-1127.**
4. **Debashree Sengupta**, Attipalli R Reddy (**2011**). Water deficit as a regulatory switch for legume root responses. **Plant Signaling & Behavior 6: 914-917.**
5. **Debashree Sengupta,** Anirban Guha, Attipalli R Reddy (2013) Interdependence of root defense responses with photosynthesis and fast kinetics of chlorophyll a fluorescence in *Vigna radiata* (L.) Wilczek under progressive soil water deficit and recovery. **Journal of Photochemistry and Photobiology**. (communicated).
6. Anirban Guha, **Debashree Sengupta**, Attipalli R Reddy (2012). Polyphasic chlorophyll a fluorescence kinetics and leaf protein analyses to track dynamics of photosynthetic performance in mulberry during progressive drought. **Journal of Photochemistry and Photobiology.** doi 10.10.16/J-JPhotoBiol. 2012.12.006
7. Anirban Guha, **Debashree Sengupta**, Girish Kumar Rasineni, Attipalli R Reddy (**2012).** Non enzymatic antioxidative defence in drought-stressed mulberry (*Morus indica* L.) genotypes. **Trees structure and function 26: 903-918**.
8. Anirban Guha, **Debashree Sengupta,** Attipalli R Reddy (**2010**). Physiological optimality, allocation trade-offs and antioxidant protection linked to better leaf yield performance in drought exposed mulberry. **Journal of Science Food and Agriculture 90: 2649-2659.**
9. Anirban Guha, **Debashree Sengupta**, Girish Kumar Rasineni, Attipalli R Reddy (**2010**). An integrated diagnostic approach to understand drought tolerance in mulberry (*Morus indica* L.). **Flora 205: 144-151**.

Accessions

1. **NCBI GenBank ID HQ999996.1**. *Vigna radiata* chloroplast gamma glutamyl cysteine syntehtase mRNA complete cds ; nuclear gene for chloroplast product.
2. **NCBI GenBank ID KC422242**. *Vigna radiata* Δ^1-pyrroline-5-carboxylate synthase, mRNA partial cds.

International/National Conferences

1. Participated and presented poster entitled "*Molecular characterization and expression analysis of γ-glutamyl cysteine synthetase gene (VrγECS) from roots of Vigna radiata L. Wilczek under low water regimes*" at the **4th EMBO meeting at Nice, France (2012).**
2. Participated and presented poster entitled "*Drought-induced regulatory mechanisms in Mungbean (Vigna radiataL. Wilczek) roots*" at **BioQuest (2010)** conducted by School of Life Sciences, University of Hyderabad.
3. Published abstract entitled "*An integrated physiological and proteomic approach for comprehending drought stress responses in Mulberry*" at **National symposium on Frontiers in Photobiology (2009)** at Bhabha Atomic Research Centre.